The cellular impact of diminished DNA origin licensing capacity and its potential therapeutic exploitation

By

Kristin Mara Zimmerman

A thesis submitted to the University of Sussex in January, 2013 for the degree of Doctor of Philosophy in Biochemistry

Declaration

I hereby declare that this thesis has not been and will not be submitted in whole or in part to another University for the award of any other degree. All data presented in this thesis have resulted from my own original work with the exception of the results depicted in Figure I.11.A and C (provided by Dr. Sarah Walker), Figure III.1.B (provided by Dr. Holly Brunton), and Figure IV.6.C-D (provided by Dr. Rebecca Jones). The results presented in Figure V.7.F are from experiments performed and repeated by myself and Liang Xue.

Kristin Zimmerman

Acknowledgements

This thesis is lovingly dedicated to my grandmother, Mara Conover, who has never failed to inspire me with her support, wisdom, strength, and beauty. I also dedicate this work to my parents, Jim and Cindy Zimmerman, who have loved and supported me throughout my life. I can only hope to be as incredible a parent for my own children as they both have been for me. Finally, I dedicate this thesis to my husband, Mark. Without his constant patience, selflessness, and encouragement, I don't know how I would have gotten through this. He truly deserves a medal.

I would like to thank Dr. Penny Jeggo for giving me the opportunity to pursue my PhD in her lab and for her supervision of my doctorate studies. I also thank Dr. Mark O'Driscoll, Dr. Aaron Goodarzi, Dr. Atsushi Shibata, Dr. Antony Oliver, and all of the members of the Jeggo lab for sharing technical advice, reagent aliquots, scientific wisdom, and, above all, moral support. Finally, I thank our scientific collaborators who have contributed to this work including Dr. Patrick Concannon, Dr. Jie Wen, Dr. Óscar Fernández-Captello, Dr. Eva Petermann, and Dr. Rebecca Jones.

I would never have been able to pursue my PhD at the University of Sussex without the generous support from Judith Hasko and The American Friends of the University, for which I am truly grateful.

UNIVERSITY OF SUSSEX

KRISTIN MARA ZIMMERMAN DOCTOR OF PHILOSOPHY BIOCHEMISTRY

THE CELLULAR IMPACT OF DIMINISHED DNA ORIGIN LICENSING CAPACITY AND ITS POTENTIAL THERAPEUTIC EXPLOITATION

SUMMARY

Genomic instability underlies various diseases including cancer. The maintenance of genomic stability requires accurate replication of the genome, proper segregation of duplicated DNA to progeny cells, and the capacity to respond effectively to DNA damage. Early sections of this thesis focus on the response to DNA double-strand breaks (DSBs) within compact regions of chromatin (heterochromatin). Here, methodology was optimised for monitoring the repair of site-specific DSBs within regions likely to be enriched for heterochromatin. This system was exploited to examine the function of the Artemis endonuclease in heterochromatic DSB repair. Later sections focus on factors involved in DNA replication and the response to replication stress. Among the various mechanisms involved in the DNA damage response (DDR) to replication stress, the licensing of excess origins of replication has been proposed to safeguard against replication failure. Here, the impact of diminished origin licensing capacity on the response to replication stress was compared in tumour and non-tumour cell lines. I present findings demonstrating that depletion of origin licensing factors causes hypersensitisation of tumour-derived but not non-tumour cell lines to replication stress-inducing agents. Further, combining diminished origin licensing capacity with depletion of the tumour suppressor, p53, or overexpression of the c-Myc oncogene impairs viability under conditions of replication stress in non-tumour fibroblasts. These findings suggest that tumour cells have a greater reliance on origin licensing capacity, raising the possibility that licensing factors might represent suitable targets for drug-based cancer therapy. Factors involved in replication origin licensing have also been implicated in the establishment of heterochromatin. Here, I examined higher-order chromatin structure and the ionizing radiation (IR)-induced DDR in cells from patients harbouring mutations in origin licensing factors. Findings from these studies provide evidence for the first time that origin licensing complex (ORC)-deficient Meier-Gorlin Syndrome (MGS) may be classified as a disordered chromatin syndrome.

Table of Contents

List of abbreviations

53BP1	p53 binding protein 1
8-oxo-dG	8-oxo-2'-deoxyguanosine
9-1-1 complex	Rad9-Rad1-Hus1
aa	Amino acids
AAA+	ATPases associated with diverse cellular activities
ADP	Adenosine diphosphate
AF-488	Alexa-Fluor 488
alt-NHEJ	Alternative nonhomologous end joining
AML	Acute lymphoblastic leukemia
AmpR	Ampicillin resistant
AOA1	Ataxia-oculomoter apraxia 1
AP site	Apurinic/apyrimidine site
APC^{Cdh1}	Cdh1-activated form of the anaphase-promoting complex
APE1	AP endonuclease 1
APS	Ammonium persulfate
ARS	Autonomously replicating sequence
ATM	Ataxia-telangiectasia mutated
ATMi	Ataxia-telangiectasia mutated inhibitor KU-55993
ATR	Ataxia-telangiectasia and Rad3-related
ATRIP	ATR-interacting protein
A.U.	Arbitrary units
BAF180	BRG1-associated factor 180
BAH	Bromo-adjacent homology
BARD1	BRCA1-associated ring domain protein 1
BER	Base excision repair
BLM	Bloom syndrome, RecQ helicase-like
bp	Base pair(s)

BRAF	V-raf murine sarcoma viral oncogene homolog B1
BRCA1	Breast cancer susceptibility 1
BRCA2	Breast cancer susceptibility 2
BRC-ABL	Breakpoint cluster region fused with V-abl Abelson murine leukemia viral oncogene homolog 1
BRCT	BRCA1 C-terminus
BrdU	Bromodeoxyuridine
BSA	bovine serum albumin
CAF-1	Chromatin assembly factor 1
CDC2	Cell division control 2
CDC28	Cell division control 28
CDC6	Cell division control 6
CDC7	Cell division control 7
CDC45	Cell division control 45
Cdk	Cyclin dependent kinase
Cdk1	Cyclin dependent kinase 1
Cdk2	Cyclin dependent kinase 2
Cdt1	Cdc10 dependent transcript 1
CENPA	Centromere protein A
CENPF	Centromere protein F
CENPJ	Centromere protein J
CEP152	Centrosomal protein 152kDa
CFS	Common fragile site
Chaos3	Chromosome aberrations occurring spontaneously 3
CHD3/Mi-2α	Chromodomain helicase DNA binding protein 3
CHD4/Mi-2β	Chromodomain helicase DNA binding protein 4
ChIP	Chromatin immunoprecipitation
Chk1	Checkpoint kinase 1
Chk2	Checkpoint kinase 2

CHO	Chinese hamster ovary
CML	Chronic myeloid leukemia
c-NHEJ	Canonical NHEJ
CO_2	Carbon dioxide
CpG	Cytosine-phosphate-guanine
CPP	Cell penetrating peptide
CSR	Class switch recombination
C-terminal/terminus	Carboxyl-terminal/terminus
CtIP	Carboxy-terminal binding protein interacting protein
Cul4/DDB1	Cullin 4/DNA damage binding protein 1
CID	CDK inhibitory domain
Cy3	Cyanine 3
Cy motif	Cyclin binding motif
DAB1	Disabled homolog 1
DAPI	4',6-diamidino-2-phenylindole
ddH_2O	Double distilled water
DDR	DNA damage response
D-loop	Displacement loop
DMEM	Dulbecco's Modified Eagle’s Medium
DMSO	Dimethyl sulfoxide
DNA	Deoxyribonucleic acid
DNA-PKcs	DNA-dependent protein kinase, catalytic subunit
DNA-PKi	DNA-dependent protein kinase inhibitor KU-57788
DNMT	DNA methyltransferases
dNTP	deoxynucleotide triphosphate
DSB	Double-strand break
dsDNA	Double-stranded DNA
ECL	Enhanced chemilluminescence

E. coli	*Escherichia coli*
EDTA	Ethylenediaminetetraacetic acid
EGFR	Epidermal growth factor receptor
EGFP	Enhanced green fluorescent protein
eNoSC	Energy-dependent Nucleolar Silencing Complex
ETS	External transcribed spacer
FCS	Fetal calf serum
FHA	Forkhead-associated
FITC	Fluorescein isothiocyanate
G0-phase/G0	Gap 0-phase
G1-phase/G1	Gap1-phase
G2-phase/G2	Gap2-phase
GEN1	Flap endonuclease gen homolog 1
GFP	Green fluorescent protein
GINS	Go, Ichi, Nii, San
H_2O_2	Hydrogen peroxide
HAT	Histone acetyltransferases
HBO1	Histone acetyltransferase binding to ORC
HDAC	Histone deacetylase
HER2	Human epidermal growth factor receptor 2
HGPS	Hutchinson-Gilford progeria syndrome
His	Polyhistidine
HJ	Holliday Junction
HMGA1a	High mobility group A 1 a
HMT	Histone methyltransferases
HNPCC	Hereditary non-polyposis colon cancer
HP1	Heterochromatin protein 1
HR	Homologous recombination

HRP	Horseradish peroxidase
hTERT	Human telomerase
HU	Hydroxyurea
IC_{50}	Half maximum inhibitory concentration
ICF	Immunodeficiency with centromere instability and facial anomalies
Ig	Immunoglobulin
I-*Ppo*I	Intron-encoded *Physarum polycephalum* endonuclease I
IPTG	Isopropyl-β-D-thio-galactoside
IR	Ionizing radiation
IRIF	Ionizing radiation-induced foci
ITS	Internal transcribed spacer
K	Lysine
KAP-1	KRAB-domain associated protein 1
KRAB	Kruppel associated box domain
kb	Kilobase(s)
kDa	Kilodalton
Kpna6/1	Karyopherin alpha 6/1
Lac	Lactose
LB	Lysogeny broth
LBL	Lymphoblastoid cell line
LET	Linear energy transfer
Lig3	Ligase 3
Lig4	Ligase 4
LSD1	Lysine-specific demethylase 1
MCM	Minichromosome maintenance
MDC1	Mediator of DNA damage protein 1
MECP2	Methyl CpG binding protein 2
MEF	Mouse embryonic fibroblast

MEM	Minimum Essential Medium
MGS	Meier-Gorlin Syndrome
Mi-2/NuRD	Mi-2/Nucleosome remodelling and deacetylase
MIR	MOD1-interacting region
MLH1	MutL homolog 1
MMEJ	Microhomology-mediated end joining
MMR	Mismatch repair
MMS	Methyl methanesulfonate
MOPD I	Microcephalic osteodysplastic primordial dwarfism type I
MOPD II	Majewski/microcephalic osteodysplastic primordial dwarfism type II
MPD	Microcephalic primordial dwarfism
M-phase/M	Mitosis-phase
MRN	Mre11/Rad50/Nbs1 complex
MSH2	MutS homolog 2
Myc/c-Myc	Avian myelocytomatosis viral oncogenes homolog
NBS1	Nijmegen breakage syndrome 1
NER	Nucleotide excision repair
NFDM	Non-fat dried milk
NHEJ	Non-homologous end joining
NLS	Nuclear localisation signal
NOR	Nucleolar organiser regions
NTA	Nickel-nitrilotriacetic acid
N-terminal/terminus	Amino-terminal/terminus
NTS	Non-transcribed spacer
OD_{600}	Optical density at a wavelength of 600 nm
ORC	Origin recognition complex
ORCA	ORC-associated
P	Phosphorylated

PACT	Pericentrin-AKAP450 centrosomal targeting
PARP1	Poly (ADP-ribose) polymerase 1
PBS	Phosphate buffered saline
PCC	Premature chromosome condensation
PCNA	Proliferating cell nuclear antigen
PCNT	Pericentrin
PCR	Polymerase chain reaction
PFA	Paraformaldehyde
PHD	Plant homeo domain
PI	Propidium iodide
PIKK	Phosphoinositol 3-kinase like kinase
PIP box	PCNA interaction protein box
PNK	Polynucleotide phosphatase/kinase
pre-RC	Pre-replication complex
PST repeat	Proline- serine- and threonine-rich repeat
PTM	Post-translational modification
PVDF	Polyvinylidene difluoride
RAG1/2	Recombination-activating genes 1/2
RB	Retinoblastoma protein
rDNA	Ribosomal DNA
RFC	Replication factor C
RNAse	Ribonuclease
RNF168	Ring finger protein 168
RNF8	Ring finger protein 8
RNR	Ribonucleotide reductase
ROS	Reactive oxygen species
RPA	Replication protein A
rpm	Revolutions per minute

RPMI	Roswell Park Memorial Institute
rRNA	Ribosomal RNA
RS-SCID	Severe combined immunodeficiency with radiation sensitivity
S. cerevisiae	*Saccharomyces cerevisiae*
SD	Standard deviation
SDS	Sodium dodecyl sulfate
SIR1	Silent information regulator 1
S-phase/S	Synthesis-phase
S. pombe	*Saccharomyces pombe*
S1	Sensor 1 motif
S2	Sensor 2 motif
SAHF	Senescence associated heterochromatin foci
SCAN1	Spinocerebellar ataxia with axonal neuropathy 1
SCID	Severe combined immunodeficiency
SCID-A	Severe combined immunodeficiency in Athabascan-speaking Native Americans
SCF	SKP1-cullin-F-box
SDS-PAGE	Sodium dodecyl sulfate polyacrylamide gel electrophoresis
SETDB1	SET domain bifurcated 1
SIRT1	Deacetylase sirtuin 1
siRNA	Small interfering ribonucleic acid
Skp2	S-phase kinase-associated protein 2
SMARCAL1	SWI/SNF-related matrix-associated, actin-dependent regulator of chromatin, subfamily A-like 1
SSB	Single-strand break
ssDNA	Single-stranded DNA
SUMO	Small ubiquitin-like modifier
SUV39H1	Suppressor of variegation 3-9 homolog 1
SUV39H2	Suppressor of variegation 3-9 homolog 2

TBE	Tris/Borate/Ethylenediaminetetraacetic acid
TBH	Tert-butyl hydroperoxide
TBS	Tris-buffered saline
TBS-T	Tris-buffered saline containing 0.1 % Tween-20
TEMED	Tetramethylethylenediamine
TERRA	Telomere-repeat-encoding RNA
tiff	Tagged image file format
TopBP1	Topoisomerase II binding protein 1
TopoI	Topoisomerase I
TopoII	Topoisomerase II
TP53	Tumour protein p53
TRF2	Telomere repeat factor 2
Ub	Ubiqutinate(d)
UV	Ultraviolet
V	Volts
V(D)J	Variable, diversity, and joining genes
VEGF	Vascular endothelial growth factor
WA	Walker A motif
WB	Walker B motif
WRN	Werner syndrome
XLF	XRCC-like factor
XRCC3	X-ray repair cross-complementing protein 3
XRCC4	X-ray repair cross-complementing protein 4

List of figures

Chapter I: Introduction

Chapter III: Examination of the role of Artemis in DSB repair during G0/G1 using a novel system of site-specific break induction

List of tables

I Introduction

I.1 Genomic instability and cancer

Cancer is currently one of the greatest health risks known to man, with an estimated 7.6 million worldwide cancer deaths reported in the year 2008 (Ferlay et al. 2010). In part as a result of longer life expectancy and increased cancer detection, cancer incidence is still on the rise in countries such as the United Kingdom (Maddams et al. 2009). However, significant progress in research, prevention, and clinical strategies has contributed to a decrease in the rate of cancer caused deaths in the United States (Maddams et al. 2009; Eheman et al. 2012). Given the enormous scope and impact of this life-altering disease, continued progress in research into therapeutic interventions is critically needed to improve the prognosis and quality of life of patients with cancer.

The term "cancer" encompasses an incredibly complex range of neoplastic diseases which involve a variety of alterations in the genome. Several hallmarks of cancer have been described, including the ability to evade cell death, sustained angiogenesis, metastatic capacity, insensitivity to anti-growth signals, self-sufficiency in growth signals, and finally, a limitless replicative potential (Hanahan et al. 2000). In addition, nearly all human cancers display genome instability which can encompass chromosomal instability, microsatellite instability, epigenetic changes, and increased rates of spontaneous mutations (Negrini et al. 2010).

The genome instability characteristic of cancer cells may be propagated by genetic alterations which impact the deoxyribonucleic acid (DNA) damage response (DDR), an elaborate series of biological pathways which function to protect genome integrity. The DDR, which acts as an anti-cancer barrier (Bartek et al. 2007b), encompasses various mechanisms involved in the arrest of the cell cycle, repair of DNA damage, and in some contexts, cell death (Hoeijmakers 2009). Depending on the type of damage occurring, the repair of DNA lesions can occur through pathways such as mismatch repair (MMR), base excision repair (BER), nucleotide excision repair (NER), single-strand break (SSB) repair, double-strand break (DSB) repair (Section I.3.1), or direct reversal of damage (Lord et al. 2012).

Reflecting the role of the DDR in preventing tumourigenesis, mutations in DDR genes have been identified in various types of hereditary cancers. For example, mutations in MMR genes such as mutL homolog 1 (*MLH1*) and mutS homolog 2 (*MSH2*) underlie hereditary non-polyposis colon cancer (HNPCC), also known as Lynch syndrome (Aaltonen et al. 1994; Peltomaki et al. 1997; Pedroni et al. 2001; Heinen et al. 2002). In addition, an estimated 80-90% of familial breast cancer cases are associated with mutations in the breast cancer susceptibility 1 (*BRCA1*) and breast cancer susceptibility 2 (*BRCA2*) genes (Ford et al. 1998; Stratton et al. 2008), both of which are involved in DSB repair (Liu et al. 2002) (Section I.3).

Further, germline mutations in tumour protein p53 (*TP53*), a tumour suppressor involved in DDR mechanisms such as cell cycle arrest and apoptosis, cause Li-Fraumeni syndrome, a disease characterised by the development of various forms of cancer from as early as childhood (Varley 2003; Hanel et al. 2012).

In addition to these examples of hereditary mutations, spontaneous alterations in DDR genes are thought to propagate tumour development and growth (Negrini et al. 2010). One model for tumourigenesis proposes that the genomic instability arising from changes in pre-cancerous cells induces replication-associated DNA damage (replication stress) (Section I.2.3), potentially contributing to the spontaneous mutagenesis of "caretaker genes" such as the DDR genes and to tumour propagation (Negrini et al. 2010). Hereditary alterations in DDR genes may also, in part, drive cancer development by further increasing mutagenesis (Bartek et al. 2007a; Murga et al. 2007). One potential source of replication stress in cancer is the aberrant expression of an oncogene (Halazonetis et al. 2008), one of the earliest lesions that may occur during tumourigenesis (Petermann et al. 2007). As described in Section I.2.4, the increased expression of an oncogene such as avian myelocytomatosis viral oncogenes homolog (Myc) can induce many cellular changes including the induction of DNA damage (ie. replication stress), changes in transcription, escalation of cellular growth, and the unscheduled activation of DNA replication origins (defined in Section I.2.4) (Vafa et al. 2002; Dominguez-Sola et al. 2007; Herold et al. 2009a). Activation of the DDR, as observed at early cancer-associated lesions (Bartkova et al. 2005), is in part attributed to oncogene-induced replication stress (Di Micco et al. 2006) and is thought to act as a barrier to tumour development by inducing cellular senescence (a state in which growth is permanently arrested) and/or cell death (Bartkova et al. 2006; Bartek et al. 2007a). Consequently, alterations in DDR genes may allow pre-cancerous cells (which harbour genome instability) to evade senescence and cell death, ultimately contributing to cancer development (Bartkova et al. 2005).

Our increased understanding of the molecular alterations which distinguish tumour cells from healthy tissue is vital in developing and improving therapeutic strategies for cancer patients. Therapeutic interventions in oncology have traditionally exploited the changes in replication observed in cancer cells. Since the discovery in the 1940's by Sidney Farber that antifolates (inhibitors of DNA replication) reduce remission in acute lymphoblastic leukaemia (AML) patients, a vast number of replication-targeting chemotherapies have been developed (Farber et al. 1948; Helleday et al. 2008). However, these agents do not discriminate between tumour cells and rapidly dividing cells in healthy tissue. As a result, clinical side effects are frequently observed with administration of replication inhibitors (Helleday et al. 2008). Strategies which selectively target alterations that distinguish tumour cells from healthy tissue have shown great promise in cancer therapy (Aggarwal 2010). This is exemplified by the success of the Breakpoint cluster region fused with V-abl Abelson murine leukaemia viral

oncogene homolog 1 (BRC-ABL) inhibitor Imantinib in the treatment of chronic myeloid leukaemia (CML), the v-raf murine sarcoma viral oncogene homolog B1 (BRAF) inhibitor Vemurafenib/Zelboraf in the treatment of melanoma, the epidermal growth factor receptor (EGFR) oncogene inhibitor Cetuximab/Erbitux in head and neck carcinoma and colorectal cancer, the human epidermal growth factor receptor 2 (HER2)-inhibiting antibody Trastuzumab/Herceptin in the treatment of breast cancer, and finally the vascular endothelial growth factor (VEGF) inhibiting antibody Bevacizumab/Avastin in a variety of tumour types (Aggarwal 2010; Yap et al. 2012).

Both the development of therapeutic interventions which target DDR proteins and an increased understanding of the impact of tumour-associated DDR alterations on drug cytotoxicity have shown promise in guiding clinical strategies for the treatment of cancer (Helleday et al. 2008; de Bono et al. 2010; Lord et al. 2012). Tumour cells deficient in one DNA repair pathway are thought to rely more heavily on other DDR pathways for survival; therefore, DDR protein inhibitors are proposed to enhance cytotoxicity specifically in these tumours (a concept known as synthetic lethality) (Helleday et al. 2008; de Bono et al. 2010; Lord et al. 2012). In support of this model, single agent treatment with inhibitors of the poly adenine diphosphate (ADP)-ribose polymerase (PARP) DNA damage signalling proteins may be beneficial specifically to patients with mutations in DNA repair genes such as *BRCA1* or *BRCA2* (Bryant et al. 2005; Farmer et al. 2005). As a further example, inhibitors of the DDR protein checkpoint kinase 1 (Chk1) are particularly lethal in tumour cells deficient in the p53 and p21 proteins (involved in DNA damage-induced cell cycle arrest and death pathways) (Origanti et al. 2012), Fanconi Anemia DNA repair proteins (Chen et al. 2009), or BRCA2 (Hattori et al. 2011).

The combined administration of DDR inhibitors with DNA damage-inducing agents may also improve the so-called “therapeutic index,” a measure used to determine the dose range in which an agent will induce beneficial therapeutic outcome with minimal side effects. For example, PARP inhibition combined with the DNA damage-inducing chemotherapeutic agent Temozolomide is reported to enhance anti-tumour activity of Temozolomide alone (Palma et al. 2008). Further, PARP inhibition has been demonstrated to enhance sensitivity to radiation-induced DNA damage particularly in cells deficient in DNA repair proteins (Loser et al. 2010) and the combined administration of a PARP inhibitor with radiation is reported to reduce tumour growth in a model for lung cancer (Albert et al. 2007). Consequently, beneficial effects may be observed at lower doses of Temozolomide or radiation under conditions of PARP inhibition, therefore improving therapeutic index.

Overall, the development of DDR-targeted therapeutics, administration of combinational drug therapy with DDR inhibitors, and exploitation of synthetic lethality have proven promising in improving clinical outcome (de Bono et al. 2010) and remain the subject of

ongoing medical research. Further understanding of the DDR will also provide insight to guide these developments.

I.2 The cellular threat of DNA damage

As previously introduced, DDR pathway activation occurs in a manner dependent on the type of damage induced. Many distinct forms of DNA damage may arise from a variety of sources. For the purpose of this thesis, specific forms of DNA damage arising from oxidative stress, IR, replication stress, and oncogenic expression will be emphasized in the context of cancer.

On a daily basis, each cell in our body must contend with tens of thousands of potentially harmful DNA lesions (Hoeijmakers 2009; Ciccia et al. 2010). Spontaneous DNA aberrations may arise from redox-cycling events such as oxidative respiration which generates DNA base damage, mis-incorporation of DNA bases during replication, deamination of cytosine which results in the transition to uracil, alteration of DNA following depurination, and DNA base modification by alkylation (Ciccia et al. 2010). DSBs are generated during cellular processes such as meiosis, variable, diversity, and joining genes (V(D)J) recombination, and immunoglobulin (Ig) class switch recombination (CSR) (Szostak et al. 1983; Alt et al. 1992; Soulas-Sprauel et al. 2007). DNA damage may also arise from environmental sources including ultraviolet (UV) radiation from sunlight, ionizing radiation (IR), as well as DNA damage-inducing chemicals such as tobacco-based products, pesticides, and various chemotherapeutic drugs (Jackson et al. 2009) (Table I.1). As introduced in Section I.1, the aberrant expression of oncogenes can induce cellular changes resulting in various types of DNA lesions (Halazonetis et al. 2008).

Damaging agent/process	Example of aberration	Sources/purpose
Endogenous damage		
Base oxidation	8-oxo-dG	ROS
Base deamination	Hydrolysis of cytosine to uracil	Spontaneous
Depurination	Apurinic site	Spontaneous, BER glycosylase
Base alkylation	3-methyladenine, 7-methylguanine, 0^6-methylguanine	Endogenous alkylating agents
Base mis-incorporation	Base transition/transversion	Replication errors
Cellular Processes		
Meiosis	DSBs	Production of gametes
V(D)J recombination	DSBs	Production of Ig and T cell receptors
CSR	DSBs	Switch of antibody class
Exogenous Damage		
UV	6-4 photoproducts, thymine dimers	Sunlight (UVA,B)
IR	8-oxo-dG, SSBs, DSBs	Cosmic radiation, radiotherapy
HU, Gemcitabine	SSBs, one-ended DSBs (replication fork stalling/collapse)	Chemotherapy
H_2O_2	8-oxo-dG, SSBs, one-ended DSBs (replication fork stalling/collapse)	Disinfectant, byproduct from aerobic respiration
Topoisomerase inhibitors	Intercalation with DNA, SSBs, DSBs	Chemotherapy
Cisplatin	DNA crosslinks	Chemotherapy

Table I.1 Sources of DNA damage. See main text for abbreviations.

I.2.1 Oxidative stress-induced base damage

Oxidative stress from excessive levels of reactive oxygen species (ROS) may result from endogenous sources such as aerobic respiration in mitochondria or from exogenous agents such as IR, hydrogen peroxide (H_2O_2), and chemotherapy (Cooke et al. 2003; Conklin 2004). The DNA damage induced by oxidative stress results from the ability of ROS, such as the hydroxyl radical and superoxide anion, to physically interact with DNA and promote the modification of DNA bases (Cooke et al. 2003). To date, the most extensively studied ROS-induced lesion is the oxidation of the deoxyguanosine nucleoside to 8-oxo-2'-deoxyguanosine (8-oxo-dG) (Figure I.1). In normal human cells, 8-oxo-dG is estimated to occur at a steady state level of 2-3 lesions per 10^6 guanine bases (Cadet et al. 1997; Cooke et al. 2003; Gedik et al. 2005; Ohno et al. 2006). This base modification can become incorporated into DNA, leading to error-prone DNA replication, replication stress, and ultimately mutagenesis (Hanes et al. 2006; David et al. 2007). In addition to the modification of DNA bases, oxidative stress leads to the induction of DNA strand breaks (Bertoncini et al. 1995), which will be introduced in Section I.2.2.

Most cancer cells can be characterised by an increase in levels of cellular ROS and oxidative stress is thought to contribute to genomic instability during tumourigenesis (Maiti 2012). The majority of chemotherapeutic agents induce further increases in ROS levels in tumour cells which can result in apoptotic cell death, presumably as a result of excess damage. However, over time, treatment with the same drug may result in a reduction in ROS levels in surviving tumour cells and chemoresistance. Therefore, maintaining high levels of ROS in tumour cells throughout therapeutic treatment may be important in clinical outcome (Maiti 2012).

In addition to contributing to carcinogenesis, the accumulation of 8-oxo-dG has also been observed during aging. In fact the free radical theory of aging, first proposed in the 1950's, postulates that ageing results from the accumulation of oxidative damage over time (Harman 1956; Kaneko et al. 2001).

I.2.2 IR-induced DNA strand breaks

DNA stand breaks, which disrupt the sugar-phosphate backbone of the DNA molecule, are potentially hazardous events and may arise from various sources. An accumulation of breaks in either a single strand or both strands of the DNA duplex may threaten chromosomal stability and, ultimately, the survival of cells.

I.2.2.a Single-strand breaks (SSBs)

SSBs are characterised by the severing of one of the two strands of DNA and are usually accompanied by damage to 5' or 3' DNA termini at the break (Figure I.1). These breaks can arise from sources of damage which generate ROS such as cellular respiration (Section I.2.1) or from exposure to exogenous agents such as H_2O_2 or IR. Direct SSB induction from ROS occurs when a sugar moiety of the DNA backbone becomes oxidized and subsequently disintegrates (Caldecott 2008). SSBs induced by damaging agents generally occur much more frequently than DSBs. For example, treatment with H_2O_2 generates roughly 2,000 SSBs for every DSB and IR induces 20 SSB for every DSB (Bradley et al. 1979). SSBs may also result in DSBs, as evidenced by the fact that closely located SSBs may result in DSBs with single-stranded DNA (ssDNA) overhangs (Chadwick et al. 1994) and that SSBs persisting during DNA replication lead to blockage or collapse of replication forks, thereby generating one-ended DSBs (Kuzminov 2001) (see Section I.2.3).

In addition to the direct induction of SSBs by IR and ROS, direct SSB induction can also occur from BER and as a result of aborted activity of topoisomerases. BER is a process initiated by DNA glycosylases which remove damaged bases and generates apurinic/apyrimidine (AP) sites. AP endonuclease 1 (APE1) may then cleave DNA at AP sites, generating SSBs (Singer et al. 1981). Topoisomerases such as topoisomerase I (TopoI), relieve torsional strain in DNA during transcription and replication by generating nicks in DNA. The collision of unsealed nicks with polymerases or close proximity to other lesions may result in SSBs covalently linked to the topoisomerase (Pommier et al. 2003).

While defects in SSB repair can result in cerebellar ataxia and neurodegeneration, as observed in disorders such as Ataxia-oculomoter apraxia I (AOAI) and spinocerebellar ataxia with axonal neuropathy 1 (SCAN1), these disorders are not marked by genomic instability and cancer, potentially as a result of alternative factors compensating for defective repair (Caldecott 2008).

I.2.2.b Double-strand breaks (DSBs)

The DSB, which occurs when both strands of the DNA helix are severed, is considered to be one of the most toxic DNA lesions that cells encounter (Helleday et al. 2007). DSBs may consist of a blunt cut across the double helix or, more commonly, of two SSBs on opposite strands within several base pairs (bp) of one another (Van Der Schans 1978) (Figure I.1). Additionally DSBs can arise when replication forks collapse, generating a structurally distinct type of break. If left unrepaired or if repaired inaccurately, DSBs can result in genomic translocations, loss of genetic material, and cell death (Ferguson et al. 2001).

I.2.2.b.1 IR-induced DSBs

Since the discovery of radiation, the process in which energy particles or waves travel through space, in the 1800's, radiation has been exploited therapeutically in the diagnosis and treatment of human diseases such as cancer (Rontgen 1896). The penetrative properties of IR allow for technologies used in medical imaging but also induce DNA damage via the production of excited and ionised molecules. IR both directly deposits energy in cells to generate excited and ionized molecules and also indirectly generates damage via the ionization of water molecules (Ward 1988). As a result, multiple types of DNA damage, ranging from modification of DNA bases to DNA strand breaks, can occur. Of all energy deposited by IR, greater than 90% generates ROS resulting in DNA damage (Section I.2.1) (Ward 1988). Both direct and indirect damage from IR can result in a variety of DNA lesions including SSBs and DSBs, with a ratio of roughly 20 SSBs for every 1 DSB generated (Lobrich et al. 2010). As depicted in Figure I.1, IR-induced DSBs usually consist of two SSBs on opposite strands within 10-20 bp of one another (Van Der Schans 1978), and therefore also contain 3' and 5' overhangs which may require processing prior to repair (Mahaney et al. 2009).

Several forms of IR exist including γ rays, which are produced by radioactive decay, particle accelerators generating X-rays and carbon ions, and radiation found in cosmic rays, such as iron ions (Charles 2001). The amount of energy transferred to a substance as an ionizing particle travels through is referred to as linear energy transfer (LET). While X-rays and γ rays are considered to be sparsely ionizing sources, and therefore have low LET, heavy ions such as carbon and iron ions are densely ionizing, have high LET, and result in greater cell death in human cells (Niemantsverdriet et al. 2012).

The induction of clustered DNA lesions, resulting from multiple forms of damage in close vicinity on the DNA, increases with increased LET and poses a challenge for the cell (Ward 1981). Results from predictive studies have demonstrated that roughly 30% of DSBs induced by a source such as γ-rays or X-rays contain clustered damage with up to 10 lesions per cluster, while roughly 70% of DSBs induced by high LET radiation have been predicted to contain clustered damage with up to 25 lesions per cluster (Nikjoo et al. 1997; Semenenko et al. 2004).

The DDR mechanisms which respond to IR-induced DSBs will be further discussed in Section I.3.

I.2.3 Replication stress and one-ended DSBs

The maintenance of stability of the replication fork, a dynamic structure which forms when two strands of DNA separate during DNA synthesis, is crucial in the prevention of genomic

aberrations. Replication stress, a term encompassing many different types of strains put on the progression of the fork, may arise from a variety of sources. For example, progression of replication forks may be delayed or completely inhibited by a variety of obstacles including protein-DNA complexes, regions that are difficult to unwind, and secondary structures arising from A-T dinucleotide-rich flexibility islands in genomic fragile sites (Burhans et al. 2007; Branzei et al. 2010; Burrow et al. 2010). The approach of a replication fork to a region of damaged DNA (for example, containing modified bases or SSBs) may also preclude further progression of replication. Alterations in the replication machinery and/or timing of replication (Section I.4) have been reported in various forms of cancer (Lau et al. 2007b; Fritz et al. 2012) and may lead to either over- or under-replication, putting strain on replication forks. Finally, exposure to replication inhibiting agents, as in the context of cancer therapy, may limit nucleotide pools or DNA polymerase activity, leading to slowed replication fork progression and the induction of replication-associated damage.

Upon stalling of a replication fork, regions of single-stranded DNA become exposed, generating unstable structures which generally require stabilization (Branzei et al. 2010). Various DDR proteins function in the stabilization of stalled forks, allowing for the preservation of genome integrity while the obstruction is resolved (Section I.4.2). However, under conditions which challenge stability of these stalled forks and after extended times of stalling, forks can collapse into structures known as "one-ended DSBs" (Figure 1.1) (Helleday et al. 2007). The MUS81-EME nuclease may also directly cleave replication forks resulting in this distinct type of DSB (Ciccia et al. 2010).

If unresolved, replication stress may result in inefficient DNA synthesis and DNA damage accumulation. Ultimately, tumourigenic genomic rearrangements or cell lethality may result. The DDR mechanisms which respond to replication stress will discussed in detail in Section I.4.

I.2.4 The various lesions induced by oncogenic stress

The aberrant expression of oncogenes such as Myc has pleiotropic cellular effects, resulting from changes in both transcriptional and non-transcriptional control of cellular processes. Using an inducible system of Myc expression in normal human fibroblasts, Vafa, Wade et al. demonstrated in 2002 that Myc overexpression results in an increase in ROS to a level similar to that generated from short treatment with H_2O_2. Consequently, an elevation in the frequency of 8-oxo-dG base modifications has been reported under conditions of Myc overexpression (KC et al. 2006). This increase in the production of ROS has been, in part, attributed to the Myc-dependent recruitment of lysine-specific demethylase 1 (LSD1) to chromatin (described in

Section I.3.3), resulting in demethylation of lysine residues and the induction of localised oxidation of DNA (Amente et al. 2010).

Myc overexpression has also been reported to increase replication stress. This is likely to occur as a result of various factors, including alterations in the regulation of DNA replication, the encountering of replication forks with ROS-induced base modifications, and aberrations in the DNA damage response. Myc overexpression in normal human fibroblasts leads to acceleration of the DNA synthesis-phase (S-phase) of the cell cycle (Robinson et al. 2009) corresponding with increased activity of origins of replication (Dominguez-Sola et al. 2007). The cellular levels of deoxynucleotide triphosphates (dNTPs), the building blocks needed for DNA synthesis, have been shown to also increase with overexpression of Myc, presumably to support ongoing rapid proliferation (Mannava et al. 2008). Further, Myc has been reported to promote aberrant replication at specific loci on DNA, which is likely to contribute to the genomic instability observed (Kuschak et al. 2002). Finally, Myc overexpression has been shown to deregulate DNA damage-induced cell cycle checkpoint components, thereby promoting S-phase progression in the presence of damage (Sheen et al. 2002; Vafa et al. 2002). This increased replication activity, premature DNA synthesis initiation, and replication in the presence of DNA damage may lead to replication fork stalling /collapse resulting from collisions between the replication and transcription machinery (Branzei et al. 2010), altered availability of dNTPs (Poli et al. 2012), and the collision of replication forks with DNA damage.

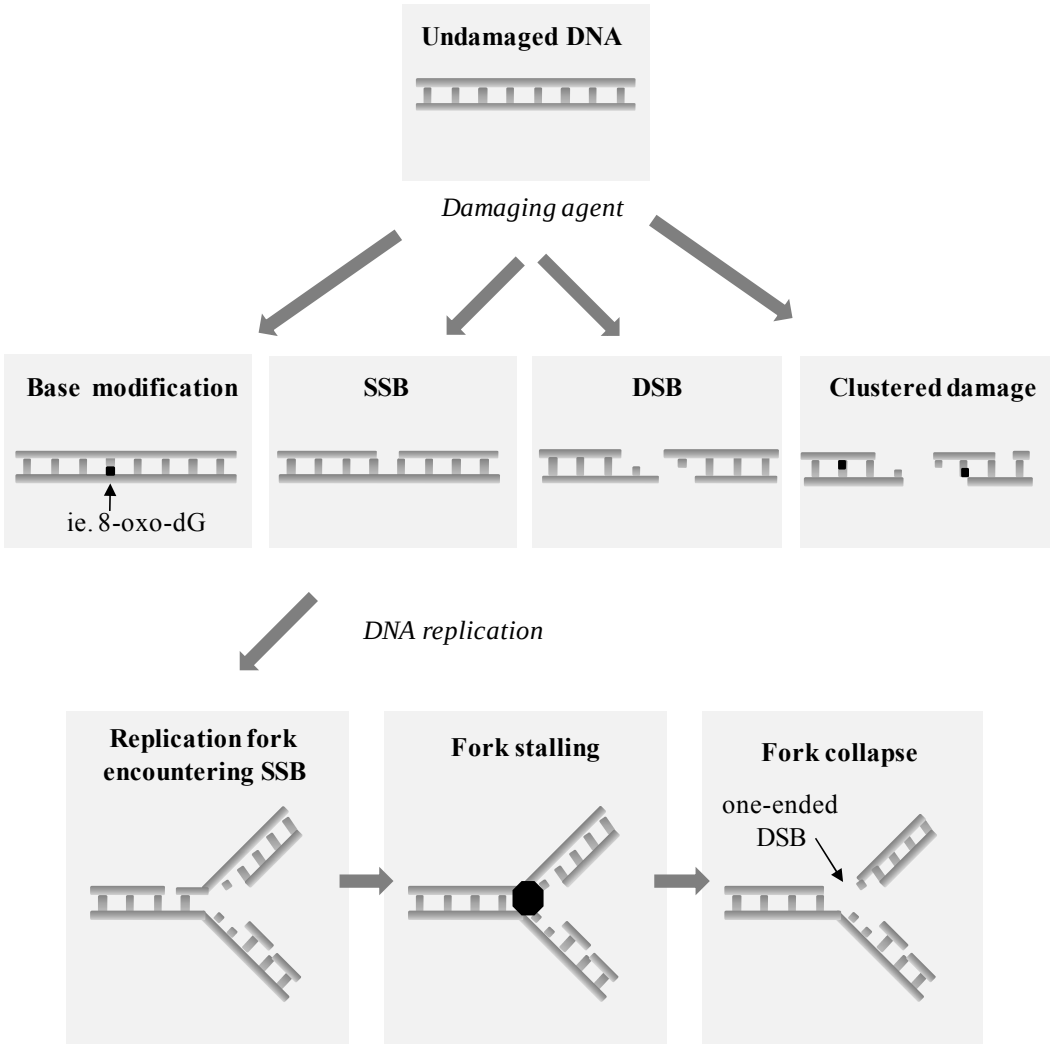

Figure I.1 Forms of DNA damage. Following induction of DNA damage via various sources, as listed in Table I.1, bases may become modified (ie. 8-oxo-dG) (indicated by black square), one strand of the DNA duplex may be severed (SSB), both strands of DNA may break (DSB), or clusters of various types of lesions can occur at the site of damage (clustered damage). If damage such as a SSB persists as a cell undergoes DNA replication, progression of the replication fork may stall (indicated by black octagon). Prolonged replication fork stalling or excessive DNA damage may then lead to collapse of the replication fork, generating a one-ended DSB.

I.3 The response to DSBs during G1 and G2 in the context of chromatin

As previously introduced, the DSB represents one of the most potentially lethal lesions to cells and elaborate molecular pathways have evolved in mammalian cells to respond to this form of damage. Cancer-associated alterations in the DDR to DSBs are thought to contribute to genome instability and cancer development (Khanna et al. 2001). Further, inherited mutations in these crucial mechanisms can lead to various debilitating diseases with symptoms that include cancer predisposition, premature aging, growth retardation, and immunodeficiency (O'Driscoll et al. 2006).

Over the past decade, results from our lab and others have demonstrated that the structural context of DNA at the site of a DSB is crucial in determining which molecular pathway is utilised in repair (Goodarzi et al. 2010). Further, the stage of cell cycle and availability of a homologous DNA template greatly impacts upon pathway selection. The following subsections will introduce mechanisms of DSB repair (Section I.3.1), protein signalling at DSBs (Section I.3.2), the structural organization of DNA (Section I.3.3), and finally, the repair of DSBs in the context of higher order DNA structure and cell cycle phase (Section I.3.4).

I.3.1 DSB repair mechanisms

As depicted in Figure I.2, the mammalian response to DSBs is comprised of two main pathways of repair: non-homologous end joining (NHEJ) and homologous recombination (HR). While NHEJ is an efficient yet potentially error-prone mechanism of repair that does not require a homologous template, HR is a slower repair process which is relatively error-free and utilises a homologous template (typically from the sister chromatid). Alternative end joining pathways have been identified, but their role in the context of a functioning classical NHEJ pathway is not clear.

I.3.1.a Non-homologous end joining (NHEJ)

NHEJ begins when a heterodimeric ring structure composed of the Ku70 and Ku80 subunits bind with high affinity to each end of the DNA at the break site rapidly after damage (Downs et al. 2004) (Figure I.2A). The Ku70/80 heterodimer then recruits the DNA-dependent protein kinase catalytic subunit (DNA-PKcs) to the DNA ends, creating the so-called “DNA-PK holoenzyme”. This results in the functional activation of the DNA-PK protein kinase and may protect and bridge DNA ends (Mahaney et al. 2009). Autophosphorylation of DNA-PKcs at two clustered sites called ABCDE and PQR then follows, ultimately leading to the exposure of DNA termini to other repair factors (Douglas et al. 2002). If the DNA ends are directly compatible,

DNA-PK may dissociate from the break site, allowing for access of a complex containing DNA Ligase 4 (Lig4), X-ray repair cross-complementing protein 4 (XRCC4), and XRCC-like factor (XLF) to Ku-bound ends to perform direct ligation (Goodarzi et al. 2006).

If DNA termini cannot be directly ligated, they must first be processed by various factors. The Artemis endonuclease, which is crucial for removing hairpins generated during V(D)J recombination (Ma et al. 2002) and can process various DNA structures *in vitro* (Ma et al. 2005c), also functions at a subset of DSBs repaired by NHEJ (Riballo et al. 2004; Beucher et al. 2009) (Section III.1.1). Additional processing factors including the Werner syndrome (WRN) helicase, DNA polymerase μ and λ, and polynucleotide phosphatase/kinase (PNK) have also been demonstrated to function in a subset of DSBs (Mahaney et al. 2009). Once ends are processed, ligation can proceed as described above.

I.3.1.b Homologous recombination (HR)

When an undamaged homologous template (a sister chromatid) is available, cells can repair DSBs using HR. The initial phase of HR involves both the recruitment of the Mre11/Rad50/Nbs1 (MRN) complex to both ends of the DSB, which initially tethers the DNA termini for repair, and the resection of DNA ends (Stracker et al. 2011). DNA end resection is promoted and carried out by various factors such as the MRN complex, BRCA1, carboxy-terminal (C-terminal) binding protein interacting protein (CtIP), and BRCA1-associated ring domain protein 1 (BARD1), generating single stranded 3' DNA overhangs (Hartlerode et al. 2009; You et al. 2009). The Artemis endonuclease is required for a subset of DSBs repaired by HR (Beucher et al. 2009) (Section III.1.1), and recent findings from our lab have supported a model in which Artemis functions during end resection in the context of HR. 3' DNA overhangs resulting from resection are immediately coated with replication protein A (RPA) molecules, stabilising the ssDNA structure and allowing HR to proceed (Eggler et al. 2002). RPA is then displaced from DNA overhangs when the Rad51 recombinase is loaded in a BRCA2-mediated process (Venkitaraman 2009), and Rad51 multimers form nucleoprotein filaments which seek homologous segments of intact double-stranded DNA (dsDNA), usually from the sister chromatid (Ogawa et al. 1993). Once this region of homology is identified, the resected strand can invade the dsDNA, forming a DNA joint or a displacement loop (D-loop) structure, and a DNA polymerase can extend the strand, converting the D-loop structure to a Holliday Junction (HJ) (Hartlerode et al. 2009). Capture of the second 3'DNA overhang and subsequent extension forms a double HJ and branch migration can occur which can be resolved by various human proteins such as Bloom syndrome, recQ helicase-like (BLM) helicase or flap endonuclease gen homolog 1 (GEN1) (a homolog of yeast YEN1) (Hartlerode et al. 2009).

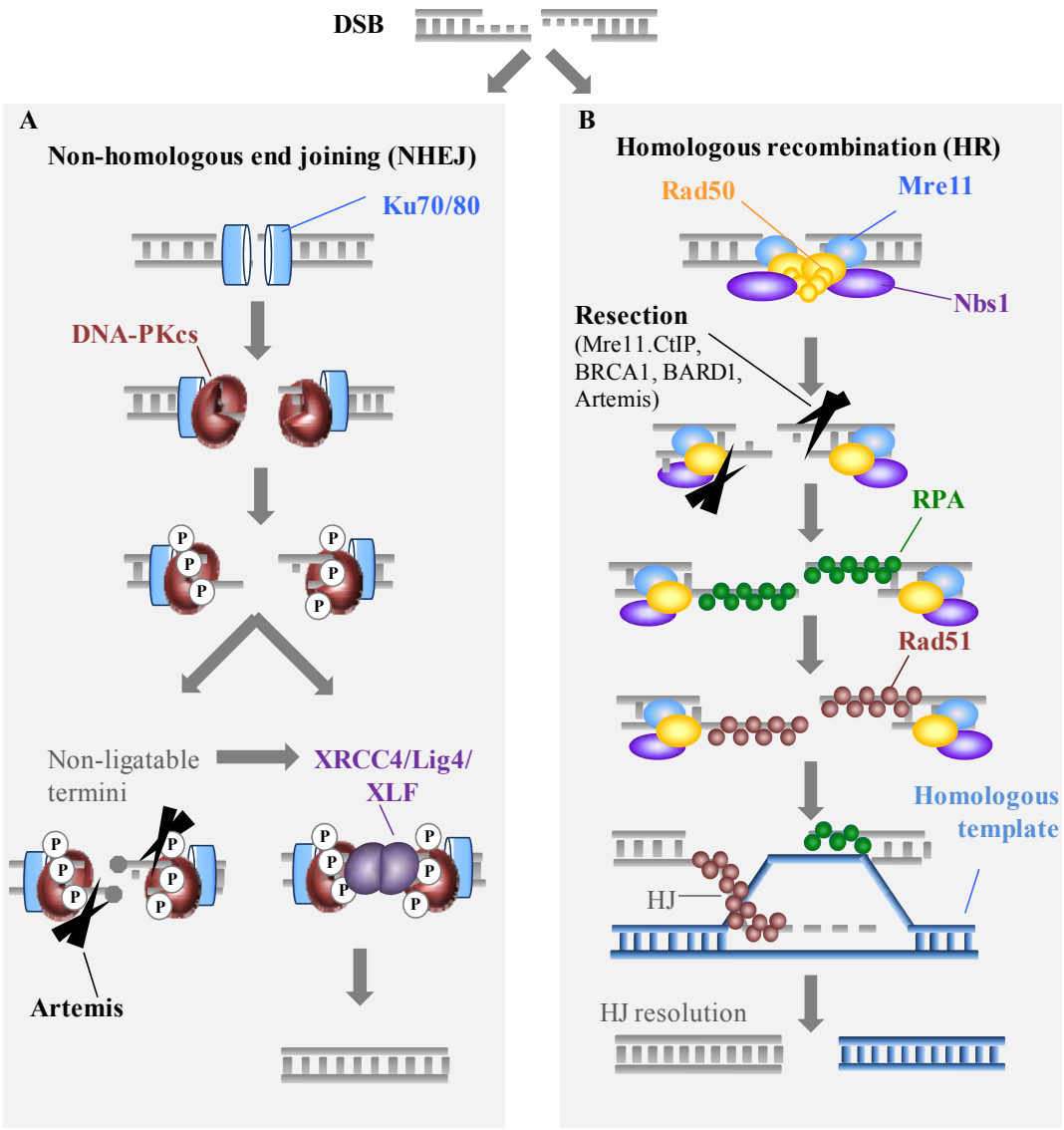

Figure I.2 Overview of the major IR-induced DSB repair pathways. HJ: Holiday junction, P: phosphorylated, see text for protein abbreviations. Following the induction of a DSB by IR, cells respond to damage primarily using either NHEJ or HR. **A**. NHEJ begins with the binding of the Ku70/80 heterodimer to damaged termini. DNA-PKcs is then recruited and autophosphorylated, inducing a conformational change that frees up DNA termini. If ends are not directly compatible for ligation, the Artemis endonuclease can be recruited to process DNA ends. Ligation of ends is completed by the Lig4/XLF/XRCC4 complex. **B**. HR may be initiated upon binding of the MRN complex (Mre11, Nbs1, Rad50) at the site of damage. Various proteins including Mre11, CtIP, BRCA1, BARD1, and Artemis are involved in promoting and carrying out resection of DNA ends, leaving 3' single stranded DNA overhangs which are rapidly coated by RPA molecules. RPA is displaced by Rad51 in a process involving BRCA2. These Rad51 molecules form nucleoprotein filaments that drive invasion of the nascent strand into the homologous duplex DNA. This generates a "D-loop" structure and HJs. The second 3' end is captured and HJs are resolved.

I.3.1.c Alternative non-homologous end joining (alt-NHEJ)

In the absence of canonical NHEJ (c-NHEJ) factors such as the Ku70/80 subunits and the Lig4 or XRCC4 ligases, alt-NHEJ can function to repair DSBs. However, this process may result in large deletions of genetic material (Roth et al. 1986) and chromosomal translocations (Bennardo et al. 2008). The genetic changes introduced by alt-NHEJ may lead to the expression of oncogenes and inhibition of tumour suppressors, therefore implicating the pathway in cancer (Bentley et al. 2004). Alt-NHEJ requires PARP1 for sensing DSBs and relies on short regions of homology that are usually only 5-25 bp long (Wang et al. 2006a; McVey et al. 2008). 5'-3' DNA end resection reveals regions of microhomology upstream and downstream of both ends of the DSB, resulting in the loss of DNA sequence (McVey et al. 2008). Increasing evidence suggests that the CtIP nuclease is involved in the resection step of alt-NHEJ. Depletion of CtIP in mouse cells reduces the frequency of chromosomal translocations and the usage of microhomology at translocation breakpoint junctions, both which are characteristics of alt-NHEJ (Zhang et al. 2011). Following end resection, DNA strands are then aligned and annealed at the regions of microhomology and overhangs are cleaved in a process termed flap trimming (McVey et al. 2008). Ligation can then proceed in a manner most likely dependent on ligase 3 (Lig3) (Wang et al. 2006a).

I.3.2 ATM-mediated DSB signalling

The response to DSBs is mediated by protein signalling at the site of damage. This signalling cascade coordinates the repair of the breaks with arrest of cell cycle progression and, in some cases, cell death. Initiation of this signalling is generally coordinated by the ataxia-telangiectasia mutated (ATM) protein, a 350 kDa (kilodalton) phosphoinositol 3-kinase like kinase (PIKK). ATM regulates various cellular activities via its ability to modify proteins by phosphorylating (transferring PO_4^{3-} groups to) serine or threonine residues on protein substrates (Shiloh 2003).

As depicted in Figure I.3.A, ATM normally exists as a homodimer but monomerises in response to induction of a DSB (ie. following IR) and becomes autophosphorylated on serine 1981 (Bakkenist et al. 2003). Binding of the MRN complex to DNA ends promotes recruitment of activated ATM to the site of damage via the C-terminus of Nbs1 (Falck et al. 2005; You et al. 2005) (Figure I.3.B). Activated ATM can then phosphorylate the histone variant H2AX (Section I.3.3), at serine 139, generating the form of H2AX referred to as γH2AX. H2AX can also be phosphorylated at serine 139 by DNA-PKcs in the response to IR, and by the ataxia-telangiectasia and Rad3-related (ATR) kinase in the response to replication stress (Ward et al. 2001; Stiff et al. 2004). The rapid assembly and subsequent spreading of γH2AX molecules at the site of a single IR-induced DSB generates a focus which can be visualised using immunofluourescence protein labelling and microscopic detection (Lobrich et al. 2010). The

enumeration of these γH2AX foci and analysis of their disappearance over time provides a valuable method to monitor the repair of DSBs which has been exploited in several sections of this thesis.

While the initial assembly of γH2AX molecules is not exclusively required for the recognition of DSBs, it is required to further promote the formation of ionizing radiation-induced foci (IRIF) and the subsequent recruitment of other DSB signalling proteins (Celeste et al. 2003). Following γH2AX foci formation at break sites, the adaptor protein mediator of DNA damage protein 1 (MDC1) is recruited to DNA. MDC1 contains an amino-terminal (N-terminal) forkhead-associated (FHA) domain, a central proline- serine- and threonine-rich repeat (PST repeat), and tandem BRCA1 C-terminus (BRCT) domains (Stewart et al. 2003; Coster et al. 2010). Via its BRCT domains, MDC1 directly interacts with γH2AX, thereby facilitating its recruitment (Stucki et al. 2005). Additionally, the FHA and BRCT domains also found in Nbs1 interact with MDC1, further promoting recruitment and retention (Figure I.3.C). The recruitment of MDC1 promotes further accumulation and amplifies the ATM-mediated tethering at DSBs (Figure I.3.D).

Next, an additional wave of ATM tethering is induced by the recruitment and accumulation of other proteins including p53 binding protein 1 (53BP1) and the E3 ubiquitin (ub)-protein ligases, ring finger protein 8 (RNF8) and ring finger protein 168 (RNF168). RNF8 is recruited to DSBs via an association with the N-terminal FHA domain of MDC1 and subsequently generates K63-linked ub chains on nearby H2A and H2AX histones (Huen et al. 2007; Mailand et al. 2007). RNF168 then binds these ub chains and propagates further K63-linked ubiquitination (Stewart et al. 2009), altogether facilitating chromatin relaxation. While 53BP1 does not appear to directly bind ub chains, its tandem tudor domains have been reported to bind methylated residues on histone proteins (Huyen et al. 2004; Botuyan et al. 2006). Ub-mediated chromatin relaxation may expose these residues, thereby promoting 53BP1 recruitment (FitzGerald et al. 2009).

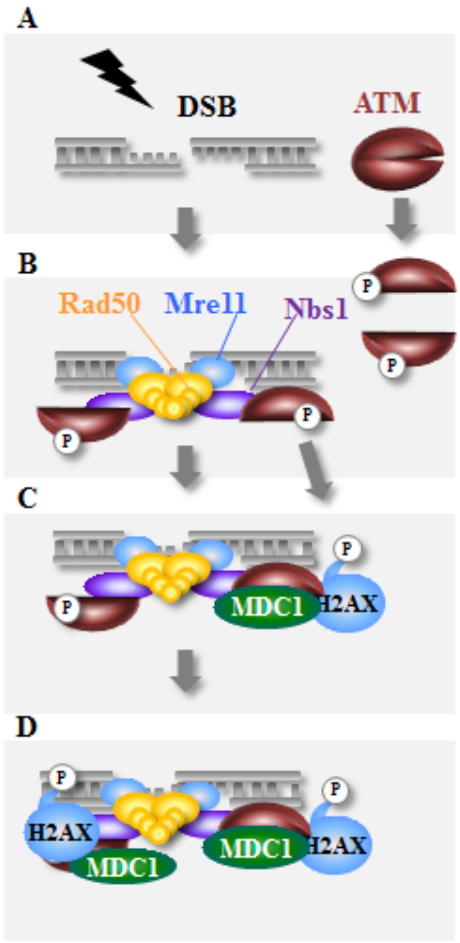

Figure I.3 Initial ATM-mediated signalling at DSBs. P: phosphorylated. **A.** ATM normally exists as a homodimer but becomes monomerised and autophosphorylated at serine 1981 following induction of a DSB (ie. from ionizing radiation). **B.** Rad50, Mre11, and Nbs1 rapidly bind and tether DSB ends and ATM gets recruited to the site via an interaction with the c-terminus of Nbs1. **C.** Next, activated ATM phosphorylates H2AX on serine 139 (γH2AX), which can interact with the BRCT domains of MDC1. MDC1 also interacts with the FHA and BRCT domains of Nbs1. **D.** Finally, accumulation of γH2AX and MDC1 further amplifies DSB signalling.

I.3.3 Chromatin organization and structure

The human genome encompasses a vast amount of DNA, comprising up to a total of 6 billion bp in diploid cells, which would encompass a distance of 2 meters if stretched linearly. This large amount of genetic material must be compacted to fit within the nucleus, which typically has a diameter of less than 10 micrometers. In order to achieve this, DNA must be packaged and organised into several layers of higher-order structure, as depicted in Figure I.4.

The first level of DNA packaging begins with the nucleosome, a structure containing 146 bp of the DNA helix wrapped around an octamer of histone proteins H2A, H2B, H3, and H4 (Luger et al. 1997) (Figure I.4.A). These four core histone proteins are highly conserved throughout evolution and also share a high degree of sequence and structural similarity (Baxevanis et al. 1996). Histones H2B, H3, and H4 form positively charged alpha helices, allowing for a strong interaction with negatively charged sugar- phosphate backbone of DNA. Each of the histone proteins has a highly flexible and accessible tail extending from the N-terminus which can contribute to the dynamic structural properties of chromatin. Histone tails may be altered by post-translational modifications (PTMs) including phosphorylation (addition of PO_4^{3-}), acetylation (addition of $COCH_3$), methylation (addition of CH_3), ubiquitination (addition of the ubiquitous immunopoietic polypeptide), SUMOylation (covalent attachment of small ubiquitin-like modifier (SUMO)), and ADP-ribosylation (transfer of ADP-ribose chains) (Sims et al. 2003) (Table I.2). PTMs of histone tails can impact upon various cellular processes involving DNA including transcription, chromosome segregation, and recombination. Additionally, modifications on histone tails function in DNA damage signalling, remodelling, and repair, as will be discussed in more depth below. These modifications may be transient events or heritable epigenetic changes which are passed to daughter cells (Delcuve et al. 2009).

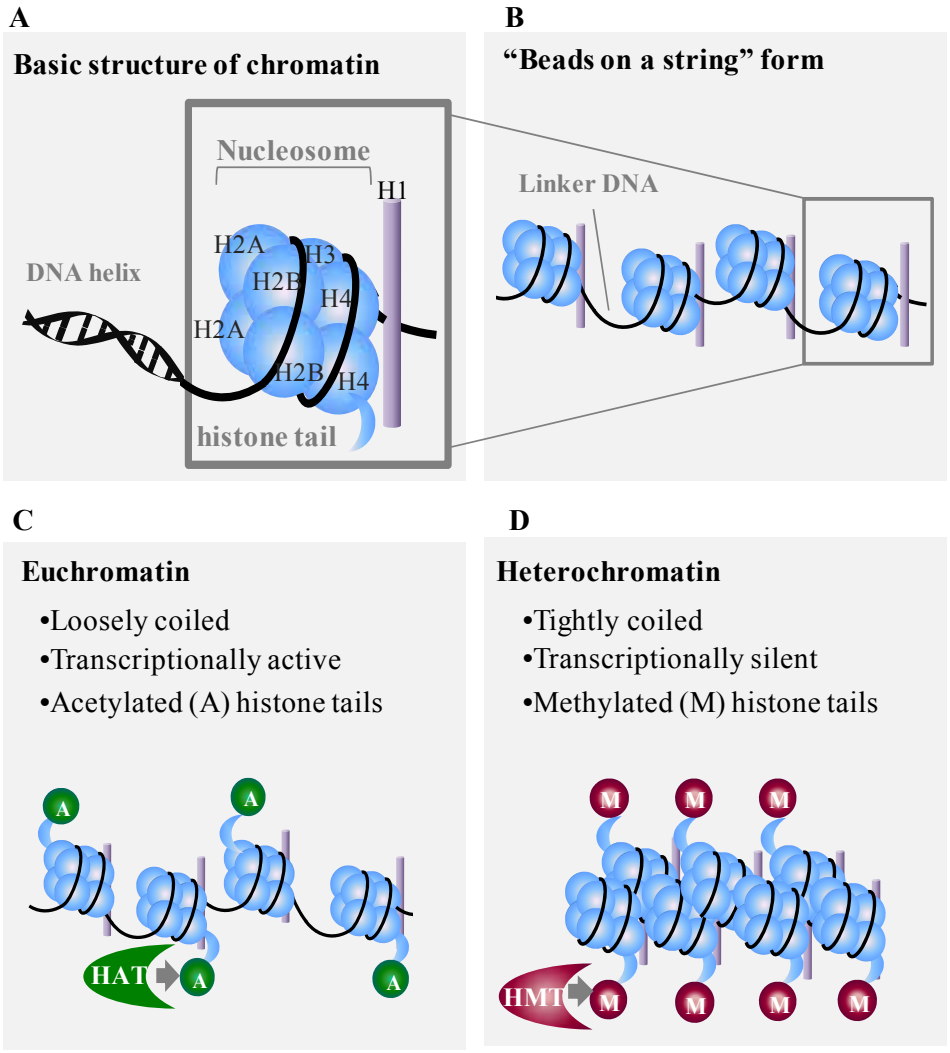

Figure I.4 The basic structure of chromatin. A. On the first level of chromatin structure, the DNA double helix is found wrapped around an octamer of the core histone proteins (H2A, H2B, H3, and H4), together making up the nucleosome. The core histones each contain highly accessible tails which can be altered by PTMs such as acetylation and methylation. The histone H1 protein binds nucleosomes and exiting DNA, locking the structure together. **B.** Repeating units of nucleosomes, separated by "linker DNA" form a structure likened to "beads on a string." Nucleosomes are locked into place by the histone H1 protein. **C-D.** Chromatin can be found to be packaged either in the form of euchromatin (C), a loosely condensed and generally transcriptionally active state in which histone tails are often acetylated by a histone acetyltransferase (HAT), or in the form of heterochromatin (D), a more compact and generally transcriptionally silent state in which histone tails may be methylated by a histone methyltransferase (HMT).

Histone	Residue	PTM
H2A	S1	p
	K5	ac
	K9	ac
	R11	me
	K13	adp
	R29	me
	K119	ub
	K120	p
H2AX	K5	ac
	K119	ub
	S139	p
	Y142	p
H2B	K5	ac
	K12	ac
	S14	p
	K15	ac
	K20	ac
	K30	adp
	K120	ub
H4	S1	p
	R3	me
	K5	ac
	K8	ac
	K12	ac
	K16	ac/adp
	K20	me
	K91	ac/ub

Histone	Residue	PTM
H3	R2	me
	T3	p
	K4	ac/me
	T6	p
	R8	me
	K9	ac/me
	S10	p
	T11	p
	K14	ac
	R17	me
	K18	ac
	K23	ac
	R26	me
	K27	ac/me/adp
	S28	p
	K36	ac/me
	K37	adp
	Y41	p
	T45	p
	K56	ac
	K79	me

Table I.2 Common histone modifications. S: serine, K: lysine, R: arginine, Y: tyrosine, T: threonine, p: phosphorylation, ac: acetylation, me: methylation, adp: adenosine diphosphate ribosylation, ub: ubiquitination, su: SUMOylation, (reviewed in (Sims et al. 2003; Bhaumik et al. 2007)).

Histone H2A, which forms a dimer with H2B, may consist of several variants including H2A.1, H2A.2, H2AX, or H2A.Z, which differ by only a small number of amino acids (aa). Following DSB induction, H2AX is phosphorylated at serine 139, a modification known as γ-H2AX which functions in the DDR (Section I.3.2) (Rogakou et al. 1998). When H2A is replaced the H2A.Z variant, as observed in nucleosomes adjacent to transcriptional start sites, stability of the dimer formed with H2B is lowered, therefore impacting upon higher order chromatin structure. (Suto et al. 2000; Placek et al. 2005; Gamble et al. 2010). Another variant of H2A, macroH2A, has been identified in nucleosomes on the inactivated X-chromosome in female mammals and in various regions on other chromosomes. Replacement of H2A with macroH2A can have either a positive or negative impact on transcription (Gamble et al. 2010).

Nucleosomes are linked together by Histone H1 to form a structure likened to "beads on a string," with up to 80 bp of linker DNA connecting the nucleosomes and contributing to stability of the structure (Figure I.4.B). The linked nucleosomes and histone H1 are then further organised into 30 nm fibres or filaments (Finch et al. 1976) which are thought to be a dynamic structure that may stretch to a loosely packed structure known as euchromatin during active transcription (Figure I.4.C). In euchromatin, histone tails can be found to be acetylated at lysine residues including lysines 9, 14, 18, 23 of histone H3, lysines 5, 8, 12, 16 of H4, lysines 5 and 9 of H2A, and on lysines 5, 12, 15 and 20 of H2B (Sims et al. 2003). The addition of acetyl groups by proteins known as histone acetyltransferases (HATs) lowers the positive charge involved in the tight interaction with DNA, therefore partially disrupting the N-terminal interaction with DNA and relaxing chromatin structure.

Alternatively, chromatin can be found in a form known as heterochromatin which plays a structural role and functions in the silencing of gene expression (Figure I.4.D). Histones in heterochromatin regions may be found to be mono-, di-, or tri-methylated on arginine or lysine residues including lysines (K) 4, 9, 27, 36, or 79 on H3 and K20 on histone H4 (Table I.2) (Sims et al. 2003). Histone methylation, a form of alkylation, involving the transfer of methyl (CH_3) groups from S-adenosyl methionine to histones, occurs via the histone methyltransferases (HMTs). Unlike the case with acetylation, methylation of histone tails does not function to modify the charge of the histones at the DNA binding site, but rather serves to "mark" regions of chromatin, allowing for protein binding and facilitating downstream heterochromatin building events.

In mammals, DNA may also be methylated, primarily at cytosine-phosphate-guanine (CpG) dinucleotides by DNA methyltransferases (DNMTs). DNMTs transfer methyl groups directly to the 5 position of the aromatic ring of cytosine, generating 5-methylcytosine. Between 70 and 80% of the CpG dinucleotides in the human genome are found to be methylated, and this essential modification has been shown to contribute to heterochromatin reorganisation,

imprinting, development, and inactivation of the X-chromosome (Jabbari et al. 2004; Ma et al. 2005a).

Heterochromatin may be found either in its constitutive form, a stable structure which remains compacted throughout various stages of cell development, or in its facultative form, which may be reversed under certain conditions, allowing for decondensation and transcriptional activity.

Regions of the genome such as centromeres and telomeres containing repetitive segments known as satellite DNA are found as constitutive heterochromatin. Organisation of heterochromatin in centromeric regions, in which nucleosomes are found to contain the histone H3 variant centromere protein A (CENPA), is crucial for proper chromosome segregation and chromosome assembly (Palmer et al. 1987; Dimitri et al. 2009). Constitutive heterochromatin can also be found at telomeres, where the compaction of chromatin plays a role in protection of chromosome ends along with other telomeric functions (Schoeftner et al. 2009).

Facultative heterochromatin has been observed to be important in regulating the expression of ribosomal DNA (rDNA), which codes for the RNA component of the ribosome. As described in more depth in Section III.1.3, rDNA, which is organised into clusters of tandem repeats in nucleoli, is under tight transcriptional regulation corresponding to the cellular requirement for ribosome generation. While actively transcribed regions of rDNA contain euchromatic histone modifications including acetylation of H3 and H4, silenced rDNA regions contain methylated H3 tails (Grummt et al. 2008). Acetylation specifically on lysine 9 of H3 (H3-K9) has been observed to be replaced by methylation under conditions of nutrient deficiency (in which ribosome synthesis shuts down). This exchange of an acetyl group for methyl groups on H3-K9 occurs via a process involving the energy-dependent nucleolar silencing complex (eNoSC), the sirtuin 1 (SIRT1) deacetylase, and the histone methyltransferase, suppressor of variegation 3-9 homolog 1 (SUV39H1) (Grummt et al. 2008).

Another example of facultative heterochromatin is the inactivation of the X chromosome (or lyonisation) which generates the Barr body in female mammals and allows for equalisation of the amount of gene expression between the sexes. The inactivated X chromosome contains uniformly distributed markers of heterochromatin such as methylated H3-K9 and lacks the acetylated forms of histones found in euchromatin (Wutz 2011).

The assembly of heterochromatin occurs over various stages, as illustrated in Figure I.5. Transcriptional silencing begins with the transcriptional repressors which bind DNA, often via a zinc finger motif (Craig 2005). Passive repressors work indirectly, either by blocking activity of transcriptional activators or by inhibiting access of activators to DNA. Active repressors can function over long distances of DNA and work to actively target regions of the genome for heterochromatin formation. The active repressor methyl CpG binding protein 2 (MECP2), for example, can be recruited to sites of methylated CpG dinucleotides in promoter regions, leading

to recruitment of the histone deacetylase (HDAC) proteins to remove acetyl groups from histone tails (Thiel et al. 2004).

Many repressors do not function independently in silencing, instead working by recruiting co-repressors such as kruppel associated box domain (KRAB) associated protein 1 (KAP-1). KAP-1 binds DNA via its zinc-finger containing KRAB (Figure I.5.A) and becomes SUMOylated in a process facilitated by its C-terminal plant homeo domain (PHD) and its bromodomain, which recognises acetylated lysines (Zeng et al. 2008) (Figure I.5.B). This SUMOylation allows for KAP-1 to act as a molecular scaffold in heterochromatin building. The SUMOylated form of KAP-1 recruits the Mi-2/ nucleosome remodelling and deacetylase (Mi-2/NuRD) complex which includes the chromodomain helicase DNA binding proteins 3 and 4 (CHD3 and CHD4), also known as Mi-2α and Mi-2β, respectively, as well as the histone deacetylase protein 1 (HDAC1) and histone deacetylase protein 2 (HDAC2) (Xue et al. 1998; Denslow et al. 2007). This unique and abundant complex coordinates the disruption of nucleosomes with the removal of acetyl groups from lysines on histone tails, therefore remodelling DNA (Xue et al. 1998; Denslow et al. 2007).

As previously introduced, lysines on histone tails are usually found to be methylated in heterochromatin. SUMOylated KAP-1 binds the methyltransferase, SET domain bifurcated 1 (SETDB1), which deposits methyl groups onto lysine 9 of histone H3 (Schultz et al. 2002). In addition to SETDB1, SUV39H1 and SUV39H2 are among other lysine methyltransferases that work to enhance chromatin compaction (O'Carroll et al. 2000).

Chromatin compaction is stabilised by chromodomain adaptor proteins such as the heterochromatin protein 1 (HP1) family. This family of adaptors, also known as chromobox homolog, or CBX, includes three paralogs in humans, known as HP1α, HP1β, and HP1γ. Unlike HP1α and HP1β, HP1γ can also be found in regions of euchromatin in mammalian cells (Minc et al. 2000). HP1α/β/γ each contain an N-terminal chromodomain, a highly conserved motif found in chromatin remodelling proteins, a chromoshadow domain near the C-terminus, and a highly flexible hinge region linking the domains together (Paro et al. 1991; Aasland et al. 1995). The chromoshadow domain of HP1 directly interacts with KAP-1, via a PxVxL motif on KAP-1, facilitating the binding of HP1 to methylated histone tails (Sripathy et al. 2006) (Figure I.5.C). HP1 forms homodimers which bridge adjacent nucleosomes together, locking them into place. In addition to binding to methylated lysines, dimerized HP1 also further promotes HDAC and SUV39H recruitment, which further contributes to heterochromatin spreading (Craig 2005). Additional interactions and functions of HP1 will be described in more detail in Chapter V.

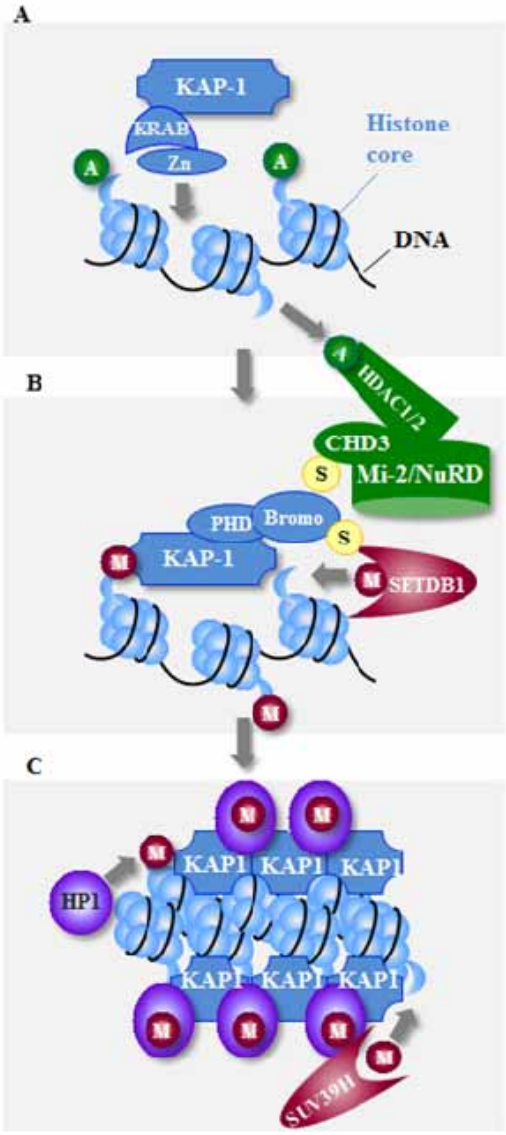

Figure I.5 Heterochromatin building. A: acetyl group, S: SUMO, M: methyl group **A**. Transcriptional silencing can commence with repressors which bind to DNA regions and recruit corepressors like KAP-1. KAP-1 can bind acetylated euchromatin via zinc finger (Zn) in its KRAB domain. **B**. SUMOylation of KAP-1 on its PHD-Bromo domain recruits the Mi-2/NurD complex, which includes deacetylation activity via HDAC1/2 and nucleosome disruption via CHD3. In addition, the methyltransferase SETDB1 can bind SUMOylated KAP-1 and transfer methyl groups to histone tails. **C**. The adaptor protein HP1 is recruited via interactions with KAP-1 and methylated lysine tails of histones. HP-1 promotes further methylation by the SUV39H methyltransferase and stabilises compaction.

I.3.3.a Heterochromatin and cancer

Heterochromatin plays an important role in the maintenance of genome stability, and changes in heterochromatin formation have been identified in various types of human cancer.

Distinct regions of facultative heterochromatin termed senescence associated heterochromatin foci (SAHF) have been identified in various types of human cells upon undergoing irreversible arrest of cell cycle (senescence) (Narita et al. 2003). SAHF formation, which ultimately contributes to gene silencing, has been demonstrated around genes which promote cellular proliferation, reflecting a role of SAHF in senescence, tumour suppression, and aging (Zhang et al. 2007).

Changes in transcriptional silencing have been reported in BRCA1-deficient breast cancer and one model proposes that BRCA1-dependent tumour suppression occurs via heterochromatin-mediated transcriptional silencing. In a recent study conducted by Zhu and colleagues, the targeted deletion of BRCA1 in mice was reported to result in a reduced number and more diffused appearance of chromocentres in neurons, suggesting that BRCA1 loss alters heterochromatin organisation (Zhu et al. 2011). Further, these authors reported that the expression of satellite repeat DNA regions, which is normally repressed by heterochromatin-mediated transcriptional silencing, was enhanced in cells from mouse or human breast tumours deficient in BRCA1 (Zhu et al. 2011). As the ectopic expression of satellite DNA was observed to induce genomic instability in human mammary cells, the authors of this study proposed that BRCA1-dependent heterochromatin-mediated transcriptional repression prevents genome instability and tumourigenesis. Further, the ubiquitin ligase activity of BRCA1 was suggested to be involved in this role in heterochromatin. In support of this notion, BRCA1 was found to be required for the enrichment of ubiquitinated histone H2A at satellite regions and the ectopic expression of H2A-ub in BRCA1-deficient human breast cancer cells restored the transcriptional silencing of satellite DNA and other cellular features associated with BRCA1 deficiency. In summary, BRCA1-mediated ubiquitination of histone H2A and subsequent heterochromatin-mediated transcriptional silencing at satellite regions has been proposed to promote genome stability and tumour suppression.

Changes in the expression and function of the heterochromatin protein HP1 have also been associated with metastasis in breast cancer (Kirschmann et al. 2000). Studies from *Drosophila melanogaster* demonstrated that while a complete loss of HP1 leads to lethality, heterozygous mutants survive and display an increase in euchromatin-like structures. Overexpression of HP1 leads to increased transcriptional silencing, consistent with heterochromatin formation (Eissenberg et al. 1990; Kirschmann et al. 2000). The role of HP1-dependent heterochromatin building in tumour suppression is complex and thought to involve centromere segregation, telomere end protection, and transcriptional regulation (Dialynas et al.

2008). In addition, HP1 appears to play a role in the response to localised DNA damage. HP1α has been reported to localise to the sites of DSBs induced by laser irradiation. Depletion of HP1α in human osteosarcoma cells leads to impaired recruitment of KAP-1 and 53BP1 to sites of laser-induced damage and decreased cell survival in response to γ-irradiation, presumably as a result of accumulating DSBs (Baldeyron et al. 2011). In cellular contexts of reduced HP1 levels, defective repair of DSBs may contribute to instability, ultimately resulting in tumourigenesis.

I.3.4 DSB repair in G1 and G2

Over the past decade, results from our lab and others have demonstrated that the structural context of DNA at the site of a DSB is crucial in determining DNA repair pathway selection (Goodarzi et al. 2010). Given the compact nature of heterochromatin, it is perhaps unsurprising that this chromatin superstructure impacts upon DNA repair. Interestingly, the repair of IR-induced DSBs during the Gap1 (G1) and Gap2 (G2) stages of the cell cycle occurs with two distinct phases of kinetics which have been shown to correspond with the two main forms of chromatin structure. The proper execution of slow and fast repair has been shown to involve distinct sets of proteins.

As previously mentioned, IR-induced DSBs can be monitored by immunofluorescence labelling and enumeration of γH2AX foci. Following irradiation of cells, γH2AX foci rapidly accumulate in cell nuclei. While some repair is likely to occur within the first 15-30 minutes after damage, assessment of the induction of breaks is commonly examined 30 minutes post IR (Lobrich et al. 2010) (Figure I.6A). Monitoring of the reduction in the number of foci over time enables assessment of DSB repair. In both G1 and G2, between 75 and 90% of the DSBs induced are repaired with rapid kinetics over the course of the first several hours (Figure I.6B). Examination of the overlap of γH2AX foci with chromocentres (which can be visualised by immunofluorescence as regions with intense 4',6-diamidino-2-phenylindole (DAPI) staining) have shown that these rapidly-repaired breaks are generally localised to euchromatic regions of DNA in which genetic material is more accessible to repair proteins (Goodarzi et al. 2010). The remaining fraction of DSBs induced (10-25%) is repaired with a significantly slower rate of repair (generally after 8 hours post IR) and these DSBs localise to regions of chromatin compaction (heterochromatin). Depletion of c-NHEJ factors such as Ku70/80, DNA-PKcs, and the Lig4/XLF/XRCC4 complex leads to defects in both fast and slow repair (Figure I.6B). However, defects exclusively in the slow repair of breaks have been observed in cells depleted for ATM-mediated signalling factors or the Artemis endonuclease. In cells lacking ATM itself, the MRN complex, H2AX, the mediator proteins (53BP1, RNF8, MDC1, RNF168), or Artemis, 15-20% of induced lesions persist for days, and in some cases over a week (Riballo et al. 2004;

Goodarzi et al. 2008; Goodarzi et al. 2010; Noon et al. 2010) (Figure I.6B). The defective repair observed in cells with deficient ATM-mediated signalling can in fact be alleviated if heterochromatin is disrupted, for example, via depletion of or a deficiency in KAP-1, HDAC1/2, HP-1, MeCP2, SETDB1, Suv39H1/2, and DNMT3B (Goodarzi et al. 2008; Brunton et al. 2011). This reflects the fact that ATM-mediated signalling is required to reduce chromatin compaction, therefore enabling access of repair proteins to DNA.

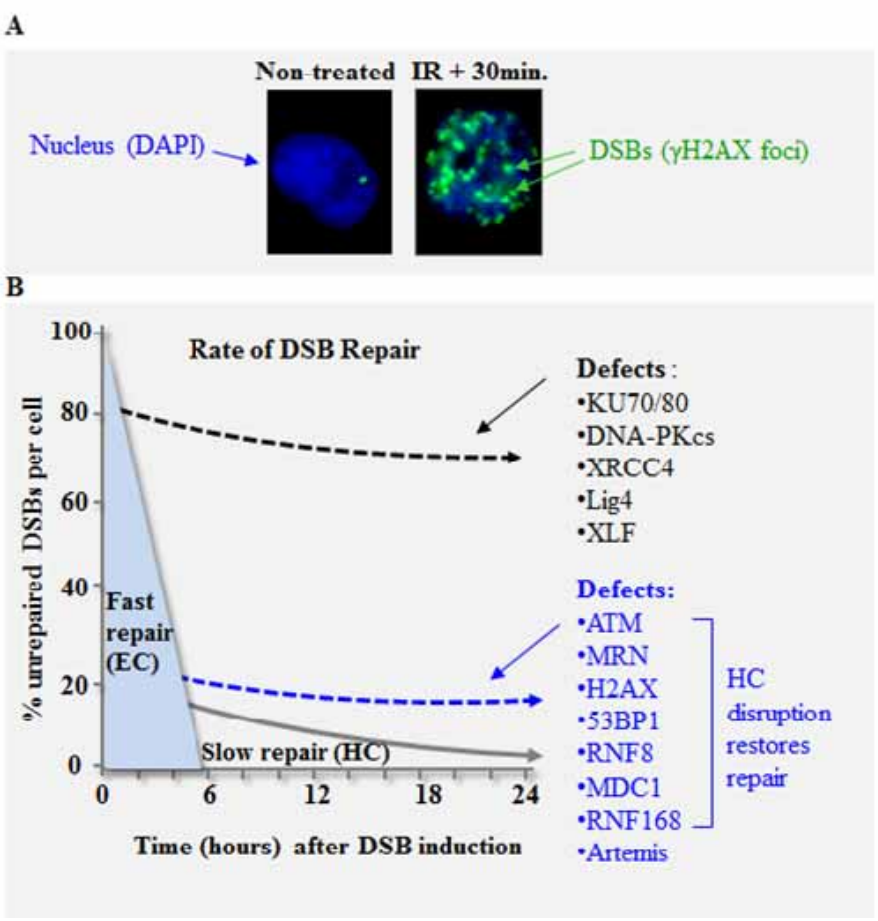

Figure I.6 DSB detection and kinetics of repair in G1 and G2. EC: euchromatin, HC: heterochromatin **A**. DSB induction may be monitored in nuclei 30 minutes following ionizing radiation (IR) using immunofluorescence labelling of γH2AX foci. **B**. The rate of DSB repair can be assessed by following the loss of γH2AX foci over time. DSB repair in G1 and G2 consists of a phase of fast repair at EC and of a slow repair phase at HC. Defects in NHEJ machinery lead to ineffective fast and slow repair whereas defects in ATM signalling proteins and in the Artemis endonuclease prevent the slow phase of repair. Defects in slow repair can be restored if heterochromatin is disrupted (Goodarzi et al. 2010; Lobrich et al. 2010).

Localised decondensation of heterochromatin at the site of a DSB is facilitated by ATM-dependent phosphorylation of the co-repressor KAP-1 on serine 824 (Ziv et al. 2006; Goodarzi et al. 2008). The role of the mediator proteins such as 53BP1, RNF8, MDC1, and RNF168 in heterochromatic DSB repair is thought to be related to concentrating and retaining ATM activity at the site of the break, thereby promoting modifications in chromatin and allowing for repair (Noon et al. 2010). ATM-dependent phosphorylation of KAP-1 has been proposed to create a structure which interferes with the interaction between the SUMO modification of KAP-1 and the CHD3 subunit of the Mi2-NuRD complex. This disruption of the interaction is thought to lead to the localised dispersal of CHD3 from chromatin, therefore disturbing heterochromatin structure and enabling repair (Goodarzi et al. 2011).

While epistatic studies have shown that the Artemis endonuclease and ATM function in the same pathway of slow DSB repair, the role of Artemis seems to be distinct from the role of ATM (Beucher et al. 2009). Given the protein's endonucleolytic processing capacity, one model presented has proposed that Artemis is required to cleave secondary structures that can arise when a DSB occurs in a highly repetitive region of DNA. Recent emerging data has indicated that Artemis plays an important role in DNA end resection, the initial process in HR and alternative end-joining. The structure and functions of Artemis will be introduced in Chapter III.

Further investigation of the fast and slow repair processes has revealed distinctions in repair pathway choice that depend on the stage of cell cycle. Given the absence of a homologous template from a sister chromatid during G1 (and Gap 0 phase, also known as G0), nearly all DSBs occurring in cells in these stages of the cell cycle are repaired using NHEJ. During G1, most DSBs are repaired with NHEJ using rapid kinetics. However, DSBs occurring within heterochromatin regions in G1 are repaired with a slower component of end joining which requires processing by the Artemis endonuclease (Beucher et al. 2009).

Despite the presence of homologous sister chromatids in G2, most DSBs in this phase are also repaired rapidly by NHEJ. However, unlike the case during G1, the slow component of repair during G2 utilises HR. Cells deficient in components exclusively required for HR such as BRCA2 or Rad51 therefore display a defect specifically in the slow component of repair during G2 (Beucher et al. 2009). The requirement for ATM-mediated signalling is observed in both G1 and G2, indicating the fact that heterochromatin decondensation resulting from ATM-dependent phosphorylation of KAP-1 occurs upstream of DSB repair.

I.4 The response to DNA damage occurring during replication

The avoidance of genomic instability in normal dividing cells requires both accurate duplication of genetic material as well as proper segregation of duplicated chromosomal DNA to the two progeny cells. Additionally, cells must be able to correctly repair any damage to DNA that can

occur from endogenous or exogenous sources to ensure that the fidelity of the genome is maintained. Erroneous DNA replication, chromosome mis-segregation, or defective repair of damaged DNA can lead to malignancies detrimental to survival, and therefore organisms have evolved vital systems to execute such tasks accurately. Elaborate molecular machines exist which precisely regulate the initiation of replication at DNA origins, progression through replication, DNA proofreading, cell cycle timing, sister chromatid separation, and, as introduced in earlier sections, the repair of breaks or deleterious modifications to DNA.

This section will introduce the regulation of DNA replication (Section I.4.1), DDR protein signalling in response to replication stress (Section I.4.2), and the activation of excess (also referred to as dormant) DNA replication origins in response to replication stress (Section I.4.3).

I.4.1 Regulation of DNA replication

Regulation of the initiation, progression, and completion of DNA replication is carried out by a host of proteins, many of which are essential to survival.

I.4.1.a The nature of replication origins

Duplication of the genome begins at DNA sequences known as replication origins. The nature of these origin sequences is varied across species. In bacteria containing a single circular DNA molecule, only one origin is needed to successfully replicate the genome. However, in eukaryotic cells, which contain linear chromosomes and larger genomes, multiple origins must fire to duplicate DNA in a timely fashion. In *Saccharomyces cerevisiae* (*S. cerevisiae*) budding yeast, origins are located in autonomously replicating sequence (ARS) elements, specific sequences rich in adenine and thymidine which are capable of replicating plasmid DNA when inserted into a vector (Stinchcomb et al. 1979; Rehman et al. 2009).

In higher eukaryotes, the locations of replication origins have proven more difficult to define. No known origin consensus sequence exists in mammalian cells, and studies have demonstrated that human licensing factors are able to functionally bind to DNA sequences indiscriminately (Schaarschmidt et al. 2004). Over the course of an unchallenged S-phase, activation of 30,000 -50,000 origins spaced ~100 kilobases (kb) apart (Huberman et al. 1966; Huberman et al. 1968) enables replication of the entire mammalian genome (Mechali 2010). Analysis of origin activation has demonstrated that replication in mammalian cells may be initiated from clusters of origins in ~1-50 kb zones termed replication or initiation zones (Little et al. 1993; Dijkwel et al. 1995; Kamath et al. 2001).

While mammalian origins are not characterised by any single consensus sequence, correlations have been observed between origin location and chromatin architecture (Alabert et

al. 2012). Active replication involves the disruption of nucleosomes ahead of replication forks, and consequently, active origins of replication have been observed in regions of low nucleosome occupancy (Gruss et al. 1993; Cayrou et al. 2011; Lubelsky et al. 2011).

Studies in *Xenopus* (Danis et al. 2004), *Drosophila* (Aggarwal et al. 2004), and human cells (Lucas et al. 2007) have demonstrated that histone modifications impacting upon the higher-order structure of chromatin play a significant role in origin determination (Zhou et al. 2005; Alabert et al. 2012). Interestingly, genomic mapping of mammalian replication origins has revealed that origin density correlates with guanine and cytosine - rich promoter regions such as CpG islands (Necsulea et al. 2009; Sequeira-Mendes et al. 2009). Activation of the 30,000-50,000 origins does not occur synchronously during S-phase, as some origins fire specifically during the early stages of S-phase and others fire only at later stages. As is the case with transcriptional activation, the regulation of the timing of origin firing has been proposed to involve heterochromatin formation. Studies examining the activity of CpG island-associated origins on the active and silent X-chromosome have demonstrated that the replication of regions surrounding methylated (and transcriptionally silenced) regions occurs later in S-phase. Conversely, unmethylated CpG islands fire early in S-phase (Gomez et al. 2004).

Importantly, multiple protein interactions between replication and heterochromatin factors have been identified. These interactions and potential implications will be discussed in more detail in Section I.5 and Chapter V.

I.4.1.b Origin licensing

Prior to firing during S-phase, origins of replication must first be licensed in a process that begins in the late stages of mitosis-phase (M-phase) and early G1-phase and involves the pre-replication complex (pre-RC) of proteins. Licensing begins in late M-phase with the binding of a complex of proteins known as the origin recognition complex (ORC) (Figure I.7.A). The interaction of ORC with chromatin was recently shown to be mediated, in part, by direct binding of ORC1 with Histone H4 dimethylated on K20 (H4K20me2) (Kuo et al. 2012) and may also be facilitated by interactions between ORC components and chaperone proteins. Following ORC recruitment, the cell division 6 (CDC6) and Cdc10 dependent transcript 1(CDT1) proteins localise to ORC-bound DNA (Figure I.7.B). This facilitates chromatin loading of the minichromosome maintenance (MCM) helicase complex to CDC6-, CDT1-, and ORC-bound DNA, altogether forming the pre-RC (Figure I.7.C)**.** CDC6 and CDT1 are released from the pre-RC, which helps to prevent re-licensing of the same origin. Cyclin dependent kinase 2 (Cdk2) and cell division 7(Cdc7) promote the recruitment of cell division control 45 (Cdc45) and the Go, Ichi, Nii, San (GINS) complex (Figure I.7.D**)** and the subsequent initiation of origin firing. Following activation of a licensed origin in S-phase, two replication forks are

formed and move in opposite directions (Figure I.7.E). Nucleosomes are disrupted ahead of replication forks to facilitate fork progression (Gruss et al. 1993), and ORC likely dissociates from DNA upon firing of an origin (Karnani et al. 2011).

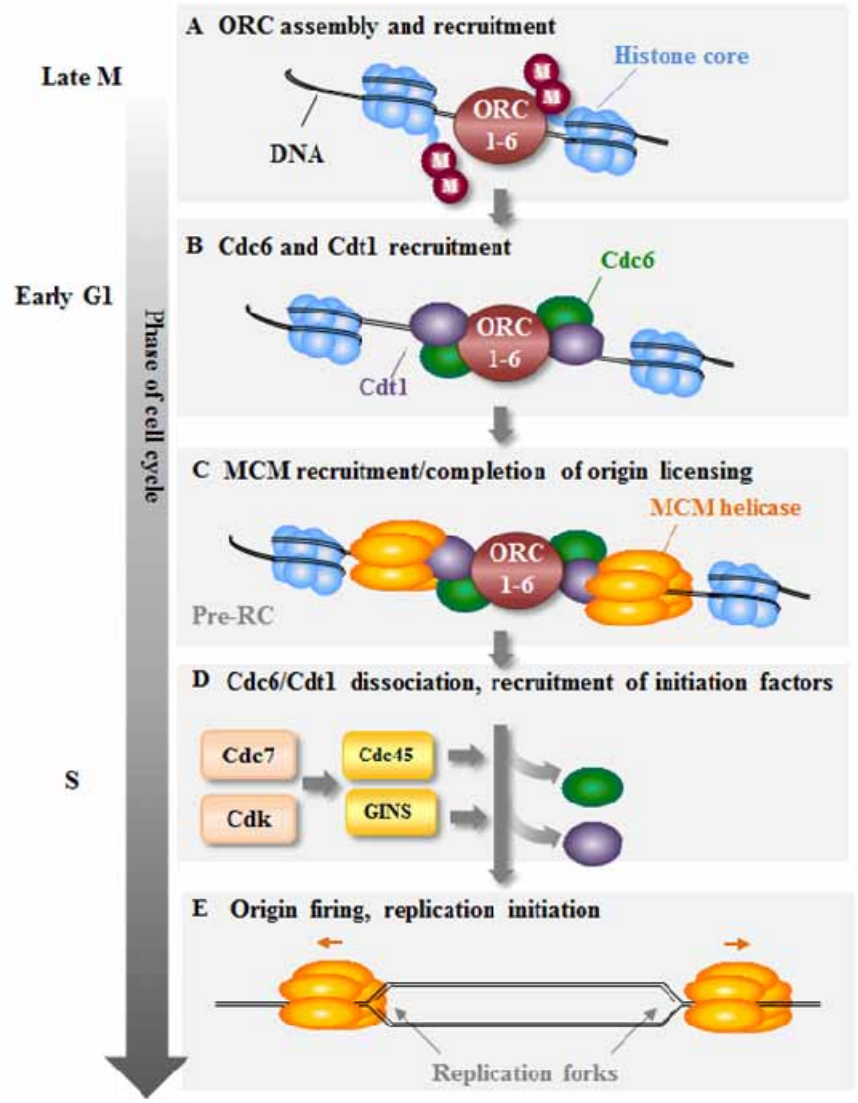

Figure I.7 Replication origin licensing and firing in mammalian cells. Pre-RC: pre-replication complex, M: methylated **A**. The licensing of origins begins with the binding of the heterohexameric ORC complex (ORC1-6) to DNA. ORC recognises and binds DNA in part, by recognition of H4K20me2 (Kuo et al. 2012). **B**. Next, CDC6 and CDT1 are recruited to ORC-bound DNA. **C**. This facilitates loading of the MCM helicase onto ORC, CDC6, and CDT1-bound DNA, altogether forming the pre-RC complex. At this stage, origin licensing is complete. **D**. Next, CDC6 and CDT1 dissociate from the complex to prevent re-licensing of the same origin and Cdc7 and Cdk proteins promote initiation of replication and recruit Cdc45 and GINS to licensed origins. **E**. Origin firing and replication initiate, generating two replication forks moving in opposite directions (as indicated by orange arrows). Nucleosomes ahead of the replication forks are disrupted in order to allow replication to proceed.

I.4.1.b.1 The origin recognition complex components

Originally identified in *S. cerevisiae*, ORC is composed of six protein members, named ORC1-6 in decreasing order of their molecular mass in yeast (Bell et al. 1992) . While the ORC1-5 proteins are highly conserved members of the ATPases associated with diverse cellular activities (AAA+) family of proteins, ORC6 is structurally distinct and less conserved across species (Duncker et al. 2009).

The human ORC1 protein consists of several domains that are highly conserved across species (Figure I.8). Human ORC1 contains an AAA+ ATP-binding domain which includes Walker A and B motifs (WA and WB, respectively) and sensor 1 and 2 motifs (S1 and S2, respectively). In addition, ORC1 contains an N-terminal bromo-adjacent homology (BAH) domain (aa 1-185) and a winged-helix (WH) domain at the C-terminus (aa783-861). In addition, a nuclear localisation signal (NLS) has been identified which spans aa240-288 in human ORC1 (Ghosh et al. 2011). More recently two additional domains have been identified in ORC1. A CDK inhibitory domain (CID), which functions in inhibiting Cyclin E-Cdk2 and Cyclin A-Cdk2 activity, has been mapped to the N-terminus (aa1-250) and a pericentrin-AKAP450 centrosomal targeting (PACT) domain has been mapped to the C-terminus (aa768-851) (Hossain et al. 2012). A role for ORC1 in regulating the duplication of centrosomes will be discussed further in Section I.5.

ATP binding of the AAA+ domain has been shown to function in the recruitment and assembly of the various subunits of the human ORC (Siddiqui et al. 2007). Studies in *S. cerevisiae* have demonstrated that the initial binding of ORC with DNA occurs in an ATP-dependent manner, but does not require hydrolysis of ATP. However, the capacity to hydrolyze ATP becomes important at later steps of pre-RC component assembly, as it is required for subsequent loading of the MCM complex (Bowers et al. 2004; Randell et al. 2006) .

While ORC2-5 also possess the ATPase and WH domains, ORC1 is the only licensing component which contains the BAH domain (Duncker et al. 2009). The ORC1 BAH domain has been demonstrated to participate directly in chromatin binding via an interaction with histone H4K20me2 (Kuo et al. 2012) and to facilitate protein-protein interactions important in replication initiation (Alabert et al. 2012). Expression of an ORC1 BAH mutant construct in human epithelial cells affects binding of ORC1 with the origin of replication in the Epstein Barr Virus (OriP), origin activity, and association of ORC2 with chromosomal DNA (Noguchi et al. 2006). While the WH domain has also been proposed to mediate ORC1 binding to DNA in archae (Gaudier et al. 2007), it is not clear how much of a role it plays in human cells.

The recruitment and activity of ORC1 may also be facilitated by interactions with protein cofactors. ORC1 (and ORC6) have been shown to interact with high mobility group A1a (HMGA1a), and this interaction is capable of generating an origin of replication in specific

sites (Thomae et al. 2008). Other ORC1 interactions, which have been proposed to be important for replication initiation and may also impact higher-order chromatin structure, will be described in more depth in Section I.5 and Chapter V.

The recent discovery of an NLS in ORC1 has revealed the fact that nuclear translocation of ORC1 can occur independently of the other ORC subunits. In studies performed with HeLa cells, deletion of the C-terminal WH domain inhibits the association of ORC1 with ORC2 and ORC3 but does not impact upon nuclear translocation (Ghosh et al. 2011). Therefore, nuclear localisation of ORC1 and the interaction between ORC1 and the other ORC subunits are proposed to be distinct events.

As depicted in Figure I.8, ORC2-5 also contain the AAA+ domain and a WH domain found in ORC1. Unlike ORC1 and ORC6, which may only loosely associate with other ORC subunits, ORC2-5 have been shown to more stably interact, thereby forming a core complex (Dhar et al. 2000; Dhar et al. 2001b; Vashee et al. 2001). In addition to the AAA+ and WH domains, ORC2 has been shown to contain two functional NLS sequences, termed NLS-A (aa 227-233) and NLS-B (aa 319-336) as well as a domain required for the assembly of ORC (aa289-451). In studies with HeLa cells, the two NLS regions have been demonstrated to be required not only for nuclear localisation of ORC2 itself, but also for nuclear accumulation of the entire ORC2-5 complex (Radichev et al. 2006). A functional NLS region has also been identified in the N-terminus of ORC3 (aa1-28). Transfection of human embryonic kidney cells with ORC3 deleted for the NLS had no impact on the interaction between ORC2 and ORC3, which has been shown to require a 200aa region of the N-terminus of ORC3 (Dhar et al. 2001a; Brand et al. 2007). This suggests that ORC2-3 interact in the cytoplasm and supports the model proposed by Ghosh and colleagues that the ORC core complex first forms in the cytoplasm, rapidly relocalises to the nucleus via a mechanism requiring the NLS regions of ORC2 and/or ORC3, and interacts with ORC1 and/or ORC6 independently translocated to the nucleus (Ghosh et al. 2011). ORC3 also contains a coiled-coil motif (aa.45-65) and a MOD1-interacting region (MIR) (213-218aa) which are both involved in the interaction of ORC3 with HP1 (Prasanth et al. 2010). This interaction will be discussed in more depth in Chapter V.

ORC6, the smallest and most structurally distinct of the ORC subunits, contains a unique domain known as the ORC6 fold superfamily domain (Duncker et al. 2009). In addition, human ORC6 is predicted to contain a coiled-coil motif towards the C-terminus (Duncker et al. 2009). In *Drosophila*, this region of ORC6 interacts with Pnut, an essential member of the septin family of structural proteins that functions in cytokinesis (Huijbregts et al. 2009). Interestingly, human ORC6 localises to kinetochores and the mitotic cleavage furrow and small interfering ribonucleic acid (siRNA)-mediated depletion of ORC6 leads to mitotic defects associated with failed cytokinesis (Prasanth et al. 2002). Recently, ORC6 was found to contain an approximately 20 aa NLS (aa 180-202) which enables nuclear localisation to occur

independently from the other ORC components and which is essential for its function. The nuclear localisation of ORC6 is reportedly facilitated by Cdk-dependent phosphorylation of a residue in the NLS and by the association of the NLS region with the nuclear transport proteins karyopherin alpha 6/1 (Kpna6/1) (Ghosh et al. 2011).While ORC6 lacks the AAA+ domain found in the other ORC subunits, it plays a crucial role in origin licensing, in part via interactions with ORC1-5, CDC6, and the ORC chaperone protein HMGA1a (Thomae et al. 2011).

Regulation of human ORC activity has been demonstrated to be multifaceted, subunit-specific, and in some cases, cell cycle dependent. The expression of human ORC1 is reported to be regulated by the E2F transcription factor and elevated levels have been observed in rapidly proliferating tissues and following growth stimulation in normal fibroblasts (Ohtani et al. 1996) (Thome et al. 2000). In addition, the chromatin-bound fraction of ORC1 has been reported to be elevated in transformed cell lines, including the tumour-derived HeLa line (Di Paola et al. 2011). ORC1 levels are generally thought to oscillate during cell cycle, with peak levels observed in G1 or at the G2/S boundary and reduced levels observed thereafter (Mendez et al. 2002; Ohta et al. 2003; Tatsumi et al. 2003). As cells transition from G1 to S-phase, ORC1 may become poly-ubiquitinated by SKP1-cullin-F-box (SCF)/S-phase kinase-associated protein 2 (Skp2) ubiquitin ligase complex (Mendez et al. 2002), and subsequently undergo proteolytic degradation by the 26S proteasome pathway (Mendez et al. 2002; Tatsumi et al. 2003). Phosphorylation of ORC1 by Cdk has also been proposed to regulate licensing by reducing the affinity of ORC binding to chromatin. As cells transition from G1 to S-phase, ORC1 can be phosphorylated by Cdk1/Cyclin B (Nguyen et al. 2001). Cdk-dependent phosphorylation levels are observed to increase during mitosis, and this hyperphosphorylated form of ORC1 inhibits ORC-chromatin binding (Li et al. 2004). In contrast to the proliferation and cell cycle dependent regulation of ORC1 levels, human ORC2-5 are reported to be expressed in tissues independently of proliferative activity (Thome et al. 2000) and generally remain bound to chromatin throughout the cell cycle (DePamphilis 2005; Takeda et al. 2005). However, Cdk-dependent phosphorylation may play a role in regulating the activities of ORC2 and ORC6. In *S. cerevisiae*, Cdk1, which is encoded by Cdc28 (cell division control 28), phosphorylates ORC2 at multiple N-terminal sites conserved across various species (Vas et al. 2001). Phosphomimetic mutants of threonine 116 and 226 on ORC2 are defective in binding of ORC2 with chromatin (Lee et al. 2012). Cdk-mediated phosphorylation of threonine 195 of ORC6 has been shown to facilitate (though is not required for) the nuclear localisation of ORC6 (Ghosh et al. 2011).

I.4.1.b.2 CDC6

Another member of the AAA+ family of ATPases originally identified in *S. cerevisiae,* the CDC6 protein, gets recruited to origins following binding of ORC. CDC6 is highly related to ORC1, both structurally and phylogenetically, and like ORC1, CDC6 has the capacity to hydrolyze ATP (Duncker et al. 2009). Cdc6-mediated ATP hydrolysis stabilises its interaction with ORC and promotes loading of the MCM helicase (Randell et al. 2006; Speck et al. 2007; Duncker et al. 2009). In addition to its AAA+ domain, human CDC6 also contains a cyclin binding (cy) motif near the N-terminus. In the U2OS osteosarcoma-derived cell line, exogenously expressed CDC6 was shown to interact with Cdk2/Cyclin A at this motif, leading to Cdk-dependent phosphorylation of various residues on CDC6 (Petersen et al. 1999). Mutation of these residues in HeLaS3 cells has been reported to impede replication and slow progression of S-phase (Herbig et al. 2000). CDC6 also contains a highly conserved leucine zipper, a motif found in DNA binding proteins (Landschulz et al. 1988) and known to mediate protein-protein interactions (Petersen et al. 1999). Like the five largest subunits of the ORC, CDC6 also contains a WH domain at its C-terminus (Liu et al. 2000) (Figure 1.8).

Like ORC1, CDC6 has been found to be hyperphosphorylated during mitosis by the CDK1/Cell division control 2 (CDC2) kinase (Fujita et al. 1999), is overexpressed in rapidly proliferating cells and tissues (Yan et al. 1998) and is regulated transcriptionally by E2F (Ohtani et al. 1998). Overexpression of CDC6 has been reported in various types of tumours (Lau et al. 2007b) and CDC6 has been considered as a biomarker in cancer (Bowers et al. 2004).

Following recruitment of the MCM helicase, CDC6 has been reported to dissociate from the chromatin-bound pre-RC, providing a mechanism for the prevention of re-licensing of replicated DNA (Blow et al. 2005; Arias et al. 2007). In *S. cerevisiae*, phosphorylation of sites on CDC6 facilitates its SCF^{Cdc4}-dependent proteolytic destruction as well as its stable association with Cdk. The association of Cdk with CDC6 can result in the inhibition of the licensing activity and/or transcription of CDC6 (Arias et al. 2007). In human cells, several studies have reported that proteolysis of CDC6 can occur by a mechanism dependent on the Cdh1 activated form of the anaphase-promoting complex (APC^{Cdh1}). Ubiquitination by this cell cycle dependent ubiquitin ligase and subsequent degradation of CDC6 has been demonstrated in G1 and in quiescent cells (Petersen et al. 2000).

Interestingly, in human cells, induction of DNA damage leads to the degradation of CDC6 by various mechanisms. Following IR, inhibition of Cdk-dependent phosphorylation of serine 54 results in subsequent APC^{Cdh1} -proteolysis (Duursma et al. 2005). p53 has been implicated in facilitating this mechanism of Cdc6 destruction after IR, and RNA interference-mediated depletion leads to increased replication and stabilization of CDC6 (Duursma et al. 2005). However, in response to treatment with MMS, which methylates DNA and induces RS

and DSBs, destruction of CDC6 has been reported to occur independently of p53 in normal human fibroblasts immortalised with telomerase. Further, MMS-induced degradation of CDC6 can occur independently of APC^{Cdh1} in HeLa cells. Instead, CDC6 proteolysis following MMS treatment requires the Huwe1 ubiquitin ligase (Hall et al. 2007).

I.4.1.b.3 CDT1

In addition to recruiting CDC6, ORC assembly initiates the recruitment of the CDT1 protein. First discovered in fission yeast, *Schizosaccharonyces pombe* (*S. pombe*) (Roukos et al. 2011), CDT1 is essential for the loading of the MCM helicase complex to origins (Nishitani et al. 2000; Randell et al. 2006). The N-terminus of CDT1 contains a proliferating cell nuclear antigen (PCNA) interaction protein box (PIP box) (aa3-9) (Arias et al. 2006) which contains a crucial lysine (K+4) which mediates degradation (Havens et al. 2009), a Cy motif (aa68-70) (Liu et al. 2004), an NLS (aa48-71) (Nishitani et al. 2004). In addition, CDT1 contains an approximately 40 aa domain important for binding with Geminin (Wohlschlegel et al. 2000), a protein which inhibits CDT1 activity by preventing binding with CDC6 and the MCM helicase (Cook et al. 2004). CDT1 interacts with the MCM complex (predominately MCM6) via its C-terminus, (aa392-471) (Zhang et al. 2010).

The regulation of CDT1 accumulation occurs by cell cycle-dependent expression, Geminin-mediated inhibition, proteolytic degradation, and Cdk-dependent phosphorylation. Studies originally performed in tumour-derived cell lines have demonstrated that human CDT1 is expressed predominately during G1-phase (Nishitani et al. 2001) in an E2F-dependent manner (Yoshida et al. 2004) and becomes destabilised as cells enter S-phase (Nishitani et al. 2001). The first 189 aa are sufficient for accumulation of CDT1 during G1 (Nishitani et al. 2004). Both Geminin binding and APC-dependent proteolytic degradation of CDT1 are thought to be important for the prevention of the re-licensing of origins, an event detrimental to precise replication of the genome. Studies using *Xenopus* egg extracts have demonstrated that inhibition of either of these regulatory mechanisms leads to re-licensing and re-replication of DNA added to extracts (Li et al. 2005). Phosphorylation of CDT1 by cyclin A-dependent Cdks is also thought to promote degradation. Cyclin A/Cdk1 and Cdk2 directly interact with the Cy motif of CDT1. While the resulting phosphorylation does not impact upon binding with Geminin, it does promote the binding of Cdt1 with the Skp2 component of the SCF ubiquitin ligase complex, therefore enabling proteolytic degradation of CDT1 (Liu et al. 2004; Sugimoto et al. 2004). In addition to the SCF-mediated degradation, CDT1 degradation can also occur via a mechanism dependent on PCNA and the Cul4/DDB1 (Cullin 4/DNA damage binding protein 1) ubiquitin ligase, predominately in the response to DNA damage (Senga et al. 2006).

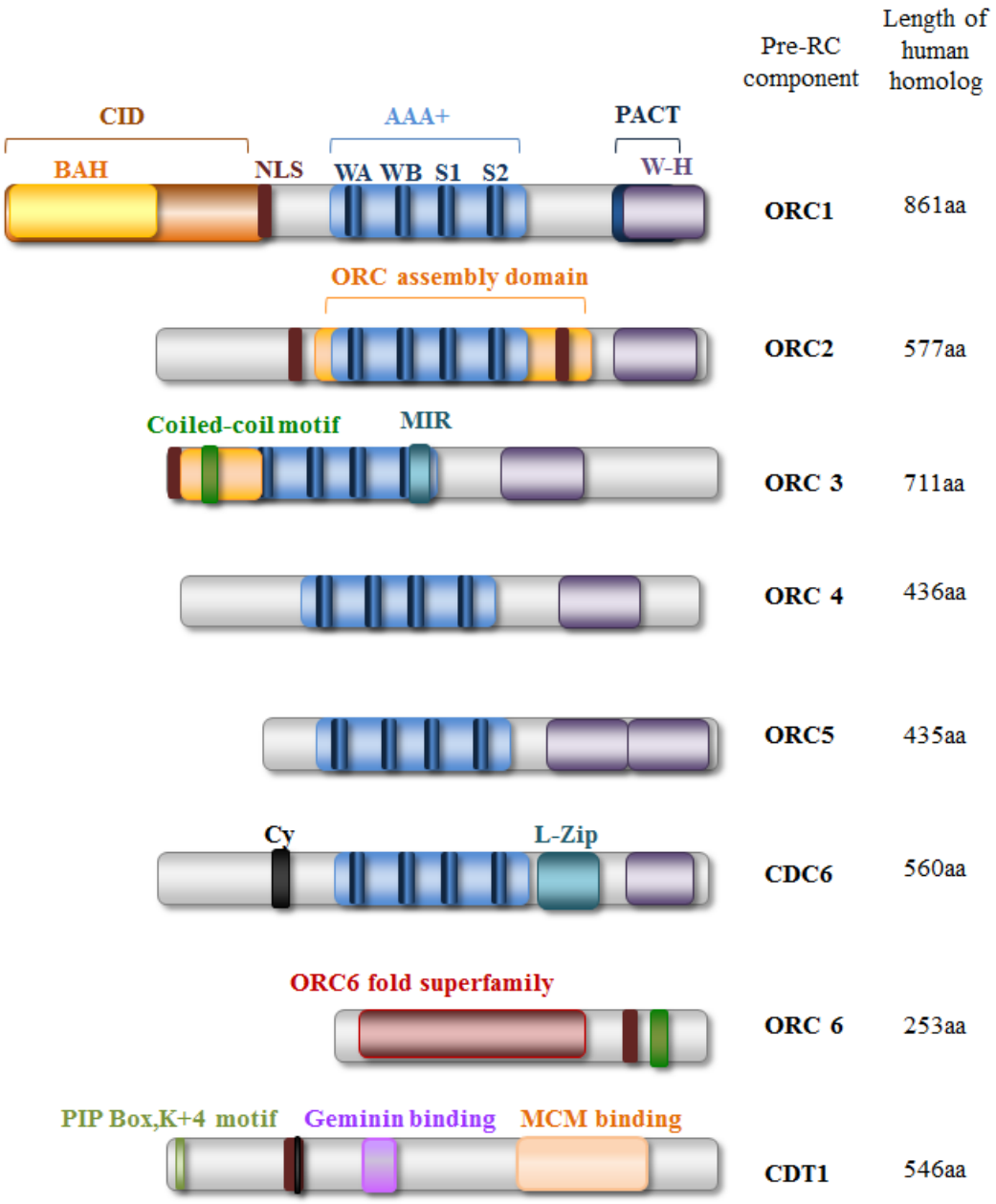

Figure I.8 Schematic representation of domains found in human ORC, CDC6, and CDT1. See text for abbreviations.

I.4.1.b.4 The MCM helicase

Following the assembly of ORC, CDC6, and CDT1 at potential sites of replication origins, the MCM helicase, a highly conserved heterohexomeric complex made up of the subunits MCM2-7, is loaded onto DNA in a ring shaped structure (Mendez et al. 2003). At each potential origin, two catalytically inactive hexomeric complexes of MCM are loaded, and the complexes are able to slide on DNA in either direction from the fork (Evrin et al. 2009). Both CDC6 and CDT1 are required for the recruitment of MCM to DNA. CDT1 directly binds MCM via the C-terminus of CDT1, and this interaction is required for MCM recruitment and impacted by CDC6 activity (Cook et al. 2004). Following recruitment of MCM to DNA, CDC6 and CDT1 are no longer required to maintain the association of MCM with DNA (Donovan et al. 1997; Cook et al. 2004) (Figure I.7.D).

The precise mechanism of MCM helicase loading remains unclear. The structural properties and ATPase activity of ORC and CDC6 could potentially facilitate the loading of the helicase by opening and closing the MCM ring structure (Evrin et al. 2009). Interestingly, CDT1 has also been implicated in chromatin decondensation, which has been proposed to enable loading of MCM as a result of increased chromatin accessibility (Wong et al. 2010).

Like several other components of the pre-RC, the MCM subunits are transcriptionally regulated by E2F and their expression peaks during late mitosis and G1-phase (Leone et al. 1998). As a complex, MCM has robust ATP hydrolysis activity (Schwacha et al. 2001) and has been shown to be involved in unwinding DNA during both initiation of replication and elongation (Labib et al. 2000; Pacek et al. 2004). Importantly, the helicase activity of MCM2-7 is induced exclusively upon association with co-factors as outlined below. Once activated, the two MCM heterohexomers allow for bidirectional replication forks moving away from each other, therefore forming a structure known as a “replication bubble” (Figure I.7.D).

I.4.1.c Replication initiation and elongation

The initiation of DNA replication by origin firing must be tightly regulated in order to avoid genomic instability. The firing of too few or too many origins, the interference with the scheduled timing of origin firing, and the re-firing of a single origin all present replication problems which can result in chromosomal instability (Blow et al. 2005; Blow et al. 2011).

Some evidence exists for a p53-dependent “licensing checkpoint” in normal human fibroblasts which prevents the premature entry of cells into S-phase if an insufficient number of origins are licensed (Nevis et al. 2009). Given the fact that a reduction in the number of available origins would result in longer distances between replication forks and therefore increased chances of replication fork stalling, this checkpoint may work to prevent replication

stress and subsequent genome instability. As a result of the strict licensing of origins exclusively during mitosis and G1, additional origins cannot be assembled once cells enter S-phase. Depletion of licensing factors such as CDC6 and CDT1 in normal human fibroblasts has been shown to result in reduced entry into S-phase and reduced Cyclin E, which is required for S-phase entry. Co-depletion of p53 in these cells restored the progression into S-phase, despite a substantial reduction in origin availability. Interestingly the prevention of S-phase entry under contexts of reduced origin licensing was not observed in tumour-derived cell lines, potentially contributing to the inherent genome instability observed in these cells (Nevis et al. 2009). Overexpression of Cyclin E, an event often found in cancer, has been shown to accelerate entry into S-phase despite insufficient licensing, and result in altered loading of the MCM helicase and defective replication initiation (Ekholm-Reed et al. 2004).

When a sufficient number of origins have been licensed and cells are ready to proceed to S-phase, replication initiates at early firing origins with the activation of the MCM helicase, enabling unwinding of origin DNA (Pacek et al. 2004). The helicase activity of the MCM complex becomes activated upon association with Cdc45 and GINS during S-phase. Structural studies performed on *Drosophila melanogaster* MCM bound to Cdc45 and GINS have demonstrated that association of the three components results in conformational changes of MCM to a more planar configuration, therefore inducing its helicase activity (Costa et al. 2011). Cdc45 and GINS are recruited by Cdk proteins as well as the Cdc7 kinase. Cdc7 also phosphorylates various MCM subunits, potentially resulting in structural changes which promote its helicase activity or increased binding with Cdc45 and GINS (Weinreich et al. 1999) (Labib 2010).

Upon unwinding of DNA and the formation of bi-directional replication forks, the semi-conservative duplication of eukaryotic DNA is carried out at a rate of ~2-3kb per minute by various proteins altogether known as the replisome (Mechali 2010). The unwinding of DNA by helicases generates ssDNA, an inherently labile structure which is stabilised in eukaryotes by binding of the heterotrimeric protein RPA (Wold et al. 1988; Wold 1997). Synthesis of DNA requires the activity of a replicative polymerase which catalyzes the polymerization of dNTPs onto a 3’ hydroxyl group of the growing daughter strand. RNA primers generated by a primase provide the 3’ hydroxyl group required for replication initiation. The 5’-3’ elongation of newly synthesized DNA occurs continuously on the leading strand and semi-discontinuously on the lagging strand through the use of 100-1000 nucleotide long Okazaki fragments. Processivity of the DNA polymerase is enhanced by loading of the sliding clamp protein PCNA onto DNA by replication factor C (RFC), (Maga et al. 2003). In addition to its role in improving processivity of the polymerase, PCNA recruits DNA ligase I to sites of replication (Montecucco et al. 1998). DNA ligase I functions to catalyze the formation of the phosphodiester bonds necessary to join Okazaki fragments. As the replicative helicase unwinds DNA to accommodate progression of

the replication fork, supercoiling occurs ahead of the fork, creating a topological problem. The DNA topoisomerases relieve this challenge by creating a nick in DNA, allowing for untangling of the double helix, and these nicks can then be sealed. In addition, DNA gyrases are thought to contribute by introducing negative supercoils.

In mammalian cells, replication occurs in discrete sites known as replication factories (Hozak et al. 1994) which can be visualised using microscopy-based methodology as foci containing replisome proteins such as PCNA (Leonhardt et al. 2000).

I.4.2 ATR-mediated signalling at the replication fork

As introduced in Section I.2.3, when a replication fork encounters a lesion in DNA, fork stalling may occur, creating an unstable structure containing ssDNA. ssDNA is also generated during the initial step of HR as ends are resected by various nucleases (Section I.3.1b). In response to the generation of ssDNA, the ATR kinase is activated and works in conjunction with its binding partner ATR-interacting protein (ATRIP) to coordinate the resulting DNA damage response (Flynn et al. 2011). Like ATM, ATR is a member of the PIKK family of protein kinases, and it phosphorylates various substrates in response to a wide range of DNA damage. The primary function of the ATR-dependent signalling pathway is to stabilise stalled replication forks and to activate cell cycle checkpoints in response to DNA damage. Therefore, this pathway plays a pivotal role in the maintenance of genome stability.

As depicted in Figure I.9A-B, upon exposure of regions of single stranded DNA resulting from replication fork stalling, DNA becomes rapidly coated with RPA**.** ATRIP recognises and directly binds to RPA coated ssDNA (Zou et al. 2003a). This facilitates the localisation of ATRIP-bound ATR molecules to stalled replication forks (or to resected regions of DNA). The clamp loading protein Rad17 is then recruited in to RPA-coated DNA. Once bound to DNA, Rad17 functions in loading the ring shaped Rad9-Rad1-Hus1 (9-1-1) complex in a manner comparable to the RFC-dependent loading of PCNA during unchallenged replication (Zou et al. 2003b) (Figure I.9.C). Full activation of ATR requires the ATRIP-dependent recruitment of the topoisomerase II binding protein 1 (TopBP1) (Kumagai et al. 2006; Choi et al. 2010). TopBP1 interacts with the 9-1-1 complex via the C-terminal region of Rad-9, which enables the interaction between ATR and TopBP1 and subsequent full activation of ATR (Lee et al. 2007) (Figure I.9.D).

Ultimately, the induction of the intra-S-phase checkpoint is dependent on phosphorylation of the Chk1 kinase by ATR. ATR-dependent phosphorylation of Chk1 is facilitated by the adaptor protein, Claspin (Kumagai et al. 2004). In response to replication stress, Rad17 is phosphorylated by ATR, and this phosphorylated form has been shown to function in Claspin recruitment and activation (Wang et al. 2006b) (Figure I.9.E). Claspin itself

also becomes phosphorylated in response to DNA damage, and this phosphorylation facilitates binding with Chk1 (Kumagai et al. 2003). ATR-dependent phosphorylation of Chk1 at serines 317 and 345 during S-phase leads to its activation and subsequent inhibitory phosphorylation of Cdc25A (Stracker et al. 2009).

The Cdc25 proteins are crucial in cell cycle progression, as they dephosphorylate the inhibitory phosphorylation at threonine 14 and tyrosine 15 on Cdk2 (Sebastian et al. 1993). The dephosphorylation of Cdk2 is required for its function in the initiation of replication at licensed origins (Section I.4.1.c). Chk1-dependent phosphorylation of Cdc25A leads to its proteolytic degradation (Mailand et al. 2000; Jin et al. 2003), thereby preventing Cdk2 dephosphorylation and inhibiting the initiation of replication.

Importantly, Chk1 has been demonstrated to exclusively inhibit the activation of origins in new replication factories (ie. late-firing clusters of origins) (Ge et al. 2010). Chk1 plays a distinct role in the initiation of origins within active replication factories experiencing replication stress which will be further discussed in Section I.4.3.

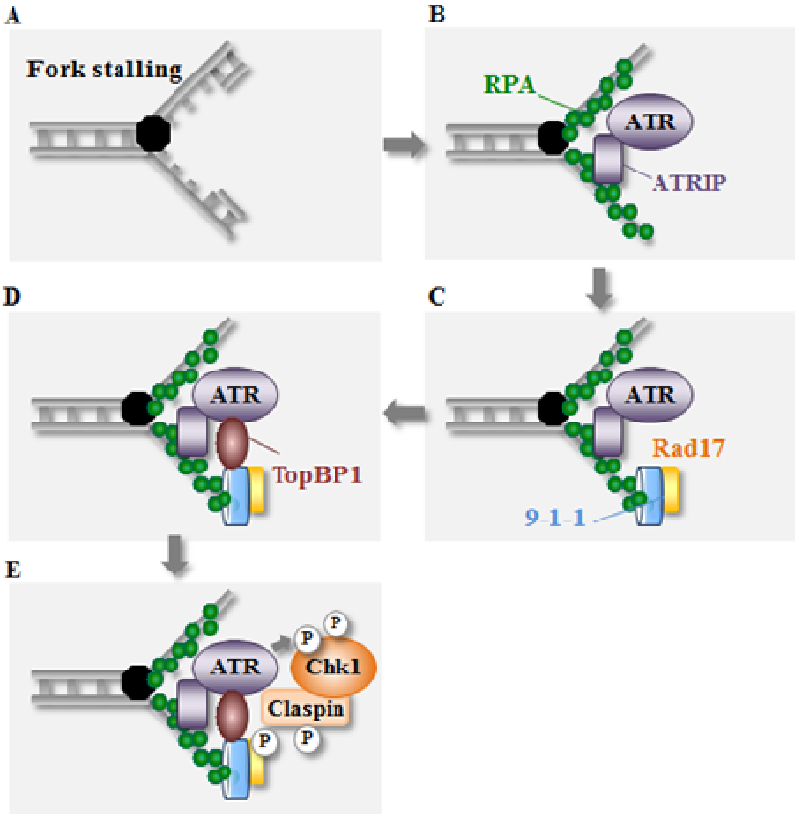

Figure I.9 Schematic representation of ATR signalling at a stalled replication fork. P: phosphorylation. **A**. Interruption of replication results in replication fork stalling, generating exposed regions of ssDNA. **B**. ssDNA is rapidly coated with RPA molecules, and ATR is recruited via the direct interaction of its binding partner, ATRIP, with RPA-ssDNA. **C**. The Rad17 clamp loader binds DNA and loads the 9-1-1 ring complex. **D**. TopBP1is recruited to the stalled fork in an ATRIP-dependent manner that also involves binding with the 9-1-1 complex. Once recruited, TopBP1 interacts with ATR, leading to full ATR activation. **E**. Rad17 and the mediator protein Claspin are both phosphorylated. This promotes the ability of Claspin to facilitate phosphorylation of Chk1 at serines 317 and 345 by ATR.

I.4.3 Dormant origin usage in the response to replication damage

While the origin licensing components are essential for cellular proliferation, cells are able to undergo replication and to proliferate when levels of the pre-RC subunits are substantially reduced. This observation reflects the fact that cells license up to 10 times more origins than are typically required during S-phase (Lei et al. 1996; Donovan et al. 1997; Wong et al. 2011). Based on computer modelling of a typical metazoan origin cluster in which origins are activated in a stochastic manner during S-phase, these excess or "dormant" origins unlikely to fire in the absence of replication stress are thought to be passively replicated by approaching forks initiated from adjacent origins (Blow et al. 2009) (Figure I.10.A-B). As described below, a growing body of evidence has supported the model that these dormant origins can be activated in response to replication stress, promoting replication recovery and cellular survival (Blow et al. 2011) (Figure 1.10.C).

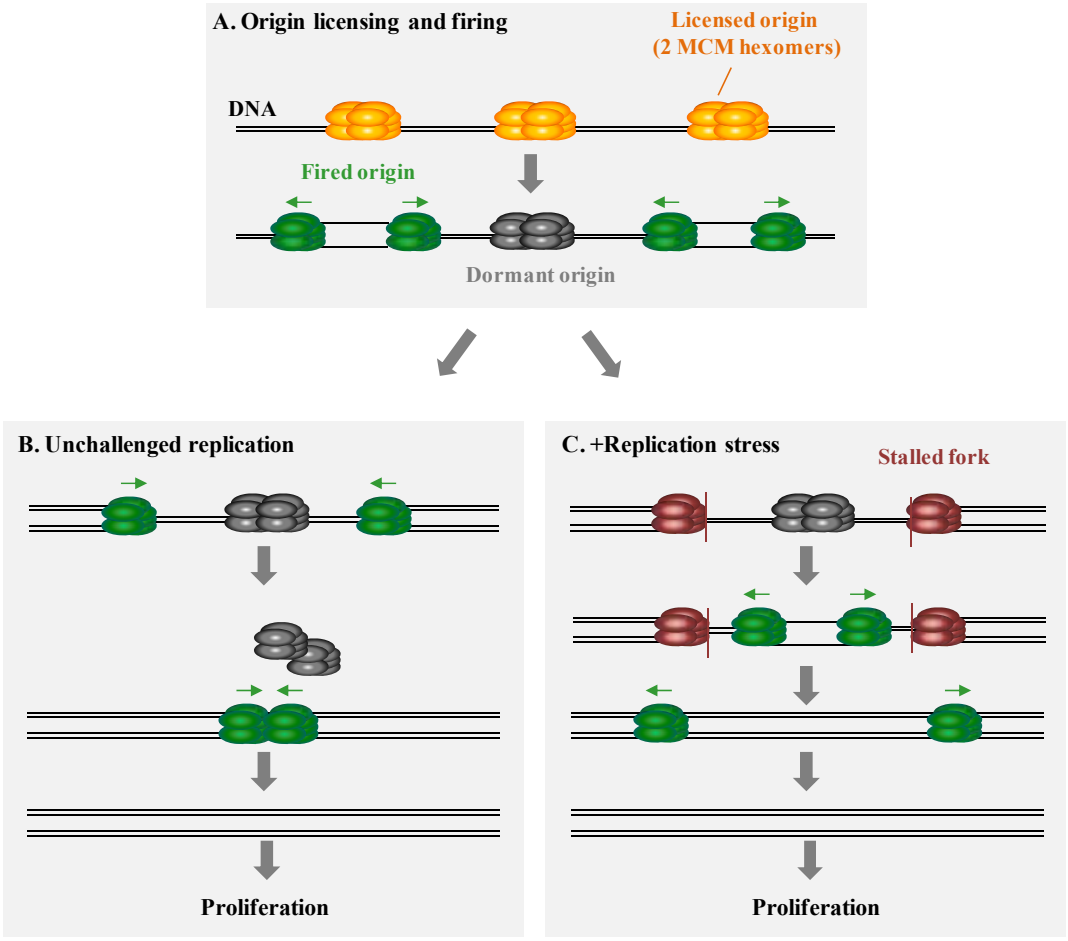

Figure I.10 A model for the usage of dormant origins in promoting cellular proliferation under conditions of replication stress. (Proposed by Blow, Ge et al, 2011). Double MCM heterohexomers are depicted at replication origins on DNA. **A**. More origins are licensed (orange) than are fired (green, green arrows indicate direction of movement of each replication fork), leaving excess or "dormant" origins (grey) inactive. **B**. Over the course of unchallenged replication, dormant origins remain inactive and are proposed to be passively replicated by nearby activated replication forks (Blow et al. 2009). **C**. Under conditions of replication stress, replication fork stalling occurs (red) and DNA between two stalled replication forks may remain unreplicated. A dormant origin within this region may become activated, enabling replication of intervening DNA, completion of replication, and cellular proliferation.

The initial observations that impaired replication fork progression increases adjacent origin firing were made nearly forty years ago (Ockey et al. 1976; Taylor 1977). Since then, these observations have been confirmed and explored by methods including the analysis of replication initiation at sites known or predicted to contain active and dormant origins in eukaryotic cells such as *S. cerevisiae* (Santocanale et al. 1999), Chinese hamster ovary (CHO) cells (Anglana et al. 2003), and, more recently, in human cells (Karnani et al. 2011). Advances in methodology for analysing single tracts of DNA replication have enabled further investigation of dormant origin firing in human cells. Nucleoside analogues can be incorporated into DNA during active replication, labelled with fluorescently-conjugated antibodies, and visualised using microscopic analysis of individual DNA fibres. These DNA fibre assays may be modified for various purposes, such as comparing inter-origin distances within replication clusters in the presence or absence of replication stress activity (Ge et al. 2007). As described below, exploitation of this or similar methods have demonstrated that replication stress-inducing agents stall the progression of forks previously activated (Merrick et al. 2004) but induce new origin firing of adjacent (most likely dormant) origins (Ge et al. 2007; Ibarra et al. 2008a; Petermann et al. 2010a; Karnani et al. 2011).

In order to study replication stress-induced dormant origin activation and subsequent cellular consequences, several studies have exploited partial siRNA-mediated depletion of pre-RC components to reduce dormant origin availability in the presence of replication inhibitors. Treatment with hydroxyurea (HU), an agent which inhibits ribonucleotide reductase (RNR) and results in decreased dNTP pools and replication fork stalling/collapse, has been shown to increase intra-cluster origin activation in U2OS osteosarcoma cells (Ge et al. 2007). This study demonstrated that the reduction but not complete ablation of origin licensing capacity via siRNA-mediated depletion of MCM5 enhances sensitivity of U2OS cells to the replication stress-inducing agents HU, aphidicolin (a DNA polymerase inhibitor) and camptothecin (a TopoI inhibitor), presumably as a result of insufficient dormant origin availability. Importantly, in the absence of treatment with replication stress-inducing agents, partial depletion of MCM5 did not significantly impact replication and cellular proliferation, implying that MCM5 depletion impacted mainly upon dormant origin availability. An independent study performed in HeLa cervical carcinoma cells demonstrated that siRNA-mediated depletion of MCM3 also enhances sensitivity of cells to aphidicolin. Increases in RPA foci, γH2AX levels, and chromosomal instability were observed in MCM3 depleted HeLa cells treated with aphidicolin for several days, reflecting enhanced DNA damage (Ibarra et al. 2008a).

Importantly, the increased origin firing observed in response to replication inhibitors has been observed primarily within previously activated replication factories. Conversely, the activation of new replication factories (ie. late-firing clusters of origins) is inhibited by replication blocks (Ge et al. 2010) in a process involving ATR and Chk1 signalling at stalled

forks (Section I.4.2) (Branzei et al. 2005; Karnani et al. 2011). Abrogation of Chk1 function via chemical inhibition or siRNA-mediated depletion results in increased origin firing (Feijoo et al. 2001; Ge et al. 2007; Maya-Mendoza et al. 2007; Karnani et al. 2011), accompanied by a decrease in the rate of fork elongation, therefore compromising efficacy of replication (Maya-Mendoza et al. 2007). Overall, these results suggest that, while ATR and Chk1inhibit the activation of late firing replication clusters in response to replication stress, the firing of dormant origins within previously activated clusters may be an important component of the DDR in these cell lines.

Dormant origin activation has also been implicated in replication within regions containing fragile sites, specific genomic regions marked by instability. Investigation of origin firing within a common fragile site (CFS) in the human genome known as FRA16C, has suggested that an increase in origin firing may promote replication completion in this region, even in normal growth conditions. Examination of FRA16C in a human lymphoblastoid cell line reported to have a normal karyotype revealed AT-rich sequences which would be predicted to form secondary structures and potentially interrupt the progression of replication forks. In fact, a correlation was observed between these AT-rich regions with replication fork slowing or stalling. A slight decrease was reported in the average inter-fork distance in the FRA16C locus when compared with the average inter-fork distance observed across the entire genome (109+/-7Kb vs. 81+/-16Kb). This suggests that slightly more origins (ie. dormant origins) may be activated in the fragile site region of these immortalised lymphoblastoid cells to promote completion of replication (Ozeri-Galai et al. 2011). However, in another study examining the FRA3B CFS, tissue-specific differences in origin density and region fragility were reported (Letessier et al. 2011). Fragility of FRA3B was much greater in lymphoblastoid cells than in various fibroblast lines, and this fragility was strongly associated with a paucity of activated origins rather than increased dormant origin firing. The reduction in origin availability in cells forces the few forks activated in the region to travel longer distances and therefore increases the chances of fork stalling and site fragility. Importantly, this scarcity of origin usage and site fragility was not observed in fibroblast cells. Therefore, many questions remain about the usage of dormant origins in normal replication of various CFSs in cells from different tissues.

In addressing the cellular function of dormant origin firing and how this process may be regulated, Blow and colleagues have presented a model based on both computer-generated modelling of origin firing within a typical 250 kb metazoan origin cluster and findings from *in vivo* studies (Blow et al. 2009; Blow et al. 2011). This model proposes that origin activation occurs in a stochastic manner, with some origins less efficient than others and therefore likely to be dormant during the course of an unchallenged S-phase. Blow and colleagues reason that in the absence of replication stress, dormant origins may be replicated passively by oncoming replication forks but that the slowing or stalling of active forks provides a longer timeframe in

which the less efficient dormant origins may become activated. Under conditions of replication stress, the probability of double fork stalling increases, potentially leaving the DNA between the forks unreplicated (Figure I.10.C**)**. Firing of dormant origins within this intervening DNA would enable completion of replication, therefore preventing under-replication and subsequent genome instability and/or cell death. Therefore, the higher the density of origins licensed, the greater protection against replication interruption and subsequent cellular consequences. Given that origin licensing occurs strictly before S-phase entry and the benefits of new origin activation in the recovery from replication stress, the availability of excess pre-licensed dormant origins has been proposed to play a role in the prevention of genome instability (Blow et al. 2011).

While the replication stress-induced activation of dormant origins has been demonstrated in a variety of cells from various eukaryotic species, the dependence of human cells on this mechanism for survival has been investigated primarily using tumour-derived cell lines. However, the dependence of cells from normal human tissue on this mechanism has yet to be fully explored. As increased expression of various components of the pre-RC has been reported in cancer (Lau et al. 2007b), perhaps reflecting increased dormant origin capacity, distinctions may exist between tumour and non-tumour cells in the reliance on dormant origin firing. Several studies have indeed examined the impact of depleting other pre-RC components on tumour and normal tissue-derived human cell lines (Prasanth et al. 2002; Machida et al. 2005; Lau et al. 2006; Feng et al. 2008; Lau et al. 2009; Nevis et al. 2009). However, these studies were generally not designed to investigate the impact of specifically depleting dormant origin capacity on the recovery from replication stress. Therefore, while the results reflect important differences between tumour-derived and normal cells in the requirement of the pre-RC components to sustain survival in the absence of damage, many questions remain unanswered. Interestingly, partial depletion of ORC6 has been reported to enhance sensitivity of a colon cancer derived cell line to the pyrimidine analogue 5-Fluorouracil, which directly inhibits replication fork progression, and the cross linking agent cisplatin, which also induces replication stress (Gavin et al. 2008). This study did not compare the impact of ORC6 depletion in tumour-derived cells with normal cells and did not examine the effect of partial ORC6 depletion on origin firing and replication. However, the enhanced sensitivity to replication stress-inducing agents caused by partial depletion of ORC6 may reflect an important role of dormant origin availability in survival of these colon cancer-derived cells under conditions of replication fork stalling and collapse.

While few patients have been identified which harbour mutations in pre-RC components, several human cell lines and mouse models with deficiencies in origin licensing have been examined. In recent years, mutations in several human pre-RC genes have been identified in patients with Meier-Gorlin Syndrome (MGS), a disorder characterised by various phenotypic traits including but not limited to pre-and post-natal growth retardation and small

head circumference (microcephaly). The clinical and cellular phenotypes of pre-RC-deficient MGS patients will be discussed in Section I.6. While mutations in the MCM helicase subunits have not been identified in humans to date, two mouse models harbouring hypomorphic mutations in MCM2 and MCM4 have been developed and used to study the impact of depleting origin licensing capacity on the entire organism. Insertion of an internal ribosome entry site (IRES) fused to the CreERT2 gene into the MCM2 transcript and subsequent targeted recombination into the wildtype MCM2 locus has provided a tamoxifen-inducible model of hypomorphic MCM2 deficiency (*MCM2*$^{IRES\text{-}CreERT2}$) (Pruitt et al. 2007). Mice homozygous for the MCM2 mutation were viable and displayed normal development up through early adulthood. However, an increase in cancer incidence was reported in these mice along with premature cancer-related death. In addition, the proliferative compartments of various tissues were found to be reduced (Pruitt et al. 2007). Mouse embryonic fibroblasts (MEFs) from homozygous *MCM2*$^{IRES\text{-}CreERT2/\ IRES\text{-}CreERT2}$ mice displayed decreased origin usage following exposure to HU as well as a modest increase in DNA damage, as measured by γH2AX and 53BP1 foci (Kunnev et al. 2010). A mutation identified in mice which results in a single amino acid change and chromosomal instability, known as *Chaos3* (chromosome aberrations occurring spontaneously 3), was identified to destabilise MCM4 (Shima et al. 2007). *MCM4*^{Chaos3} was observed to be hypomorphic and result in increased aphidicolin-induced chromosome instability and cancer incidence (Shima et al. 2007; Kawabata et al. 2011b). MEFs from *MCM4*$^{Chaos3/Chaos3}$ mice displayed reduced levels of chromatin-bound MCM2-7, decreased origin firing, and increased γH2AX and RPA foci, (Kawabata et al. 2011b). Unlike the *MCM2*$^{IRES\text{-}CreERT2}$ mice, *MCM4*$^{Chaos3/Chaos3}$ mice displayed some embryonic lethality and a small (~15%) decrease in embryonic body weight. Further, proliferation of *MCM4*$^{Chaos3/Chaos3}$ MEFs has been reported to be impaired, which correlates with the upregulation of p21 (Kawabata et al. 2011c). Whether deficiencies in the other pre-RC components would also result in increased cancer incidence in humans remains unknown. While there are no reports of increased cancer incidence in MGS patients with mutations in ORC1, ORC4, ORC6, CDC6, and CDT1, the number of patients is too limited to accurately assess this.

I.5 Additional cellular roles of origin licensing machinery

In addition to their crucial role in licensing of replication origins, various components of the pre-RC have been found to function in other cellular processes. As a result, depletion or deficiency of these components may result in pleiotropic cellular effects.

Recent unpublished findings from our lab have identified a role for origin licensing factors in the ATR-dependent G2/M checkpoint. Cells from MGS patients with hypomorphic mutations in *ORC1* (Bicknell et al. 2011b) fail to activate the G2/M checkpoint in response to

UV (S. Walker, unpublished results) (Figure I.11A). The activation of this checkpoint, which is regulated by ATR signalling (Stiff et al. 2008), involves the inhibition of Plk1 (van Vugt et al. 2001) and Aurora A kinase activity (Marumoto et al. 2002). Interestingly, this UV-induced G2/M checkpoint defect in ORC1-deficient cells can be overcome by treatment with Plk1 or Aurora A inhibitors (S. Walker, unpublished results). Similar results have been observed in cells from a CDC6-deficient MGS patient (Bicknell et al. 2011a) (S. Walker, unpublished results, data not shown). While a role for CDC6 in ATR activation has already been proposed during S-phase and thought to be mediated by the direct interaction of CDC6 with ATR (Yoshida et al. 2010), these findings have implicated the origin licensing components in regulating the UV-induced ATR-dependent G2/M checkpoint upstream of Plk1 and Aurora A inhibition.

In addition to this role in regulating the transition from G2 to M-phase, components of the pre-RC have been shown to function in the regulation of centrosome duplication. Enhanced green fluorescent protein (EGFP) –tagged pre-RC components overexpressed in mouse cells are reported to colocalise with centrosomes (Stuermer et al. 2007), the microtubule organising centres in metazoan cells. Centrosomes are composed of two centrioles as well as surrounding pericentriolar material which must be duplicated only once during cell cycle to ensure proper organisation of microtubules (Figure I.11B) (Nigg et al. 2011). Given the importance of the bipolar microtubule spindle in the segregation of chromosomes to the two progeny cells during mitosis, abnormalities in the formation, function, or duplication of centrosomes can result in abnormal cytokinesis, genetic aberrations, and genome instability. siRNA-mediated depletion of ORC1 has been reported to result in Cdk2 and Cyclin E-dependent re-duplication of centromeres and centrioles, while overexpression blocks re-duplication (Hemerly et al. 2009). Cyclin A-dependent localisation of ORC1 to centrosomes via the PACT domain of ORC1 has been proposed to regulate the prevention of re-duplication (Hossain et al. 2012). Depletion of ORC2 in HeLa cells has been reported to result in multipolar spindles and multinucleation (Prasanth et al. 2002). ORC6 has implicated in the regulation of centrosome copy number, as depletion of ORC6 in DT40 chicken cells results in supernumary centrosomes and subsequent mis-segregation of chromosomes (Bernal et al. 2011). Recent unpublished findings from our lab have further supported the model that origin licensing components are required for proper centrosome and centriole duplication. Cells from an ORC1-deficient MGS patient (ORC1-P1) (Bicknell et al. 2011b) display supernumary centrosomes and abnormal centrioles (S. Walker, unpublished findings) (Figure I.11C). In addition, siRNA-mediated depletion of ORC4, ORC6, CDC6, and CDT1 lead to an increase in the fraction of cells containing supernumary centrosomes (T. Stiff, unpublished findings).

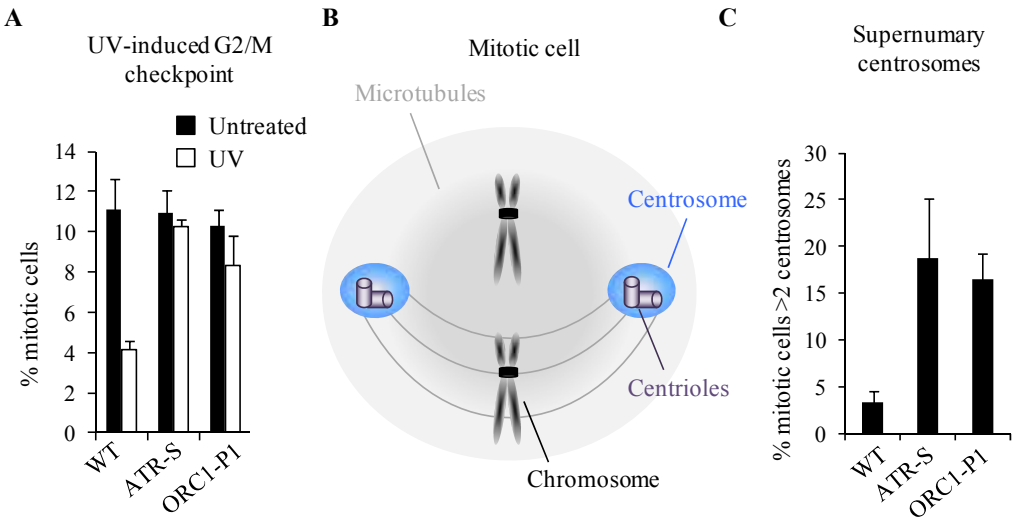

Figure I.11 Additional roles of ORC1. A. ORC1-deficient cells are defective in the UV-induced G2/M checkpoint. Cells from a normal individual (WT), an ATR-deficient Seckel Syndrome patient (ATR-S), or an ORC1-deficient MGS patient (ORC1-P1) individuals were untreated or treated with 5J/m^2 UV. One hour later, the fraction of mitotic cells was assessed (Section II.6.3). A decrease in the mitotic fraction indicates activation of the G2/M checkpoint (S. Walker, unpublished results). **B**. Schematic depicting the location of chromosomes, centrosomes, centrioles, and microtubules in a mitotic (metaphase) cell. **C**. ORC1-deficient cells contain supernumary centrosomes. Cells described in (A) were treated with nocodazole for 24 hours to increase mitotic fraction, centrosomes were examined by immunofluorescence (Section II.6) using an antibody to γ-tubulin, and the fraction of mitotic containing >2 centrosomes was scored (S. Walker, unpublished results).

Several pre-RC components have also been implicated in the building and/or maintenance of higher-order chromatin structure (Chakraborty et al. 2011). Various components of the pre-RC have been reported to localise to heterochromatin and interact with chromatin factors (Table I.3) (Alabert et al. 2012). ORC1, CDT1, and MCM2 interact with the Histone H3 and H4 acetyltransferase, histone acetyltransferase binding to ORC (HBO1) (Iizuka et al. 1999; Burke et al. 2001). As introduced in Section I.4, ORC1 and ORC6 have been reported to interact with an AT-rich domain in HMGA1a, a high mobility group protein which binds to the minor groove of A-T dinucleotide regions and induces structural changes (Thomae et al. 2008). The interaction localises to heterochromatin regions and has been shown to affect the recruitment of ORC to DNA. However, whether the ORC-HMGA1a interaction directly impacts upon chromatin structure is unknown. More recently, ORC2 and CDT1 have been shown to interact with ORC-associated (ORCA) (Shen et al. 2012). This interaction is thought to participate in the recruitment ORC to DNA (Shen et al. 2010). ORC1 has been reported to interact with telomere repeat factor 2 (TRF2) and telomere-repeat-encoding RNA (TERRA) and these interaction promote localisation of ORC to telomeres to facilitate heterochromatin formation and/or replication initiation (Atanasiu et al. 2006; Deng et al. 2009). Finally, ORC1 and ORC3 directly interact with HP1α. As discussed in more depth in Chapter V, the interaction between ORC and HP1α has been demonstrated to impact upon heterochromatin structure (Prasanth et al. 2010).

Chromatin factors	Proposed function	Interaction
HBO1 (Zn domain)	RI	ORC1 (aa210-861)
		CDT1
H4 (K20me2)	RI	ORC1 (BAH domain)
ORCA (WD-repeat domain)	RI	ORC2
		CDT1
HMGA1a (AT-rich domain)	RI	ORC1
	RI	ORC6
TRF2 (N-term)	RI, ORC localisation at telomeres	ORC1
HP1α (chromoshadow domain)	RI, ORC recruitment, HC organisation	ORC1 (N-term)
		ORC3 (MIR domain)

Table I.3. Interactions reported in humans between chromatin factors and ORC, CDC6 or CDT1. RI: replication initiation, HC: heterochromatin

I.6 Microcephalic primordial dwarfism

Microcephalic primordial dwarfism (MPD) encompasses a group of syndromes including Seckel Syndrome (Majewski et al. 1982), Microcephalic/Majewski osteodysplastic primordial dwarfism types I and II (MOPD I/II), (Majewski et al. 1982; Hall et al. 2004), and MGS (Gorlin 1992). MPD syndromes are characterised by microcephaly accompanied by severe pre- and post-natal growth retardation. Seckel Syndrome patients harbouring mutations in *ATR* (O'Driscoll et al. 2003), centromere protein J (*CENPJ)* (Al-Dosari et al. 2010), centrosomal protein 152 kDa (*CEP152*) (Kalay et al. 2011), *CtIP* (Qvist et al. 2011), and *ATRIP* (Ogi et al. 2012) have been identified. Mutations in the centrosomal protein pericentrin (*PCNT)* have been reported in MOPD II patients and patients originally classified as having Seckel Syndrome (Griffith et al. 2008; Rauch et al. 2008; Willems et al. 2010). Mutations in a component of the spliceosome, U4atac snRNA, have also been reported in patients with MOPD I (He et al. 2011; Abdel-Salam et al. 2012; Nagy et al. 2012).

Recently, hypomorphic mutations in the origin licensing components *ORC1, ORC4, ORC6, CDC6 and CDT1* have been identified in MGS patients (Bicknell et al. 2011a; Bicknell et al. 2011b; Guernsey et al. 2011; de Munnik et al. 2012) (Table I.4). These mutations are observed to result in either a reduction in protein level or in chromatin binding capacity. Because cells license up to 10 fold more origins than are required for a typical round of replication, (Section I.4.3), cells from these MGS patients are able to proliferate despite a substantial reduction in origin licensing capacity.

In addition to the short stature and microcephaly characteristic of MPD disorders, most of the origin licensing-deficient MGS patients also displayed microtia (abnormal ear development), delayed bone age, abnormal or absent patellae (kneecaps) and full lips (de Munnik et al. 2012).

Selected clinical features	ORC1 (n=10)	ORC4 (n=7)	ORC6 (=7)	CDC6 (n=1)	CDT1 (n=10)
Microcephaly	8/8	2/5	1/6	0/1	2/9
Head circumference (cm)*	-9.8 to -4	-3.2 to -0.7	-3.3 to -1.6	-1.8	-5 to -1.7
Height (cm) *	-5.2 to -9.6	-6.4 to -1.8	-3.3 to -0.8	-3.5	-6 to -0.4
Short stature	10/10	6/7	6/7	1/1	8/10
Microtia	9/10	7/7	7/7	1/1	10/10
Delayed bone age	3/4	4/7	4/5	1/1	2/5
Abnormal/absent patellae	6/7	7/7	6/7	1/1	10/10
Full lips	7/10	2/5	5/7	1/1	6/9

Table I.4. Selected clinical features of MGS patients with biallelic mutations in origin licensing factors. Data and images compiled from (Bicknell et al. 2011a; Bicknell et al. 2011b; Guernsey et al. 2011; de Munnik et al. 2012). *standard deviations from the age-related normal population mean

While the limited number of individuals with origin licensing-deficient MGS makes it difficult to accurately identify distinctions between these patients, microcephaly seems to be more severe in ORC1-deficient patients compared with patients with defects in other licensing components (Table I.4). To date, all ORC1-deficient MGS patients have been identified to have at least one mutation located within the BAH domain (de Munnik et al. 2012), the region involved in interactions with chromatin at H4K20me2 and with HP1α (Figure I.12). In addition to having a deficiency in activating replication origins, cells from patients with ORC1-deficient MGS display slowed S-phase entry and progression (Bicknell et al. 2011b), abnormal activation of the UV-induced G2/M checkpoint, and supernumary centrosomes and centrioles (Figure I.11).

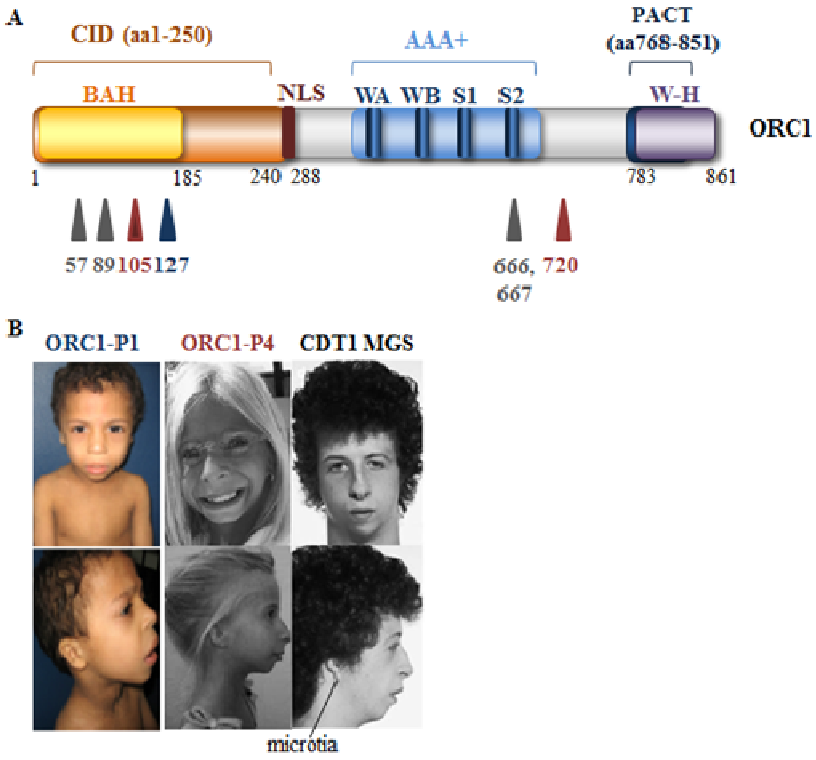

Figure I.12 ORC1-deficient MGS. A. Schematic depicting the locations of amino acid alterations resulting from ORC1 mutations in MGS patients. Blue arrows and numbers depict the amino acid alteration in patient 1 (ORC1-P1), red numbers and arrows depict two amino acid alterations identified in patient 4 (ORC1-P4), and grey arrows and numbers depict amino acid changes identified in other patients. **B.** Photographs of ORC1-P1, ORC1-P4, and CDT1-deficient MGS (individual 11). Microtia can clearly be observed in individual 11 (Bicknell et al. 2011b; de Munnik et al. 2012).

I.7 Thesis aims

In recent years, there has been much progress in our understanding of the crucial biological mechanisms which preserve genomic stability. However, many questions remain unresolved.

Important advances in technology and methodology have enabled the study of DNA repair processes at the level of a single DNA break. DNA damage signalling and repair is now being investigated in the context of higher-order chromatin structure, which has revealed interesting distinctions in pathway selection in the response to DSBs occurring within euchromatin or heterochromatin. However many questions about the precise role of various proteins in damage signalling and/or repair in chromatin regions remain unanswered. For example, while the role of ATM in heterochromatic DSB repair has been established, the precise function of the Artemis endonuclease in repair has yet to be fully elucidated. In Chapter III, I will describe a method of site-specific DSB induction using direct delivery of an endonuclease capable of introducing breaks within the highly repetitive regions of rDNA. Optimisation of this system has allowed for the assessment of DSB repair at regions likely to be enriched for heterochromatin. Findings obtained through the use of this methodology have consolidated the notion that Artemis functions in heterochromatic DSB repair in a manner that is independent of heterochromatin opening.

Chapters IV and V will then shift to focus on applied research, reflecting my interest in therapeutic and disease-related research.

The identification of MGS patients harbouring mutations in origin licensing machinery has opened up many questions about the importance of these factors in cellular processes. Availability of cell lines from these patients has enabled the study of the cellular impact of diminished origin licensing capacity. As described in Chapter IV, the role of origin licensing in the recovery from replication stress was examined in cell lines derived from healthy individuals or ORC-deficient MGS patients as well as in tumour-derived cell lines. My findings have suggested that while tumour-derived cell lines rely on dormant origin firing to recover from replication stress, non-tumour fibroblast cells can recover from replication stress despite a substantial reduction in origin licensing.

Factors involved in replication origin licensing have also been implicated in higher-order chromatin structure, though questions remain about their precise role. In Chapter V, I will present findings which substantiate published results showing that siRNA-mediated depletion of ORC results in changes in higher-order chromatin structure. Further, I will demonstrate that cells from ORC-deficient MGS patients also display characteristics consistent with disordered chromatin and that these chromatin alterations impact the DDR. These findings contribute to our understanding of the cellular phenotype of patients with ORC-deficient MGS.

Overall, this thesis aims to examine the cellular impact of diminished origin licensing capacity with a focus on the response to replication stress and higher-order chromatin structure. The implications of the findings presented in this thesis, including the potential therapeutic exploitation of origin licensing capacity, will be discussed in Chapter VI.

II Materials and methods

Unless otherwise stated, lab reagents were obtained from Sigma-Aldrich (Gillingham, UK).

II.1 Mammalian cell culture

Reagents for tissue culture were obtained from Gibco®, Invitrogen ™ (Paisley, UK). Cell culture dishes and flasks were obtained from Corning®Costar®, Sigma-Aldrich (Gillingham, UK). All growth medium described below was additionally supplemented with 2 mM L-Glutamine and 1% antibiotics (100 U/ml penicillin G and 100 mg/ml streptomycin).

The wildtype primary fibroblast line 48BR (Keyse et al. 1985) and human telomerase (hTERT)-immortalised fibroblast cell lines 1BR3hTERT (wildtype), BJhTERT (Jiang et al. 1999) (wildtype), F02/385hTERT (Riballo et al. 2004) (Artemis null), and ORC1-P4hTERT (Bicknell et al. 2011b) (ORC1 deficient) were cultured in Dulbecco's Modified Eagle's Medium (DMEM) supplemented with 15% fetal calf serum (FCS). Growth medium for BJ-MYC-ER, a derivative of BJhTERT which stably expresses a tamoxifen-inducible *c-Myc* gene (Littlewood et al. 1995; Murga et al. 2011) (kindly provided by Dr. Óscar Fernández-Captello), was additionally supplemented with 2 μM puromycin.

MRC-5 (wildtype lung fibroblast), U2OS (osteosarcoma), A549 (adenocarcinomic alveolar basal epithelial), HeLa (cervical adenocarcinoma) cell lines (obtained from ATCC) and NIH3T3 mouse embryonic fibroblasts (MEFs) were cultured in Minimum Essential Medium (MEM) supplemented with 10% FCS. MDA-MB-231 breast adenocarcinoma cells (ATCC) were cultured in DMEM supplemented with 10% FCS.

Lymphoblastoid cell lines (LBLs) derived from healthy individuals (GM02188 and AG09387, wild-type) or MGS patients deficient in ORC1 (Bicknell et al. 2011b), ORC6, CDC6, or CDT1 (Bicknell et al. 2011a) were cultured in Roswell Park Memorial Institute (RPMI)-1640 supplemented with 15% FCS.

All cell lines were maintained at 37°C in 5% carbon dioxide (CO_2) and passaged every 2-3 days. Adherent cells were passaged by trypsinization with 0.25% trypsin in 1 mM Ethylenediaminetetraacetic acid (EDTA)/ phosphate buffered saline (PBS). Stocks of cell lines were stored in liquid nitrogen in 70% growth medium, an additional 20% FCS, and 10% dimethyl sulfoxide (DMSO).

II.2 siRNA depletion

HiPerFect (Qiagen, Hilden, Germany) or Metafectene-Pro (Biotex, Planegg, Germany) transfection reagents were used to transfect logarithmically growing cells with siRNA oligonucleotides (Table II.1) according to manufacturer's instructions. Briefly, for transfection

with HiPerFect, siRNA oligonucleotides were mixed with HiPerFect transfection reagent and Opti-MEM® (Invitrogen, Paisley, UK) and incubated for 10 minutes prior to mixing with cells in suspension. For transfection with Metafectene-Pro, siRNA oligonucleotides and the transfection reagent were each mixed with Opti-MEM® (Invitrogen, Paisley, UK) in separate eppendorf tubes. These mixtures were combined and incubated for 15 minutes prior to mixing with cells in suspension. Unless otherwise stated in text, 0.5-1x10^5 cells per ml were transfected with 20 nM siRNA duplexes and grown for 48-72 hours prior to further analysis.

For experiments involving titrations of siRNA oligonucleotides, 2 fold serial dilutions were initially performed in 1x siRNA buffer (Dharmacon, Thermo Scientific, Loughborough, UK) prior to mixing with the transfection reagent and delivery to cells. Each siRNA titration was performed in triplicate.

ON-TARGETplus SMART pool siRNA oligonucleotides are reported to being highly specific, as verified by microarray analysis, as a result of unique dual-strand modification patterns used to synthesise the reagents (http://www.thermoscientificbio.com/uploadedFiles/Resources/sirna-libraries-brochure.pdf).

siRNA	Species	Description	Supplier
siControl	N/a	Randomly scrambled control sequence	Dharmacon
siORC1single	human	5'CGUAUGUUGCUAAAUUGCUUGAGUU3	Invitrogen
siORC1pool	human	ON-TARGETplus SMART pool	Dharmacon
siORC1	mouse	ON-TARGETplus SMART pool	Dharmacon
siORC6	human	ON-TARGETplus SMART pool	Dharmacon
siCDT1	human	ON-TARGETplus SMART pool	Dharmacon
siCDC6	human	ON-TARGETplus SMART pool	Dharmacon
sip53	human	ON-TARGETplus SMART pool	Dharmacon
siKAP-1	human	5'CAGUGCUGCACUAGCUGUGAGGAUA3'	Invitrogen
siKAP-1	mouse	5'AAGAUGCAGUGAGGAACCAACGUAA3	Invitrogen
siArtemis	human	ON-TARGETplus SMART pool	Dharmacon
si53BP1	human	5'AGAACGAGGAGACGGUAAUAGUGGG3	Qiagen
siRNF8	human	'A' 5'GGACAAUUAUGGACAACAA3' 'B' 5'UGCGGAGUAUGAAUAUGAA3'	Invitrogen
siHP1α	human	5'GGUUAAGGGACAAGUGGAAUAUCUA3	Invitrogen

Table II.1. siRNA oligonucleotides.

II.3 I-*Ppo*I system of site-specific DSB induction

II.3.1 Plasmids used for I-*Ppo*I expression and *in vitro* analysis of activity

Expression of the intron-encoded Physarum polycephalum endonuclease (I-*PpoI*) was carried out using a pET-45b(+) expression vector (I-PpoI-his / pET-45b(+)) (Wen, Cerosaletti et al. 2012) constructed and kindly provided by Dr. Jie Wen and Dr. Patrick Concannon. Briefly, the open reading frame of I-*Ppo*I was synthesised and cloned into the pUC57 vector, excised by restriction digestion, and ligated into the pET-45b(+) expression vector (containing a T7 promoter, ampicillin resistance (AmpR) gene, and polyhistidine (his)-epitope tag) (Figure III.3B).

For analysis of I-*Ppo*I functional activity *in vitro*, the 15 bp I-*Ppo*I recognition sequence was cloned into the pcDNA3.1 vector (containing a T7 promoter and AmpR gene) (I-*Ppo*I site/ pcDNA3.1A(+), Figure III.4A) (also constructed and kindly provided by Dr. Jie Wen and Dr. Patrick Concannon).

These and all other plasmids exploited in this thesis were amplified using DH5α competent cells, and isolated by the MaxiPrep purification according to manufacturer's instructions (Qiagen, Hilden, Germany).

II.3.2 I-*Ppo*I protein expression in *Escherichia coli*

An inducible system of protein expression exploiting the lac operon regulatory process in *Escherichia coli* (*E. coli*) was used to generate sufficient volumes of his-tagged I-*Ppo*I. BL21 (DE3) competent *E. coli* (New England Biolabs, Hitchin, UK) were transformed with 500 ng of the (I-*Ppo*I-his / pET-45b(+)) (Section II.3.1, Figure III.3B) and cultured overnight on lysogeny broth (LB)-agar plates supplemented with 100 µg/l ampicillin. The following day, ampicillin-resistant clones were selected and cultured in a shaking incubator at 225 revolutions per minute (rpm) at 37˚C. Cultures were scaled up and grown in LB supplemented with 100 µg/L ampicillin as well as 1 mM zinc acetate to allow for proper protein folding and stability. The optical density at a wavelength of 600 nm (OD_{600}) was monitored periodically over time using the Ultraspec 2100 pro UV spectrophotometer (Amersham, GE Healthcare Life Sciences, Buckinghamshire, UK). Once an OD_{600} reading of approximately 0.4 was obtained, protein expression was induced by adding 1 mM Isopropyl-β-D-thio-galactoside (IPTG) and an additional 1mM zinc acetate to the culture. BL21 (DE3) cells were then harvested 3.5-4 hours later. Following a wash in PBS, and centrifugation at 8,000 rpm for 10 minutes at 4°C, pellets were resuspended in cold lysis buffer (25 mM MOPS-NaOH, 1.25 mM EDTA, deoxyribonuclease, and PMSF in PBS) supplemented with 1mM $MgCl_2$ (AnalaR NORMAPUR®, VWR, East Grinstead, UK) and a protease inhibitor cocktail (Complete Mini

tablet) (Roche Applied Sciences, Burgess Hill, UK). Bacterial plasma membrane was disrupted using a French pressure cell press and cellular debris and membranes were separated from lysates by centrifugation at 4°C.

II.3.3 I-*Ppo*I protein purification

Purification of his-tagged I-*Ppo*I protein was performed using a nickel-nitrilotriacetic acid (NTA) purification system. Bacterial lysates were mixed with Nickel-NTA agarose beads (Qiagen, Hilden, Germany) to allow for binding of the his tag with nickel ions. Protein-bound beads were washed three times in wash buffer (50 mM $NaH_2PO_4.H_2O$, 300 mM NaCl, 20 mM imidazole, pH 8) and the his-tagged I-*Ppo*I protein was eluted from beads using elution buffer (50 mM NaH_2PO_4, 300 mM NaCl, 250 mM imidazole at pH 8.0) supplemented with the protease inhibitors (Roche Applied Sciences, Burgess Hill, UK). 15 µl of each wash and elution fraction were mixed with 3 µl sodium dodecyl sulfate (SDS) loading buffer (10% w/v SDS, 50% glycerol, 5% β-mercaptoethanol, 0.4 M Tris pH6.8, and 0.6 % w/v bromophenol blue) and stored at -20°C.

Protein samples were separated by SDS polyacrylamide gel electrophoresis (SDS-PAGE) and gels were stained using Coomassie Blue to examine protein yield at each stage of wash and elution (Section II.4). Vivaspin™ centrifugal concentrators (Sartorius, Epsom, UK) were used to concentrate protein into storage buffer (0.5 M Tris pH 8.0, 2 mM EDTA, 50% glycerol, 75 mM KCl) supplemented with protease inhibitors (Roche Applied Sciences, Burgess Hill, UK). Protein concentration was assessed using the colorimetric DC assay (Bio-Rad, Hemel Hempstead, UK) according to supplier's instructions. Purity of concentrated protein was assessed by SDS-PAGE electrophoresis and Coomassie Blue staining (Section II.4).

II.3.4 *In vitro* I-*Ppo*I plasmid assay

In vitro activity of purified and concentrated his-tagged I-*Ppo*I was verified using the I-*Ppo*I site/ pcDNA3.1A(+) vector (Section II.3.1, Figure III.4A). Indicated concentrations of purified I-*Ppo*I protein were incubated with 4 µg of plasmid DNA in I-*Ppo*I buffer (Promega, Southampton, UK) diluted in 50 mM Tris-Hydrochloric acid (HCl) pH7.4, 1mM EDTA, 1 mM DTT, 10% glycerol and 100 ng/µl bovine serum albumin (BSA) (Promega, Southampton, UK). Protein digestion of plasmid DNA was performed at 37ºC for 45 minutes and was then inhibited by incubating samples at 60ºC for 20 minutes. Samples were diluted in 6x DNA loading buffer (Invitrogen ™, Paisley, UK) and loaded alongside a DNA ladder (Invitrogen ™, Paisley, UK) on gel made up of 1% agarose and 0.5µg/ml ethidium bromide intercalating agent in Tris/Borate/Ethylenediaminetetraacetic acid (TBE) buffer (89 mM Tris base, 89 mM Boric acid, 2 mM EDTA). DNA was separated with 100 V for approximately 1 hour in TBE buffer and UV

illumination of the gel was used to visualise ethidium bromide labeled DNA bands. Images were captured with a gel imaging system (InGenius, Syngene, Cambridge, UK). Efficiency of the DNA digestion was assessed by comparing the size of the DNA product after each digestion with that of an undigested plasmid control.

II.3.5 Delivery of I-*Ppo*I to cells

Purified his-tagged I-*Ppo*I protein and/or Alexa-Fluor 488 (AF-488) (Invitrogen™, Paisley, UK) were delivered to cells using the synthetic peptide carrier Pep-1 Cysteamine (Anaspec, Cambridge, UK). First, cells were seeded onto glass coverslips and grown in normal growth medium for 24-48 hours. Next, peptide carrier and protein complexes were allowed to form for 30 minutes at 37°C in 500 µl serum-free MEM per sample. A peptide: protein molar ratio of 1:20-1:40 was used for efficient macromolecule formation (Morris et al. 2001). 1 ml of normal growth medium was then added to the volume and media on cells was replaced with the peptide: protein complex mixture. At indicated time points following I-*Ppo*I protein delivery, cells were fixed for immunofluorescence analysis. DSB induction and repair was assessed by immunofluorescence labelling of γH2AX and/or 53BP1 (Section II.6).

II.4 SDS-PAGE protein analysis

II.4.1 Preparation of cell extracts

Cells were seeded in tissue culture flasks ($1x10^6$ cells per flask) and grown for 48 hours. Cells were washed in 1 mM EDTA and trypsinized with 0.25% trypsin/EDTA. Trypsin was quenched by adding an equal volume of growth medium, and cells were collected and pelleted by centrifugation at 1500 rpm for 5 minutes. Cell pellets were washed twice in ice cold PBS, and pellets were lysed on ice, in ~20 µL of lysis buffer per 1 million cells.

For whole cell extracts, cells were lysed in Lysis Buffer A (50 mM Tris-HCl, 2 mM EDTA, 2 mM EGTA, 25 mM NaF, 25 mM B-glycerophosphate, 0.1 mM NaOrthovanadate, 0.2% Triton X-100, and 0.3% NP-40) containing 500 mM NaCl and supplemented with protease inhibitor (Sigma Aldrich, Gillingham, UK or Roche Applied Sciences, Burgess Hill, UK) and phosphotase inhibitor cocktails (Thermo Fisher, Loughborough, UK or Roche Applied Sciences, Burgess Hill, UK) for one hour, vortexing every 15 minutes. Pulsed sonication was applied to lysates in a 4°C water bath for 15 minutes and lysates were centrifuged at 14,000 rpm at 4°C for 20 minutes to separate any remaining cellular residue.

For fractionation of soluble and insoluble proteins, cells were scored and an equal number of cells for each sample were first lysed in Lysis Buffer A containing 150 mM NaCl and supplemented with protease and phosphatase inhibitors as described above. One hour later,

extracts were centrifuged at 14,000 rpm at 4°C for 10 minutes and the supernatant, containing soluble proteins, was transferred to fresh pre-chilled tubes. Pellets were resuspended in Lysis Buffer A containing 300 mM NaCl and supplemented as described above and pulsed sonication was applied to lysates in a 4°C water bath for 15 minutes.

All cellular lysates were stored at -80°C, avoiding multiple freeze-thaw cycles to minimize protein degradation. Protein concentrations of whole cell extracts and extracts containing unbound proteins were estimated using the Bradford Protein Assay (Bio-Rad, Hemel Hempstead, UK), according to manufacturer's instructions, at a UV absorbance of 595 nM. Prior to SDS-PAGE, the volume of lysate needed to achieve the desired amount of protein was transferred to a new tube and diluted in 2x high SDS loading buffer (5% SDS, 10% glycerol, 10% β-mercaptoethanol, 0.125 M Tris pH6.8, and 0.2% w/v bromophenol blue). Insoluble fractions were directly diluted in 2X SDS loading buffer. Samples diluted in SDS loading buffer were boiled in a 99°C water bath for 5-10 minutes to denature protein, centrifuged briefly and loaded onto pre-cast polyacrylamide gels as described below.

II.4.2 Gel electrophoresis

Proteins were separated using the Laemilli SDS-PAGE system. Resolving gels made up of 0.375 M Tris pH8.8, 0.1% SDS, 0.1% ammonium persulfate (APS), 0.1% Tetramethylethylenediamine (TEMED) (Fluka, Sigma-Aldrich, Gillingham, UK), and either 8%, 10%, or 17.5% polyacrylamide (Protogel, National Diagnostics, Fisher Scientific, Loughborough, UK) and stacking gels comprised of 0.125 M Tris pH6.8, 0.1% SDS, 0.1% APS, 0.1% TEMED, and 4%, 5%, or 6% polyacrylamide (Table II.2) were prepared prior to electrophoresis. Samples were loaded onto pre-cast polyacrylamide gels in 1 mm gel cassettes (Invitrogen ™, Paisley, UK). In order to monitor migration of proteins of various sizes, the 250kDa Precision Plus Protein™ standard (Bio-Rad, Hemel Hempstead, UK) was also loaded onto each gel. Polyacrylamide gels were resolved with 100-150 volts (V) in SDS running buffer (25 mM Tris-base, 192 mM Glycine, and 0.1% w/v SDS, pH8.3) for 1-2.5 hours using the X-cell SureLock^{TM} Mini-Cell electrophoresis system (Invitrogen ™, Paisley, UK). Gels were removed and subjected either to Coomassie blue staining or immunoblotting.

A. Resolving gels.

Reagent	8% resolving	10% resolving	17.5% resolving
ddH_2O	2.7 ml	2.2 ml	0.2 ml
30% polyacrylamide	2.13 ml	2.67 ml	4.67 ml
1 M Tris pH 8.8	3 ml	3 ml	3 ml
10% SDS	80 µl	80 µl	80 µl
10% APS	80 µl	80 µl	80 µl
TEMED	8 µl	8 µl	8 µl
Total Volume	8 ml	8 ml	8 ml

B. Stacking gels.

Reagent	4% stacking	5% stacking	6% stacking
ddH_2O	3.00 ml	2.812 ml	2.6 ml
30% polyacrylamide	0.67 ml	0.833 ml	1 ml
0.5 M Tris pH 6.8	1.25 ml	1.25 ml	1.25 ml
10% SDS	50 µl	50 µl	50 µl
10% APS	50 µl	50 µl	50 µl
TEMED	5 µl	5 µl	5 µl
Total Volume	5 ml	5 ml	5 ml

Table II.2. 1mm mini SDS-PAGE gels.

II.4.3 Coomassie blue staining

For analysis of total protein levels following electrophoresis of purified I-*Ppo*I protein samples (Section II.3), gels were rinsed in water and incubated in Coomassie brilliant blue staining solution (0.05% Brilliant Blue R-250, 50% methanol, and ddH_2O) for 15 minutes on a shaker. Gels were rinsed in ddH_2O and washed three times in de-stain buffer (10% v/v acetic acid, 40% v/v methanol in ddH_2O) for 15 minutes each wash. Gels were dried using a gel dryer and vacuum system and were imaged with an Epsom (Hemel Hempstead, UK) scanner.

II.4.4 Immunoblotting

Proteins were transferred from gels onto pre-wet 0.4 µm Hybond™-P polyvinylidene difluoride (PVDF) (GE Healthcare Life Sciences, Buckinghamshire, UK) or 0.2 µm nitrocellulose (Bio-Rad, Hemel Hempstead, UK) membranes in cold transfer buffer (25 mM Tris, 192 mM Glycine, 20% methanol, pH8.3) with 100 V for 1 hour using the Mini Trans-Blot® system (Bio-Rad, Hemel Hempstead, UK) according to manufacturer's instructions. Membranes were then washed with Tris-buffered saline (TBS) (150mM NaCl, 10mM Tris, pH7.5) with 0.1 % Tween-20 (TSB-T) for 5 minutes on a shaker.

Membranes were blocked with gentle shaking for 20-60 minutes at room temperature in blocking buffer, consisting of 5% w/v non-fat dried milk (NFDM) (Marvel, Premier Foods, St. Albans, UK) or 5% BSA in TBS-T. Following a brief wash in TBS-T, membranes were then incubated with primary antibodies (Table II.3) diluted in blocking buffer with gentle shaking for 1 hour at room temperature or overnight at 4°C. Membranes were then subjected to three 10 minute washes in TBS-T with vigorous shaking. Anti-goat, rabbit, or mouse-horseradish peroxidase (HRP)-conjugated secondary antibodies (Dako, Cambridgeshire, UK) were diluted at 1:2000 in blocking buffer and applied to membranes for 45-60 minutes at room temperature with gentle shaking. Membranes were again subjected to three 10 minute washes in TBS-T, excess moisture was removed, and enhanced chemilluminescence (ECL) detection reagents (Pierce Biotechnology, Thermo Scientific, Loughborough, UK) were applied according to manufacturers' instructions. Membranes were exposed onto high performance chemilluminescence film (Amersham, GE Healthcare Life Sciences, Buckinghamshire, UK) to visualise protein bands. Films were developed using an x-ray film processor (Xograph, Gloucester, UK) and imaged with an Epsom scanner (Hemel Hempstead, UK).

Semi-quantitative analysis was performed on tagged image file format (tiff) files from scanned images of films using Image J software (National Institutes of Health, http://rsbweb.nih.gov/ij/).

Protein	Clone/#	Raised against	Species	Supp	kDa	Dilution
ORC1	N-17	N-terminus	Goat polyclonal	SCB	120	1:200
ORC2	H-300	C-terminus (aa275-577)	Rabbit polyclonal	SCB	70	1:200
ORC4	L-15	Internal region	Goat polyclonal	SCB	45	1:200
ORC6	FL-252	Full length (aa1-252)	Rabbit polyclonal	SCB	30	1:200
CDT1	H-300	C-terminus (aa247-546)	Rabbit polyclonal	SCB	65	1:200
CDC6	180.2	Full length	Mouse monoclonal	SCB	62	1:200
KAP-1	3831	C-terminus (aa741-753)	Goat polyclonal	AB	110	1:1000
p53	DO-1	N-terminus (aa11-25)	Mouse monoclonal	SCB	53	1:200
β-actin	8226	N-terminus (aa1-100)	Mouse monoclonal	AB	42	1:10,000

Table II.3. Primary antibodies for immunoblotting. AB: Abcam® (Cambridge, UK); SCB: Santa Cruz Biotechnology, Inc. (Heidelberg, Germany); Supp: supplier

II.5 DNA damage-inducing reagents and IR

Cells were grown for 48 hours prior to treatment with DNA damage-inducing reagents unless otherwise stated.

For experiments involving IR treatment, cells were grown on glass coverslips in tissue culture dishes and were irradiated using a ^{137}Cs source (9 Gy per minute) or with 250 kV X-rays, delivered at 12 mA (0.5 Gy/minute). The ATM inhibitor (ATMi), KU-55933 (Calbiochem, VWR, East Grinstead, UK), was administered to cells at 10 μM 30 minutes prior to IR or I-*Ppo*I transduction. KU-55933 is reported to inhibit ATM kinase activity at low concentrations, with the half maximum inhibitory concentration (IC_{50}) of ~13 nM, and at a concentration of 10 μM, this compound was not found to inhibit other kinases in a commercially-available panel (Hickson et al. 2004). The DNA-PK inhibitor (DNA-PKi), NU-7441/KU-57788 (a gift from KuDOS Pharmaceuticals) is a highly selective inhibitor of DNA-PK with the IC_{50} of ~14 nM and at a concentration of 10 μM, this compound was also not found to inhibit other kinases in a commercially-available panel (Leahy et al. 2004). DNA-PKi was administered to cells at 10 μM 30 minutes prior to IR or I-*Ppo*I transduction. 4μM of the DNA polymerase inhibitor, aphidicolin, was added at the time of IR to prevent cells irradiated in S-phase from progressing into G2-phase and to distinguish S-phase cells during analyses.

For experiments examining the response to replication stress, serial dilutions of reagents were initially performed in an appropriate solvent (PBS or DMSO) prior to addition to cells in growth medium. HU or H_2O_2 (Acros Organics, Thermo Scientific, Loughborough, UK) were used at concentrations indicated for 24 hours (unless otherwise stated). Cells were then washed three times in PBS and incubated in fresh growth media for the indicated times. UCN-01, a Chk1/2 kinase inhibitor (Busby et al. 2000; Graves et al. 2000), was either administered as single agents to cells at various doses, as indicated, or were added in combination with HU. For combination treatments, 50 nM UCN-01 were added 1 hour prior to treatment with HU and were re-administered at the same dose following release from HU. Overexpression of the c-Myc oncogene was induced in BJ-MYC-ER cells via the addition of tamoxifen to cells at the indicated doses.

II.6 Immunofluorescence

For immunofluorescence analysis of adherent siRNA-treated cell lines, cells were transfected with siRNA oligonucleotides as indicated (Section II.2), seeded onto glass coverslips in 30 mm tissue culture dishes, and grown for 48 hours. Cells were then treated with IR/damage-inducing agents (Section II.5) or were incubated with purified I-*Ppo*I protein mixed with Pep-1 Cysteamine (Section II.3). At the indicated time, cells were then washed in PBS, fixed in 3%

w/v paraformaldehyde (PFA)/2% w/v sucrose/PBS for 10 minutes, and washed again in PBS. Coverslips were stored in PBS at 4°C.

Permeabilization was performed at room temperature for 3 minutes in 0.2% w/v Triton X-100/PBS. Following three washes in PBS, cells were incubated with the indicated primary antibodies (Table II.4) diluted in 2% w/v BSA/PBS for one hour at room temperature. Then, cells were washed three times and incubated with anti-mouse- Fluorescein isothiocyanate (FITC)-conjugated or anti-rabbit-Cyanine 3(Cy3)-conjugated secondary antibodies diluted at 1:200 in 2% w/v BSA/PBS for 30 minutes at room temperature away from light. Cells were washed again and DNA was fluorescently labeled by incubating cells in 1µg/ml DAPI/PBS for 10 minutes away from light. Following a final three washes in PBS, cover slips were mounted onto glass slides using Vectashield mounting media (Vector Laboratories, Peterborough, UK) and edges were sealed using nail varnish. Slides were stored at 4°C prior to analysis.

Fixation and immunofluorescence labelling in LBLs was performed as described in Section II.6.3.

Protein	Clone/ #	Raised against	Species	Supp	Dilution
H3K9me3	8898	aa1-100	Rabbit	AB	1:800
H4K20me3	9053	aa1-100	Rabbit	AB	1:200
HP1(αβγ)	FL-191	Full length (aa1-191)	Rabbit	SCB	1:100
CENP-F	ab5	C-terminus	Rabbit	AB	1:1000
p-H3(Ser10)	06-570	phosphorylated Ser10	Rabbit	UCM	1:400
53BP1	21083	C-terminus	Rabbit	AB	1:1000
γH2AX	18311	phosphorylated Ser139	Mouse	AB	1:800

Table II.4. Primary antibodies for immunofluorescence assays. AB: Abcam® (Cambridge, UK); SCB: Santa Cruz Biotechnology, Inc. (Heidelberg, Germany); Supp: supplier; UCM: Upstate & Chemicon, Merck Millipore, Watford, UK).

II.6.1 DSB repair analysis in G0/G1 cells

DSBs can be measured by the appearance of distinct γH2AX foci and repair of these breaks can be determined by the rate of disappearance of the foci (Lobrich et al. 2010; Brunton et al. 2011). Given the fact that DSB repair pathway choice varies with cell cycle phase (Beucher et al. 2009), methodology was used to distinguish G0/G1-, S-, G2-, and M-phase cells during analysis. To achieve this, 4μM aphidicolin was added at the time of damage (Section II.5), which prevents cells damaged in S-phase from progressing through the cell cycle and enables discrimination of these cells, given the striking pan-nuclear γH2AX signal observed rapidly after aphidicolin-induced S-phase damage. Previous studies have demonstrated that the repair of DSBs in G0/G1 and G2 is not affected by aphidicolin (Deckbar et al. 2007; Shibata et al. 2010). In addition, co-staining slides with an antibody to the cell cycle marker, centromere protein F (CENPF) (Table II.4), enables the discrimination of G2- or M-phase cells from other phases of cell cycle. Mitotic cells may be distinguished from G2-phase cells by morphological changes in chromatin condensation, which may also be observed in the DAPI channel (Beucher et al. 2009; Lobrich et al. 2010; Shibata et al. 2010).

The number of γH2AX foci per G0/G1 nucleus were manually scored in >90 cells per condition (unless otherwise stated) using a 100x lens on a Zeiss Axioplan (Carl Zeiss Ltd., Cambridge, UK) microscope. Images were acquired with identical exposure settings using SimplePCI software and a digital camera (Hamamatsu, Welwyn Garden City, UK). Data is presented in box plots including all data from three independent experiments or in bar graphs depicting the mean values +/- SD from at least three independent experiments. Statistical significance was determined using t-test or Mann-Whitney analyses in SigmaPlot (Systat Software, Inc., Hounslow, UK).

II.6.2 Analysis of replication stress-induced damage

The accumulation of S-phase damage was assessed in cells treated with damage-inducing agents (Section II.5) using immunofluorescence labelling of γH2AX, the cell cycle marker CENPF (Table II.4), and DNA (DAPI). As described above, S-phase damaged cells display a striking pan-nuclear γH2AX signal with minimal CENPF signal (termed $\gamma H2AX^{+}$). The fraction of $\gamma H2AX^{+}$cells was determined by manually scoring >500 cells per condition. Plots represent the mean values +/- SD from at least three independent experiments. Images were acquired as described above using a 40x lens.

II.6.3 G2/M checkpoint assay

To assess efficiency of the IR-induced G2/M checkpoint induction, cells were treated with the indicated doses of IR, treated with aphidicolin (Section II.5) to prevent S-phase damaged cells from progressing through cell cycle, and harvested after 1 or 2 hours for analysis of LBLs or fibroblasts, respectively. For examination of the maintenance of this checkpoint, cells were treated with 2Gy IR and aphidicolin and were grown for the indicated times prior to harvesting.

For analysis of the G2/M checkpoint using LBLs, cells were centrifuged at 18,000 RPM for 3 minutes, pellets were resuspended in hypotonic buffer (75 mM KCl), and cells were incubated for 10 minutes at 37°C to allow for cell swelling. Cells were then centrifuged at 700 RPM for 5 minutes and resuspended in 1µg/ml DAPI/PBS. LBLs were then mounted onto glass slides by cytospinning (700 RPM for 4 minutes), fixed with 3% w/v PFA/2% w/v sucrose/PBS for 10 minutes, and washed again in PBS. Mitotic cells were identified by characteristic changes in chromatin condensation, as observed by DAPI analysis.

For analysis of the G2/M checkpoint in fibroblasts, cells were labelled with 1µg/ml DAPI/PBS and an antibody to the M-phase marker, Histone H3 phosphorylated at Ser10 (p-H3(Ser10)) (Table II.4). As described previously (Brunton et al. 2011), mitotic cells were identified by positive labelling with p-H3(Ser10) and changes in chromatin condensation, as observed by DAPI analysis.

For all G2/M checkpoint analysis, >400 cells were manually scored per condition. Plots depict mean values +/- SD from at least three independent experiments unless otherwise stated.

II.6.4 γH2AX foci expansion into chromocentres

Exponentially growing but nearly confluent NIH3T3 MEFs were transfected with siRNA oligonucleotides (Section II.2), seeded onto glass coverslips in tissue culture dishes, and grown to confluency. Cells were then treated with 3Gy IR and aphidicolin (Section II.5), grown for 20-30 minutes, and fixed. Labelling with DAPI, anti-γH2AX, and anti-p-H3(Ser10) was performed to enable analysis of DSBs in G0/G1 and to identify DAPI-dense heterochromatin (chromocentres) as previously described (Brunton et al. 2011).

Z-stacked images of G0/G1 cells were taken using a 100x lens, an DeltaVision RT Olympus IX70 deconvolution microscope and digital camera, and softWoRx® Suite software (Applied Precision, Inc., Image Solutions, Preston, UK). For each cell, 25 sections (~5 µm thick) were imaged. Images were deconvolved and regions of γH2AX foci colocalising with DAPI-dense regions of HC (chromocentres) were identified in the red channel using SoftWoRx®. To assess the size of overlap between γH2AX foci and chromocentres, the total area of overlapping regions (depicted in the red channel) was quantified per cell using ImageJ

software (National Institutes of Health, Bethesda, Maryland, USA) and normalised to chromocentre number. For each experimental condition, all normalised cellular values were then averaged. Averaged values were further normalised to the average area of overlap per chromocentre in siControl-treated cells, generating values referred to as arbitrary units (A.U.). To assess the size of γH2AX foci regions which do no overlap with chromocentres, the area of each γH2AX foci (the square pixel number of regions microscopically detected in the green channel) was determined using ImageJ. Regions which overlap with chromocentres (detected in the red channel as described above) were eliminated from the analysis. The square pixel number of non-overlapping γH2AX foci regions was averaged for each experimental condition. All plots depict mean values +/- SD >2 independent experiments (n>200 chromocentres).

II.6.5 Analysis of nuclear signal intensity

siRNA-transfected cells were grown on glass coverslips for 48 hours, left untreated or treated with 3Gy IR and aphidicolin (Section II.5), grown for 20-30 minutes, and fixed. Coverslips were then stained with DAPI and anti-γH2AX as well as anti-H3K9me3, H4K20me3, or HP (αβγ) (Table II.4). Visualisation, imaging, and analysis were performed using a 40x objective on a Zeiss Axioplan (Carl Zeiss Ltd., Cambridge, UK) microscope. Images were acquired with identical exposure settings using SimplePCI software and a digital camera (Hamamatsu, Welwyn Garden City, UK). Nuclear intensity was quantified using SimplePCI in 40-100 cells per condition. Box plots depict representative results from a single experiment. Statistical significance was determined using t-test or Mann-Whitney analyses in SigmaPlot (Systat Software, Inc., Hounslow, UK).At least three independent experiments were performed to assess reproducibility.

II.7 Cell viability, clonogenic survival, and growth rate assays

II.7.1 Viability assay

Cells transfected with siRNA (Section II.2) were seeded in 96 well tissue culture dishes (700 cells per well), grown, and left untreated or treated with damage-inducing reagents (Section II.5). Test conditions were carried out in triplicate wells within each dish. Unless otherwise stated, viability was assessed seven days after seeding, using the CellTiter-Blue® viability assay (Promega, Southampton, UK), which measures the ability of cells to actively metabolize resazurin, a redox dye, into resorufin, a fluorescent product. 20 µl CellTiter-Blue® reagent was added to 100 µl cell growth medium on cells and to negative control wells (containing growth medium but no cells). Dishes were then incubated for 3-4 hours at 37°C in 5% CO_2 atmosphere, and readings of resorufin fluorescence were taken using the GloMax® multiwall plate reader

(Promega, Southampton, UK). Background correction was performed by subtracting the mean fluorescence reading from negative control wells from all other readings.

For assessment of the impact of siRNA treatment on viability in the absence of exogenous DNA damage, the mean background-corrected value of the test siRNA-transfected but untreated controls was normalized to that of the siControl. Plots depict mean viability (% siControl) +/- SD from at least three independent experiments.

To examine the impact of siRNA treatment on proliferation in the presence of damage-inducing agents, viability values were obtained by normalizing background-corrected readings to the mean value of siRNA-transfected but untreated controls for each siRNA condition. Representative plots depict mean viability (% untreated control) +/- standard deviation (SD) from triplicate samples (y-axis) versus concentration of the damage inducing agent (x-axis).

Sensitivity to DNA damage-inducing agents was estimated by calculating the IC_{50} from triplicate dose response curves in each dish with SigmaPlot (Systat Software, Inc., Hounslow, UK) using the five-parameter logistic nonlinear regression model. The impact of siRNA depletion on sensitivity was compared between cell lines by normalizing the IC_{50} value of the test siRNA to that of the siControl condition. Plots depict mean IC_{50} values (% siControl) +/- SD from at least three independent experiments.

II.7.2 Clonogenic survival

II.7.2.a Clonogenic survival in U2OS cells

U2OS cells were transfected with siRNA oligonucleotides (Section II.2), seeded at ~100 cells per well in tissue culture dishes, grown for 48 hours, and treated with HU for 24 hours (Section II.5). Dishes were then incubated for 10 days, stained with 1% w/v methylene blue (Fisher Scientific Loughborough, UK), washed twice with ddH_2O, and left to dry overnight at 37°C. Colonies of at least 50 cells were scored manually using the 1x objective on a light microscope. The surviving fraction was normalized to that of the untreated control. Plots depict mean values +/- SD from at least three independent experiments.

II.7.2.b Clonogenic survival in 1BR3hTERT cells

1BR3hTERT cells were transfected with siRNA oligonucleotides (Section II.2), grown for 48 hours, and treated with HU for 48 hours (Section II.5). 24 hours prior to release from HU, feeder cells were irradiated with 35 Gy γ-rays (Section II.5) and plated in MEM supplemented with 15% newborn calf serum and additional supplements (Section II.1) at $4x10^4$ cells/dish in 10 cm dishes. 24 hours after plating feeder cells, 1BR3hTERT cells were washed in 1XPBS,

trypsinized, and seeded at 100 cells per dish onto feeder plates. Dishes were then incubated for 21 days and colonies were labeled and assessed as described in Section II.7.2.a.

II.7.3 Growth rate studies

Exponentially growing cells were seeded at densities comparable to those used for the viability assay. Following incubation in normal growth medium at 37°C in 5% CO_2 atmosphere for indicated times, cells were harvested by trypsinization. Non-viable cells were labeled with trypan blue (Gibco®, Invitrogen ™, Paisley, UK) and healthy viable cells were manually scored. Cell number was normalized to the initial seeding density. Results represent mean values +/- SD from three experiments. Approximate doubling times were calculated from growth curves.

II.8 Flow cytometry

Cells were transfected with siRNA oligonucleotides (Section II.2), grown in tissue culture flasks for 48 hours, and treated with HU for 24 hours (Section II.5). 30 minutes prior to harvesting cells at the indicated times, newly synthesized DNA was labeled with 50 µM of the nucleoside analogue bromodeoxyuridine (BrdU) (BD, Oxford, UK) for 30 minutes at 37°C in 5% CO_2 atmosphere. Cells were then collected by trypsinization, washed twice at room temperature in 1% w/v BSA/PBS with 15 minute 500 g spins, resuspended into 200 µl cold PBS, and fixed by slowly pipetting cell suspension into 5 ml 70% aqueous ethanol in polypropylene tubes (Falcon™, BD, Oxford, UK). Fixed cells were then incubated at -20°C for at least 24 hours.

BrdU staining was carried out with a FITC-conjugated antibody (BD, Oxford, UK) as described by the manufacturer. Briefly, fixed cells were centrifuged at 500 g for 10 minutes at 10°C. Denaturation of DNA was achieved by slowly adding 1 ml 2 M HCl/ddH_20 while loosening the pellet, and cells were incubated at room temperature for 30 minutes. Cells were centrifuged again as described above and 0.1 M sodium tetraborate/water was added to cells for 2 minutes to neutralize the acid. Cells were pelleted and washed once in 1% BSA/PBS or directly incubated with the FITC-conjugated BrdU antibody diluted 20-25 fold in 1% BSA/PBS/0.25% Tween-20 for 30-60 minutes at 37°C or room temperature away from light. After a final centrifugation, DNA was stained with 10 µg/ml propidium iodide (PI) and 0.5 mg/ml ribonuclease (RNAse) in PBS for 10-20 minutes.

Cellular BrdU and PI levels were detected by flow cytometry using FACSCanto™ instrumentation (BD, Oxford, UK) and analysed using FACSDiva™ (BD, Oxford, UK) and WinMDI2.9 (The Scripps Research Institute, La Jolla, California, USA, http://facs.scripps.edu/software.html) software. Gating for specific cell cycle and BrdU-labelled

($BrdU^+$) populations was determined using experiment controls and applied to all samples within each experiment.

PI histograms are representative of reproducible results. Dot plots depict representative images of BrdU versus PI staining; boxed regions containing data points indicate $BrdU^+$ cells and adjacent numbers representing the $BrdU^+$ fraction. Bar plots depict mean values +/- SD from at least three independent experiments.

II.9 Complementation analysis

II.9.1 ORC1-GFP plasmid

A vector for expression of green fluorescent protein (GFP)-tagged ORC1 (ORC1-GFP) (Bicknell et al. 2011b) and empty vector were provided by Dr. Andrew Jackson. The coding sequence of ORC1 from the open reading frame shuttle clone IOH9757 (ImaGene) was cloned into a GFP epitope–tagged mammalian expression vector using Gateway cloning (Invitrogen ™, Paisley, UK).

II.9.2 ORC1 complementation in LBLs

GM02188 (WT) or ORC1-P1 LBLs in log phase growth were transfected with 2 μg empty vector or ORC1-GFP using GeneJuice® transfection reagent (Novagen/Merck Chemicals, Nottingham, UK) according to manufacturer's instructions every 24 hours for 72 hours. Efficiency of the G2/M checkpoint was performed as described in II.6.3 in cells positive for GFP signal.

II.9.3 ORC1 complementation in hTERT fibroblasts

1BR3hTERT (WT) or ORC1-P4hTERT cells were grown for 48 hours prior to transfection to achieve log phase growth. Cells were then transfected with indicated concentrations of empty vector or ORC1-GFP using Metafectene® Pro transfection reagent (Biotex, Planegg, Germany) according to manufacturer's instructions. Viability was assessed as in Section II.7.1 and replication associated DNA damage was assessed as in Section II.6.2 in cells positive for GFP signal.

III Examination of the role of Artemis in DSB repair during G0/G1 using a novel system of site-specific break induction

III.1 Introduction

III.1.1 The Artemis endonuclease and DSB repair

Artemis, a member of the metallo-β-lactamase family of nucleases, functions in both V(D)J recombination and the slow component of DSB repair at a subset of breaks (Ma et al. 2002; Riballo et al. 2004). Artemis is classified as an endonuclease and has the capacity to cleave a variety of DNA structures including 5' or 3' overhangs, flaps, gapped substrates, hairpins, pseudo Y structures, stem-loops, symmetrical bubbles, heterologous loops, and gapped DNA (Ma et al. 2005c). Artemis consists of an N-terminal β-lactamase domain (aa1-135) and a β-CASP domain (aa155-385) (Ma et al. 2005b) (Figure III.1.A). The C-terminal region of Artemis contains multiple PIKK target phosphorylation sites and appears to represent a regulatory region (Ma et al. 2005b; Goodarzi et al. 2006). While Artemis is phosphorylated by ATM in response to IR (Riballo et al. 2004), mutation of the phosphorylation sites does not impact upon DSB repair (Goodarzi et al. 2006). The function of these phosphorylation events still remains unknown.

Artemis was originally identified as the causal genetic defect in a group of Athabascan-speaking Native Americans with severe combined immunodeficiency (SCID) (SCID-A) (Li et al. 1998; Moshous et al. 2001). Mutations in *Artemis* were also identified in a subset of SCID patients with increased cellular radiation sensitivity (RS-SCID) (Moshous et al. 2001). The absence of T and B cells and severe immunodeficiency observed in Artemis-defective SCID reflects the critical role of Artemis in V(D)J recombination (Jackson et al. 1995). V(D)J recombination, which generates sequence diversity of T- and B-cell receptors, involves the induction of DSBs by the lymphocyte-specific recombination-activating genes 1 and 2 (RAG1 and RAG2) proteins in recombination signal sequences near the V(D)J segments. A DNA hairpin is generated at each coding end which must subsequently be opened to enable joining of segments by the NHEJ machinery. In complex with DNA-PK, Artemis is capable of performing the endonucleolytic cleavage 3' to RAG-generated hairpins (Ma et al. 2001) and alterations in this endonuclease lead to defects in the hairpin opening stage of V(D)J recombination (Mansilla-Soto et al. 2003). Therefore the critical function of Artemis in V(D)J recombination is thought to occur at the hairpin opening stage.

As introduced in Section I.3, in addition to this role in V(D)J recombination, Artemis is known to function in the repair of a subset of DSBs. Cells lacking Artemis display a defect exclusively in the slow repair of IR-induced DSBs during G0/G1 or G2-phase, a defect similar

to that observed in ATM-defective cells (Riballo et al. 2004) or in cells depleted for the mediator proteins (Noon et al. 2010). As introduced in Section I.3.4, the role of ATM in DSB repair during both G0/G1 and G2 involves the phosphorylation of KAP-1 on serine 824, which is proposed to promote localised decondensation of heterochromatin and DSB repair (Ziv et al. 2006; Goodarzi et al. 2008). The role of the mediator proteins such as 53BP1 and RNF8 is thought to involve the concentration of ATM activity at the site of the break (Noon et al. 2010). Under conditions of abnormal global chromatin compaction, the requirement for ATM and the mediator proteins in DSB repair can be bypassed since localised heterochromatin decondensation is no longer needed. Disruption of heterochromatin, for example, via depletion of KAP-1, the histone deacetylases (HDAC1/2), HP-1α/β/γ, MECP2, Suv39H1/2, DNMT3B (Goodarzi et al. 2008; Brunton et al. 2011) and SETDB1 (Y. Katsuki, unpublished findings) results in an alleviation of the DSB repair defect during G0/G1 as observed in cells depleted for ATM or the mediator proteins.

Similar to observations made in ATM-deficient cells, DSBs persisting in cells lacking Artemis have been demonstrated to localise to heterochromatic regions. Recent results from our lab have demonstrated that DSBs arising endogenously or from treatment with the oxidative damaging agent tert-butyl hydroperoxide (TBH) localise to regions of heterochromatin marked by KAP-1 serine 824 phosphorylation in Artemis-deficient cells (Woodbine et al. 2011). Further support for a role of Artemis in heterochromatic DSB repair has come from studies exploiting IR. 24 hours following IR, persisting DSBs localise to heterochromatin-rich chromocentres in Artemis-depleted MEFs (H. Brunton, unpublished findings) (Figure III.1.B) or to phosphorylated KAP-1 foci in Artemis defective human fibroblasts (Woodbine et al. 2011) to a similar extent as in Ataxia-telangiectasia patient cells which lack ATM. Also similar to ATM-deficient cells, cells lacking Artemis display a defect in a subset of DSBs repaired by NHEJ during G0/G1 (Riballo et al. 2004; Darroudi et al. 2007) and by HR during G2 (Beucher et al. 2009). However, unlike observations made in cells defective in ATM signalling, the requirement of Artemis for repair of IR or TBH-induced DSBs is not relieved in Artemis-deficient cells by depletion of KAP-1 (Woodbine et al. 2011). These results suggest that Artemis does not participate in heterochromatin relaxation, and instead has a role in promoting NHEJ or HR-mediated heterochromatic DSB repair distinct to that of ATM and downstream of KAP-1 phosphorylation. Overall, while findings from recent studies suggest that Artemis functions in the slow repair of heterochromatic DSBs, the precise nature of this role is still being investigated.

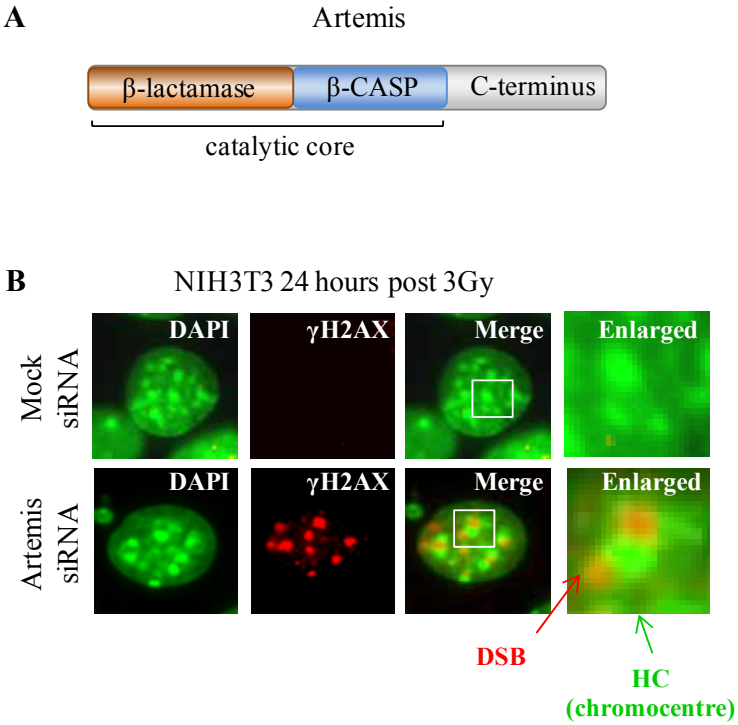

Figure III.1 The Artemis endonuclease and localisation of DSBs persisting in Artemis-depleted cells A. Schematic depicting domains in the Artemis protein. **B**. Images of immunofluorescence labelling of γH2AX (red) and DAPI (green) in Control or Artemis siRNA-transfected NIH3T3 MEFs 24 hours after 3 Gy IR (H. Brunton, unpublished findings).

The relatively low percentage of IR-induced DSBs that localise to heterochromatic regions of the genome poses limitations for monitoring IR-induced heterochromatic DSB repair. As introduced in Section I.2.2, IR induces a variety of DNA lesions, including SSBs that outnumber DSBs 20:1 (Bradley et al. 1979). Given that the lesions induced by IR occur indiscriminately across the genome and that most DNA is organised into euchromatin at any given time, the majority of these lesions do not tend to be localised to heterochromatin (Cowell et al. 2007; Goodarzi et al. 2008). Aside from generating DNA damage by IR, several systems of site-specific DSB induction exist, but these breaks rarely localise to heterochromatin. Further, these methods often require stable integration of a target sequence for a cleaving enzyme into the genome of a cell line, therefore restricting experiments to particular cell lines. These systems of site-specific DSB induction are not ideal for monitoring the kinetics of repair by enumeration of γH2AX foci since they are plagued by restrictions such as low cutting frequency and the capacity of active enzymes to re-cut at the same site.

To further examine the requirement for Artemis in DSB repair during G0/G1 and avoid the limitations introduced by DSB induction using IR or other existing systems of DSB induction, I have utilised a novel system introduced by Dr. Jie Wen and Dr. Patrick Concannon exploiting the rDNA-cleaving endonuclease, I-*Ppo*I (Wen et al. 2012).

III.1.2 I-*Ppo*I endonuclease

Several group I introns have the ability to act as mobile genetic elements by encoding rare-cutting endonucleases which can recognise and cleave DNA at a specific site 12-40 bp within an intron-free gene (Dujon 1989). Following induction of a DSB, a group I intron can act as a DNA template for repair of the break, thereby incorporating intronic DNA into the previously intron-free gene unit via recombination. This mechanism of endonuclease-driven gene conversion is known as homing (Dujon 1989; Belfort et al. 1997). Multiple homing endonucleases have been identified which recognise and cleave rDNA sequences in various species, including I-*Sce*I, which was discovered in the mitochondrial rDNA of *S. cerevisiae* (Colleaux et al. 1990), I-*Cre*I in the chloroplast 23S rDNA of *Chlamydomonas reinhardtii* (single celled green algae) (Sklar et al. 1986), and I-*Ppo*I in the nuclear rDNA of *Physarum polycephalum* (slime mold) (Muscarella et al. 1990). I-*Sce*I, I-*Cre*I, and I-*Ppo*I cleave rDNA at 18, 24, and 15 bp recognition sequences, respectively, generating four base 3' -OH overhangs (Sklar et al. 1986; Monteilhet et al. 1990; Muscarella et al. 1990). While the human genome does not contain endogenous I-*Sce*I recognition sites, the homing sites for I-*Cre*I and I-*Ppo*I are highly conserved, and these endonucleases can cleave sequences in human 28s rDNA when exogenously expressed in cells (Monnat et al. 1999).

Interestingly, in a study using a system of tamoxifen-inducible I-*Ppo*I expression in MCF7 human cells and chromatin immunoprecipitation (ChIP) at I-*Ppo*I sites on chromosomes 1 and 8, ATM was reported to be required for I-*Ppo*I-induced localised chromatin changes and DSB repair (Berkovich et al. 2007). While inherent limitations in this particular system make it difficult to accurately assess this role in repair (Section III.I.1), the reported requirement for ATM appeared to be greater than that observed following IR. A possible explanation for this finding is that I-*Ppo*I-induced DSBs occur in regions enriched for heterochromatin such as rDNA.

III.1.3 The nature of rDNA

rDNA encodes the RNA that is central to protein biosynthesis in the ribosome. Eukaryotic ribosomes are composed of a small (40s) and large (60s) subunit, and contain ribosomal proteins and ribosomal RNA (rRNA) (Taylor et al. 2009). The 40s subunit is made up of 18s rRNA and ~33 proteins and the 60s subunit is composed of 5s, 5.8s, and 28s rRNA along with approximately 46 proteins (Ben-Shem et al. 2011; Rabl et al. 2011). Eukaryotic rDNA is organised into the separately-transcribed 5s gene and a 45s gene cluster. The sequences encoding 18s, 5.8s, and 28s rRNA are found within the 45S gene cluster and are divided by internal transcribed spacer (ITS) units (Gonzalez et al. 1995). 45S gene clusters flanked by an external transcribed spacer (ETS) and non-transcribed spacers (NTS) are found in 30-40 tandem repeats and localise to the nucleolus, the location of ribosome synthesis (Stults et al. 2008) (Figure III.2B, E). *In situ* hybridization studies using ^{3}H labeled rRNA demonstrated that the 30-40 tandem repeat rDNA units are located between satellite regions and the short arm of the five acrocentric chromosomes (13, 14, 15, 21, and 22) (Henderson et al. 1972) (Figure III.2D).

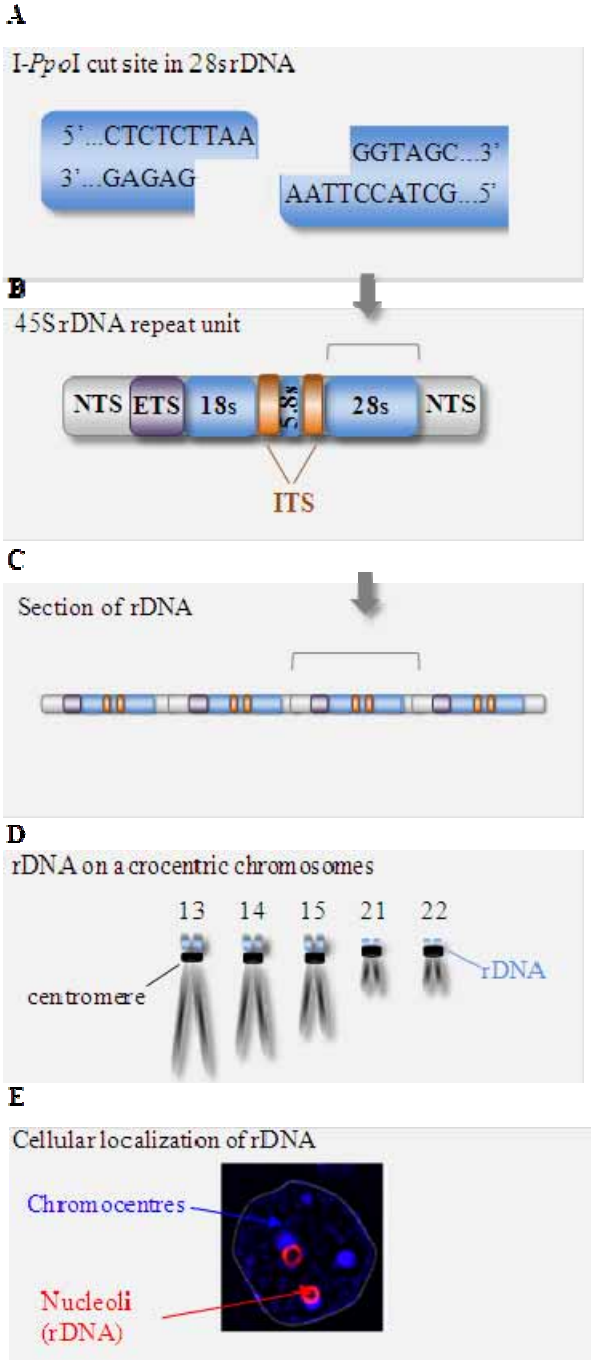

Figure III.2 The nature of rDNA and the I-*Ppo*I recognition site A. I-*Ppo*I binds, recognises and cleaves a 15 bp recognition sequence found in the 28s unit of rDNA. I-*Ppo*I cleavage generates a DSB with 4 bp 3' overhangs. **B**. The 18S, 5.8S, and 28S rDNA sequences are clustered in transcriptional units containing internal transcribed spacers (ITS), and are flanked by an external transcribed spacer (ETS) and non-transcribed spacers (NTS). **C**. rDNA clusters are found in 30-40 tandem repeats **D**. In humans, rDNA tandem repeats are found on the short arm of the 5 acrocentric chromosomes (13, 14, 15, 21, 22). **E**. rDNA is organised within nucleoli. 50% of rDNA is found to exist within heterochromatin regions, with transcriptionally silenced rDNA localising to the periphery of chromocentres. A microscopic image of the nucleus of a mouse neuron depicting the close proximity of nucleoli (red) to heterochromatic chromocentres (blue) (Singleton et al. 2011).

While transcription of the rRNA genes is necessary to accommodate the cellular requirement for ribosomal biogenesis, a substantial fraction of rDNA remains transcriptionally silent (Santoro 2005). Unlike other regions of the genome, approximately half of rDNA is found in a transcriptionally silent structure throughout the cell cycle (Conconi et al. 1989). Non-transcribed rDNA repeat units localise to the periphery of chromocentres (Akhmanova et al. 2000), suggesting that transcriptionally silenced rDNA genes are associated with heterochromatin. rDNA repeat regions on the acrocentric chromosomes, termed nucleolar organiser regions (NORs), are key to the formation and structural integrity of the nucleolus (Bartova et al. 2010). In support of the notion that rDNA genes are frequently found to be associated with heterochromatin, analysis of 28S rDNA in mouse-human hybrid cells has demonstrated that transcriptionally-silenced NOR regions of the acrocentric chromosomes associate with nucleoli (Sullivan et al. 2001) and nucleoli are reported to colocalise with chromocentres in MEFs (Singleton et al. 2011). Consequently, the 28S rDNA region, which contains the I-*Ppo*I recognition site, is likely to be more highly enriched for heterochromatin than non-rDNA regions of the genome.

III.1.4 Systems of site-specific DSB induction which exploit I-*Ppo*I

In recent years, several studies have exploited the I-*Ppo*I endonuclease for the study of protein dynamics at site-specific DSBs (Berkovich et al. 2007; Berkovich et al. 2008; McCord et al. 2009; Wen et al. 2012). Studies performed by Berkovich, Kastan and colleagues and by Michishita, Chua, et al., employed a tamoxifen-inducible system of I-*Ppo*I expression. Using this method, I-*Ppo*I-induced DDR protein recruitment was primarily assessed at a cut site identified on chromosome 1 within an intron of *disabled homolog 1 (DAB1),* a gene involved in brain development (Lambert de Rouvroit et al. 1998; Berkovich et al. 2007). Quantitative polymerase chain reaction (PCR) analysis of cutting at the chromosome 1 site and southern blotting with a 28S rDNA probe demonstrated that I-*Ppo*I-mediated cleavage occurs within the first several hours after induction of expression in this system (Berkovich et al. 2007). While this methodology has proven successful for assessment of protein recruitment to the sites of breaks by ChIP, inherent limitations preclude its exploitation for accurate assessment of DSB repair. One major disadvantage of the inducible system originally developed by Berkovich *et al.* is that a second wave of I-*Ppo*I-induced cleavage and DSB signalling is observed after 8 hours post induction of protein expression (Berkovich et al. 2007). As cells are exposed to tamoxifen continuously upon its addition, the expression of active protein is likely an ongoing process over the course of several hours. The ongoing presence of I-*Ppo*I in cells likely results in multiple rounds of enzymatic cleavage at I-*Ppo*I recognition sites. In contexts in which DSB induction is continual, the precise monitoring of repair is impossible. Further confounding DSB repair

analysis following continual expression of I-*Ppo*I over time, cellular overexpression of I-*Ppo*I is detrimental to cell viability (Monnat et al. 1999). In addition to these limitations, this system requires the establishment of stably transduced cell lines containing the inducible protein construct, which ultimately limits the use of this system to specific cell lines. None the less, examination of 28S rDNA cleavage following tamoxifen induction of I-*Ppo*I expression revealed a substantial (~2-2.5 fold) increase in maximum cutting efficiency which persisted over time in the presence of ATM inhibition (Berkovich et al. 2007). This result not only suggests that ATM is required for the repair of I-*Ppo*I-induced DSBs within 28S rDNA (since these DSBs persist unrepaired), but also, as discussed in later sections, supports the notion that multiple cycles of enzymatic cleavage may occur in this system. As ATM has been demonstrated to function in the slow component of DSB repair at heterochromatin regions (Goodarzi et al. 2008), this finding may imply that the rDNA site recognised by I-*Ppo*I is more likely to be found within heterochromatin than other sites in the genome. Therefore, a system of site-specific DSB induction which exploits I-*Ppo*I may provide a model for the study of DSB repair in regions enriched for heterochromatin.

In order to address some of the restrictions associated with previous I-*Ppo*I-based methodologies, Dr. Jie Wen, Dr. Patrick Concannon, and colleagues have developed a novel system of I-*Ppo*I DSB induction using direct protein transduction of his-tagged I-*Ppo*I (I-*Ppo*I-his) with cell-penetrating peptides (CPPs) (Wen et al. 2012). Synthetically generated CPPs have the capacity to translocate across cellular membranes and deliver cargoes such as purified proteins to both cytoplasmic and nuclear compartments (Milletti 2012). Importantly, this method of protein delivery is highly efficient, results in little to no cytotoxicity, and is not limited to specific cell lines (Henriques et al. 2005a; Milletti 2012). Using this system, rapid accumulation (within one hour) of functional I-*Ppo*I was observed both by immunoblot and quantitative PCR analysis of cleavage at the cut site on chromosome 1 (Wen et al. 2012). Additionally, ChIP-based analysis of both NBS and phosphorylated ATM recruitment and immunofluorescence-based analysis of nuclear γH2AX levels demonstrated that DDR signalling at the site of I-*Ppo*I-induced DSBs can be detected within one hour after transduction. However, examination of DSB repair in specific phases of cell cycle by γH2AX foci analysis was not specifically examined. Importantly, I-*Ppo*I levels were observed to decline 5 hours following I-*Ppo*I delivery, a finding likely to reflect rapid turnover of purified I-*Ppo*I in cells. Further, while a defect in I-*Ppo*I-induced DSB repair was observed in NHEJ-defective cells, enzymatic cutting efficiency (assessed by quantitative PCR) was not enhanced in these cells (Wen et al. 2012). Importantly, this result suggests that the system introduced by Wen et al. is not limited by the repeated cycles of cleavage and repair observed in the tamoxifen-inducible system of I-*Ppo*I expression.

Aside from system-specific limitations, other factors must be considered in the use of I-*Ppo*I to study heterochromatic DSB repair. In addition to the well-characterised I-*Ppo*I recognition sites in 28s rDNA and the *DAB1* gene, at least ten additional I-*Ppo*I recognition sites have been identified in other locations in the human genome on chromosomes 1, 2, 3, 7, and 11 (Berkovich et al. 2007; Wen et al. 2012) and the efficiency of I-*Ppo*I cutting at these regions must also be considered. As demonstrated by quantitative PCR using primers spanning the site within *DAB1* and these newly identified recognition sites, cutting efficiency of CPP-delivered I-*Ppo*I is similar across these sites and never exceeds 30% (Wen et al. 2012). While the cutting efficiency of CPP-delivered I-*Ppo*I at the 28S rDNA repeat sites has not fully been explored, the potential availability of up to 300 rDNA-associated recognition sites in the genome (Berkovich et al. 2008) may result in the majority of I-*Ppo*I-induced DSBs occurring within rDNA.

III.1.5 Aims of this chapter

Results from a previous study (Berkovich et al. 2008) have suggested that there is a substantial requirement for ATM in the repair of I-*Ppo*I-induced DSBs. ATM has previously been demonstrated to be required for the repair of DSBs occurring within regions of heterochromatin (Goodarzi et al. 2008). Therefore, one possible explanation for the observations made by Berkovich and colleagues may be that the genomic loci targeted by I-*Ppo*I are enriched for heterochromatin. Consequently, the repair of I-*Ppo*I-induced DSBs may require ATM to a greater extent than the repair of IR-induced DSBs, which are induced at random throughout the genome. However, limitations in the system used for monitoring I-*Ppo*I-induced DSB repair have made it difficult to interpret this data. Further, the requirement for Artemis and the ATM signalling mediator proteins in the repair of I-*Ppo*I-induced DSBs has not previously been explored. ATM, the mediator proteins, and Artemis are required for the repair of a subset of DSBs (Riballo et al. 2004; Goodarzi et al. 2008; Noon et al. 2010). The function of ATM and the mediator proteins in DSB repair has been demonstrated to involve phosphorylation of the heterochromatin factor KAP-1, a process thought to regulate chromosome remodeling (Goodarzi et al. 2008; Noon et al. 2010; Goodarzi et al. 2011). In contrast, the precise role of Artemis in DSB repair is still being examined.

Here, I have investigated the requirement for Artemis in DSB repair using a novel system of I-*Ppo*I-mediated DSB induction developed by Wen, Concannon, and colleagues (Wen et al. 2012). This system addresses multiple limitations associated with previous methodology, thereby enabling its utilisation for DSB repair analysis. I aimed to consolidate previous findings which suggest that I-*Ppo*I-induced DSBs occur within regions enriched for heterochromatin and to examine the requirement for Artemis in the repair of these DSBs using γH2AX foci analysis.

As DSB repair pathway choice is impacted by cell cycle phase (Beucher et al. 2009), I have restricted my analyses to G0/G1 cells. In Sections III.2.1-2, I will present results from optimisation experiments for the expression, purification, and CPP-mediated cellular delivery of functional I-*Ppo*I protein. Section III.2.3 will introduce my methodology for analysis of DSB repair in G0/G1 cells and in Section III.2.4, I will present findings demonstrating that Artemis and the ATM signalling mediator proteins are required for a substantial fraction of I-*Ppo*I-induced DSBs and that depletion of the heterochromatin factor KAP-1 alleviates the requirement for the mediator proteins but not for Artemis. Finally, in Section III.2.5, I will discuss my conclusions and the implications of these findings.

III.2 Results

III.2.1 Expression of the I-*Ppo*I protein in *E.coli*

As introduced in Section III.1, I set out to exploit a system of site-specific DSB induction within regions enriched for heterochromatin for the study of DSB repair factors. To do so, I aimed to introduce purified I-*Ppo*I protein directly into cells using CPP-mediated delivery as recently described (Wen et al. 2012). To obtain sufficient amounts of purified I-*Ppo*I for the subsequent delivery of the protein to cells, a system of protein expression in *E.coli* and Nickel-NTA purification was first optimised (Figure III.3.A).

Protein expression was achieved by transforming BL21 (DE3) competent *E. coli* (a T7 expression strain) with a pET-45b(+) expression vector containing the genetic sequences encoding his-tagged I-*Ppo*I (I-*Ppo*I-his / pET-45b(+)). As depicted in Figure III.3.B, the pET-45b(+) vector also contains sequences encoding an *AmpR* gene to enable selection of efficiently transformed bacteria, the bacterial origin of replication (ori), the lactose (lac) operator which blocks transcription of the *lacI* gene encoding the lac repressor, and the T7 RNA polymerase promoter. In the absence of a lac analogue such as IPTG, the lac repressor binds the lac operator, therefore blocking transcription of the adjacent sequence encoding I-*Ppo*I-his. However, upon addition of IPTG, this block is removed, with transcription initiating from the T7 promoter and hence expression of protein.

Ampicillin-resistant I-*Ppo*I-his-transformed bacterial clones were selected and grown in the presence of zinc acetate, as proper protein folding and stability of I-*Ppo*I has been reported to require divalent metal ions (Flick et al. 1997). Growth of bacteria was monitored carefully by taking OD_{600} readings periodically, and upon entry into log phase of growth, protein expression was induced by adding IPTG, again in the presence of zinc acetate. While bacterial growth rate varied slightly between preparations, cells usually reached early log phase within ~4 hours, and therefore IPTG was typically added around 5 hours after initial growth (Figure III.3.C). Given the slightly toxic nature of IPTG and zinc acetate treatment, bacteria entered a quasi-stationary

phase state upon addition of these reagents. Several trial experiments demonstrated that following IPTG induction, 3-4 hours of protein expression is sufficient to generate working material of I-*Ppo*I protein. Therefore, cells were typically harvested and lysed 8-9 hours after initial growth.

A system of purification exploiting the affinity of the his-epitope tag for Nickel-NTA was used to isolate I-*Ppo*I-his from all other proteins. Efficiency of the purification was assessed by subjecting eluted protein to SDS-PAGE and labelling proteins with Coomassie blue. A substantial amount of a ~22 kDa protein was detected in the purified elutions, corresponding to the size of the ~18-20 kDa I-*Ppo*I protein (Monnat et al. 1999), his-epitope tag, and intervening linker (Wen et al. 2012) (Figure III.3.D). While bands corresponding with 30kDa and 60kDa proteins were also detected, levels of these proteins were significantly lower than that of the ~22 kDa I-*Ppo*I-his fusion protein. Eluted protein samples were next subjected to concentration by ultrafiltration and protein levels were subsequently assessed by SDS-PAGE and Coomassie blue staining. Again, the ~22 kDa I-*Ppo*I-his fusion protein was observed to be the main product within the purified protein sample (Figure III.3.E).

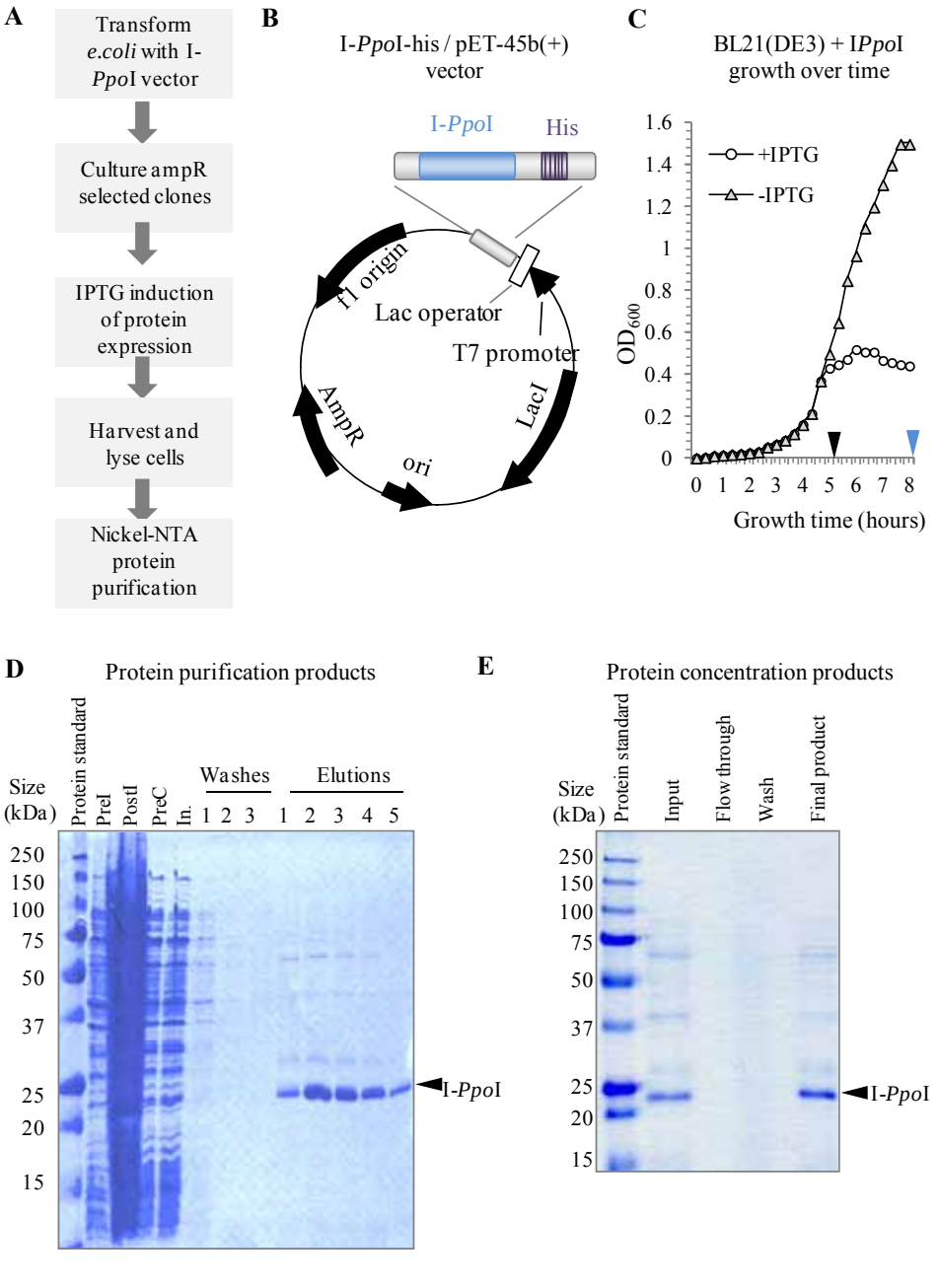

Figure III.3 Expression of I-*Ppo*I in *E.coli* **A**. Schematic representation of I-*Ppo*I protein expression and purification. **B**. Map of I-*Ppo*I-his / pET-45b(+) expression vector **C**. Representative growth curve of subclones of BL21(DE3) *E.coli* transfected with the I-*Ppo*I expression vector. Black arrow indicates the time of IPTG addition in the +IPTG sample. Blue arrow indicates the time bacteria were harvested. Growth was determined by taking OD_{600} readings at indicated times after initial seeding in flasks. **D**. Samples of bacteria were harvested pre- or post-IPTG addition (PreI and PostI respectively) and lysed. PostI lysates were cleared, providing input (In.) samples for purification. Pre-cleared (PreC) samples were saved. Protein purification was performed with Nickel-NTA beads, and samples from all wash and elution steps were saved. Indicated lysates were then subjected to SDS-PAGE and gels were stained with Coomassie Blue. Black arrow indicates a band corresponding to the ~22 kDa I-*Ppo*I-his. **E**. Concentration of elutions from (D) was performed using ultrafiltration columns. I-*Ppo*I protein levels were assessed in the input, flow through, wash, and the final product samples as in (D).

Next I verified that the purified I-*Ppo*I-his protein was functionally active using an *in vitro* assay. To test for enzymatic activity, a pcDNA3.1A(+) plasmid containing the 15 bp I-*Ppo*I recognition sequence was used as a DNA substrate for the I-*Ppo*I enzyme (Figure III.4.A). Purified I-*Ppo*I-his protein was incubated with I-*Ppo*I site/ pcDNA3.1A(+) plasmid DNA to allow enzymatic cleavage of the recognition site. A digestion reaction containing commercially purchased I-*Ppo*I was used as a positive control for active protein, and a reaction containing DNA but no protein was included as a negative control (undigested plasmid). Following digestion, DNA was separated on an agarose gel and visualised using ethidium bromide labelling and UV illumination. The primary DNA product following digestion with commercially purchased I-*Ppo*I or I-*Ppo*I-his was approximately 5.5-6 kb, corresponding to the predicted size of the linearized I-*Ppo*I site/ pcDNA3.1A(+) plasmid (Figure III.4.B). DNA digested with 1.5 µg commercially purchased I-*Ppo*I or 0.5 µg I-*Ppo*I-his also contained a much less abundant product which migrated at the same size as the undigested control, most likely representing a small amount of uncut DNA. However, incubation of DNA with 0.75 µg I-*Ppo*I-his resulted in complete digestion, indicating high enzymatic activity (Figure III.4.B).

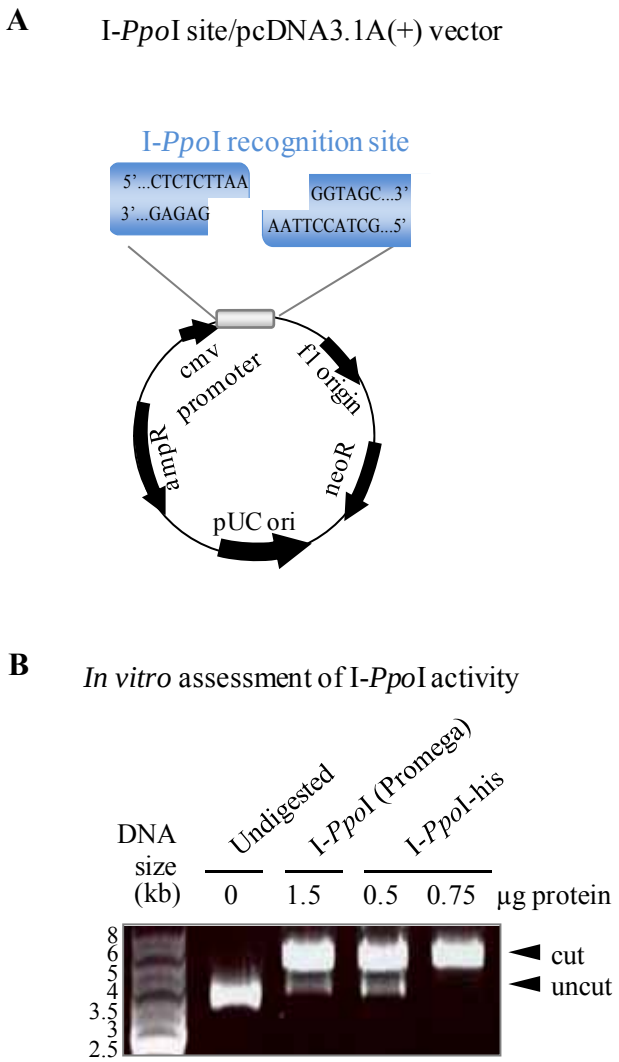

Figure III.4 Purified I-*Ppo*I protein is functionally active. **A**. Map of I-*Ppo*I site / pcDNA3.1A(+) vector **B**. Indicated µg of purified I-*Ppo*I was incubated with the *Ppo*I site /pcDNA3.1A(+) vector for 45 minutes, the digestion was stopped, and DNA samples were separated alongside a DNA size standard on a 1% agarose-TBE gel containing ethidium bromide to enable DNA detection by UV illumination. Black arrows indicate sizes corresponding to cut or uncut plasmid.

III.2.2 Optimisation of peptide-mediated protein delivery to cells

Next, the functional I-*Ppo*I-his protein obtained by *E.coli* expression and Nickel-NTA purification was delivered to human cells using the pep-1-cysteamine delivery reagent, a technique also exploited by Dr. Jie Wen, Dr. Patrick Concannon, et al. (Wen et al. 2012). Pep-1 is a short amphipathic CPP that can be used to deliver biologically active protein across the cell and nuclear membranes in a transmembrane-potential-mediated process (Morris et al. 2001; Henriques et al. 2005b). The ampiphatic nature of pep-1 allows interaction with lipid membranes and addition of a cysteamine group enhances the shuttling of the protein (Figure III.5.A). Pep-1 contains a flexible spacer region flanked by an N-terminal hydrophobic domain which enables cell membrane penetration and a hydrophilic C-terminus which acts as an NLS (Morris et al. 2001). Incubation of protein molecules with this CPP generates complexes which can then be shuttled across the cell membrane and distributed within the cytoplasm, nucleus, or both compartments (Figure III.5.B). Importantly, the ratio of pep-1 to protein molecules has been reported to impact upon the efficacy of delivery (Morris et al. 2001).

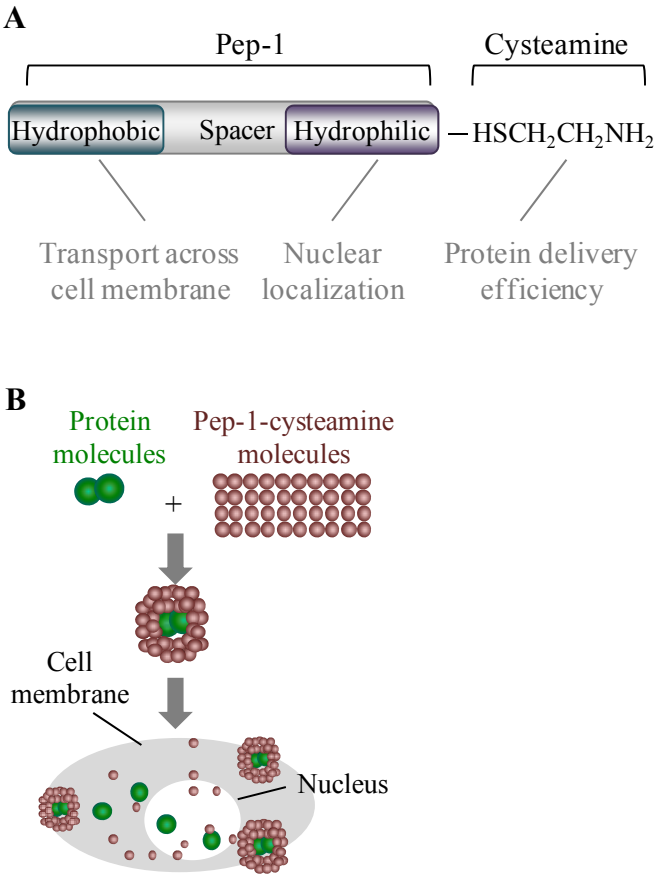

Figure III.5 The CPP pep-1-cysteamine as a tool for protein delivery. A. Schematic depiction of the regions of the pep-1-cysteamine CPP. Functions of domains are indicated in grey text. **B**. Schematic depiction of the delivery of protein molecules to cells using pep-1-cysteamine (see text for details).

I first tested the efficiency of this system of pep-1-cysteamine-mediated protein transduction in the tumour-derived HeLa cell line. To this end, cells were transduced with pep-1-cysteamine and an IgG antibody conjugated to the AF-488 fluorescein fluorophore, and efficiency was monitored by immunofluorescence-based detection of fluorescein. While covalent fluorescence labelling alters the physiochemical properties of CPPs and therefore cannot be used for accurate monitoring of peptide delivery efficiency (Szeto et al. 2005), introduction of a fluorescent protein or fluorescently labelled antibody such as AF-488 provides a tool for monitoring the protein distribution in cells.

The efficacy of pep-1-cysteamine-mediated protein delivery was first assessed in HeLa cells using a range of α-AF-488 concentrations (0.05-1µg). A peptide:protein molar ratio of 1:20-1:40 was used as ratios within this range are reported to facilitate maximum efficiency of macromolecule formation (Morris et al. 2001). As negative controls, I included samples of cells treated with pep-1 mixed with BSA or with AF-488 alone. Cells were fixed 1, 2, 3, or 6 hours following exposure of cells to peptide:protein mixtures and the cellular distribution of AF-488 was analysed using immunofluorescence microscopy. As early as 1-2 hours after protein transduction, AF-488 signal was observed in cells exposed to both pep-1-cysteamine and AF-488 (Figure III.6.A). AF-488 signal was observed both as diffused signal and in aggregates consistent with published observations following pep-1-mediated protein delivery (Morris et al. 2001); detection of large protein aggregates increased with increasing antibody (Figure III.6.A) or pep-1-cysteamine concentrations.

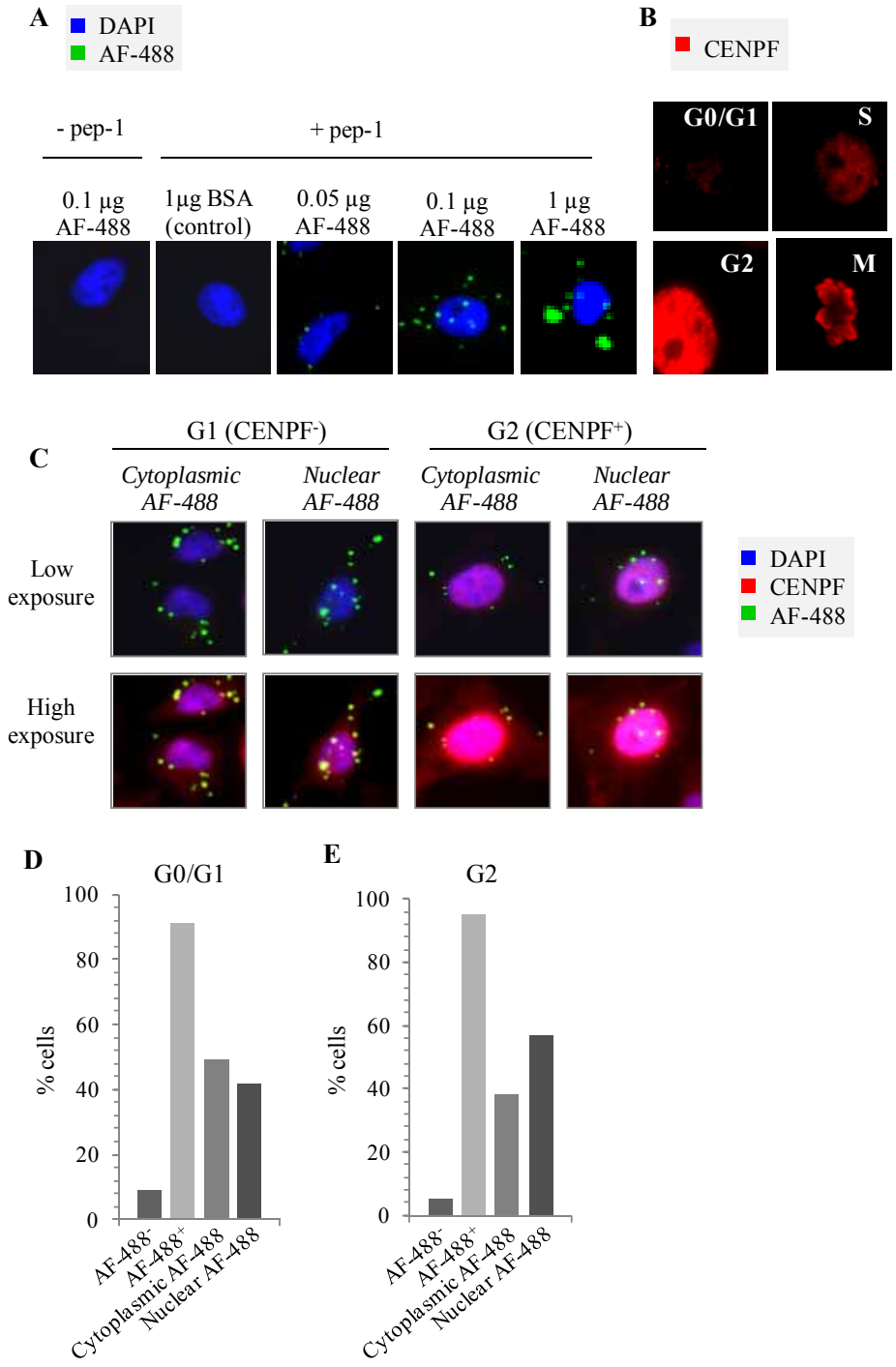

Figure III.6 Direct protein delivery by pep-1-cysteamine results in high transduction efficiency. A. HeLa cells grown on coverslips were treated with indicated pep-1:protein mixtures and fixed 2 hours later. Nuclei were labelled with DAPI and cells were visualised and imaged using immunofluorescence microscopy. **B.** Cell cycle phase can be distinguished by immunofluorescence labelling of CENPF. Representative images of CENPF levels in G0/G1-, S-, G2-, and M-phase cells are shown. **C-E.** HeLa cells were exposed to pep-1-cysteamine and 0.1 µg α-IgG-AF-488 and fixed 2 hours later. Immunofluorescence labelling with DAPI and α-CENPF was performed and AF-488 localisation was assessed by immunofluorescence microscopy in >200 G0/G1 or G2 cells. Representative images are displayed in (C) and quantification of the fraction of AF-488$^-$ and AF-488$^+$ cells or cells displaying exclusively cytoplasmic AF-488, or nuclear AF-488 cells are presented in (D-E).

Efficiency of protein delivery was next assessed specifically in G0/G1 and G2 cells 2 hours after delivery of 0.1 μg AF-488. To distinguish cell cycle phase, immunofluorescence staining for CENPF was performed. CENPF staining is bright in G2/M-phase, mild in S-phase, and minimal to absent during G0/G1 and mitotic cells can be distinguished by morphological changes such as chromatin condensation (Lobrich et al. 2010; Brunton et al. 2011) (Figure III.6.B). The distribution of AF-488 was assessed in $CENPF^-$ G0/G1 and $CENPF^+$ G2 cells, and cytoplasmic and/or nuclear localisation was noted. High exposure images were captured allowing distinction of the cytoplasmic compartment from extracellular background (Figure III.6.C). Quantification of the fraction of $AF\text{-}488^-$ or $AF\text{-}488^+$ cells provided an initial assessment of transduction efficiency. Complete absence of AF-488 ($AF\text{-}488^-$) was observed in very few G0/G1 or G2 cells (10% or 5%, respectively) 2 hours following transduction, reflecting the high (>90 %) efficiency of pep-1-mediated protein delivery also reported by Wen, Concannon and colleagues (Wen et al. 2012) (Figure III.6.D-E). Consistent with published findings (Morris et al. 2001), no cellular toxicity was observed following addition of pep-1 at concentrations used in these and subsequent experiments (3-5 μM). Cytoplasmic distribution of AF-488 was observed in most cells, but ~40-50% of cells displayed exclusive cytoplasmic localisation, with the remaining fraction containing both nuclear and cytoplasmic distribution (Figure III.6.D-E). Very few cells displayed an exclusively nuclear distribution (data not shown). It is important to note, however, that some levels of transduced AF-488 may be below the limit of visual detection using the assay.

III.2.3 Analysis of DSB induction and repair of I-*Ppo*I induced breaks

Next, pep-1-mediated delivery of I-*Ppo*I was assessed. Cells were exposed to varying concentrations of I-*Ppo*I protein with pep-1-cysteamine and aphidicolin was added at the time of protein delivery to facilitate identification of S-phase cells and prevent cells from progressing to later stages of cell cycle (Section II.6.1). As negative controls, samples of cells treated with pep-1 mixed with BSA or with I-*Ppo*I-his alone were included in each experiment. Cells were fixed at one hour intervals following exposure to peptide:protein mixtures. Immunofluorescence labelling of DNA (DAPI), DSBs (γH2AX or 53BP1), and cell cycle (CENPF) allowed the analysis of site-specific DSB induction in G0/G1 cells as described above.

Within one to three hours following pep-1-cysteamine-mediated delivery of 0.5-1 μg I-*Ppo*I-his, an increase was observed in γH2AX (or 53BP1) foci per G0/G1 cell, indicating efficient induction of I-*Ppo*I-generated DSBs (Figure III.7.A). 1 μg protein was used for CPP-mediated I-*Ppo*I delivery in all subsequent experiments. Using similar transduction conditions, Wen, Concannon and colleagues, routinely detect I-*Ppo*I-his in the nuclear fraction of cells and efficient cutting of various recognition sites as early as 1 hour following CPP-mediated protein

delivery (Wen et al. 2012). In contrast to 3Gy IR-induced DSBs, I-*Ppo*I-induced DSBs were less numerous, less uniform in size (with some larger foci most likely containing clustered DSBs), and often (though not exclusively) observed near the periphery of nucleoli, which appear as dark regions in the DAPI channel (Figure III.7.A). A maximum number of ~30 γH2AX foci were typically observed in G0/G1 cells exposed to I-*Ppo*I, consistent with previous reports that I-*Ppo*I expression results in cleavage of 10 % of the ~300 rDNA target sites in the human genome (Monnat et al. 1999; Berkovich et al. 2007).

Enumeration of γH2AX foci revealed that I-*Ppo*I-induced DSB number peaked within 3 hours after protein transduction and that repair of most DSBs occurred after a further 2-3 hours later (Figure III.7.B). Similarly, quantitative PCR analysis (indiscriminate of cell cycle) has demonstrated that, for most of the ten additional I-*Ppo*I recognition sites recently identified, enzymatic cleavage peaks 1-3 hours after protein transduction and resolution of cleavage has been completed within a further 3 hours later (Wen et al. 2012). Importantly, no accumulation of DSBs was observed after the first several hours post I-*Ppo*I transduction (between 3-24 hours post I-*Ppo*I transduction) (Figure III.7.B), similar to observations made by Wen and colleagues using quantitative PCR analysis. In addition, no cellular toxicity was observed over time following pep1-mediated I-*Ppo*I delivery. As previously introduced, using their tamoxifen-inducible system of I-*Ppo*I expression in MCF7 cells, Berkovich and colleagues observed a potential second wave of enzymatic cleavage and DSB signalling after 8 hours post-tamoxifen administration, suggesting that continuous expression of I-*Ppo*I in their system may result in multiple rounds of enzymatic cleavage (Berkovich et al. 2007). As discussed in Section III.3, I considered my findings likely to reflect the fact that CPP-mediated delivery of I-*Ppo*I does not result in the ongoing/continuous cycles of enzymatic cleavage likely to be associated with tamoxifen-induced I-*Ppo*I expression.

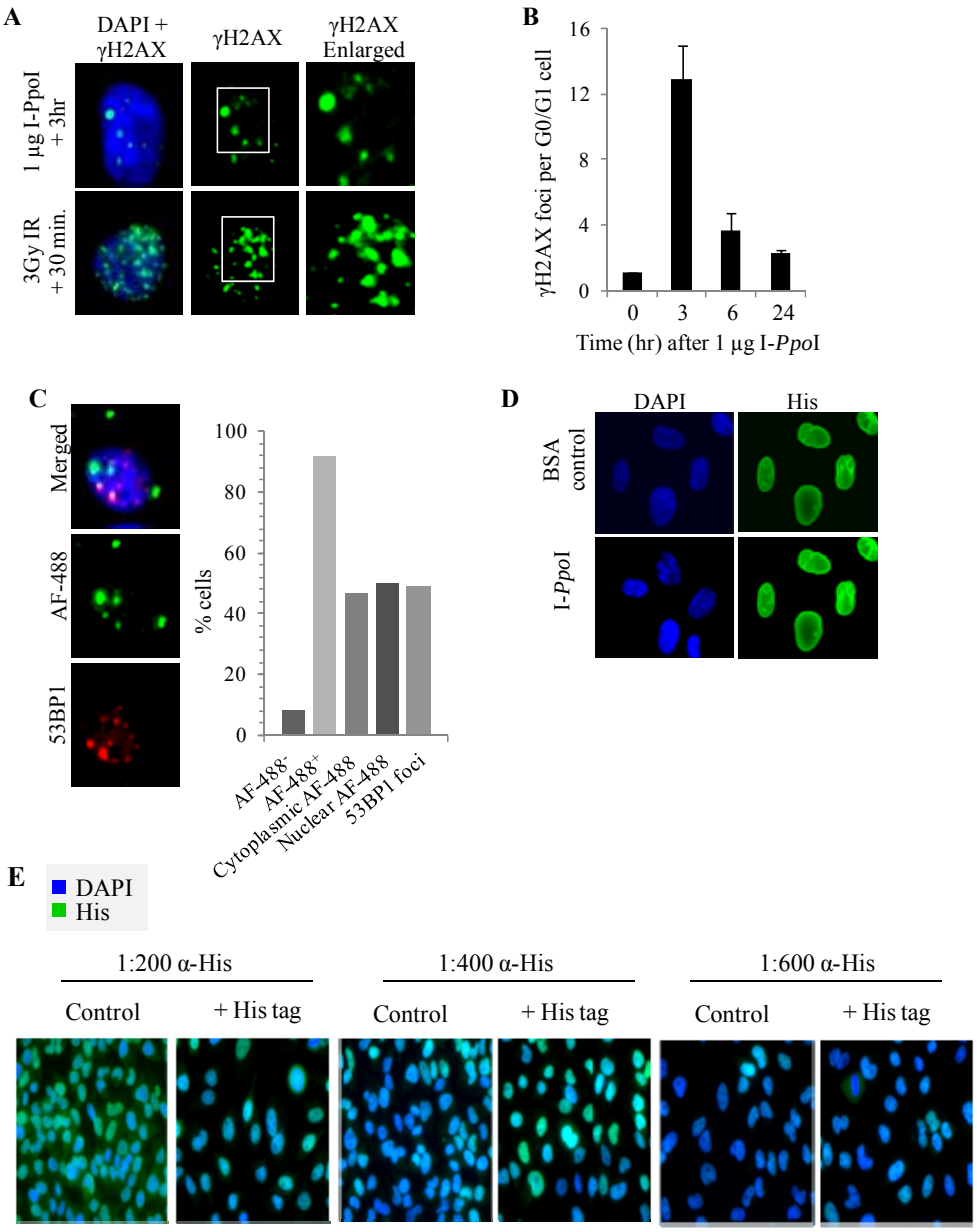

Figure III.7 Direct delivery of the I-*Ppo*I endonuclease delivery by pep-1-cysteamine results in DSB induction in HeLa cells. A. HeLa cells were exposed to 1 μg I-*Ppo*I and fixed 3 hours later or irradiated with 3Gy and fixed 30 minutes later. 4 μM aphidicolin was added at the time of treatment to facilitate identification of S-phase cells and prevent cells from progressing to later stages of cell cycle. Immunofluorescence labelling with DAPI, α-γH2AX, and α-CENPF was carried out and images of CENPF$^-$ G0/G1 cells were captured. Regions within white boxes are enlarged in far right panels. **B.** Cells were exposed to I-*Ppo*I as in (A) and harvested at indicated times. γH2AX foci per G0/G1 cell were scored. Plots depict mean +/- SD from 3 independent experiments. **C.** 1 μg I-*Ppo*I was delivered with 0.1 μg α-AF-488, cells were fixed 3 hours later, and immunofluorescence labelling was carried out with DAPI and α-53BP1. Representative images are displayed in left panels, results from quantification of cell fractions containing AF-488 (as in Fig. III.6D) and 53BP1 foci are displayed in right panel. **D.** BSA (control) or 1 μg I-*Ppo*I was delivered to cells, and 3 hours later, cells were fixed and immunofluorescence labelling with DAPI and α-His was carried out. **E.** As in (D) except cells were transfected with an empty vector or a control vector with a His-tag and fixed 24 hours later. Indicated dilutions of α-His were tested.

As measured by 53BP1 foci formation, pep-1-cysteamine-mediated delivery of I-*Ppo*I to HeLa cells results in DSB induction in ~50% of cells (Figure III.7.C). This fraction of cells, likely to represent those with nuclear levels of I-*Ppo*I, was comparable to the fraction of cells which display detectable nuclear fluorescein after CPP transduction of AF-488 (Figure III.6.D). Similarly, co-delivery of both 1 μg I-*Ppo*I and 0.1 μg α-AF-488 revealed a comparable transduction efficiency (>90%) and cellular distribution of protein cargo (nuclear AF-488 detected in ~50% of cells) (Figure III.7.C). While attempts were made to monitor I-*Ppo*I-his protein delivery by immunofluorescence staining with α-his, no change in his levels were observed after pep-1-mediated I-*Ppo*I delivery (Figure III.7.D). However, this most likely reflected inefficiency of the antibody for use in immunofluorescence, as changes in his levels were also not observed upon efficient transfection of cells with a control vector containing a his-tag (Figure III.7.E).

The variation in γH2AX foci characteristics observed after I-*Ppo*I protein delivery has posed a challenge in monitoring repair of I-*Ppo*I-induced DSBs over time by γH2AX foci enumeration. As described above, a range in DSB size, intensity, and distribution was observed within cells following I-*Ppo*I protein delivery when compared with DSBs arising from IR. Further, intercellular variations in nuclear uptake were observed. Given these intracellular and intercellular variations, γH2AX foci were scored in a higher number of G0/G1 cells (60) per experiment than typically scored for assessment of IR-induced DSB repair (20-30 cells (Goodarzi et al. 2008). In addition, experiments were repeated at least three times and all data was combined and presented in box plots to enable visualisation of data distribution. The significant variation in intercellular DSB number is highlighted by comparison of box plots depicting the number of γH2AX foci per cell in endonuclease versus IR-treated cells (Figure III.8.A-B). However, as presented previously by bar graph (Figure III.7.B), the peak induction of I-*Ppo*I-generated DSBs 3 hours after protein delivery and repair of most DSBs after a further 3 hours remains evident when plotting these results by box plot (Figure III.8.A). Overall, while intercellular variation in IR-induced DSB number is generally low, enabling analysis of mean values presented in column/bar graphs, I-*Ppo*I-generated DSBs display substantial intercellular variation and were plotted by box plot for subsequent analysis.

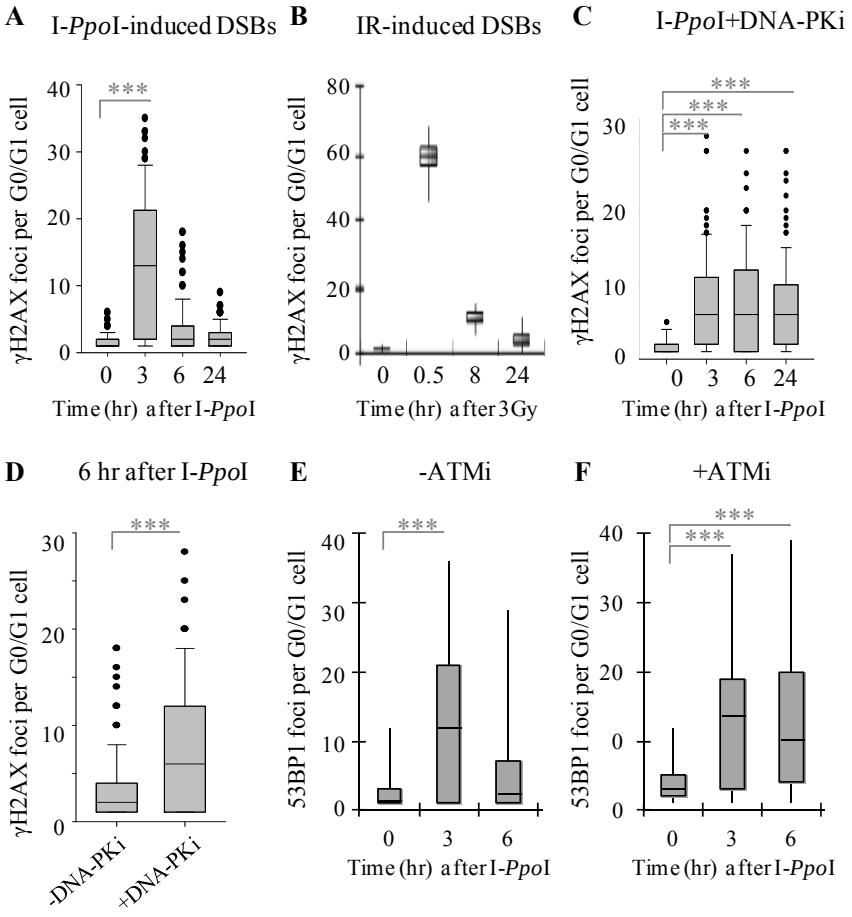

Figure III.8 DNA-PK and ATM are required for the repair of a substantial fraction of I-*Ppo*I-induced DSBs in HeLa G0/G1-phase cells. For descriptions of the DNA-PKi and ATMi, see Section II.5. **A**. As in Figure III.7.B except all data from 3 independent experiments (60 G0/G1 cells scored per experiment) are displayed in box plots. Asterix indicate a statistically significant difference compared with 0hr or – DNA-PKi samples, depending on plots (*** $p<0.001$). **B**. HeLa cells were treated with 3Gy IR, fixed at indicated times, and enumeration of γH2AX foci in at least 30 cells per experiment was performed. Results are depicted as in (A). **C**. Cells were treated with 10 μM DNA-PKi for 30 minutes prior to I-*Ppo*I protein delivery as described. **D**. As in (C) except cells were treated with 10 μM KU-55933 (+ATMi) or a DMSO control (-ATMi). Repair of DSBs was monitored by immunofluorescence labelling and enumeration of 53BP1 foci.

Using this method of data analysis and presentation, I went on to examine the impact of small molecule inhibition or siRNA-mediated depletion of DSB factors on the repair of I-*Ppo*I-induced DSBs during G0/G1.

As previously introduced, the repair of DSBs in G0/G1 cells occurs mainly by c-NHEJ, a process mediated by the DNA-PK holoenzyme (Section I. 3). Treatment of cells with NU-7441/KU-57788, a highly selective inhibitor of DNA-PK (DNA-PKi) (Section II.5) is reported to inhibit DNA-PK kinase activity at low doses, with an IC_{50} of ~14 nM (Leahy et al. 2004). Treatment of primary human fibroblasts with a related DNA-PKi, NU7026, results in a substantial defect in the repair of IR-induced DSBs in G1- and G2-phase cells, consistent with the notion that c-NHEJ plays a significant role in DSB repair during these phases of cell cycle (Beucher et al. 2009).

To assess the impact of inhibiting c-NHEJ on the number of I-*Ppo*I-induced DSBs over time in G0/G1 cells, NU-7441/KU-57788, an inhibitor of DNA-PK (DNA-PKi) was added to cells 30 minutes prior to the time of protein delivery (Section II.5). Consistent with the notion that I-*Ppo*I-generated DSB repair occurs primarily by c-NHEJ in G0/G1 cells, DSBs induced in the presence of the DNA-PKi remained unrepaired 6 hours and up to 24 hours after addition of I-*Ppo*I (Figure III.8.C-D). Importantly, I observed no increase in the maximum number of DSBs induced by pep-1-delivered I-*Ppo*I in DNA-PKi-treated cells compared with control cells (Figure III.8.A,C). Similarly, Wen and colleagues have observed no increase in the maximum cutting efficiency of CPP-delivered I-*Ppo*I in cells lacking functional Lig4, another component of c-NHEJ (Wen et al. 2012). These findings again support the notion that CPP-mediated I-*Ppo*I delivery may not result in ongoing cycles of enzymatic cutting since, if this did result, one might predict to see an increase in the maximum number of I-*Ppo*I-induced DSBs in DSB repair-deficient cells compared with repair-proficient cells (the number of initially induced DSBs which remain unrepaired would be added to the number of newly induced DSBs).

Next, to substantiate previous reports that the repair of a substantial fraction of I-*Ppo*I-induced DSBs require ATM (Berkovich et al. 2007) using direct delivery of I-*Ppo*I, cells were treated with KU-55933, an inhibitor of ATM (ATMi) (Section II.5), 30 minutes prior to protein delivery and DSB number assessed 0, 3, or 6 hours after transduction (Figure III.8.E-F). As ATM inhibition results in reduced γH2AX foci size in specific cell lines such as NIH3T3 (Brunton et al. 2011) and HeLa (unpublished observations), and a fraction of I-*Ppo*I-induced DSBs are small and difficult to score, DSBs were monitored by 53BP1 foci, another marker of DSBs. Using this measure, ATM inhibition was observed to result in a significant defect in I-*Ppo*I-induced DSB repair (Figure III.8.E-F). Comparison of the median values of I-*Ppo*I-induced 53BP1 foci per cell revealed that ~ 60% of DSBs detected at 3 hours (median =15) persisted 6 hours after transduction (median=9) in ATMi-treated cells, while only ~15% of DSBs persist at this timepoint in control cells. As ATM is required for the repair of 10-20% of

DSBs induced by IR (Riballo et al. 2004) (Figure III.12.A), this result may indicate a greater requirement for ATM in the repair of I-*Ppo*I-induced DSBs. However, as previously stressed and discussed in Section III.3, variations in DSB induction associated with I-*Ppo*I delivery may impact upon interpretation of these results and must be carefully considered. Importantly, while the maximum cutting efficiency of I-*Ppo*I was enhanced in ATM defective cells using the system described by Berkovich et al. (Berkovich et al. 2008), I did not observe a significant difference in the maximum number of DSBs using CPP-mediated I-*Ppo*I delivery in ATMi-treated cells (Figure III.8.E-F). As discussed above and in Section III.3, this finding again supports the notion that repeated cycles of enzymatic cutting, which would be predicted to result in an increase in maximum DSB number in repair-deficient cells, is not a major factor in the system of CPP-mediated I-*Ppo*I delivery.

To confirm that observations of I-*Ppo*I-induced DSB repair kinetics and foci variation were not restricted to the tumour-derived HeLa cell line, I-*Ppo*I induction of DSBs was also assessed in an hTERT-immortalised fibroblast line (1BR3hTERT) derived from a normal individual. 1BR3hTERT cells have a stable karyotype, show genomic stability, and have an intact G1/S checkpoint (unpublished observations). Delivery of 1 μg I-*Ppo*I to an hTERT-immortalised control fibroblast line (1BR3hTERT) resulted in maximal DSB induction by 3 hours. Similar to that observed in HeLa cells, most I-*Ppo*I-induced were repaired within several hours in 1BR3hTERT cells (Figure III.9.A). As observed in HeLa cells, I-*Ppo*I-induced DSBs (measured by γH2AX or 53BP1 foci) in 1BR3hTERT cells displayed variation in size and intensity compared to IR-induced DSBs (Figure III.9.B).

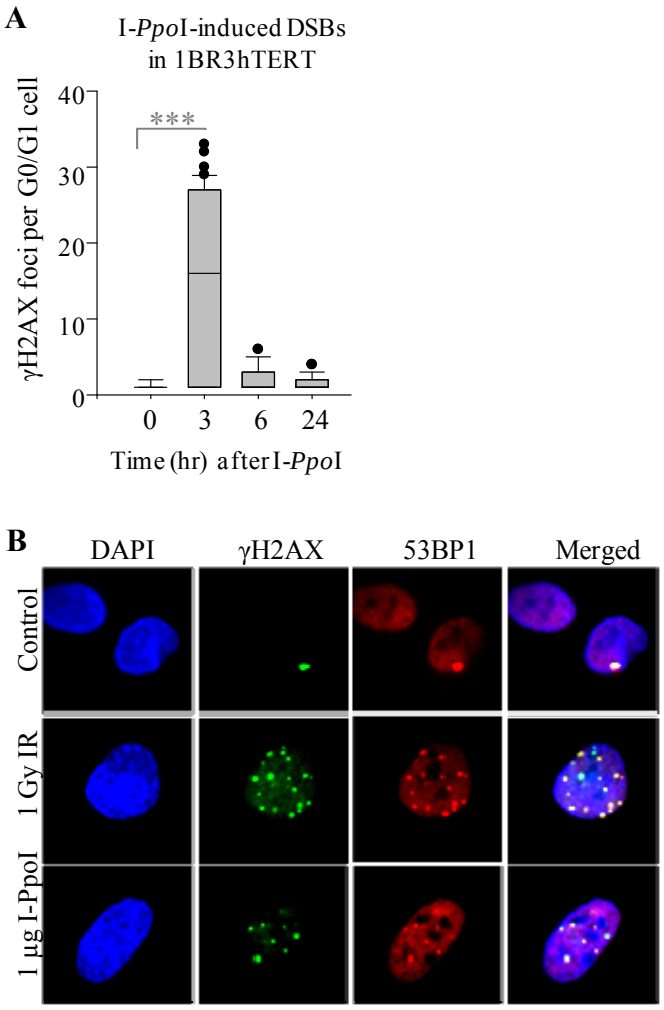

Figure III.9 Direct delivery of the I-*Ppo*I endonuclease delivery by pep-1-cysteamine results in DSB induction in control human fibroblasts. A. I-*Ppo*I-induced DSBs were assessed in 1BR3hTERT control fibroblasts as in Figures III.7.A-B and 8.A. **B**. Representative images of DAPI, γH2AX, and 53BP1 immunofluorescence labelling in 1BR3hTERT cells 30 minutes after 1Gy IR or 3 hours after I-*Ppo*I delivery.

III.2.4 Artemis, 53BP1, and RNF8 are required for the repair of I-PpoI-induced DSBs

The availability of an hTERT-immortalised fibroblast cell line from an Artemis-defective RS-SCID patient (F02/385hTERT) has enabled analysis of I-*Ppo*I-induced DSB repair in the absence of the Artemis endonuclease. F02/385hTERT cells have a normal cell cycle but are radiosensitive as a result of a defect in the repair of ~10-20% IR-induced DSBs (Riballo et al. 2004) (Figure III.10.A) and display endogenous DSB accumulation over extended times of culture (Woodbine et al. 2011). Delivery of 1 μg I-*Ppo*I to F02/385hTERT resulted in maximal DSB induction within 3 hours, similar to 1BR3hTERT control fibroblasts (Figure III.10.B-C). However, most I-*Ppo*I-induced DSBs remained unrepaired 6-24 hours following protein delivery in F02/385hTERT (Figure III.10.C-D). As the fraction of DSBs requiring Artemis for repair have been observed to localise to heterochromatin regions in MEFs (Figure III.1) and human cells (Woodbine et al. 2011), this observation suggests that a substantial fraction of I-*Ppo*I-induced DSBs may occur within heterochromatin regions.

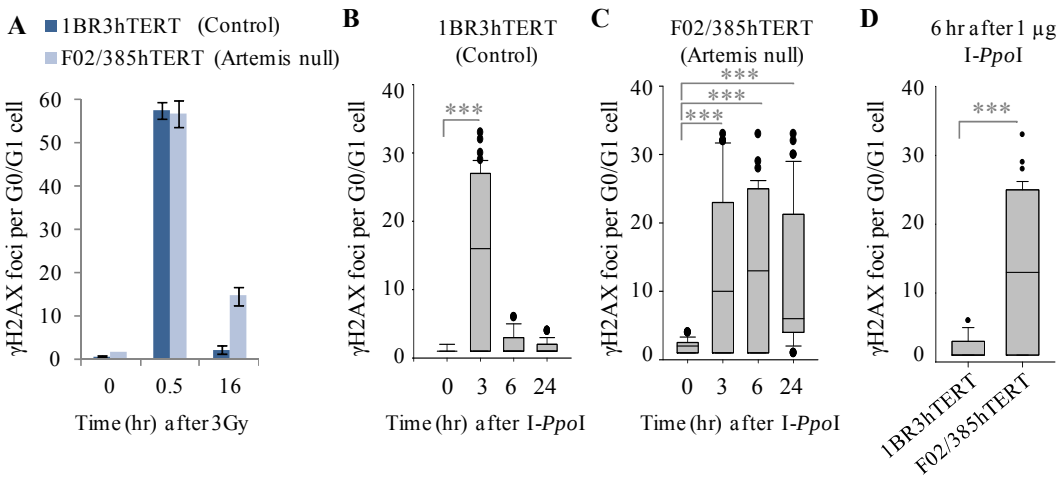

Figure III.10 Artemis-null human fibroblasts display a substantial defect in the repair of I-*Ppo*I-induced DSBs during G0/G1. A. IR-induced DSB repair efficiency was assessed in 1BR3hTERT (control) (A) or F02/385hTERT (Artemis null) (B) G0/G1-phase fibroblasts as in Figure III.8.B. **C-D**. I-*Ppo*I-induced DSB repair efficiency was assessed in 1BR3hTERT (control) (C) or F02/385hTERT (D) G0/G1-phase fibroblasts as in Figures III.7.A-B and 8.A. E. Comparison of the number of DSBs per G0/G1 cell 6 hours after protein transduction in 1BR3hTERT versus F02/385hTERT (as in D-E).

To extend these findings, the requirement for Artemis in the repair of I-*Ppo*I-induced DSBs was also confirmed by siRNA depletion in HeLa cells using siRNA conditions routinely used in our lab and shown to effectively deplete the endonuclease. HeLa cells were transfected with ON-TARGETplus SMART pool siRNA oligonucleotides targeting Artemis which are reported by the manufacturer to being highly specific (Section II.2), though this was not verified here. Cells were transfected with 20 nM siControl or siArtemis, grown for 24 hours, transfected a second time with siRNA oligonucleotides, and grown for a further 48 hours. While I found the currently available α-Artemis antibodies to be inefficient for analysis by immunofluorescence or immunoblotting, my colleagues have previously been able to demonstrate effective depletion of Artemis in HeLa cells by immunoblot 48 hours after a single transfection with the same oligonucleotide pool used for the purpose of this thesis (Beucher et al. 2009). Here, I assessed the efficiency of Artemis depletion in HeLa cells indirectly by assessing IR-induced DSB repair efficiency in siControl vs. siArtemis cells. As previously published and confirmed above, Artemis-defective fibroblasts are deficient in the repair in ~10-20% IR-induced DSBs (Figure III.10.A, Riballo et al. 2004). A similar DSB repair defect has also been demonstrated in Artemis-depleted HeLa cells using the siRNA knockdown conditions described above (Beucher et al. 2009). Here, I assessed the IR-induced DSB repair efficiency of siControl vs. siArtemis-treated HeLa cells and again observed defective repair of ~10-20% IR-induced DSBs in siArtemis-treated cells (Figure III.11.A). Therefore, I considered my siRNA knockdown conditions likely to be efficient in the depletion of the Artemis endonuclease. Using these knockdown conditions, the impact of siRNA depletion of Artemis on I-*Ppo*I-induced DSBs was assessed. Similar to observations in Artemis-defective fibroblasts, depletion of Artemis resulted in defective repair of the majority of I-*Ppo*I-induced DSBs (Figure III.11.B-C). Unrepaired DSBs in siArtemis-treated cells persisted 6-24 hours following I-*Ppo*I delivery (Figure III.11.D-E) and were observed to vary in size and distribution (Figure III.11. E).

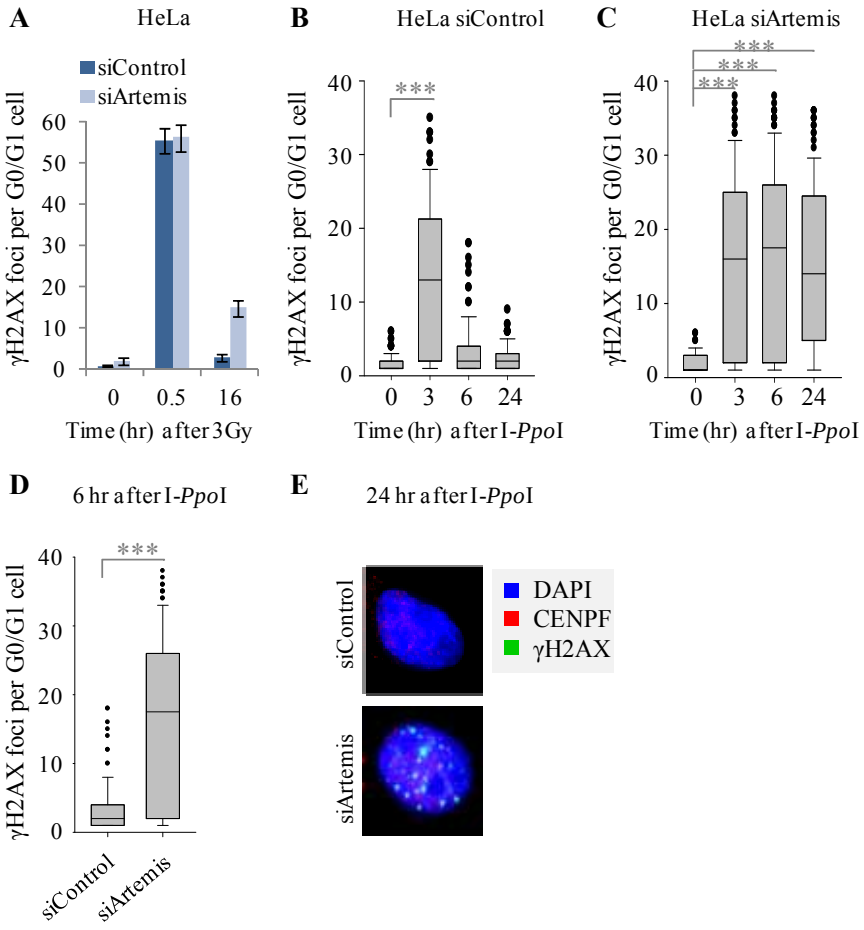

Figure III.11 Artemis depletion in HeLa results in a defect in the repair of substantial fraction of I-*Ppo*I-induced DSBs during G0/G1. HeLa cells were transfected with control or Artemis siRNA, grown for 24 hours, transfected again, and grown for a further 48 hours. **A.** IR-induced DSB repair efficiency was assessed as in Figure III.8.B. **B-C**. I-*Ppo*I-induced DSB repair efficiency was assessed as in Figures III.7.A and 8.A. **D**. Comparison of the number of DSBs per G0/G1 cell 6 hours after protein transduction in siControl versus siArtemis treated HeLa cells (as in B-C). **E**. Representative images of siControl or siArtemis treated HeLa cells 24 hours after I-*Ppo*I protein delivery.

Next, I examined the requirement for the ATM signalling mediator proteins RNF8 and 53BP1 in the repair of I-*Ppo*I-induced DSBs in G0/G1. Mediator proteins such as RNF8 and 53BP1 are thought to concentrate ATM signalling at DSBs and are required for robust ATM-dependent phosphorylation of KAP-1 (Noon et al. 2010). Consistent with this, siRNA-mediated depletion of these factors results in a defect in the repair of ~10-20% IR-induced DSBs which is comparable to that observed in ATM- or Artemis-defective cells (Noon et al. 2010). RNF8 or 53BP1 were depleted in HeLa cells by transfection with siRNA oligonucleotides characterised in Noon et al. 2010 and as described in Table II.1. For the purpose of this thesis, I used identical 53BP1 and RNF8 siRNA depletion conditions previously demonstrated to be efficient based on an observed reduction in nuclear protein levels (in the case of 53BP1, by immunofluorescence), inability of cells to form 53BP1 foci, and reduction in localised KAP-1 phosphorylation (Noon et al. 2010). These siRNA conditions are routinely observed in our lab to result in the DSB repair defect described above and specificity of the 53BP1 siRNA oligonucleotide has previously been confirmed by complementation of the DSB repair defect after expression of siRNA-resistant 53BP1 (Noon et al. 2010). Here, I assessed the efficiency of si53BP1 or siRNF8 knockdown indirectly by assessing IR-induced DSB repair efficiency in these cells. Similar to the reported findings described, I observed a defect in the repair of 10-20% IR-induced DSBs (Figure III.12A) and therefore considered these knockdown conditions likely to efficiently deplete the proteins. Using these conditions, I-*Ppo*I-induced DSB repair was monitored as described above. Similar to observations made after depletion of Artemis or inhibition of ATM, depletion of RNF8 or 53BP1 resulted in a substantial defect in the repair of I-*Ppo*I-induced DSBs (Figure III.12B-G).

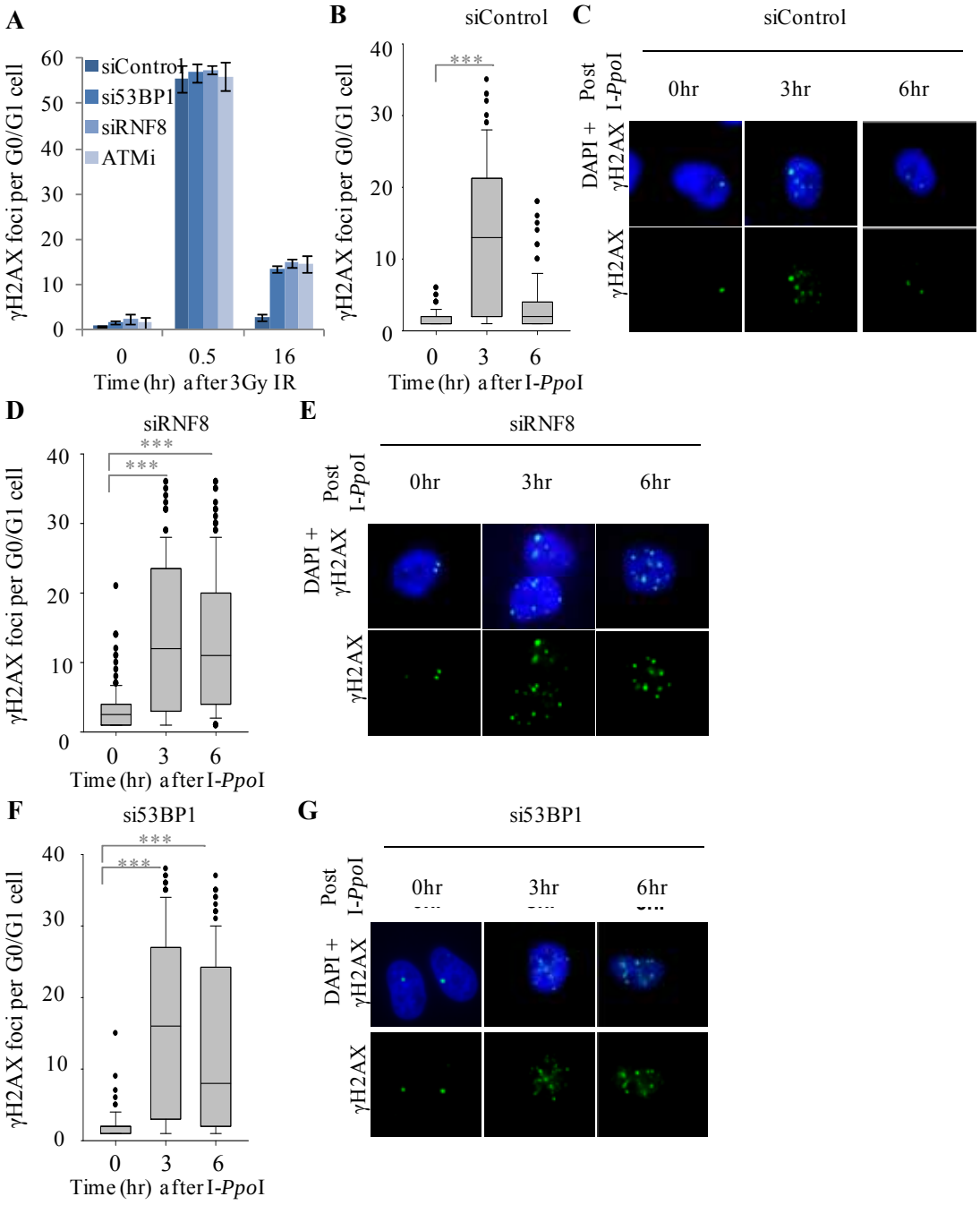

Figure III.12 The mediator proteins RNF8 and 53BP1 are required for the repair of the majority of I-*Ppo*I-induced DSBs in HeLa G0/G1-phase cells. A. HeLa cells were transfected twice over 72 hours with indicated siRNA oligonucleotides. ATM was added 30 minutes prior to IR. Cells were treated with 3Gy IR, aphidicolin was added at the time of IR, and cells were harvested at indicated times later. For each experiment, γH2AX foci enumeration was performed in 30 cells per sample. Plot depicts mean values +/- SD from three independent experiments. **B-G**. HeLa cells were transfected with siControl (B-C), siRNF8 (D-E), or si53BP1 (F-G) as described in Figure III.10.C and repair of DSBs was monitored after delivery of 1 µg I-*Ppo*I. Plots depict γH2AX foci number per G0/G1 cell. Representative images of DAPI and/or γH2AX staining in cells fixed at indicated times after I-*Ppo*I delivery.

Findings from our lab have demonstrated that global heterochromatin relaxation by KAP-1 depletion relieves the requirement for ATM and the mediator proteins in IR-induced DSB repair (Goodarzi et al. 2008; Noon et al. 2010; Brunton et al. 2011). Here, I examined the impact of heterochromatin relaxation on the requirement for Artemis, RNF8, or 53BP1 in the repair of I-*Ppo*I-induced DSBs.

To this end, siRNA-mediated depletion of KAP-1 was performed using an siRNA oligonucleotide (Table II.1) and knockdown conditions previously demonstrated to efficiently deplete KAP-1 in HeLa cells by immunofluorescence analysis and to relieve the requirement for ATM and the mediator proteins in IR-induced DSB repair (Goodarzi et al. 2008; Goodarzi et al. 2011) . The specificity of this siKAP-1 oligonucleotide was previously illustrated by the finding that expression of siRNA-resistant KAP-1 in cells treated with siKAP-1 and ATMi restores ATM-dependent repair (Goodarzi et al. 2008). While in Chapter V, I demonstrate the efficiency of KAP-1 depletion in human fibroblasts by immunoblot, here I verified KAP-1 knockdown in HeLa cells indirectly by assessing the impact of siKAP-1 treatment on the requirement for ATM, 53BP1, and RNF8 in IR-induced DSB repair (Figure III.13.A). Similar to published results by Goodarzi and colleagues, I observed that depletion of KAP-1 combined with siRNF8, si53BP1, or ATMi successfully alleviated the DSB repair defect associated with treatment with siRNF8, si53BP1, or ATMi alone; therefore I considered KAP-1 knockdown and siKAP-1-mediated heterochromatin relaxation to be efficient (Figure III.13.A). Importantly, I observed an IR-induced DSB repair defect in cells co-depleted for KAP-1 and Artemis. This result substantiated similar findings from our lab that were recently published (Woodbine et al. 2011) and will be discussed in later sections.

Next, cells were co-depleted for KAP-1 and RNF8, 53BP1, or Artemis and the number of DSBs per G0/G1 cell was assessed at indicated times after I-*Ppo*I delivery. 6 hours after direct delivery of I-*Ppo*I, a similar number of DSBs were observed in cells treated with siKAP-1 and 53BP1 (Figure III.13.D-E) or siKAP-1 and RNF8 (Figure III.13.F- G) as observed in cells treated with siControl and siKAP-1 (Figure III.13.B-C) or siControl alone (Figure III.12.B). This finding suggests that RNF8 and 53BP1 function in I-*Ppo*I-induced DSB repair to facilitate heterochromatin decompaction, similar to observations made after IR (Noon et al. 2010). Further, as cells co-depleted for KAP-1 and the mediator proteins fully repair most I-*Ppo*I-induced DSBs within six hours after transduction, the repair defect observed at this time in cells transfected exclusively with siRNF8 or si53BP1 is most likely related to defective heterochromatin decompaction. In contrast to these observations, cells co-depleted for KAP-1 and Artemis displayed a defective in I-*Ppo*I-induced DSB repair similar to that observed in cells depleted for Artemis alone (Figure III.13.H-I). This observation strongly suggests that Artemis functions downstream of localised heterochromatin relaxation in I-*Ppo*I-induced DSB repair.

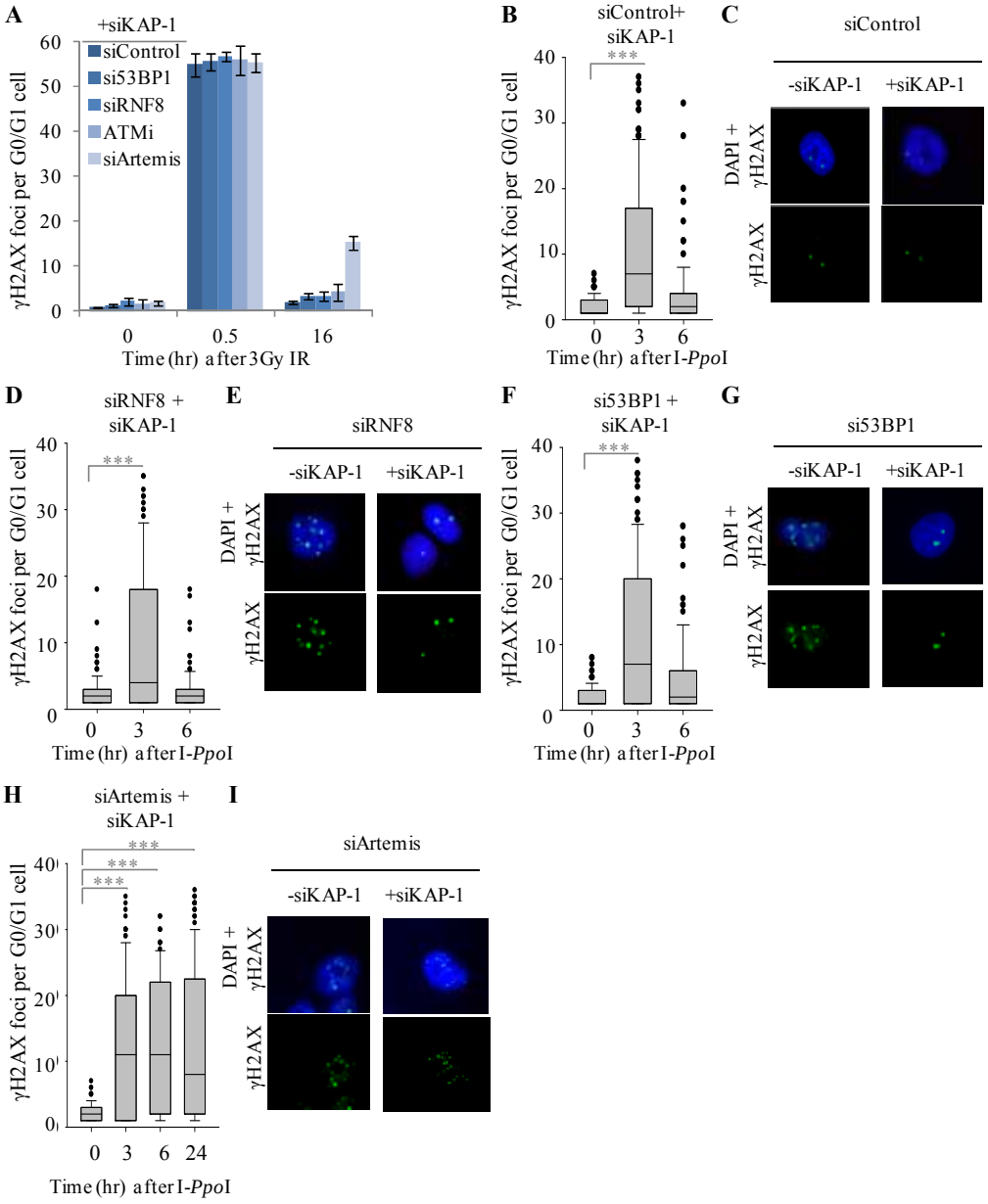

Figure III.13 Depletion of KAP-1 alleviates the requirement for RNF8 and 53BP1 but not for Artemis in the repair of I-*Ppo*I-induced DSBs in G0/G1. HeLa cells were transfected with siKAP-1 in combination with siControl (**A-B**), siRNF8 (**C-D**), si53BP1 (**E-F**), or siArtemis (**G-H**) as described in Figure III.10.C and repair of DSBs was monitored after delivery of 1 µg I-*Ppo*I. Plots depict γH2AX foci number per G0/G1 cell. Representative images of DAPI and/or γH2AX staining in cells fixed 6 hours after I-*Ppo*I delivery.

III.3 Discussion

While recent studies have shed light on the function of ATM signalling in heterochromatic DSB repair, the precise role of Artemis in this process is still being explored. Here I have optimised a system for site-specific DSB induction in regions likely to be enriched for heterochromatin using direct delivery of the I-*Ppo*I endonuclease. This system has been exploited to investigate the cellular requirement for Artemis in DSB repair. These findings have demonstrated that Artemis as well as ATM, DNA-PK, and the mediator proteins are required for the repair of a very substantial fraction of I-*Ppo*I-generated DSBs during G0/G1. Further, these results have indicated that unlike the requirement for ATM signalling factors, the requirement for Artemis in I-*Ppo*I-induced DSB repair cannot be overcome by heterochromatin relaxation.

Various techniques for inducing DNA damage and monitoring DSB repair may be exploited for the study of DDR factors and are accompanied by distinct advantages and disadvantages. As discussed below, several of the advantages and disadvantages associated with these techniques must be considered in their use for heterochromatic DSB repair analysis in the context of G0/G1.

Some commonly used methods for monitoring DSB repair include γH2AX foci enumeration, pulse-field gel electrophoresis (allowing for physical assessment of DNA size), and analysis of breakage on the level of chromosomes (Lobrich et al. 2010). γH2AX foci enumeration is currently a favoured assay in our lab for assessment of DSB repair in G0/G1. Advantages of this technique include the ability to discriminate cells based on cell cycle phase or protein expression, the sensitivity of the assay (single DSBs can be visualised as a γH2AX focus, enabling assessment after very low and physiologically relevant levels of damage), and the application of this methodology for live cell analysis. However, disadvantages include the fact that γH2AX foci represent an indirect measure of DSBs, that γH2AX may also mark lesions other than DSBs, and that multiple clustered DSBs may be contained within a single γH2AX focus, therefore leading to underestimation of DSB number. While pulse-field gel electrophoresis has also proven to be useful in DSB repair analysis, much higher cell numbers and IR doses (10-80 Gy) are required for this technique than for γH2AX foci enumeration. Analysis of chromosome breaks in G0/G1 cells may be performed by fusion of G0/G1 and M-phase cells. However, only ~1 in 3-6 DSBs may be visualised as a chromosome break in these fused cells, limiting sensitivity of the assay. In this section, I aimed to assess the repair of I-*Ppo*I-induced DSBs (which occur at a relatively low frequency) specifically in G0/G1 cells; therefore γH2AX foci enumeration was selected for analysis.

DSB induction is typically performed by treatment with chemical agents, irradiation, or inducible expression of an endonuclease. However, treatment with IR and most chemical reagents generates multiple types of DNA lesions (ie. IR induces ~20 SSBs for every 1 DSB

generated (Lobrich et al. 2010)) across the genome. As previously introduced, throughout the genome, the majority of chromatin is found as euchromatin, with only ~10-20% DNA found as heterochromatin. As IR-induced damage may occur at random in the genome, this poses limitations for its use in site-specific DSB analysis at heterochromatin. Systems of site-specific DSB induction exploiting endonucleases such as I-*Sce*I (Pierce et al. 1999; Pierce et al. 2005; Mao et al. 2008) have proven valuable in the study of NHEJ- and HR-mediated repair pathways. However, these systems typically involve establishing cell lines with stably integrated enzymatic recognition sites and transfection with a protein expression vector. Further, these systems generally do not induce DSBs in regions specifically enriched for heterochromatin. Recently developed systems exploiting the I-*Ppo*I endonuclease and ChIP methodology have proven valuable in the analysis of DDR protein recruitment at site-specific DSBs. As I-*Ppo*I cleaves 28S rDNA (Monnat et al. 1999), heterochromatin content is generally higher in rDNA regions than other regions of the genome (Conconi et al. 1989), and a previous study reported that ATM-defective cells have a very substantial defect in I-*Ppo*I-induced DSBs (Berkovich et al. 2007), I considered that I-*Ppo*I may introduce DSBs in regions enriched for heterochromatin and provide a useful tool for examining the DDR at heterochromatic DSBs. However, earlier I-*Ppo*I-based techniques have relied on inducible protein expression in a stable cell line (Berkovich et al. 2007) or transfection with an I-*Ppo*I expression vector (Monnat et al. 1999) and result in cytotoxicity and repeated cycles of enzymatic cleavage. Here, I have exploited a novel system developed by Dr. Jie Wen, Dr. Patrick Concannon, et al. based on CPP-mediated delivery of purified I-*Ppo*I (Wen et al. 2012). This system has addressed several disadvantages associated with previous techniques and, as presented here, enabled analysis of I-*Ppo*I-mediated DSB repair by γH2AX foci enumeration in multiple cell lines.

As outlined in the results section, prior to using this system to examine the role of Artemis in DSB repair, optimisation of I-*Ppo*I expression (using a vector kindly provided by Dr. Wen and Dr. Concannon) and purification, CPP-mediated protein delivery, and I-*Ppo*I-generated DSB induction was performed. Conditions were identified which enabled the generation of sufficient amounts of purified I-*Ppo*I-his and purified protein was demonstrated to be functional in an *in vitro* plasmid-based assay. CPP-mediated protein delivery, using pep-1-cysteamine, was observed to be non-toxic and efficient, as measured by observation of cellular morphology and detection of fluorescein following AF-488 transduction. Using conditions for Pep-1-mediated delivery of I-*Ppo*I reported to result in detectable nuclear protein and enzymatic cutting of recognition sites (Wen et al. 2012), DSB induction (detected by immunofluorescence labelling of γH2AX foci) was observed within 1-3 hours following transduction. However, inter- and intra-cellular variations in DSB number, size, and distribution were evident.

Several experimental and physiological factors are likely to contribute to the variation in DSBs observed after CPP-mediated I-*Ppo*I delivery, and their impact upon the accurate

analysis of DSB repair must be carefully considered. First, intercellular variation in the uptake of pep-1:protein complexes and sub-cellular distribution of delivered protein may be a contributing factor to γH2AX foci variation. Unlike IR, which generally induces DNA damage in a synchronous fashion across all cells in a treated population, it is possible that CPP-mediated delivery of the endonuclease occurs over time, therefore posing a challenge in determining the total number of DSBs induced. If I-*Ppo*I-induced DSBs are indeed generated asynchronously and if a fraction of these DSBs are repaired rapidly, the precise monitoring of DSB repair over time would prove difficult using most assays. Further, while protein transduction is observed to be highly efficient (>90%), the intracellular distribution of delivered I-*Ppo*I may not be uniform, potentially impacting upon the probability of enzymatic cutting at recognition sequences. In addition, the efficiency of enzymatic cutting may be recognition site-dependent. Cutting efficiency of CPP-delivered I-*Ppo*I is reported to be similar (10-30%) at the 11 non-rDNA recognition sites in the human genome (Wen et al. 2012) but this analysis was not performed in a cell- (or cell cycle-) specific manner. Further, cutting efficiency of 28S rDNA has not been investigated with this novel system. Previous systems which exploit the expression of I-*Ppo*I protein in human cells have reported that I-*Ppo*I cleaves ~10% of the ~300 rDNA target sites in the genome (Monnat et al. 1999; Berkovich et al. 2007), a finding consistent with my observation that CPP-delivered I-*Ppo*I induces up to 30 γH2AX foci. As rDNA contain ~300 I-*Ppo*I recognition sites while only 11 additional recognition sites have been identified in the genome, it is likely that the majority of I-*Ppo*I-generated DSBs occur within the rDNA. However, this has not directly been shown. Another potentially confounding variable is the induction of clustered DSBs. As the 28S rDNA I-*Ppo*I recognition sequence is found in a repeating gene cluster, I-*Ppo*I-induced DSBs may occur within close proximity to one another. This clustered damage may make it difficult to distinguish between foci representing single DSBs or multiple DSBs. In support of this hypothesis, a fraction of I-*Ppo*I-induced γH2AX foci were observed to be brightly staining and large, potentially due to clustered damage within rDNA. Given the observed variation in I-*Ppo*I-induced γH2AX foci, potentially arising from these or other factors, γH2AX foci were scored in a greater number of cells than typically scored and all results from at least three independent experiments were presented in box plots to display variation.

While the potentially confounding factors described above are also likely to be associated with other I-*Ppo*I-based systems, CPP-mediated I-*Ppo*I delivery has addressed several factors associated with previous systems which originally prevented accurate assessment of DSB repair across cell lines. For example, I have suggested that multiple rounds of enzymatic cutting over extended times are less likely to confound DSB repair analysis after CPP delivery of I-*Ppo*I than after induction of tamoxifen-dependent protein expression. In a system in which the continuous presence and activity of the enzyme results in ongoing rounds of cleavage, an

increase in DSB number may be predicted to occur at times following the initial wave of DSB induction. Further, an increase in the overall maximal cutting frequency would be predicted to occur in cells depleted for key DSB repair factors as the number of newly generated DSBs over time would be added to the number of unrepaired DSBs in these cells. Consistent with this prediction, analysis of cutting efficiency in cells expressing tamoxifen-induced I-*Ppo*I indicate a possible second wave of cutting after 8 hours post-induction and an increase in the maximum cutting efficiency in cells lacking functional ATM or treated with an ATMi (Berkovich et al. 2007). In contrast, here I have reported that the maximum number of DSBs detected by immunofluorescence analysis of γH2AX foci does not increase after 3 hours post CPP delivery of I-*Ppo*I to cells, suggesting that the majority of enzymatic cleavage occurs within the first 3 hours and does not recur over time. Further, I have reported that inhibition or depletion of the DSB repair factors ATM and DNA-PK (or of Artemis, RNF8, or 53BP1) impacts upon the repair of I-*Ppo*I-induced DSBs but does not result in an increase in the maximum number of DSBs scored at any time. As described above, this suggests that while the DSBs induced within the first 3 hours after protein delivery remain unrepaired in these DSB repair-deficient cells, no new DSBs are induced after this time. Further supporting my findings are the observations made by Wen and colleagues using quantitative PCR analysis of the recognition site on chromosome 1 that cutting efficiency of I-*Ppo*I does not increase after the first 3 hours following CPP-mediated delivery and that there is no increase in maximum cutting efficiency in cells defective in c-NHEJ (lack Lig4) (Wen et al. 2012). Together, these findings suggest that multiple rounds of enzymatic cutting and re-cutting are likely to occur after inducible protein expression but to be minimal after direct protein delivery. Wen, Conannon, et al have proposed that I-*Ppo*I, once delivered to the cell using CPPs, is turned over rapidly, and in support of this, levels of I-*Ppo*I-his are detected early (1-2 hours) after transduction but rapidly diminish over time (Wen et al. 2012). In addition, potentially as a result of rapid protein turnover and/or the low toxicity associated with CPP-mediated protein delivery, the method of protein introduction exploited here was not observed to affect cell viability. Finally, as CPP-mediated I-*Ppo*I delivery is not restricted to specific cell lines, DSB repair can be assessed and compared in cell lines from various genetic backgrounds (ie. from patients with mutations in DDR genes).

Using this system of CPP-mediated protein delivery and DSB repair analysis by γH2AX foci enumeration, I have demonstrated that a very substantial fraction of I-*Ppo*I-induced DSBs require Artemis, ATM, RNF8, 53BP1 and DNA-PK for repair during G0/G1. While, for the reasons described above, the precise assessment of the % I-*Ppo*I-induced DSBs which require these factors for repair is not feasible, comparison of median or the value range in the upper and lower quartiles (25-75%) over time allows for very rough approximations of the fraction of persisting DSBs. Using this method of comparison, in control cells, only a small fraction of DSBs scored at 3 hours (25-75 % range ~1-21, median~13) persist at later times (6-24 hours) in

control cells, with DSB number returning to base line values (range 1-3, median~2). In contrast, while the number of DSBs scored 3 hours after transduction was similar in Artemis, ATM, RNF8, 53BP1 or DNA-PK inhibited/depleted cells, anywhere from 50-90 % of DSBs persisted 6-24 hours later in these cells (median values between 8-12). Importantly, KAP-1 depletion was observed to alleviate this repair defect in cells treated with ATMi, siRNF8, or si53BP1, with the median number of DSBs falling to baseline levels. As KAP-1 depletion results in global heterochromatin relaxation, this suggests that the very substantial repair defect observed in ATMi, siRNF8, or si53BP1-treated cells is associated with an inability to promote the localised heterochromatin decompaction which normally facilitates DSB repair (Goodarzi et al. 2008). Further, this finding suggests that I-*Ppo*I delivery may induce a high fraction of DSBs within heterochromatin (presumably at rDNA regions), therefore resulting in an enhanced reliance on these specific DDR factors.

A substantial defect in I-*Ppo*I-generated DSB repair was observed in Artemis-depleted cells even after co-depletion of KAP-1. Similarly, depletion of KAP-1 did not alleviate the requirement for Artemis in repair of IR-induced DSBs. These observations substantiated findings from IR- and TBH-based experiments recently published (Woodbine et al. 2011) and suggest that Artemis functions in DSB repair in a process distinct to ATM signalling-dependent heterochromatin opening. While the function of ATM and Artemis may be distinct, epistasis analysis has demonstrated that ATM and Artemis operate in the same pathway, both promoting NHEJ during G0/G1 and HR during G2 (Riballo et al. 2004; Beucher et al. 2009).

In considering the role of the Artemis endonuclease in heterochromatic DSB repair, several possible models exist. One model postulates that the endonucleolytic activity of Artemis helps to remove lesions or secondary structures inhibitory to the completion of NHEJ or HR. During G0/G1, Artemis activity is reported to require DNA-PK (Goodarzi et al. 2006) and is thought to promote NHEJ (Beucher et al. 2009). Goodarzi et al. originally proposed that Artemis functions in NHEJ to process DSBs with long overhangs (ie .two SSBs in close proximity) that cannot readily be ligated (Goodarzi et al. 2006). This model proposes that DNA ends are first bound by Ku and DNA-PKCs and subsequent autophosphorylation of DNA-PKcs induces structural changes which activate Artemis-dependent processing of ends, thereby facilitating end ligation (Goodarzi et al. 2006). During G2, Artemis activity does not require DNA-PK and is instead thought to promote HR (Beucher et al. 2009). As DNA end resection is required for HR, Beucher, Lobrich et al. have proposed that Artemis promotes repair during G2 by cleaving secondary structures which block the progression of DNA end resection. Given the structural complexity of heterochromatin and tendency to contain repeat sequences such as satellite regions, one might expect that secondary structures (such as hairpins) may arise more frequently in heterochromatic DSBs and therefore require Artemis-dependent processing.

Another more recent model postulates that some level of resection may occur at heterochromatic DSBs during both G0/G1 and G2 and that the function of Artemis involves promoting DNA end resection. While resection can be readily detected in G2 by techniques such as immunofluorescence labelling of RPA or BrdU foci, these foci are generally more difficult to detect in IR-treated G0/G1 cells. However, some resection may still occur in G0/G1, though less extensive than the resection visualised in G2 cells. As DSBs arising within heterochromatin regions rapidly relocalise to the periphery of heterochromatic regions (Jakob et al. 2011), one potential function of resection may be to promote this relocalisation, ultimately facilitating repair. As described below, further analysis of resection at I-*Ppo*I-induced DSBs within rDNA could potentially further these studies.

While the findings presented here provide insight into the nature of I-*Ppo*I-generated DSBs and factors required for their repair, further studies are needed to extend these findings and fully exploit the potential utility of this novel system of I-*Ppo*I delivery. Quantitative PCR analysis has previously been used to monitor induction and repair of I-*Ppo*I-induced cleavage at non-rDNA recognition sites (Berkovich et al. 2007; Wen et al. 2012). This methodology has been useful in examining certain DDR aspects such as the role of ATM-dependent phosphorylation of NBS. However, the likelihood of these genomic regions falling within heterochromatin regions is low and, therefore, other strategies may be needed to examine I-*Ppo*I-generated DSBs which occur within heterochromatin-rich regions. In order to substantiate my findings, quantitative PCR using primers spanning the 28S rDNA site or southern blotting using a 28S rDNA probe could feasibly be used to assess I-*Ppo*I associated DNA cleavage and repair. For example, control or Artemis-null fibroblasts grown to confluency (to enrich for G0/G1) could be exposed to I-*Ppo*I and harvested at various times after protein transduction for DNA extraction. Analysis of rDNA site cleavage over time by quantitative PCR or southern blot may then provide a measure for repair which could be compared in control and Artemis-defective fibroblasts. Further, the requirement for Artemis and extent of DNA end resection at DSBs in rDNA could be examined in G0/G1 cells using this system of I-*Ppo*I delivery. Quantitative PCR primer sets which vary in distance from the rDNA recognition site could be used to assess the extent of I-*Ppo*I-induced DSB end processing. This method may be applied to examine the molecular requirements for resection. ChIP-based assays could also be applied to samples from control and Artemis-null cells treated with I-*Ppo*I, to assess chromatin binding of resection factors, again using primers which recognise sequences at various distances from the 28S rDNA site. However, the repetitive nature of rDNA may present difficulties for primer efficiency.

In summary, here I have exploited a novel system of site-specific DSB induction by CPP-mediated delivery of I-*Ppo*I to examine the requirement for Artemis in DSB repair. Artemis, ATM, RNF8, 53BP1, and DNA-PK were found to be required for the repair of a

substantial fraction of I-*Ppo*I-induced DSBs during G0/G1 and heterochromatin relaxation via KAP-1depletion relieved the requirement for ATM, RNF8, and 53BP1 but not for Artemis. As ATM, RNF8, and 53BP1 are required specifically for the repair of heterochromatic DSBs, these results have suggested that I-*Ppo*I-induced DSBs may occur in regions enriched for heterochromatin (ie. within rDNA). In addition, these findings have implicated Artemis as functioning downstream of heterochromatin decompaction to promote DSB repair, a result also recently observed and reported in IR-based studies (Woodbine et al. 2011). Further exploitation of this system of site-specific DSB induction may extend our understanding of the precise role of Artemis in DSB repair.

Later chapters will now transition to the primary focus of this thesis: examination of the cellular impact of diminished capacity for DNA replication origin licensing. The effects of diminished origin licensing capacity were investigated in the context of potential therapeutic exploitation in oncology and in the context of ORC-deficient MGS. This transition has reflected my interest in disease-relevant research.

IV The impact of diminished origin licensing capacity on sensitivity to replication stress in tumour versus non-tumour cells

IV.1 Introduction

IV.1.1 Cellular alterations associated with cancer

As introduced in Chapter I, some of the earliest changes which occur during tumour development include the increased expression of oncogenes and decreased expression of tumour suppressor genes (Pedraza-Farina 2006). These changes are associated with a host of other alterations including, but not limited to, hyper-replication, altered regulation of DNA replication factors, genome instability, changes in survival and/or apoptotic pathways, and alterations in the mechanisms required to respond to the cellular threat of DNA damage such as cell cycle checkpoints and repair pathways (Hanahan et al. 2000; Halazonetis et al. 2008) . These changes each promote the proliferation of cancer cells and can propagate further alterations conducive to tumour development and survival.

One source of DNA damage found to be enhanced in tumours is replication stress (Bartek et al. 2012) (Section I.2.3). Replication stress may result from cellular changes associated with cancer such as the aberrant expression of the c-Myc oncogene (Murga et al. 2011), hyper-replication, structures or lesions which block the progression of replication forks or replication inhibiting reagents (Burhans et al. 2007). Alterations in genes involved in regulating the transition from G1 to S-phase are frequently associated with cancer and these alterations are thought to contribute to replication stress. Up to 50% of tumours harbour mutations in *TP53* (Vogelstein et al. 2000), which implies that p53 plays a crucial role in prevention of tumourigenesis. Alterations in other factors with regulate the G1-S transition, such as p16 or the retinoblastoma (RB) protein, are associated with a wide variety of tumour types (Bartkova et al. 1997; Bartek et al. 2001). In the context of such alterations, inappropriate S-phase entry of cells harbouring DNA damage may occur (Bartkova et al. 1997; Bartek et al. 2001), resulting in an increase in replication, replication-associated damage and genome instability. Under conditions of insufficient replication origin licensing capacity, regulation of the G1-S-phase transition is also thought to be crucial to prevent unscheduled S-phase entry and subsequent genome instability (Nevis et al. 2009).

Replication inhibitors are frequently used in the treatment of cancer but they can also impact upon any rapidly dividing normal tissue, which underlies the clinical side effects associated with chemotherapy (Helleday et al. 2008). Alternative therapeutic strategies which selectively target cancer cells may reduce these potential side effects. In this chapter, I aim to examine a potential therapeutic strategy of this nature.

IV.1.2 Mechanisms of replication stress recovery

As previously introduced (Section I.4.3), one of the ways in which cells may withstand replication stress is via the activation of dormant origins, allowing replication through DNA between two stalled forks, completion of genome replication and survival (Blow et al. 2011). However, most studies examining replication stress-induced dormant origin firing have been performed in tumour-derived cell lines using agents such as HU and aphidicolin (Ge et al. 2007; Ibarra et al. 2008a; Ge et al. 2010; Karnani et al. 2011). Overexpression of various pre-RC components has been observed in tumour cells (Lau et al. 2007b), and could function both to accommodate hyper-replication and to provide increased dormant origin availability to facilitate proliferation in the face of enhanced replication stress. Dormant origin firing has also been proposed to promote genome stability and tumour suppression in MEFs even in the absence of replication stress-inducing reagents (Kawabata et al. 2011b). However, these studies were performed using mice expressing hypomorphic mutations in the MCM helicase and it is unclear whether a similar effect would be observed in human cells deficient in ORC, CDC6, or CDT1. While no increase in cancer predisposition has been reported in human patients with deficiencies in the pre-RC components, MGS is a rare disorder, and it is therefore difficult to accurately assess changes in cancer incidence.

In addition to dormant origin firing, several other mechanisms exist which may promote recovery from replication fork stalling and/or collapse (Petermann et al. 2010a). As briefly introduced in Section I.2.3 and reviewed by Petermann and Helleday, replication fork stalling refers to a potentially transient delay in the progression of active replication forks which can be caused by a variety of obstacles. Replication fork stalling generates a DNA structure which requires stabilisation and, under contexts in which replication fork stability is compromised, forks may ultimately collapse. While the progression of stalled replication forks may be resumed following removal of the obstacle, collapsed replication forks are proposed to represent inactivated replication structures from which the replication machinery has dissociated (Petermann et al. 2010a). The term “replication fork collapse” is only loosely defined and refers to the generation of a variety of replication structures vulnerable to additional processing. For example, under certain contexts, replication forks may collapse into structures known as “one-ended DSBs” which require processing by DSB repair proteins, as described below.

As depicted in Figure IV.1, recovery from replication stress inducing agents such as HU involves fork remodelling and/or HR-mediated repair. HU-induced fork stalling is reported to result in the binding and activation of PARP1, subsequent recruitment of Mre11, activation of Mre11-dependent resection (Bryant et al. 2009), and X-ray repair cross-complementing protein 3 (XRCC3)-dependent replication fork restart and/or repair (Petermann et al. 2010b). Recovery from replication inhibition is also promoted by the DNA helicases, WRN (Sidorova et al. 2008),

BLM (Davies et al. 2007), and SWI/SNF-related matrix-associated, actin-dependent regulator of chromatin, subfamily A-like 1 (SMARCAL1) (Ciccia et al. 2009). While Rad51 activity promotes replication recovery after both short (ie. 2 hours) or long (ie. 24 hours) treatments with HU (Arnaudeau et al. 2001; Saintigny et al. 2001; Petermann et al. 2010c), Rad51 foci formation has been reported mainly after longer replication blocks (Petermann et al. 2010b). Therefore, Rad51 loading may be more extensive after longer exposures to HU, perhaps in order to support HR-mediated recovery. In response to 24 hour treatment with HU, PARP-1 is thought to promote HR-mediated repair of damaged forks and, as a consequence, PARP1 inhibition results in reduced Rad51 foci formation, recombination frequency, and survival (Bryant et al. 2009). These findings support a model proposed by Dr. Eva Petermann and Dr. Thomas Helleday that replication stress recovery may be dependent on the length of time in which replication is inhibited. Shorter arrest times (ie. 2 hours) may be associated mainly with fork stalling which activates HR-independent but Rad51-dependent replication fork remodelling. In contrast, longer periods of arrest (ie. 24 hours) may result in increased replication fork collapse, generating one-ended DSBs which require HR for repair (Petermann et al. 2010b). Overall, these mechanisms of replication fork restart and/or repair may act alongside dormant origin firing to promote efficient cellular recovery from replication arrest.

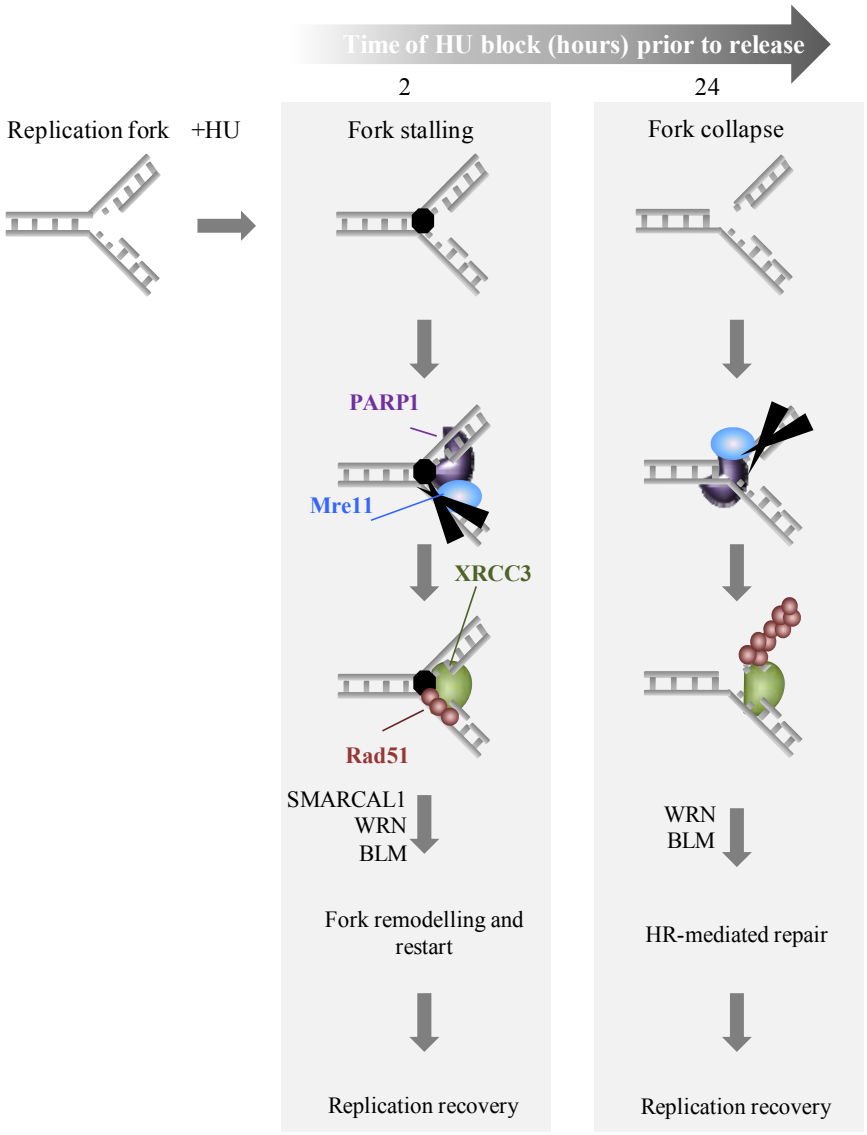

Figure IV.1 Pathways of Rad51-dependent recovery from replication stress. Adapted from (Petermann et al. 2010a). Treatment with HU blocks the progression of replication forks. Release from short or long periods of HU treatment (2 or 24 hours, respectively) results in the recruitment of PARP1 and subsequent Mre11-dependent end resection at stalled replication forks. XRCC3 is recruited to forks, leading to Rad51 loading. A 2 hour treatment with HU results in more minimal Rad51 loading while 24 hour HU treatment results in more extensive Rad51 loading and filament formation. DNA helicases may promote fork remodelling after short HU treatments, or HR-mediated repair after longer HU treatments, leading to replication recovery.

IV.1.3 Aims of this chapter

While dormant origin firing has been demonstrated to promote recovery from reagents such as HU or aphidicolin in tumour-derived cell lines (Ge et al. 2007; Ibarra et al. 2008a; Ge et al. 2010; Karnani et al. 2011), questions remain about whether normal human fibroblasts depend on dormant origin firing for recovery from replication stress. This is an important question because if cells in normal tissue have a diminished dependency upon dormant origin usage (perhaps by exploiting other pathways of recovery), therapeutic treatment with inhibitors of origin licensing components may be predicted to specifically sensitise tumour cells to replication stress without greatly affecting non-tumour tissue. Therefore, inhibitors of origin licensing components could be potentially useful therapeutic agents in combination with replication stress-inducing treatments.

Here, I aimed to compare the ability of non-tumour and tumour cells to recover from replication stress under conditions of diminished origin licensing capacity. To test this, I have employed siRNA-mediated depletion of licensing components such as ORC1, using conditions likely to deplete dormant origin availability without impacting upon cell growth, combined with HU treatment. In Sections IV.2.1-2, work will be presented from the comparison of ORC1 expression and reliance on ORC1 to maintain proliferation in the presence or absence of HU in 1BR3hTERT non-tumour fibroblasts and U2OS osteosarcoma cells. In addition, this section will describe findings from the comparison of ORC1-deficient MGS patient cell lines with control cells. Section IV.2.3 will present results from the examination of HU-induced new origin firing in U2OS cells depleted for ORC1 and Sections IV.2.4-5 will present results from the comparison of replication recovery and S-phase associated DNA damage in 1BR3hTERT and U2OS cells after treatment with HU. In Section IV.2.6, I will present findings from the combined partial depletion of additional licensing components and HU treatment in 1BR3hTERT and U2OS cells and Section IV.2.7 will compare HU sensitivity of additional non-tumour and tumour-derived cell lines following ORC1 depletion. Section IV.2.8 will examine the impact of ORC1 depletion on sensitivity to H_2O_2, an agent which induces oxidative stress and indirectly generates replication stress. Section IV.2.9 will describe findings demonstrating that the combined depletion of p53 and ORC1 results in enhanced loss of viability in the presence or absence of HU in 1BR3hTERT non-tumour cells. Section IV.2.10 will examine the impact of diminished origin licensing capacity on proliferation following aberrant expression of the c-Myc oncogene, and Section IV.2.11 will present finding from the combined treatment of U2OS osteosarcoma cells with ORC1 siRNA, UCN-01 (a Chk1 inhibitor at low doses), and HU. Finally, all findings presented in this chapter will be discussed in Section IV.3.

IV.2 Results

IV.2.1 Substantial depletion of origin licensing capacity does not impact upon viability in non-tumour and tumour-derived cells

To examine the cellular impact of reduced origin licensing capacity, I began by exploiting siRNA-mediated depletion of ORC1 in the non-tumour fibroblast line 1BR3hTERT and the tumour-derived line U2OS. 1BR3hTERT, an hTERT-immortalised fibroblast line derived from a normal individual, has a stable karyotype, shows genomic stability, and has an intact G1/S checkpoint (unpublished observations). The U2OS cell line is derived from an osteosarcoma, expresses normal p53 and RB but lacks p16 (Grossel et al. 1999). These cells are reported to lack the so-called "licensing checkpoint" (Hall et al. 2007). Further, the use of dormant origin firing has been reported to promote recovery from HU in this cell line (Ge et al. 2007).
While ORC1 is essential for cellular replication and viability, cells can survive with a significant reduction in ORC1, as shown by the viability of ORC1-deficient MGS patient cells (Bicknell et al. 2011b). This likely reflects the fact that a reduction in ORC1 levels may diminish dormant origin availability, while a sufficient number of origins remain to promote replication. Here, I aimed to identify conditions of ORC1 siRNA (siORC1) treatment in 1BR3hTERT and U2OS cells which reduced the level of protein and thus the availability of dormant origins while not impairing viability in the absence of exogenous damage. To this end, a single siRNA oligonucleotide targeting ORC1 which was previously described (Bicknell et al. 2011b) (Table II. 1) was used. While specificity of this siRNA oligonucleotide has not been verified by complementation studies, treatment of 1BR3hTERT cells with siORC1 results in a similar delay in the progression of cells from G1 to S-phase as observed in hTERT-immortalised fibroblast cells from an ORC1-deficient MGS patient (Bicknell et al. 2011b).
Here, cells were transfected with a range of siRNA oligonucleotide concentrations, incubated for 7 days, and assessed for viability using the fluorescence-based CellTiter-Blue® assay which measures the metabolic activity characteristic of viable cells. As positive controls for viability, non-transfected cells (0 nM siRNA) or cells transfected with various concentrations of randomly scrambled oligonucleotides (siControl) were examined. As negative controls for background fluorescence, samples including growth medium and the CellTiter-Blue® reagent but no cells were included in each experiment, and all samples were performed in triplicate within each experiment.

Using this assay, I observed diminished proliferation with increasing siORC1 concentrations, consistent with the notion that oligonucleotide concentration correlates with knockdown efficiency (Figure IV.2.A-B). No significant change was observed in viability between non-transfected or siControl-transfected cells. Interestingly, a greater loss of viability

was observed after lower siORC1 concentrations in U2OS cells compared with 1BR3hTERT cells. This result may reflect differences in siRNA-mediated knockdown efficiency between tumour and non-tumour cell lines. In addition, it may reflect a greater reliance of the tumour-derived cell line on ORC1-dependent origin licensing to maintain viability under conditions of hyper-replication and/or replication stress. The maximum ORC1 siRNA concentrations which did not inhibit viability (5 nM or 0.6 nM in 1BR3hTERT or U2OS cells, respectively) were selected from the siRNA dose response experiments and results were confirmed in three independent experiments (Figure IV.2.C).

Next, the efficiency of ORC1 protein depletion was assessed 48 hours after cells were transfected with siControl or siORC1 at the concentrations indicated above (Figure IV.2.D). Immunoblotting revealed that U20S cells express higher levels of ORC1 compared with 1BR3hTERT cells, consistent with previous findings that tumour-derived cells overexpress ORC proteins (Karakaidos et al. 2004; McNairn et al. 2005; Lau et al. 2007a; Di Paola et al. 2012). Although α-ORC1 antibodies are inefficient for immunoblotting, a marked reduction in ORC1 protein could be observed in both lines following siORC1 (Figure IV.2.D). Low levels of residual ORC1 were routinely detected in siORC1-treated U20S but not 1BR3hTERT cells. However, since ORC1 is essential, it is likely that 1BR3hTERT cells retain residual, although undetectable, ORC1. Nonetheless, these results suggest that U20S cells require a higher level of ORC1, and therefore origin licensing capacity, to maintain viability compared to normal fibroblasts.

I considered these siORC1 conditions likely to diminish dormant origin licensing capacity and went on to use them in subsequent experiments.

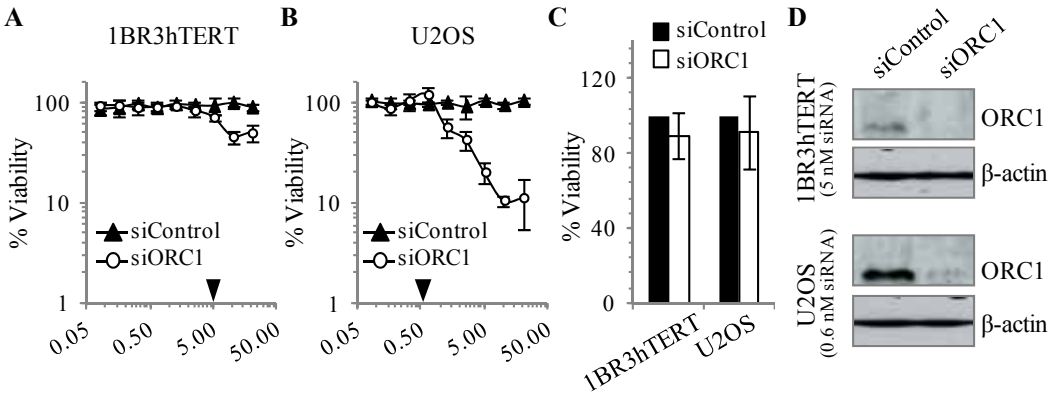

Figure IV.2 Substantial depletion of ORC1 does not impact upon viability in non-tumour 1BR3hTERT fibroblasts and osteosarcoma-derivedU2OS cells. A-B. 1BR3hTERT (A) or U2OS (B) cells were transfected with siControl or siORC1 oligonucleotides (0.1-20 nM), and viability assessed 7 days later. Results represent mean +/- SD from triplicate samples within one representative experiment. Black arrows indicate the oligonucleotide concentration subsequently utilised. **C.** As in (A-B), except 1BR3hTERT and U2OS cells were transfected with 5 or 0.6 nM siORC1, respectively and results depict mean % viability +/- SD from three independent experiments. **D**. 1BR3hTERT and U2OS cells were transfected with 5 or 0.6 nM siORC1, respectively. ORC1 protein levels were assessed by immunoblotting 48 hours later. β-actin was a loading control.

IV.2.2 ORC1 depletion differentially impacts upon the recovery of non-tumour and tumour-derived cells from HU-induced replication stress

Next, the impact of ORC1 depletion on recovery from replication stress was assessed in 1BR3hTERT and U2OS cells. To this end, HU, a clinically relevant chemotherapeutic agent which induces replication fork stalling and/or collapses, was exploited. As previously introduced, HU inhibits RNR, the enzyme required to supply cells with the nucleotide pools required for DNA synthesis, and has been demonstrated to induce dormant origin firing in U2OS cells (Ge et al. 2007). siRNA transfection was as performed as described above and cells were exposed to differing concentrations of HU for 24 hours. HU was removed and viability monitored 4 days later. Despite efficient protein depletion, as verified by immunoblot (Figure IV.2.D), treatment of 1BR3hTERT with siORC1 did not impact upon HU-induced loss of viability (Figure IV.3.A). However, ORC1 depletion resulted in a marked increase in HU-induced loss of viability in U2OS cells (Figure IV.3.B).

To verify that the viability assay reflects cellular survival and clonogenicity, clonogenic survival was examined in U2OS cells 10 days after HU removal **(**Figure IV.3.C). Although these two assays monitor different endpoints, a similarly enhanced sensitivity to HU was observed in siORC1-treated U2OS cells. I therefore considered the viability assay to be a valid measure of HU sensitivity and used it for subsequent experiments.

I next went on to verify that the effect of ORC1 depletion on HU sensitivity was not limited to the single ORC1-targeting oligonucleotide (siORC1 single) by testing the effect of transfection with a distinct ON-TARGETplus SMART pool targeting ORC1 (siORC1 pool). Again, while specificity of siORC1 pool was not verified here, ON-TARGETplus SMART pool oligonucleotides are reported by the manufacturer to being highly specific (Section II.2). 1BR3hTERT and U2OS cells were transfected with 5 nM or 0.6 nM, respectively, of siORC1 pool and 48 hours later ORC1 depletion was verified by western blot. Similar to observations made after transfection with siORC1 single, depletion of ORC1 was efficient in both cell lines using these conditions **(**Figure IV.3.D). Cells were then transfected with siControl, siORC1 single, or siORC1 pool as described, treated with HU for 24 hours, and assessed for viability 4 days after HU removal. Similar results were observed after treatment with either siORC1 single or siORC1 pool, confirming that the effects observed were reproducible with separate siRNA oligonucleotides.

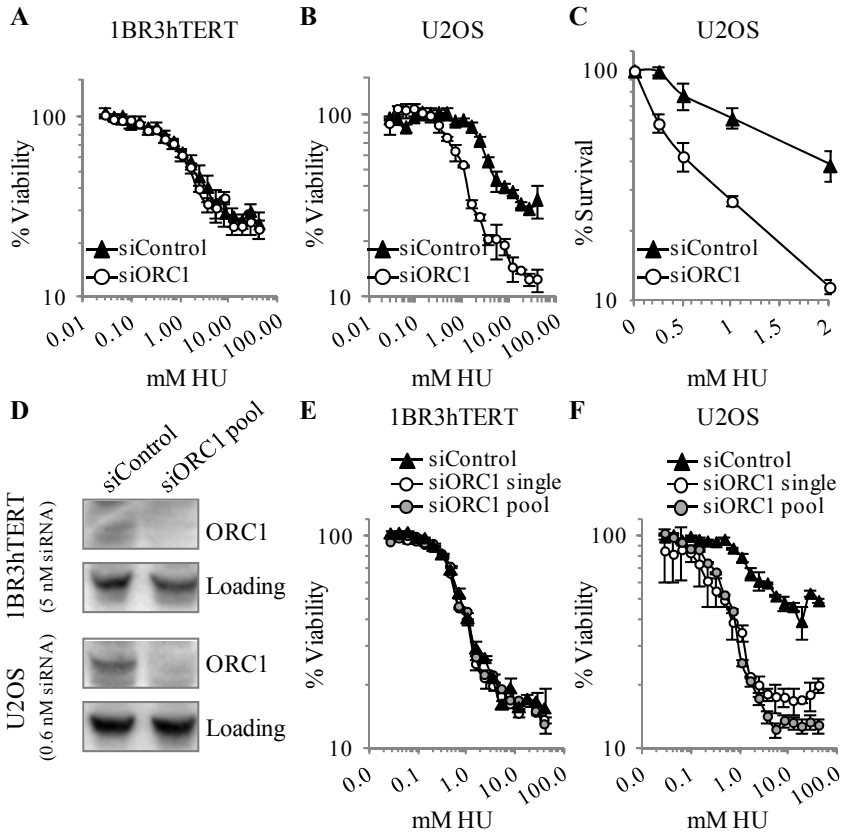

Figure IV.3 ORC1 depletion enhances sensitivity of tumour-derived U2OS cells but not non-tumour 1BR3hTERT cells to 24 hour treatment with HU. A-B. 1BR3hTERT (A) or U2OS (B) cells were transfected with siControl or siORC1 oligonucleotides (0.1-20 nM), and viability assessed 7 days later. Results represent mean +/- SD from triplicate samples within one representative experiment. Reproducibility was verified in at least six independent experiments. **C.** U2OS cells transfected with siRNA as described were treated with HU (0.05-2 mM) for 24 hours. Clonogenic survival was estimated 10 days following HU removal. Results represent mean +/- SD from three independent experiments. **D.** As in Figure IV.2.D except cells were transfected with siControl or a distinct pool of ORC1 siRNA oligonucleotides (siORC1 pool). **E-F.** As in (A-B), except cells were transfected with siControl, siORC1 single, or siORC1 pool. Reproducibility was verified in three independent experiments.

In considering possible explanations for the observation that ORC1 depletion specifically sensitises tumour-derived U2OS cells to HU, I reasoned that differences in the rate of cell cycle progression and/or DNA replication between tumour and non-tumour cells may impact upon the effects of HU, which specifically impacts cells during S-phase. Therefore, I monitored the population doubling time (Figure IV.4.A-B) and rate of HU-induced replication stress accumulation in a given cellular population (Figure IV.4C-D). The growth of 1BR3hTERT and U2OS cells was monitored for up to 96 hours (Figure IV.4.A) and the doubling time was estimated from the results (Figure IV.4.B). As expected, the tumour-derived U2OS cell line doubled more quickly than 1BR3hTERT cells, with U2OS cells doubling within ~30 hours. In contrast, 1BR3hTERT cells doubled every ~48 hours; hence there could be a fraction of cells that have not entered S-phase within the 24 hour HU exposure time tested above. As the effects of HU are specific to S-phase, a 24 hour exposure time is therefore unlikely to affect the entire population of 1BR3hTERT fibroblasts. To determine the fraction of cells which display the effects of HU after various exposure times, HU-induced replication stress was monitored by immunofluorescence labelling with γH2AX and the G2/M-phase marker, CENPF (Figure IV.4.C-D). Cells harbouring S-phase specific damage can be visualised as having bright, pan-nuclear γH2AX levels and minimal CENPF staining (here referred to as $\gamma H2AX^{+}$). Examination of the % $\gamma H2AX^{+}$ population at various times after HU addition revealed that >95% cells had undergone replication fork arrest by ~48 hours after HU in 1BR3hTERT cells (Figure IV.4.C) or ~30 hours after HU in U2OS cells treated with siControl or siORC1 (Figure IV.4.D).

1BR3hTERT cells were next transfected with siRNA oligonucleotides as previously described and treated with HU for 48 hours, a treatment time observed to induce replication stress in most cells in the population. HU was then removed and both cellular viability (Figure IV.4.E) and clonogenic survival (Figure IV.4.F) were assessed after a further 4 or 21 days, respectively. Despite this longer HU exposure and efficient ORC1 depletion, as routinely observed by western blot (Figure IV.2.D), treatment with siORC1 was not observed to impact the HU sensitivity of 1BR3hTERT cells measured in either of these assays (Figure IV.4.E-F).

To compare relative sensitivity of 1BR3hTERT and U2OS cells to 24 or 48 hour HU exposure times, the concentration at which viability was reduced by 50% (IC_{50}) was calculated from viability curves. The relative IC_{50} value was then estimated by comparison of the IC_{50} of siORC1-transfected cells to that of siControl-transfected cells (Figure IV.4.H). Whilst siORC1 did not affect sensitivity in 1BR3hTERT to both 24 and 48 hour treatments with HU, it enhanced sensitivity in U20S cells. Therefore, the resistance of 1BR3hTERT cells to siORC1-induced hypersensitivity is not explained by their slower cell cycle progression.

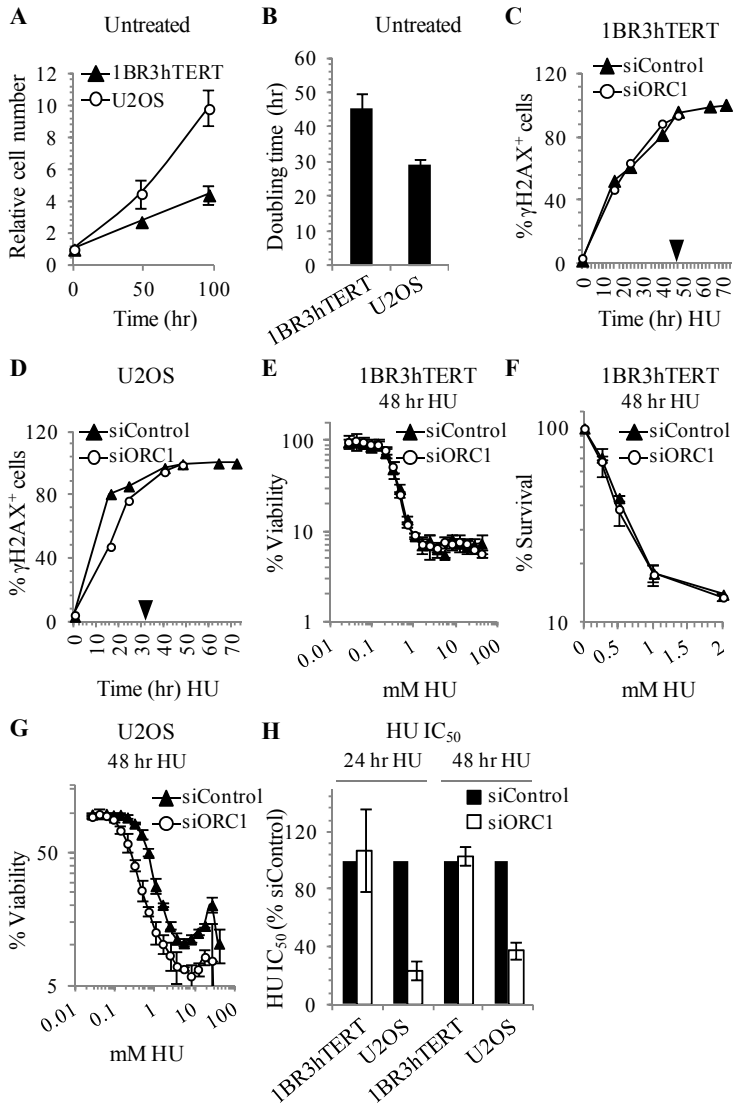

Figure IV.4 ORC1 depletion does not impact upon sensitivity of 1BR3hTERT fibroblasts to 48 hours of HU exposure. A. Exponentially growing 1BR3hTERT and U2OS cells were seeded at sub-confluent numbers similar to those used for the viability assay. Cells were grown in normal growth medium and harvested at the indicated time points. Cell number was assessed by manual scoring of live cells. Dead cells were detected by trypan blue staining and excluded. Cell number was normalized to the number seeded (t=0hr). Results represent the mean and SD from three experiments **B.** Cell doubling time was estimated from data in (A). Results represent mean and SD from three experiments. **C-D.** 1BR3hTERT (C) and U2OS (D) cells transfected with siRNA as described were treated with 2 mM HU for indicated times and HU-induced S-phase damage was assessed by immunofluorescence labelling of γH2AX. Nuclei containing bright γH2AX pan-nuclear staining were scored as $\gamma H2AX^+$. Black arrows indicate the time of HU treatment required to obtain >95% $\gamma H2AX^+$ cells. **E.** As in Fig.IV.3.A except cells were exposed to HU for 48 hours. **F.** Clonogenic survival was assessed as in Figure IV.3.C except siRNA-treated 1BR3hTERT cells were seeded on a feeder layer and survival was estimated 21 days following removal from 48 hour HU removal. **G.** As in Fig.IV.3.B except cells were exposed to HU for 48 hours. **H.** Relative HU IC_{50} values were estimated from the viability curves obtained in cells treated with HU for 24 (Fig.IV.3A-B) or 48 hours (E, G) Results depict mean values +/- SD from three independent experiments.

To substantiate these findings without relying on siRNA-mediated depletion, I next examined non-tumour cell lines derived from two MGS patients which carry mutations in ORC1. As previously introduced, MGS is characterised by microcephaly, both pre- and post-natal growth retardation, and skeletal abnormalities. Mutations in the origin licensing components *ORC1, ORC4, ORC6, CDC6, and CDT1* have been identified in patients with MGS (de Munnik et al. 2012). ORC1-deficient MGS cells display diminished replication efficiency in a plasmid-based assay and slowed S-phase entry and progression (Bicknell et al. 2011b).

ORC1-P1 LBLs have homozygous mutations in the BAH domain of ORC1 (p.Glu127Gly) (Bicknell et al. 2011b). Similar to published findings (Bicknell et al. 2011b), ORC1-P1 displayed reduced cellular levels of ORC1 (Figure IV.5.A). Examination of viability 5 days after treatment with HU (Figure IV.5.B) or aphidicolin (Figure IV.5.C) revealed that ORC1-P1 LBLs were slightly more resistant than control LBLs to HU or aphidicolin at concentrations greater than 1 mM and 5 μM, respectively, with no enhanced sensitivity observed at any concentrations tested.

Next, I examined an hTERT-immortalised fibroblast line derived from a distinct ORC1-deficient MGS patient (ORC1-P4hTERT). ORC1-P4hTERT cells have hypomorphic mutations in the BAH domain (p.Arg105Gln) and C-terminus (p.Arg720Gln) (Bicknell et al. 2011b). Examination of ORC1 levels in insoluble (proteins bound to chromatin or other structures) or soluble (unbound) protein extracts from 1BR3hTERT and ORC1-P4hTERT suggested that ORC1 chromatin binding is partially impaired in the MGS patient cells (Figure IV.5.D), as previously reported (Bicknell et al. 2011b). Interestingly, I observed resistance at higher HU concentrations rather than marked sensitivity of ORC1-P4hTERT to 24 hour treatment with HU (Figure IV.5.E). To confirm that this observed resistance to HU was not related to a slower cell cycle progression, HU treatment time was adjusted to achieve complete S-phase arrest in 1BR3hTERT and ORC-P4hTERT (representing 48 or 72 hour exposures, respectively) (Figure IV.5.F). Under these conditions, resistance but not sensitivity to 0.5 mM HU was also observed (Figure IV.5.G).

Overall, as depletion of ORC1 was observed to enhance sensitivity of tumour-derived U2OS cells but not non-tumour 1BR3hTERT cells to HU in both viability and clonogenic survival assays, I considered that of tumour-derived cells may have an increased reliance on dormant origin firing to recover from replication stress.

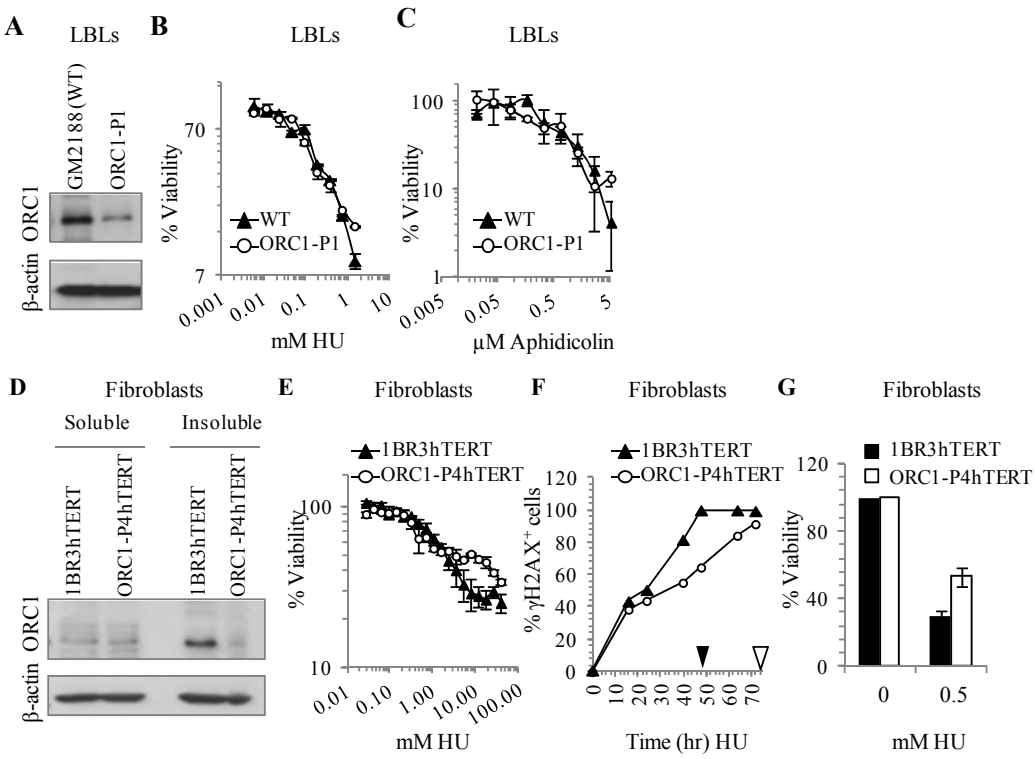

Figure IV.5 ORC1-deficient MGS patient cells do not display enhanced HU sensitivity. A. ORC1 protein levels were assessed by immunoblot in control (GM02188, WT) LBLs or in LBLs derived from an ORC1-deficient MGS patient (ORC1-P1). **B-C.** Viability was assessed 4 days after release from 24 hour HU (B) or aphidicolin (C) treatment in Control or ORC1-deficient fibroblasts. **D**. ORC1 protein levels were assessed in soluble and insoluble fractions in 1BR3hTERT and ORC1-P4hTERT by immunoblotting. **E**. 1BR3hTERT or ORC1-P4hTERT were treated with HU (0.03-40 mM) for 24 hours. Viability was assessed 4 days post HU removal. **F.** HU-induced S-phase damage was assessed in1BR3hTERT or ORC1-P4hTERT cells as in Figure IV.4.C-D. Arrows indicate the time of HU treatment required to obtain 100% $\gamma H2AX^+$ cells in 1BR3hTERT (black fill) and ORC1-P4hTERT (white fill). **G.** 1BR3hTERT or ORC1-P4hTERT cells were treated with 0.5 mM HU for 48 or 72 hours, respectively. Viability was assessed as above.

IV.2.3 ORC1 depletion reduces HU-induced new origin firing in tumour-derived U2OS cells

To verify that ORC1 depletion results in diminished new origin firing after HU, as assumed in my hypothesis, HU-induced new origin firing was assessed using the DNA fibre assay in collaboration with Dr. Eva Petermann and Dr. Rebecca Jones (University of Birmingham). The DNA fibre assay can be exploited to measure origin activity by transiently labelling replicating DNA with two distinct nucleoside analogues prior to HU treatment or following release from the agent (Petermann et al. 2010b). As depicted in Figure IV.6.A, U2OS cells were treated with 0.6 nM siORC1, grown for 48 hours, pulsed with CldU for 20 minutes, exposed to 2 mM HU for 24 hours, and pulsed with IdU for 1 hour. Cells were harvested and acid treated DNA fibre spreads were prepared, stained, and imaged using immunofluorescence methodology. $CldU^+/IdU^+$ replication tracks are considered to represent either ongoing tracts or tracts which restarted after HU removal, $CldU^+/IdU^-$ replication tracks are considered to represent stalled forks that have not reinitiated replication and $CldU^-/IdU^+$ tracks represent tracts with newly fired origins (such as dormant origins) (Figure IV.6.B).

To assess levels of fork stalling and new origin firing in siControl or siORC1-transfected cells, the number of these structures was quantified and normalised to the total number of replication tracks labelled with CldU (referred to as "% all CldU labelled").While the fraction of forks stalled was similar after both siRNA treatments, siORC1-transfected U2OS cells displayed reduced new origin firing. As a control, fork stalling and new origin firing was assessed in cells not treated with HU and were found to be similar after siControl or siORC1 (Figure IV.6.C).

These findings strongly suggest that depletion of ORC1 diminishes dormant origin firing after HU whilst not affecting origin firing in unperturbed U2OS cells. Further examination into the impact of ORC1 depletion on HU-induced new origin firing in 1BR3hTERT cells may shed light on whether non-tumour cells are able to restart stalled forks despite diminished dormant origin availability.

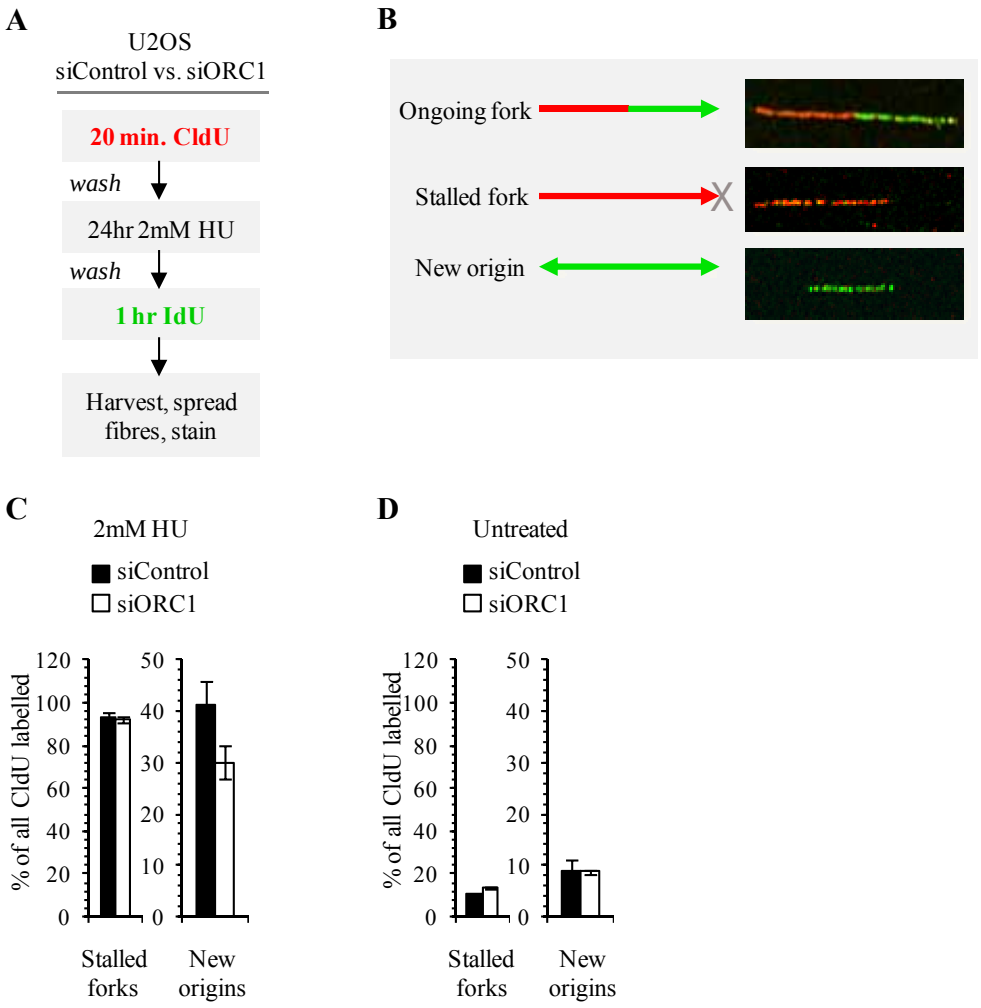

Figure IV.6 ORC1 depletion reduces HU-induced new origin firing in U2OS cells (Experiments performed by E. Petermann and R. Jones). **A**. Schematic of experimental setup for the DNA fibre assay. **B**. Representative images of labelled DNA fibres. $CldU^+$ (red) and IdU^+ (green)-labelled tracks represent ongoing/progressing forks, $CldU^+$ IdU^- represent fork stalling, and $CldU^-$ IdU^+ represent new origin firing. **C-D**. The fraction of replication tracts containing stalled forks or newly fired origins was determined by scoring at least 130 structures per experiment. Values were then normalised to the number of all CldU labelled tracts. Results represent the mean values +/- SD from multiple independent experiments.

IV.2.4 ORC1 depletion reduces replication restart in tumour-derived U2OS cells but not in non-tumour 1BR3hTERT cells following release from HU

Next, the impact of ORC1 depletion on overall replication restart was assessed in 1BR3hTERT and U2OS cells released from HU using a BrdU-based assay. While this assay does not distinguish between fork restart and dormant origin firing, it can provide a measure of replication re-entry at early times after release from HU.

As depicted in Figure IV.7.A, siRNA-transfected cells were grown for 48 hours and exposed to 2 mM HU for 24 hours. Either immediately (0 hours) or at various times after release from HU (2, 4, or 24 hours), cells were pulse labeled with the nucleoside analogue, BrdU, which is incorporated into actively replicating DNA. Cells were then harvested, BrdU was labeled with an FITC-conjugated antibody to BrdU, DNA was stained by PI, and cells were analysed by flow cytometry. Both positive controls for active replication (cells untreated with HU but pulse-labeled with BrdU) and negative controls (cells untreated with either HU or BrdU) were included in each experiment. BrdU intensity was plotted vs. PI intensity, and the fraction of $BrdU^+$ actively replicating cells was determined from control samples (Figure IV.7.B-D).

Consistent with the analysis of replication inhibition, 24 hour HU treatment abolished BrdU incorporation in both cell lines (Figure IV.7.B-D). In 1BR3hTERT, BrdU incorporation was substantially recovered at 2 hours post HU removal and was similar in siControl or siORC1-treated cells. In marked contrast, although siControl-treated U20S cells also recovered DNA synthesis at 2 hours following HU removal, DNA synthesis was dramatically reduced at this time in siORC1-treated U20S cells. Since this difference is observed at early times (2 hours) post HU removal, this suggests that siORC1 does not impair early replication restart in HU-treated 1BR3hTERT but does so in U20S.

The DNA fragmentation associated with apoptosis can be identified as a sub-G1 population by PI staining and flow cytometry (Darzynkiewicz et al. 1997). In siControl or siORC1-treated U2OS cells, the fraction of cells displaying sub-G1 DNA content was determined at early times after release from HU (Figure IV.7.D). As early as 0.5 hours following release from HU, an increase in sub-G1 cells was observed in ORC1-depleted samples, suggesting that at least some loss of viability may be attributed to the induction of replication stress-associated apoptosis (Figure IV.7.E).

Together with the results obtained in the fibre assay, these findings strongly suggest that depletion of ORC1in U2OS cells impairs replication restart after release from HU via diminished dormant origin firing. In contrast, despite substantially reduced ORC1 levels, 1BR3hTERT cells are able to recover replication after release from HU, potentially via alternative replication recovery mechanisms (Figure IV.1).

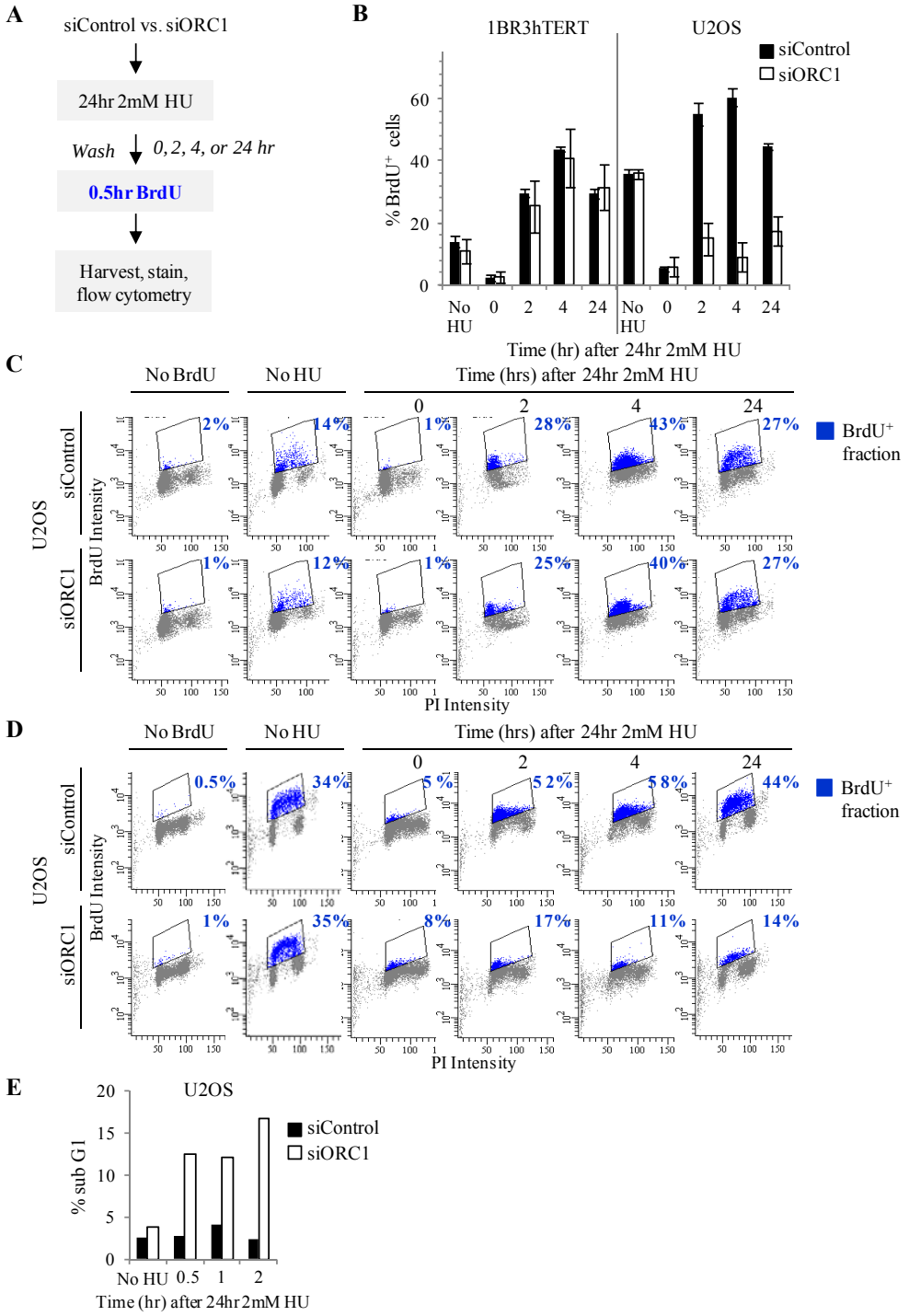

Figure IV.7 ORC1 depletion reduces replication restart following release from HU in U2OS but not 1BR3hTERT cells. A. Schematic of experimental setup for the BrdU assay. **B-D.** The BrdU$^+$ fraction of cells, representing active replication, was determined in siRNA-treated 1BR3hTERT or U2OS cells 0, 2, 4, or 24 hours after release from 24 hour treatment with 2mM HU. (B) depicts mean values +/- SD from three independent experiments and representative plots of BrdU vs. PI are depicted in (C-D), with the boxed regions containing blue data points indicating BrdU$^+$ cells and numbers in blue text representing the BrdU+ cell fraction. **E.** The fraction of sub-G1 cells was quantified in U2OS cells as in (C) except cells were harvested 0.5, 1, or 2 hours following release from HU.

IV.2.5 ORC1 depletion results in the persistence of S-phase DNA damage in U2OS cells but not in 1BR3hTERT cells following release from HU

Next, I examined whether the reduced replication restart observed in ORC1-depleted U2OS cells results in an accumulation of S-phase DNA damage, a threat to cell viability if left unrepaired. As depicted in Figure IV.8.A, siRNA-transfected cells were treated with HU as described, HU was washed out, and cells were fixed either immediately (0 hours) or 24 hours after release from HU. Immunofluorescence labelling of nuclei with DAPI, DNA damage with α-γH2AX, and G2/M-phase cells with α-CENPF was performed and staining was analysed using microscopic techniques. Replication stress from sources such as oncogene overexpression (Murga et al. 2011) or treatment with HU or aphidicolin (Lobrich et al. 2010), results in bright, pan nuclear γH2AX staining in $CENPF^-$ S-phase cells. The fraction of $\gamma H2AX^+CENPF^-$ cells was scored and compared across samples (Figure IV.8.B-C). Immediately following HU treatment, most cells were $CENPF^-$ (consistent with S-phase arrest) and showed pan-nuclear γH2AX staining, demonstrating the presence of collapsed/stalled replication forks; untreated cells had a lower fraction of $\gamma H2AX^+$cells. 24 hours post HU removal, few siControl or siORC1-transfected 1BR3hTERT cells were $\gamma H2AX^+$, consistent with the observed recovery of replication. Similarly, the number of $\gamma H2AX^+$siControl-treated U20S cells was dramatically reduced 24 hours post HU removal. In stark contrast, approximately 50 % of siORC1-treated U20S cells retained γH2AX staining 24 hours post HU removal while not staining for CENPF, consistent with the notion that they represent damaged S-phase cells. This analysis shows that 1BR3hTERT undergo replication fork arrest and activate the DNA damage response after HU treatment but efficiently recover despite substantial depletion of ORC1.

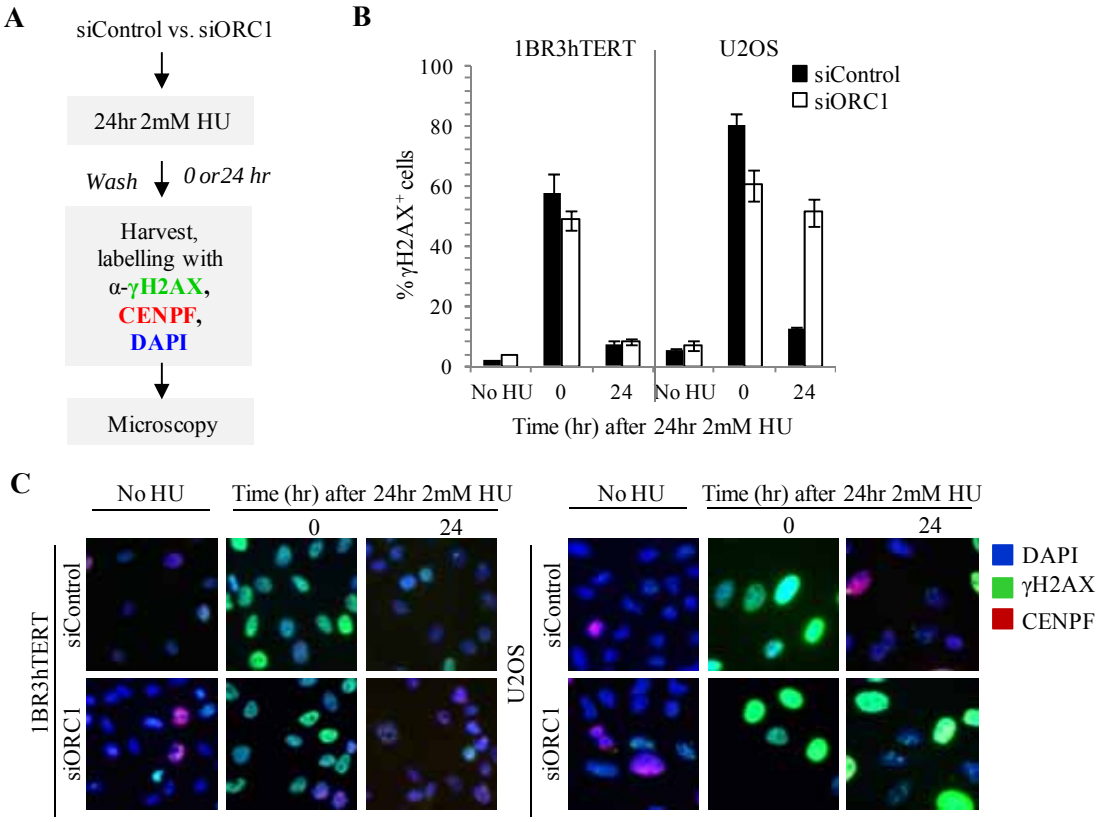

Figure IV.8 ORC1 depletion results in the persistence of HU-induced S-phase DNA damage in U2OS but not 1BR3hTERT cells. A. Schematic of experimental setup for the S-phase DNA damage assay. **B-C**. The γH2AX^{+} CENPF^{-} fraction of cells, representing cells harbouring S-phase DNA damage, was determined in siRNA-treated 1BR3hTERT or U2OS cells 0 or 24 hours after release from 24 hour treatment with 2mM HU. (B) depicts mean values +/- SD from three independent experiments. (C) depicts representative immunofluorescence images showing DAPI (blue, DNA), CENPF (red, cell cycle phase) or γH2AX (green, DNA damage).

IV.2.6 Depletion of additional licensing components sensitises tumour-derived but not non-tumour cells to HU-induced replication stress

In order to verify that the effects observed were not specific to ORC1 depletion, I next examined the impact of depleting additional licensing components on HU sensitivity. First the expression levels of ORC6 and CDC6 in exponentially growing 1BR3hTERT and U2OS cells were assessed by western blot. Similar to the observed increased in ORC1 expression in U2OS cells, the expression of both ORC6 and CDC6 was found to be enhanced in U2OS cells compared to 1BR3hTERT (Figure IV.9.A).

Next, the impact of depletion of ORC6 and CDC6 on HU sensitivity was assessed. 1BR3hTERT or U2OS cells were transfected with 5 nM or 0.6 nM, respectively, of ON-TARGETplus SMART pool siRNA oligonucleotides targeting ORC6 or CDC6 (Section II.2) and protein depletion was confirmed by western blotting 48 hours later. Transfection of 1BR3hTERT and U2OS cells with 5 nM or 0.6 nM, respectively, of siRNA oligonucleotides substantially depleted ORC6 or CDC6 (Figure IV.9.B-C) but did not impede cellular proliferation. Specificity of these siRNA oligonucleotide pools was not verified here.

Viability assessment in 1BR3hTERT cells revealed that neither siORC6 nor siCDC6 affected HU sensitivity (Figure IV.9.D), similar to findings obtained with siORC1 transfection. In marked contrast, HU sensitivity was enhanced in U2OS cells following treatment with siORC6 or CDC6 similar to that observed after treatment with siORC1 (Figure IV.9.E).

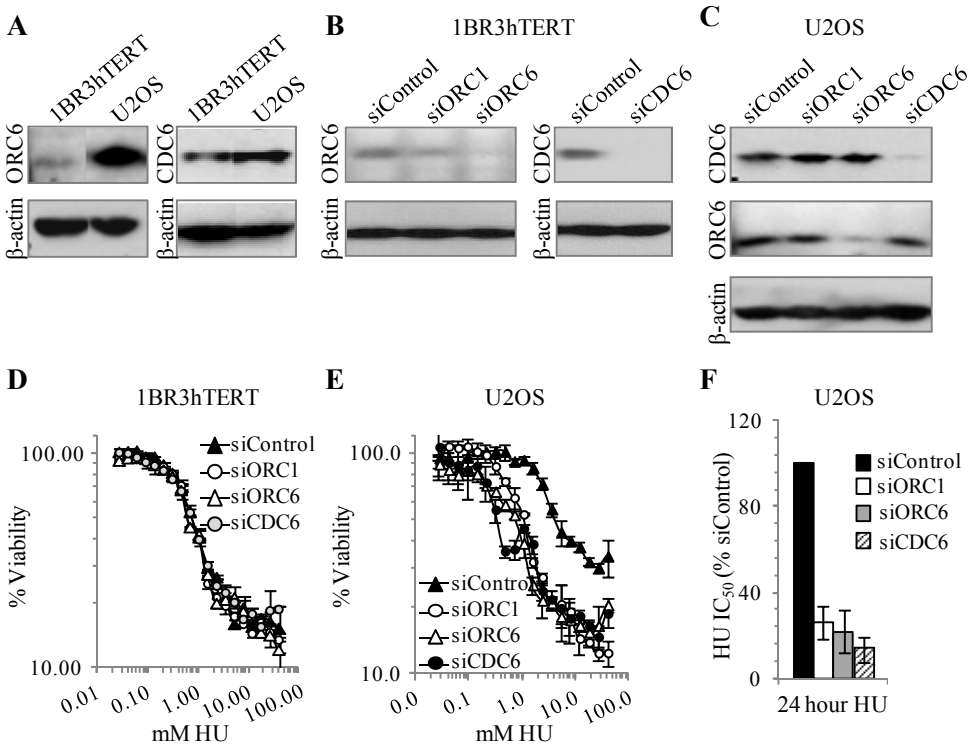

Figure IV.9 Depletion of ORC6 or CDC6 enhances HU sensitivity of U2OS but not 1BR3hTERT cells. A. Whole cell extracts were separated by SDS-PAGE and indicated protein levels were assessed by western blot. β-actin served as a loading control. **B**. As in (A) except 1BR3hTERT cells were transfected with 5 nM of ORC1, ORC6 or CDC6, and grown for 48 hours prior to lysis. **C.** As in (B) except U2OS cells transfected with 0.6 nM siORC1, siORC6, or siCDC6. **D-E.** 1BR3hTERT or U2OS cells were treated with siRNA as described in (A-B), treated with HU for 24 hours, and assessed for viability 4 days after release from HU. Viability plots from triplicate samples within representative experiments are depicted **F.** Relative HU IC_{50} values from U2OS viability plots from three independent experiments are depicted.

IV.2.7 ORC1 deficiency or depletion results in enhanced HU sensitivity in additional tumour-derived cell lines without affecting HU sensitivity of additional non-tumour cell lines

Next, in order to verify that the observations made were not specific to 1BR3hTERT and U2OS cells, the impact of reduced ORC1 levels on HU sensitivity was investigated in additional non-tumour fibroblasts (BJhTERT, 48BR, and MRC-5) and tumour-derived lines (HeLa and MDA-MB-231). BJhTERT is derived from foreskin tissue and immortalised with hTERT. 48BR (derived from skin tissue) and MRC5 (derived from fetal lung tissue) represent primary fibroblast lines to complement the analysis of hTERT-immortalised lines. HeLa cells, derived from cervical carcinoma, are reported to have a defective origin licensing checkpoint (Nevis et al. 2009) and require dormant origin firing to efficiently recovery from treatment with replication stress-inducing agents (Ibarra et al. 2008a). MDA-MB-231 cells are derived from breast adenocarcinoma and carry mutations in genes encoding proteins such as p16 (deleted) (Herman et al. 1995), p53 (Olivier et al. 2002), and the BRAF and KRAS oncogenes (activating mutations) (Wan et al. 2004).

For all lines, the optimum siORC1 oligonucleotide concentration that failed to impact upon viability was examined (Figure IV.10). BJhTERT cells showed slightly diminished viability above 5 nM siORC1 similar to 1BR3hTERT cells; 5 nM was chosen for analysis (Figure IV.10.A). HeLa cells were resistant to high oligonucleotide concentrations; 0.6 nM was chosen to allow comparison to U20S (Figure IV.10.B). 48BR, MDA-MB-231, and MRC-5 displayed diminished viability above 1 nM siORC1; 1 nM was chosen for analysis (Figure IV.10.C-E). The failure of these ORC1 knockdown conditions to impact upon viability was verified in three additional independent experiments (Figure IV.10.C-G). ORC1 depletion was also verified by immunoblot in all additional cell lines using siRNA oligonucleotide concentrations selected. Similar to observations made when comparing ORC1 levels in 1BR3hTERT and U2OS cells, ORC1 expression was enhanced in HeLa and MDA-MB-231 tumour-derived cell lines compared to BJhTERT, 48BR, and MRC-5 non-tumour cells (Figure IV.10.F). Importantly, the treatment of each additional cell line with siORC1 using the conditions selected was observed to result in a reduction in ORC1 protein levels.

The time of HU treatment required to achieve complete HU-induced S-phase damage was also assessed in each cell line (Figure IV.11.A-E) and used for subsequent viability experiments. Similar to the observations previously made using 1BR3hTERT and U20S cells, siORC1 enhanced HU sensitivity of HeLa and MDA-MB-231 without substantially impacting upon sensitivity of BJhTERT, 48BR or MRC-5 cells (Figure IV.11.F-J). For MRC-5, slightly enhanced sensitivity was observed at high HU doses but there was no impact on the IC_{50} value.

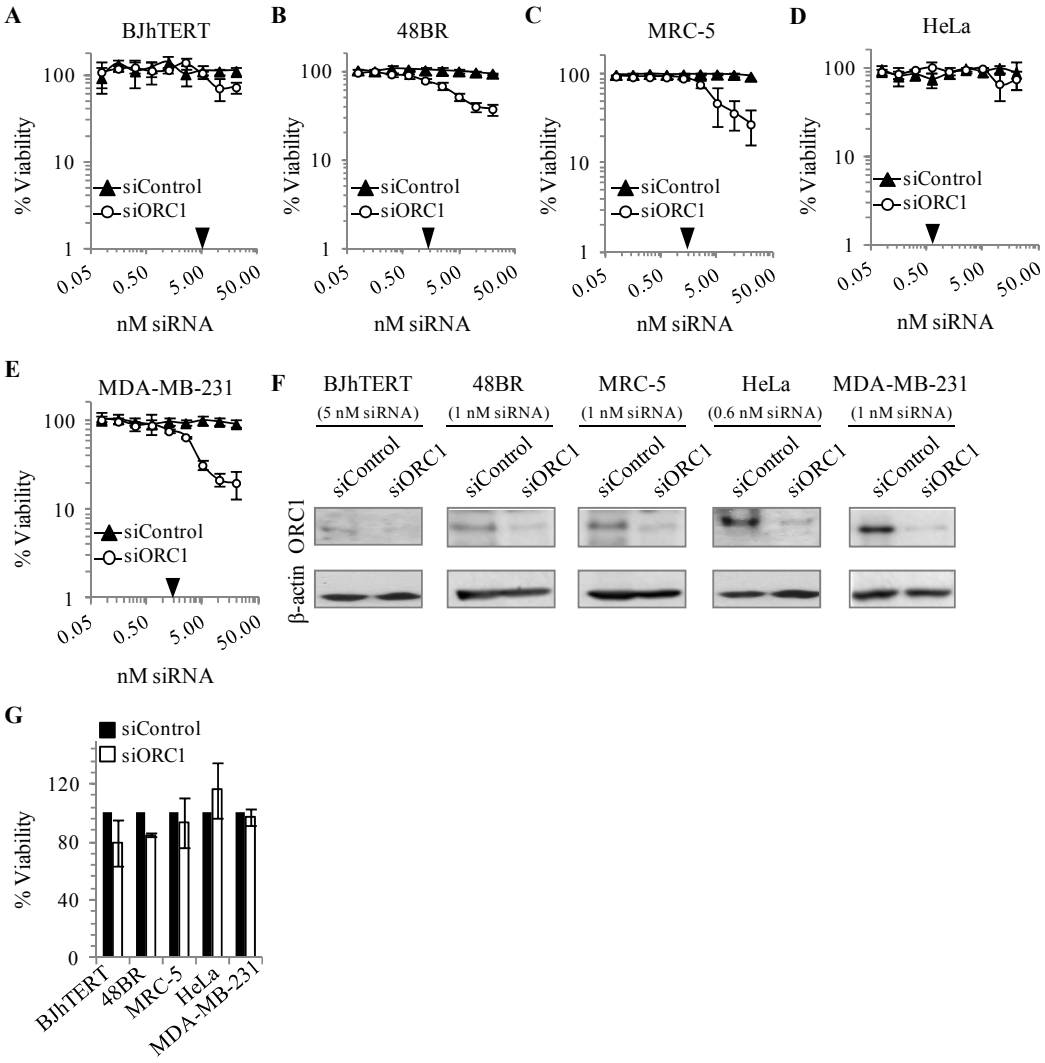

Figure IV.10 Identification of siORC1 conditions likely to deplete dormant origin licensing capacity in additional non-tumour (BJhTERT, 48BR, and MRC-5) and tumour-derived cell lines (HeLa and MDA-MB-231). A-E. The impact of increasing siORC1 concentrations on viability was assessed as in Figure IV.2.A-B in BJhTERT (A), 48BR (B), MRC-5(C), HeLa (D), or MDA-MB-231 (E). **F**. ORC1 depletion using conditions identified in A-E was verified by immunoblot. **G**. The impact of siRNA oligonucleotides (using conditions identified in A-E) was assessed as in Figure IV.2.C.

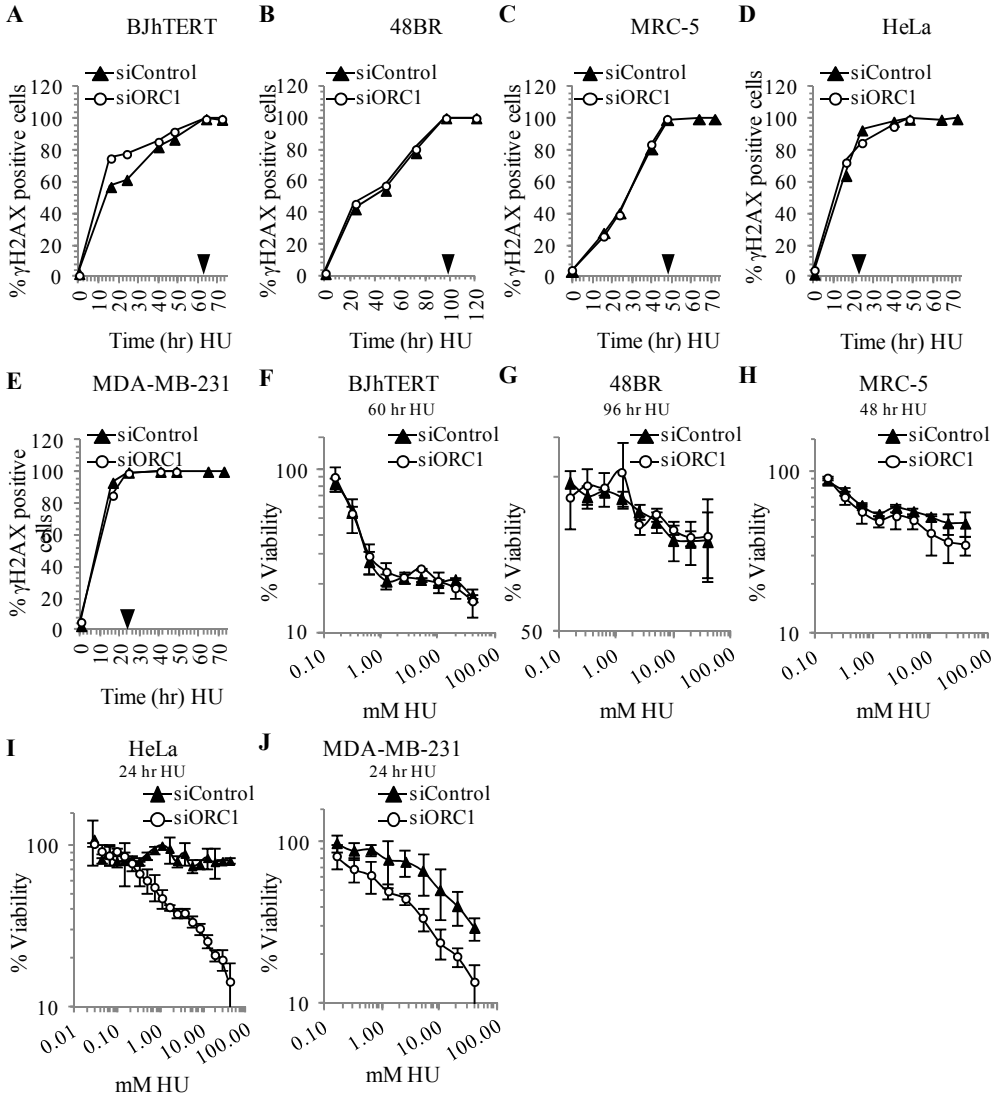

Figure IV.11 ORC1 depletion enhances HU sensitivity of additional tumour-derived cell lines (HeLa and MDA-MB-23) but not of additional non-tumour cell lines (BJhTERT, 48BR, and MRC-5). A-E. HU-induced S-phase damage was assessed in BJhTERT (A), 48BR (B), MRC-5(C), HeLa (D), or MDA-MB-231 (E) cells as in Figure IV.4.C-D. The impact of increasing siORC1 concentrations on viability was assessed as in Figure IV.2.A-B in BJhTERT (A), 48BR (B), MRC-5(C), HeLa (D), or MDA-MB-231 (E). **F**. ORC1 depletion using conditions identified in A-E was verified by immunoblot. **G**. The impact of siRNA oligonucleotides (using conditions identified in A-E) was assessed as in Figure IV.2.C.

IV.2.8 ORC1 depletion enhances sensitivity of tumour-derived HeLa and U2OS cells but not of non-tumour 1BR3hTERT and BJhTERT to H_2O_2-induced oxidative damage

Having shown that ORC1 depletion hypersensitises U20S and HeLa but not 1BR3hTERT or BJhTERT cells to HU-induced replication fork stalling/collapse, I next used a similar approach to examine recovery from oxidative stress, which is also found to be enhanced in tumour cells (Szatrowski et al. 1991). The primary lesions generated by H_2O_2 involve ROS-mediated DNA base damage (Section I.2.1) and are distinct to those induced by HU. While the primary lesions induced by H_2O_2 are not replication-specific, a fraction of H_2O_2-induced lesions may be encountered by the replication fork during S-phase, causing replication stalling. Consistent with this notion, H_2O_2-induced DNA damage signalling (detected by γH2AX labelling) is found to colocalise with replication factories (Zhao et al. 2011). Therefore, H_2O_2 is likely to indirectly induce replication fork stalling/collapse.

To assess the impact of diminished origin licensing on the recovery of non-tumour or tumour cells from oxidative stress, cells were treated with siRNA oligonucleotides as previously described, and H_2O_2 was added in differing concentrations. 24 hours later, H_2O_2 was washed out and after a further four days, viability was assessed. Strikingly, whilst siORC1 did not affect sensitivity of 1BR3hTERT or BJhTERT to H_20_2, U20S and HeLa cells showed marked hypersensitivity (Figure IV.12.A-E).

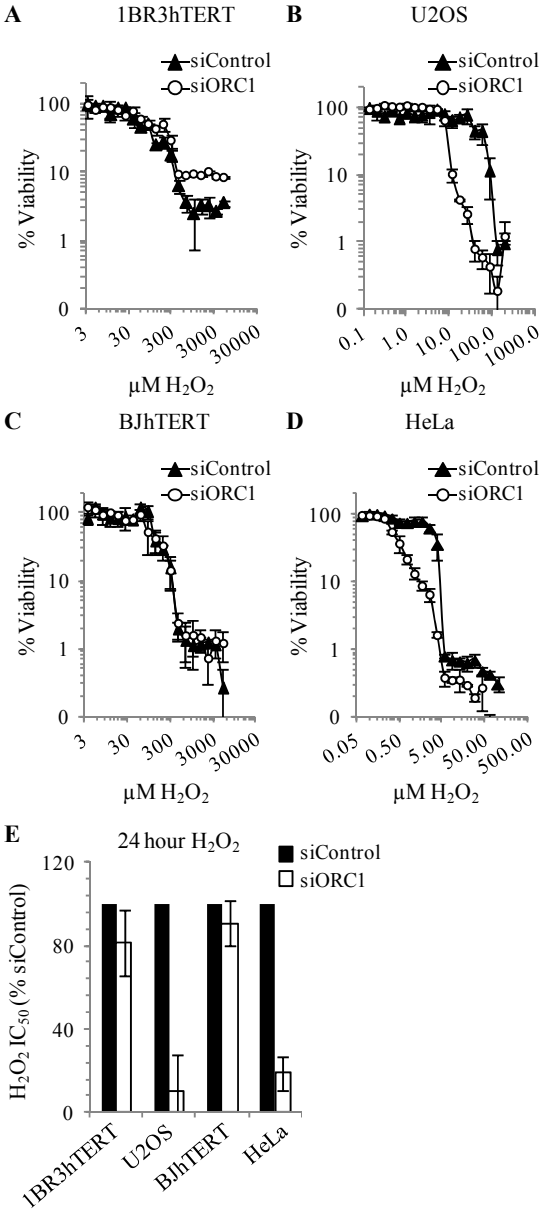

Figure IV.12 ORC1 depletion sensitises tumour-derived but not non-tumour cell lines to H_2O_2-induced oxidative damage. 1BR3hTERT (A), U20S (B), BJhTERT (C), or Hela (D) cells were transfected with siRNA as described in Figures IV.3 and IV.11. 48 hours later, cells were treated with H_2O_2, with concentrations adjusted to account for substantial differences in sensitivity between cell lines. 24 hours later, $H_2O_2$was removed and viability assessed 4 days later. **A-D**. Representative viability plots. **E**. Estimated IC_{50} values.

IV.2.9 Co-depletion of ORC1 and the p53 tumour suppressor in 1BR3hTERT cells enhances loss of viability in the presence and absence of HU.

p53 loss abrogates the damage-induced G1/S checkpoint, enhancing S-phase progression and replication stalling (Wahl et al. 1997). Additionally, p53 is required for a licensing checkpoint which prevents S-phase entry until sufficient origins have been licensed (Shreeram et al. 2002; Ge et al. 2009). Here, I examined whether p53 depletion in 1BR3hTERT, using an ON-TARGETplus SMART pool targeting p53 (Dharmacon, Thermo Scientific, Loughborough, UK) affects viability and HU sensitivity when combined with diminished origin licensing. As previously described (Section II.2), ON-TARGETplus SMART pool siRNA oligonucleotides are reported by the manufacturer to being highly specific as a result of unique dual-strand modification patterns used to synthesise the reagents. While, specificity of this oligonucleotide pool was not verified here, efficiency of p53 depletion was tested by immunoblot.

1BR3hTERT cells were transfected with siControl, sip53, siORC1 or combined siORC1+sip53 using 5 nM siRNA oligonucleotides. Depletion of p53 was verified by western blot 48 hours after siRNA transfection and found to be efficient in both sip53 and siORC1+sip53-transfected cells (Figure IV.13A). Next, viability was assessed in the absence of HU 7 days after siRNA transfection. While no significant impact on viability was observed after transfection with siORC1 or sip53 alone, treatment with both sip53+siORC1 diminished viability by ~1.7x (Figure IV.13B). Assuming that the siRNA oligonucleotide pool employed in these studies specifically targets p53, and therefore these results reflect the impact of p53 depletion, these findings suggest that in undamaged cells, siORC1 more markedly affects viability in the absence of p53. Assessment of sensitivity to 24 hour treatment with HU revealed that combined depletion of ORC1 and p53 also resulted in enhanced sensitivity to replication stress (Figure IV.13C).

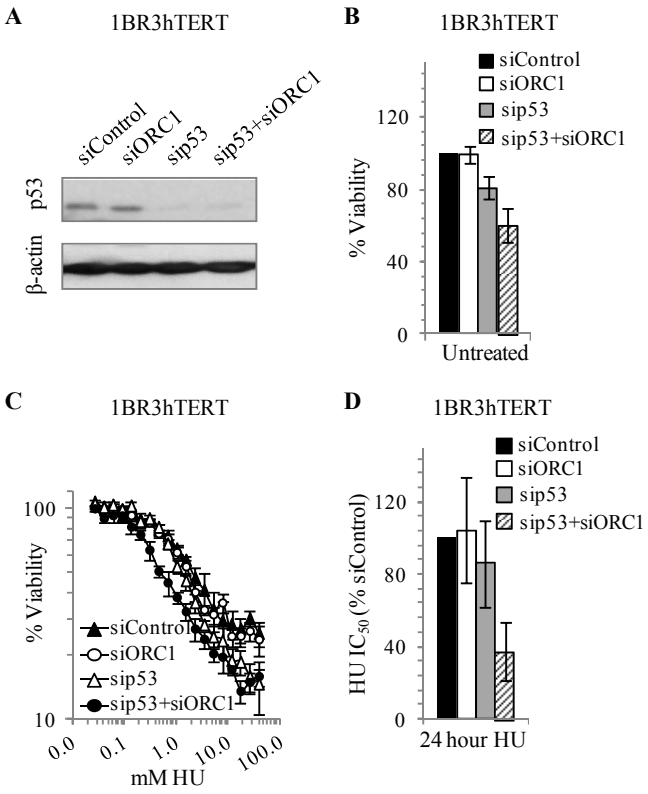

Figure IV.13 Co-depletion of ORC1 and p53 in 1BR3hTERT cells enhances loss of viability in the presence and absence of HU. A. 1BR3hTERT cells were transfected with 5 nM of indicated siRNA oligonucleotides and 48 hours later, efficiency of protein depletion was verified by immunoblotting. **B**. Cells transfected with siRNA as in (A) were assessed for viability 7 days after transfection as in Figure IV.2.C. **C-D**. HU sensitivity was assessed as in Figure IV.3.A-B. Viability plots are depicted in (C) and HU IC_{50} plots in (D).

IV.2.10 Depletion of ORC1 combined with aberrant oncogene expression results in enhanced DNA damage and loss of viability

Overexpression of the c-Myc oncogene, which is frequently observed during carcinogenesis, enhances DNA damage, hyper-replication, replication stress, and proliferation (Dominguez-Sola et al. 2007; Herold et al. 2009b; Robinson et al. 2009). Further, c-Myc overexpression is reported to increase ROS levels and to disrupt p53 function, therefore allowing cells containing damage to progress into S-phase (Vafa et al. 2002). This consequence of c-Myc expression may contribute to the enhanced replication stress observed.

The proliferative requirement for dormant origin licensing capacity was examined in a BJhTERT derivative cell line expressing c-Myc fused to a tamoxifen-inducible estrogen receptor (BJ-MYC-ER) (Dominguez-Sola et al. 2007; Herold et al. 2009b; Robinson et al. 2009) (kindly provided by Dr. Óscar Fernández-Capetillo) (Figure IV.14.A). First, efficiency of ORC1 depletion was verified after treatment of BJ-MYC-ER cells with 5 nM siORC1 (Figure IV.14.B). Efficient tamoxifen-dependent induction of c-Myc expression has been demonstrated in a similar system to result in enhanced replication stress, as monitored by pan-nuclear γH2AX staining (Murga et al. 2011). This assay was therefore used to monitor efficiency of c-Myc induction and to examine the impact of diminished origin licensing capacity on c-Myc-induced replication stress. 24 hours post tamoxifen addition, ~30 % of siControl-transfected BJ-MYC-ER cells were $\gamma H2AX^{+}$, suggesting that c-Myc overexpression induces replication stress (Figure IV.14.C). Following siORC1, ~60 % of BJ-MYC-ER cells were $\gamma H2AX^{+}$, raising the possibility that siORC1 causes enhanced or persistent c-Myc-induced replication arrest.

Next, the viability of siControl or siORC1-treated BJ-MYC-ER cells was assessed following addition of tamoxifen/induction of c-Myc overexpression. First, viability was assessed 5 days following addition of 2 μM tamoxifen, a dose found to induce replication stress, as described above. BJhTERT cells not containing the c-Myc-expressing system were included to verify that addition of 2 μM tamoxifen did not impact upon viability in the absence of oncogene-induced replication stress. An approximately 70% loss in viability was observed in ORC1-depleted BJ-MYC-ER cells following tamoxifen-mediated induction of c-Myc expression while no loss of viability was observed in tamoxifen-treated BJhTERT cells (Figure IV.14.C). These results suggest that viability is specifically impacted by increased expression of the c-Myc oncogene in ORC1-depleted non-tumour fibroblasts. To extend these findings, viability was assessed in siControl or siORC1-treated BJ-MYC-ER 5 days after the addition of a range of tamoxifen concentrations. ORC1-depletion was again observed to result in viability loss at multiple concentrations of tamoxifen (Figure IV.14.D-E).

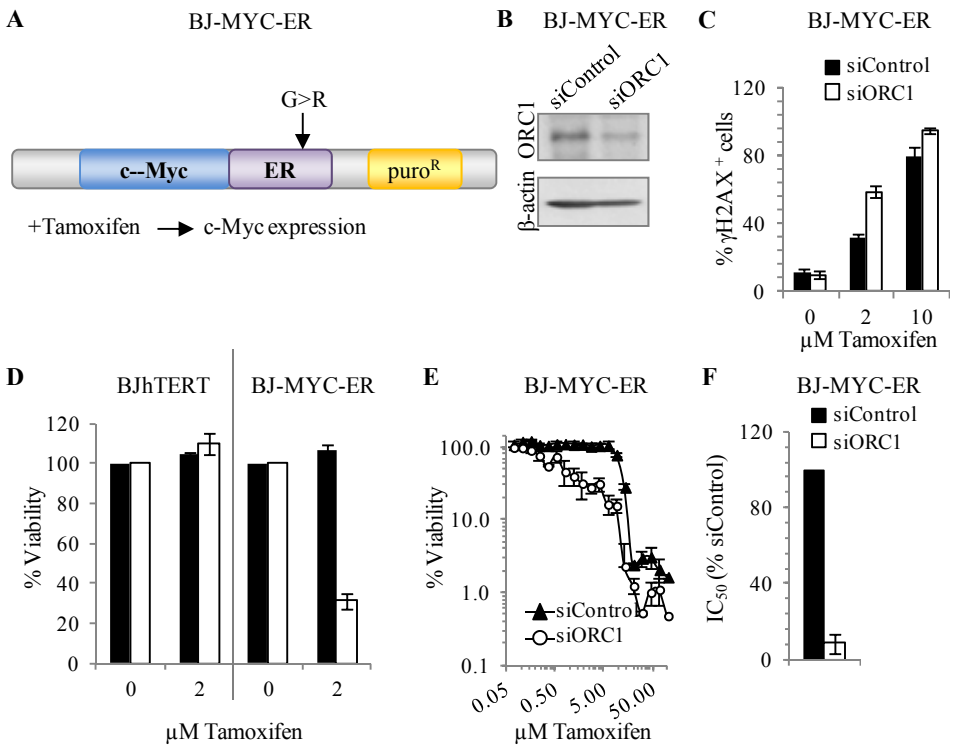

Figure IV.14 Depletion of ORC1 combined with overexpression of the c-Myc oncogene in BJhTERT cells results in enhanced DNA damage and loss of viability. A. Schematic of the inducible c-Myc expression system in BJhTERT cells (BJ-MYC-ER). **B**. BJ-MYC-ER cells were transfected with 5 nM siControl or siORC1, grown for 48 hours, and ORC1 depleted was verified by immunoblot. **C**. BJ-MYC-ER cells were treated with siRNA oligonucleotides as in (B) and tamoxifen was added for 24 hours to induce expression of c-Myc. S-phase-induced DNA damage was then assessed by immunofluorescence labelling with γH2AX as previously described. **D**. BJhTERT or BJ-MYC-ER cells were transfected with siRNA oligonucleotides as described and treated with tamoxifen. 5 days later, viability was assessed. **E**. As in (D) except BJ-MYC-ER cells were treated with a range of tamoxifen concentrations. **F**. IC_{50} values were estimated from viability plots in (E).

IV.2.11 Chk1 inhibition further enhances the sensitivity of ORC1 or ORC6-depleted tumour-derived U2OS cells to HU

The DNA damage response kinase Chk1 is reported to be required for inhibition of late firing origins, promoting the firing of dormant origins within active replication clusters (Ge et al. 2010). In response to HU-induced DNA damage, Chk1 is also reported to play a role in promoting Rad51 phosphorylation and subsequent HR-mediated repair (Sorensen et al. 2005). Chk1 inhibitors show promise as therapeutic agents in the treatment of cancer (Dai et al. 2010) in combination with replication stress-inducing agents such as HU or Gemcitabine (Montano et al. 2012). Here, I aimed to investigate whether the combined depletion of origin licensing inhibition, inhibition of Chk1 and treatment with HU could enhance cell death in tumour-derived cells and therefore represent a potential therapeutic strategy.

To examine this question, U2OS cells were transfected with siControl, siORC1, and siORC6 as previously described and treated with a range of HU concentrations for 24 hours. 50nM of UCN-01, a selective inhibitor of Chk1 at submicromolar doses (Graves et al. 2000), was added for the last 0.5 hours of HU treatment and following release from HU (Figure IV.15.A) to examine the impact of Chk1 inhibition on the recovery from replication arrest. Assessment of viability revealed that the depletion of ORC1 or ORC6 enhanced sensitivity to UCN-01+HU in U2OS cells (Figure IV.15.B).

These findings have positive implications for chemotherapeutic treatment with origin licensing inhibitors, Chk1 inhibitors, and HU, and tumour cells may be particularly sensitive to this combination.

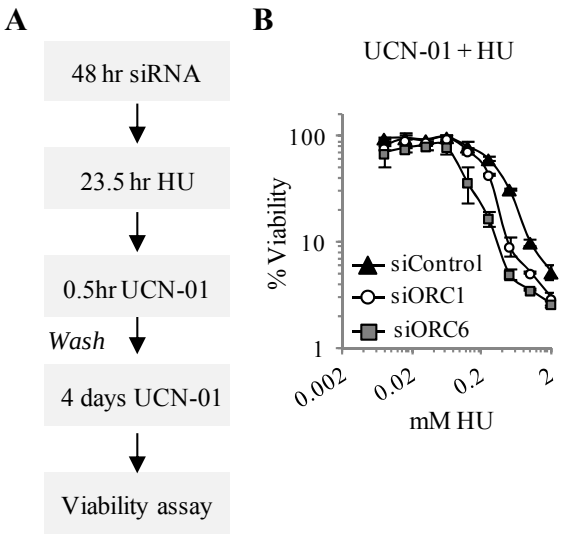

Figure IV.15 Combined treatment with siORC1 or siORC6 and UCN-01 enhances HU sensitivity in U2OS cells. A. Schematic depicted experimental setup. Cells were transfected with 0.6 nM of siControl, siORC1, or siORC6. 48 hours later, HU was added at a range of concentrations (0.01-2 mM). 23.5 hours after HU addition, 50 nM UCN-01 was added to HU and cells. After a further 30 minutes, cells were washed, UCN-01 was re-administered, and cells were incubated for a further 4 days prior to viability assessment. **B.** Viability plots are depicted.

IV.3 Discussion

Recent studies primarily from work using tumour-derived cell lines have provided evidence that dormant origins can be utilised to promote recovery from replication fork stalling or collapse (Woodward et al. 2006; Ge et al. 2007; Ibarra et al. 2008b; Blow et al. 2009; Kawabata et al. 2011a). Since tumour cells display elevated oxidative damage (Maiti 2012) and replicative stress (Negrini et al. 2010) as well as increased expression of origin licensing components (Lau et al. 2007b), I reasoned that the requirement for dormant origin availability to maintain proliferation may be elevated in tumour cells. This raises the possibility that targeting origin licensing components could specifically inhibit cancer cell growth, potentially implicating origin licensing as a potential therapeutic target. Here, I have evaluated this by examining the reliance of various non-tumour and tumour-derived cell lines on origin licensing capacity to maintain viability under conditions of increased replication stress.

Consistent with previous findings (Karakaidos, Taraviras et al. 2004; McNairn and Gilbert 2005; Lau, Tsuji et al. 2007; Di Paola and Zannis-Hadjopoulos 2012), I observed higher ORC1 expression in tumour-derived cell lines (U2OS, HeLa, and MDA-MB-231) than non-tumour cells (1BR3hTERT, BJhTERT, 48BR, and MRC-5). Further, higher levels of ORC1 were required to maintain viability in U2OS and HeLa cells compared to non-tumour cells. While the increased expression of licensing components is likely to support increased DNA replication, this change may also provide enhanced dormant origin licensing capacity to promote ongoing proliferation in the face of enhanced replication stress. Consistent with findings that only 10 % of licensed origins are utilised during unchallenged replication (Anglana et al. 2003; DePamphilis et al. 2006; Gilbert 2010), I observed that both viability and replication could be maintained in both non-tumour and tumour-derived cells despite substantial depletion of origin licensing factors such as ORC1. I was able to identify siORC1 conditions which substantially depleted ORC1 levels but allowed for viability in the absence of exogenous replication stress in both non-tumour and tumour-derived cells, and considered these conditions to mainly deplete dormant origin licensing capacity. In support of this notion, conditions of ORC1 depletion which did not impact upon viability or replication fork stalling in the absence of HU were observed to reduce new origin firing (assessed by the DNA fibre assay) 1 hour after release from HU in U2OS cells.

The exploitation of these siORC1 treatment conditions revealed a marked sensitisation of the tumour-derived lines to HU, compared to non-tumour cells. Further, these observations were similar after ORC1 depletion using distinct oligonucleotides and after HU treatment times adjusted to result in complete S-phase arrest, indicating that the findings were not specific to the

siORC1 oligonucleotide or HU exposure time selected. Using the longer term clonogenic survival assay, considered the "gold standard" for measuring cell killing, I continued to observe enhanced HU sensitivity in ORC1-depleted U2OS cells but similar sensitivity in ORC1-depleted 1BR3hTERT cells, therefore validating the viability assay and substantiating my findings. The ability to routinely detect residual ORC1 in the siORC1-treated tumour but not in siORC1-treated non-tumour cells demonstrates that the observed distinctions between the cell lines cannot simply be explained by more efficient ORC1 knockdown in the tumour cells. In addition, no enhanced sensitivity was observed in the non-tumour ORC1-deficient MGS patient cells, despite the reduced levels of chromatin-bound ORC1 and replication licensing capacity reported in these cells (Bicknell et al. 2011b). Similar observations were observed when depleting additional licensing components ORC6 and CDC6 in 1BR3hTERT and U2OS cells.

Overall replication restart, as measured by BrdU incorporation, was found to be unaffected in siORC1-treated non-tumour cells, while it was markedly impaired in siORC1-treated U2OS cells by 2 hours and out to 24 hours following release from HU. Further, DNA fragmentation, identified by flow cytometry-based analysis of a sub-G1 population, was observed in siORC1-treated U2OS cells within 0.5-2 hours after release from HU. As detection of a sub-G1 population is associated with apoptosis (Darzynkiewicz et al. 1997), this result may suggest that the depletion of dormant origin capacity in tumour-derived U2OS cells results in some induction of cell death rapidly after release from HU. The distinctions in replication restart observed in siORC1 treated non-tumour and tumour cells were found to correlate with the persistence of S-phase-associated DNA damage 24 hours after release from HU and, ultimately, viability. Further investigation of replication recovery, S-phase damage resolution, and induction of cell death after extended times following HU release may be informative. As tumour-derived cells display increased expression of licensing components and increased proliferation compared with non-tumour cells, the number of active replication origins required to support replication is likely to be greater in tumour cells even under conditions of diminished dormant origin supply. It is feasible, therefore, that the recovery of the rapid replication observed in U2OS cells requires a longer timeframe than was measured in these experiments.

These results described above suggest that 1BR3hTERT cells can efficiently employ other mechanisms of recovery from replication inhibition while U2OS cells have a greater reliance on dormant origin firing to do so. As previously introduced, HR-independent replication fork remodelling and HR-mediated repair of one-ended DSBs may represent potential mechanisms of recovery from replication stress (Petermann et al. 2010a). Perhaps these alternative mechanisms are exploited more readily in non-tumour cells than tumour cell lines and therefore may be used to promote efficient replication recovery in the absence of dormant origins. Further DNA fibre experiments which assess the ability of ORC1-depleted 1BR3hTERT cells to restart stalled forks may shed light on this hypothesis.

One possible explanation for differential usage of replication recovery mechanisms in non-tumour and tumour cells may be related to differences in the stability of stalled replication forks. The prevention of fork collapse (inactivation of a replication fork) is required to avoid genome instability, one of the hallmarks of cancer (Segurado et al. 2009). If replication fork stability is compromised and sources of replication stress are enhanced in tumour-derived cells, this could feasibly result in increased fork collapse, although this has yet to be definitively demonstrated. Comparison of fork restart and new origin firing after various HU treatment times have suggested that new (dormant) origin firing is enhanced after conditions which induce replication fork collapse while fork restart may represent the main recovery mechanism activated by conditions which induce transient fork stalling (Petermann et al. 2010b). An enhanced reliance on dormant origin firing in contexts of increased fork collapse may be attributed to the fact that the replication machinery is thought to dissociate from collapsed forks, perhaps precluding efficient fork restart via HR-independent mechanisms (Forment et al. 2012). Therefore, both HR-mediated repair of inactivated forks and dormant origin firing may promote efficient recovery of replication in response to fork collapse. While this model may be appealing, more thorough investigation is needed to examine its validity.

Extending my findings of a differential impact of diminished licensing capacity on HU sensitivity, I obtained similar results when examining sensitivity to H_2O_2-induced oxidative damage. Tumour cells have been reported to produce higher levels of ROS than non-tumour cells, in part resulting from the overexpression of oncogenes such as c-Myc (Vafa et al. 2002). While ROS may induce DNA lesions irrespective of cell cycle, replication stress may also be indirectly induced when forks encounter ROS-induced base damage. In support of this notion, a fraction of H_2O_2–induced damage signalling (as measured by γH2AX labelling) colocalises with replication factories (Zhao et al. 2011). Therefore, my observations that ORC1 depletion specifically sensitises tumour-derived cell lines to H_2O_2 demonstrate that my findings are not specific to HU treatment and extend to other sources of replication stress.

My findings have demonstrated that co-depletion of p53 and ORC1 in non-tumour 1BR3hTERT cells results in an enhanced loss of viability both in the absence and presence of HU. These results suggest that p53-depleted 1BR3hTERT cells have a greater reliance on dormant origin availability, potentially as a result of enhanced replication stress and/or reduced ability to recover using alternative mechanisms. Consistent with this notion, $p53^{-/-}$ MEFs treated with 2mM HU for 24 hours display increased Rad51 formation, enhanced DSBs (as measured by PFGE), and reduced replication recovery compared to $p53^{+/+}$ MEFs (Kumari et al. 2004). In addition to the well-characterised role of p53 in cell death and preventing cells which harbour DNA damage from proceeding to S-phase (Di Leonardo et al. 1994), p53 signalling has been implicated in preventing premature S-phase entry in normal human fibroblasts depleted for origin licensing machinery (Nevis et al. 2009). Therefore, loss of factors such as p53 which

regulate the G1-S-phase transition may enhance endogenous replication stress by allowing cells with DNA lesions or, under conditions of diminished dormant origin supply, with too few origins to enter into S-phase. This premature S-phase entry may ultimately result in increased fork stalling/collapse. In response to HU, p53 has also been reported to associate with stalled forks in a BLM-dependent but ATM and Chk1-independent manner (Ho et al. 2006) where it is thought to regulate the DDR (Sengupta et al. 2003). p53 has also been shown to regulate the activity of RNR, reflecting a role in replication regulation, particularly in the presence of damage (Xue et al. 2003). dNTP pools are rate limiting for replication elongation, but upregulation of RNR and increased dNTP levels promote fork progression in the presence of DNA damage (Poli et al. 2012). Therefore, p53 loss is likely to have pleiotropic effects. Overall, p53 loss may enhance replication stress or prevent recovery from fork stalling/collapse by multiple mechanisms, placing a greater reliance on dormant origin firing to recover replication. As loss of viability is observed in HU-treated cells depleted for both ORC1 and p53, some p53-independent cell death may contribute to HU sensitivity in these experiments.

As described in Section IV.2.10, overexpression of c-Myc in normal human fibroblasts (BJhTERT) was observed to result in an enhanced reliance on origin licensing capacity to maintain viability. Overexpression of the c-Myc oncogene has been reported to increase replication stress, accelerate S-phase progression, and lead to the accumulation of ROS (Vafa et al. 2002; Dominguez-Sola et al. 2007; Robinson et al. 2009; Murga et al. 2011). Perhaps to support increased replication, c-Myc has also been shown to impact upon cellular dNTP levels (Mannava et al. 2008). Further, c-Myc expression has be demonstrated to impede the DNA damage response (Guerra et al. 2010), interfere with p53 function (Vafa et al. 2002), and facilitate proliferation in the presence of damage (Herold et al. 2009a). Therefore, as c-Myc overexpression may lead to enhanced S-phase entry, hyper-replication, and replication stress, dormant origin firing may be more crucial to maintain proliferation in this context. Further examination of the impact of diminished dormant origin supply on the proliferative capacity of cells which overexpress additional oncogenes such as Ras may extend these findings.

Finally, I demonstrated that ORC depletion further sensitises tumour cells to combined treatment with HU and a Chk1 inhibitor. As Chk1 inhibitors have shown promise in clinical trials studying the outcome of treatment with Chk1 and replication inhibitors, my findings implicate that origin licensing inhibition could provide added benefit to current clinical strategies.

As discussed in more depth in Chapter VI, further examination of tumour types particularly sensitive to ORC depletion may increase our understanding of the potential clinical utility of diminished origin licensing capacity. As both HR-mediated repair and dormant origin firing may promote recovery from replication stress, tumours with mutations in HR factors such as *BRCA1* or *BRCA2* may be particularly sensitive to inhibitors of licensing components.

Further, combination treatment with reagents which inhibit factors required for HR, replication restart, or replication fork stability (ie. inhibitors of Chk1, PARP1, or ATR) may yield interesting results.

Altogether, my findings have demonstrated that the 3 tumour cell lines selected for analysis have a greater reliance on dormant origin firing than the 4 non-tumour cell lines examined to maintain viability and recovery from replication stress. Importantly, ORC1 expression was observed to be increased in all of the selected tumour-derived cell lines in comparison to that observed in the selected non-tumour cell lines. Upregulation of origin licensing factors may not, however, be universal across all tumours. In support of this notion, a previous study reported that CDT1 and CDC6 expression is elevated in ~50% of NSCLC tumours from a selected panel (Karakaidos et al. 2004). While the frequency of ORC1 overexpression in tumours has not been thoroughly examined, it may be similar to that reported for CDT1 and CDC6. Further examination of a broader panel of cell lines may help to substantiate my findings and to determine whether tumour cells which do not overexpress licensing components also display enhanced sensitivity to replication stress under conditions of reduced origin licensing capacity.

As depicted in the model depicted in Figure IV.16, non-tumour cells display normal replication, cell cycle checkpoints, and DDR mechanisms. Therefore multiple mechanisms of replication stress recovery may be available in these cells. In non-tumour cells, the partial depletion of licensing factors, which reduces licensing capacity and availability of dormant origins, does not impact upon sensitivity to replication stress, as alternative mechanisms may promote replication restart, DNA damage recovery and viability (Figure IV.16.A). In contrast, as a result of alterations such as the increased expression of oncogenes and decreased expression of tumour suppressor genes, tumour cells often display hyper-replication, increased expression of origin licensing factors, enhanced oxidative damage and/or replication stress, defective cell cycle checkpoints, and altered DDR mechanisms. These changes result in a greater reliance on dormant origin firing to recover from replication stress. Depletion of dormant origin availability in these cells results in impaired replication restart, DNA damage recovery, and viability (Figure IV.16.B).

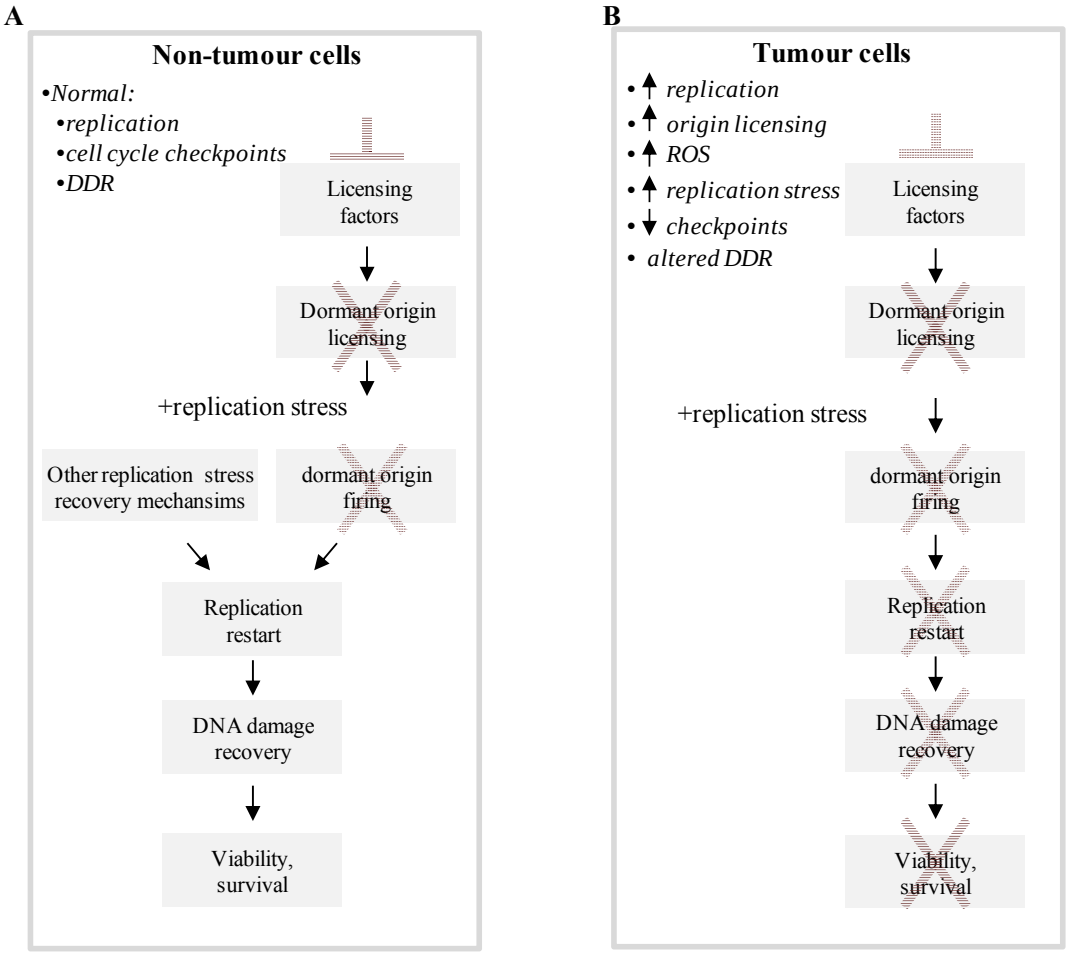

Figure IV.16 Model for the differential reliance on dormant origin firing in non-tumour and tumour cells. A. Non-tumour cells have normal levels of replication, normal cell cycle checkpoint activity, and a fully functional DDR. Depletion or inhibition of licensing factors reduces dormant origin firing (as indicated by the x). Under conditions of elevated replication stress and diminished dormant origin firing, alternative replication stress recovery mechanisms allow for replication restart, DNA damage recovery, and viability/survival. **B.** Tumour cells frequently display hyper-replication, increased expression of origin licensing factors, enhanced ROS and replication stress, defects in cell cycle checkpoints, and alterations in other DDR mechanisms. Therefore, these cells rely more heavily on dormant origin firing to recover from replication stress. Inhibition or depletion of licensing factors results in diminished origin licensing and reduced dormant origin firing in response to replication stress. After excess replication stress or treatment with replication inhibiting reagents, diminished dormant origin firing results in impaired replicating restart, DNA damage recovery, and viability.

The findings presented in this chapter provide evidence that the down-regulation of origin licensing components enhances the sensitivity of various tumour but not non-tumour cell lines to replicative stress, providing a potential route for specific sensitisation of tumour cells. Therefore, origin licensing may represent a suitable target for drug-based cancer therapy which may be particularly efficient in tumours which display high levels of replication stress or in combination with replication stress-inducing chemotherapeutic agents. Based on my findings, inhibition of licensing may be particularly effective in tumours deficient in p53 or which overexpress c-Myc. Further, combined treatment with origin licensing and Chk1 inhibitors may enhance sensitivity of tumours to replication-inhibiting chemotherapeutics. However, more work is needed to assess the feasibility of using small molecules to target licensing components. The binding of ORC1 to chromatin, a prerequisite for origin licensing, has recently been reported to occur via a highly specific interaction between the BAH domain of ORC1 and H4 dimethylated at lysine 20. A dynamic aromatic cage within the BAH domain of ORC1 mediates high affinity binding with H4K20me2 (Kuo et al. 2012). While further investigation is needed, this site could provide a route for drug targeting.

V The impact of reduced levels of origin licensing factors on higher-order chromatin structure and the IR-induced DDR

V.1 Introduction

As previously introduced, components of the pre-RC function in processes distinct to origin licensing including regulating centrosome duplication and transcriptional silencing. For the purpose of this chapter, evidence for a role of licensing factors in heterochromatin will be discussed.

V.1.1 HP1 and heterochromatin

As introduced in Chapter I, the mammalian HP1 adaptor protein family consists of the α, β and γ subunits which each contain a chromodomain and chromoshadow domain (Paro et al. 1991; Aasland et al. 1995) (Figure V.1.A). While HP1α and HP1β are predominantly found at heterochromatin regions and promote stabilization of chromatin compaction, HP1γ can also be found in euchromatin regions (Minc et al. 2000). In HeLa cells, HP1α is found to localise primarily to the periphery of nucleoli (the site of centromeric and pericentric heterochromatin) during interphase and to centromeric regions of chromosomes during mitosis (Minc et al. 1999).

The binding of HP1 with chromatin has been attributed mainly to the interaction between the chromodomain of HP1 and trimethylated Histone H3K9 (H3K9me3) (Bannister et al. 2001; Lachner et al. 2001), a well-established marker of heterochromatin. Dimers of HP1 linked by the chromoshadow domain (Cowieson et al. 2000) bridge neighbouring nucleosomes together and act as molecular scaffolds for binding of other heterochromatin factors such as HDAC and the SUV39H1 methyltransferase (Craig 2005; Grewal et al. 2007). Once targeted to heterochromatin, HP1 can promote further H3K9 trimethylation (Kourmouli et al. 2005) and spreading of chromatin compaction across extended regions of DNA (Verschure et al. 2005).

The association of HP1 with chromatin is highly dynamic (Cheutin et al. 2003) and is thought to be regulated by multiple protein-protein interactions which occur primarily via the chromoshadow domain of HP1. The association of the HP1 chromoshadow domain with a PxVxL motif of KAP-1 facilitates binding of HP1 to methylated histone residues (Sripathy et al. 2006). HP1 chromatin association is also promoted and regulated by SUV39H1 (Melcher et al. 2000), which selectively methylates H3K9 residues (Rea et al. 2000). In addition to providing the H3K9me3 residues which facilitate chromatin binding of HP1, a direct interaction between the chromoshadow domain of HP1 and SUV39H1 has been identified and is thought to contribute to HP1 binding (Yamamoto et al. 2003; Stewart et al. 2005).

However, the interactions between HP1 and H3K9me3 or SUV39H1 are not alone sufficient to recruit HP1 (Stewart et al. 2005) and HP1 recruitment may also occur in an H3K9me3-independent manner (Luijsterburg et al. 2009) (Quivy et al. 2004). Therefore other protein-protein interactions are required to promote the dynamic association of HP1 with chromatin. During S-phase in mouse cells, HP1α is reported to interact with chromatin assembly factor 1 (CAF-1) in a manner independent of SUV39H1 activity and H3K9me3 near pericentric heterochromatin (Quivy et al. 2004). As nucleosomes are disrupted ahead of replication forks during S-phase (Groth et al. 2007), CAF-1-dependent recruitment of HP1α may function to facilitate H3K9 methylation on newly synthesized DNA, therefore promoting epigenetic inheritance of the histone mark. Similarly, in replicating HeLa cells, a complex containing CAF-1, HP1α, and the SETDB1 methyltransferase has been observed near pericentric heterochromatin (Loyola et al. 2009). A model has been proposed in which CAF-1 first directs the deposition of H3 onto newly synthesized DNA and subsequently promotes monomethylation of H3K9 tails at pericentric heterochromatin via recruitment of HP1α/SETDB1. Monomethylated H3K9 tails may then serve as a platform for trimethylation by SUV39H1/2, resulting in further spreading of HP1α binding and chromatin compaction (Loyola et al. 2009). In addition to these protein interactions and as described in the next section, the direct binding of HP1 with various ORC subunits is reported to promote HP1α recruitment.

HP1 targeting to specific regions of heterochromatin and/or retention on chromatin may also be regulated by various PTMs identified on both the chromo- and chromoshadow domains of the HP1 subunits (LeRoy et al. 2009) or on various residues of interacting partners. SUMOylation of HP1α was recently reported to target the protein to regions of pericentric heterochromatin (Maison et al. 2011) and subsequent deSUMOylation has been proposed to promote its retention in these regions (Maison et al. 2012). During mitosis, HP1 has been observed to dissociate from chromatin in a process mediated by Aurora kinase B-dependent phosphorylation of H3 serine 10 (pH3(S10)). This phosphorylation event may disrupt the interaction between HP1 and H3K9me3, leading to the ejection of HP1 from chromatin (Fischle et al. 2005).

V.1.2 Pre-RC factors and heterochromatin across eukaryotic species

As previously introduced, the six subunits of human ORC are required for the efficient licensing of DNA replication origins and various subunits have also been demonstrated to participate in chromatin compaction. The function of the ORC subunits ORC1-5 in replication initiation is known to be highly conserved across species. While current evidence suggests that a role for ORC in heterochromatin may also be conserved, distinctions are apparent in the protein interactions thought to govern this role.

A link between replication licensing factors and transcriptional silencing was first identified in *S. cerevisiae* (Foss et al. 1993) and has since been shown to involve the interaction of an N-terminal region of ORC1 with silent information regulator 1 (SIR1), a trans-acting factor involved in silencing of the *HM* mating-type loci (Triolo et al. 1996). In addition, binding sites for ORC1 have been identified in the four silencer sequences that flank the repressed *HM* mating-type region (Rusche et al. 2003). Binding of ORC1 with SIR1 at silencer sequences is sufficient to silence transcription, using a mechanism comparable to heterochromatin formation in higher eukaryotes (Triolo et al. 1996). Importantly, the functions of ORC components in silencing and replication initiation are genetically separable. Introduction of *Drosophila melanogaster* ORC2 complements the silencing defect but not the replication defect of a yeast *ORC2* mutant (Ehrenhofer-Murray et al. 1995). Further, targeting of SIR1 to the *HM* mating-type silencer alleviates the requirement for ORC in transcriptional silencing (Chien et al. 1993; Fox et al. 1997). In addition, ORC5 alleles which are functional in replication initiation but non-functional in heterochromatin building and vice versa have been identified in *S. cerevisiae* (Dillin et al. 1997).

In other eukaryotic species such as *Drosophila melanogaster*, *Xenopus* (Pak et al. 1997), mouse (Auth et al. 2006), and human (Prasanth et al. 2010), various pre-RC components have been reported to interact with the chromoshadow domain of HP1α (Figure V.1A-B). In *Drosophila,* ORC2 colocalises with heterochromatin regions and HP1 (Pak et al. 1997). In the maternally loaded cytoplasm of early *Drosophila* embryos, both ORC2 and ORC6 co-immunoprecipitate with HP1, and HP1 localization is altered in *ORC2* mutants (Shareef et al. 2003). In *Drosophila*, the compaction of euchromatin into heterochromatin can be observed as position effect variegation, resulting in altered gene expression patterns. This process was found to be altered in *ORC2* or *HP1* mutants (Pak et al. 1997). In mouse, both ORC2 and CDC6 have been reported to interact with HP1α (Auth et al. 2006). As described in more depth below, human ORC1 and ORC3 directly interact with the chromoshadow domain of HP1α. These interactions requires a domain overlapping with the BAH domain of ORC1 or the MIR and coiled-coil motif of ORC3 (Prasanth et al. 2010) (Figure V.1).

While *S. cerevisiae* SIR1 bears no sequence similarity to *Drosophila melanogaster*, *Xenopus*, mouse, or human HP1, both proteins are crucial in transcriptional silencing and are thought to be regulated, in part, by interactions with ORC. The functionally conserved role for ORC in chromatin compaction may therefore reflect a need for replication licensing proteins to regulate heterochromatin (Leatherwood et al. 2003).

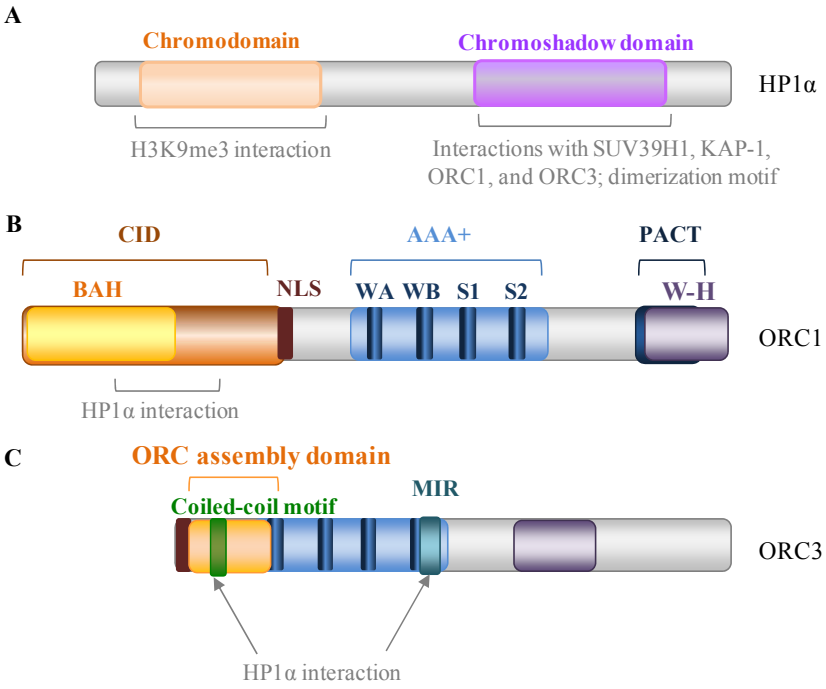

Figure V.1 Schematic depicting human ORC1, ORC3, and HP1α interaction domains. A. HP1α contains a chromodomain and chromoshadow domain connected by a hinge region. Domains involved in protein interactions described here are depicted in grey text. **B**. Schematic of ORC1 domains as in Figure I.8 with the region required for its interaction with HP1α indicated by grey text. **C**. Regions of ORC3 are depicted as in (B).

V.1.3 The role of human pre-RC factors in regulating chromatin compaction

To date, much of the evidence for a role of human pre-RC factors in the establishment of pericentric and/or centromeric heterochromatin has been reported by Dr. Supriya Prasanth, Dr. Bruce Stillman, and associated colleagues. Interestingly, this group has proposed that individual ORC subunits may play distinct roles in heterochromatin formation (Chakraborty et al. 2011). The authors have suggested that differences in the chromatin binding characteristics of various ORC subunits may, in part, underlie these distinctions.

In 2002, Prasanth and colleagues demonstrated that ORC6 functions in chromosome segregation (Prasanth et al. 2002), a process also found to be regulated by HP1-dependent centromeric heterochromatin formation (Kellum et al. 1995; Taddei et al. 2001). In 2004, the same group demonstrated that human ORC2 colocalises with HP1α and HP1β at heterochromatin regions during G1- and S-phase. During G1 and mitosis, ORC2 was found to localise specifically to centromeric heterochromatin. This study also demonstrated that depletion of ORC2 results in altered HP1α and HP1β localisation, changes in S-phase progression, and chromosome abnormalities during mitosis (Prasanth et al. 2004).

In a comprehensive study published in 2010, Prasanth and colleagues demonstrated that human ORC1 and ORC3 (but not ORC2, ORC4, ORC5, or ORC6) interact directly with HP1α (Prasanth et al. 2010). However, it is likely that, when associated in a complex, other ORC components may also indirectly interact with HP1α. In this study, distinctions were observed when examining the association of individual ORC subunits with HP1α. While the chromatin association of HP1α and ORC3 (and ORC2) were found to be highly dynamic, ORC1 association was found to be significantly more stable. Further, depletion of ORC1 or ORC5 was reported to result in the redistribution of HP1α to the periphery of nucleoli whereas depletion of ORC2 or ORC3 results in loss of HP1α foci. Interestingly, ORC1-depleted cells were reported to display abnormal chromatin organization. Here, ORC1 depletion was observed to result in clustering of centromeres which colocalised with HP1α at the periphery of nucleoli. While the authors demonstrated that depletion of ORC3 or ORC2 resulted in abnormal compaction of the satellite repeats in centromeric heterochromatin, the impact of depletion of ORC1, ORC5, or ORC6 on satellite repeat compaction was not presented. Finally, this study demonstrated that depletion of ORC1, ORC2, or ORC3 does not impact upon Polycomb-associated repressive marks such as H3K27me3 (Prasanth et al. 2010). However, results demonstrating the impact of ORC depletion on H3K9me3 or the additional heterochromatin marker H4K20me3 were not presented.

In addition to the role of the human ORC in establishing pericentric and/or centromeric heterochromatin, ORC subunits have been demonstrated to function in heterochromatin formation at telomeres. In a manner dependent on TERRA and a direct interaction with TRF2,

ORC is recruited to telomeres. Interruption of this interaction (via ORC2 depletion) results in a reduction in H3K9me3 levels at telomeres (Deng et al. 2009).

V.1.4 Heterochromatin and the ATM-dependent DDR

As previously introduced, the DDR to IR-induced DSBs occurring in G0/G1 and G2 is mediated primarily by ATM-dependent protein signalling. Following treatment with IR, ATM becomes autophosphorylated and dissociates into active monomers (Bakkenist et al. 2003). In response to DSBs, activated ATM rapidly phosphorylates H2AX at Ser139 (generating γH2AX) (Burma et al. 2001). γH2AX accumulation facilitates the recruitment of DDR proteins to sites of damaged DNA, which can be visualised as IRIF. In addition, ATM signalling coordinates the IR-induced arrest of cell cycle progression, a crucial process which provides time for the repair of DSBs and prevents genome instability (Lukas et al. 2004; Deckbar et al. 2011). ATM-dependent activation of the G2/M checkpoint involves phosphorylation of the Chk2 kinase, resulting in Cdc25 phosphorylation and inactivation of Cyclin B1 and Cdk1. The ATM-dependent G2/M checkpoint has been proposed to have a defined threshold of sensitivity as both the induction and maintenance of the checkpoint are influenced by the number of DSBs present (Buscemi et al. 2004; Deckbar et al. 2007). While ATM autophosphorylation and γH2AX foci can be detected after IR doses as low as 0.2 Gy (Bakkenist et al. 2003), Chk2 phosphorylation and full induction of cell cycle arrest is reported to occur only after doses above 0.5-1Gy, corresponding to >20 DSBs (Buscemi et al. 2004; Deckbar et al. 2007). Further, wildtype fibroblast cells irradiated with 1 Gy only sustain the G2/M arrest for 4 hours and progress into mitosis despite persisting DSBs. Analysis of premature chromosome condensation (PCC) breaks, which each correspond to 3-6 DSBs, has revealed that cells re-enter cell cycle progression when 3-4 PCC breaks or ~10-25 DSBs γH2AX foci can still be detected in G2-phase cells (Deckbar et al. 2007). Importantly, the majority of mitotic chromosome breaks arise in cells that have been released from checkpoint arrest rather than in irradiated mitotic cells.

As introduced in Chapter I.3.4, an accumulating body of evidence has demonstrated that heterochromatin acts as a barrier to IR-induced DSB repair which may be overcome by ATM-dependent signalling events (Ziv et al. 2006; Goodarzi et al. 2008; Goodarzi et al. 2010). Importantly, heterochromatin relaxation overcomes the requirement for ATM in DSB repair, as demonstrated in cells depleted for KAP-1, HP1αβγ, HDAC1/2, MeCP2, and DNMT3B (Goodarzi et al. 2008; Brunton et al. 2011) and in SUV39H1/2 $^{-/-}$ MEFs (Goodarzi et al. 2008). As discussed below, the requirement for ATM is also alleviated in cells from patients with disordered chromatin syndromes (Brunton et al. 2011).

Various human syndromes have been characterised which are associated with disordered chromatin including Rett syndrome, immunodeficiency with centromere instability and facial anomalies (ICF), and Hutchinson-Gilford progeria syndrome (HGPS) (Ausio et al. 2003). Rett syndrome, a progressive neurodevelopmental disorder, is associated with mutations in MeCP2 which result in an altered capacity to organise heterochromatin (Amir et al. 1999; Agarwal et al. 2011). In addition to the role of MeCP2 in transcriptional silencing mediated by its binding to methylated CpG islands and subsequent recruitment of corepressors proteins such as HDAC1/2 (Section I.3.3), MeCP2 directly interacts with HP1. This interaction has been proposed to stabilise the association of both proteins with heterochromatin (Agarwal et al. 2007). A large fraction of patients with ICF, a rare syndrome associated with immunodeficiency and facial anomalies, carry mutations in DNMT3B methyltransferase (Hansen et al. 1999). Cells from ICF patients are reported to display hypomethylation of satellite repeats, disruption of constitutive heterochromatin, and abnormal subcellular distribution of HP1 subunits (Luciani et al. 2005; Brun et al. 2011). Finally, HGPS is a premature aging syndrome associated with mutations in lamin A (Shumaker et al. 2006). As nuclear lamins not only provide the structural composition of the nucleus but also play a role in transcriptional silencing, lamin A-deficient HGPS patients display heterochromatin loss (Dechat et al. 2008).

Findings from the examination of disordered chromatin syndrome patient cells have supported the model that heterochromatin not only poses a barrier to DSB repair but also restricts IR-induced DSB signalling (Brunton et al. 2011). Consistent with the notion that heterochromatin compaction is altered in these patient cells, precluding the requirement for ATM-dependent heterochromatin relaxation in DSB repair, treatment with an ATMi was not observed to impact upon DSB repair. Interestingly, IR-induced γH2AX signalling was enhanced in primary fibroblasts from a patient with Rett syndrome. Importantly, this enhanced γH2AX signalling was associated with regions of heterochromatin, as demonstrated by immunoprecipitation with H3K9me3. As heterochromatin regions can readily be visualised in MEFs as DAPI-dense chromocentres, siRNA-mediated depletion has been exploited in NIH3T3 cells to examine the impact of altered chromatin structure on the expansion of γH2AX signalling at heterochromatin regions. While depletion of KAP-1, MeCP2, or DNMT3B did not impact upon the size or structure of chromocentres, depletion of these factors was found to enhance the expansion of γH2AX signalling at regions of heterochromatin. Both IR-induced ATM autophosphorylation and Chk2 phosphorylation were also enhanced in primary fibroblasts from a patient with Rett syndrome. Further examination demonstrated that this enhanced signalling results in increased sensitivity of the ATM-dependent G2/M checkpoint. Full activation of the G2/M checkpoint is inefficient in control cells, with little to no induction of the checkpoint observed at doses <0.25 Gy and complete induction was only observed at doses >1 Gy, corresponding to >20 DSBs (Buscemi et al. 2004; Deckbar et al. 2007; Fernet et al. 2010).

However, cells from patients with Rett syndrome, ICF, or HGPS exhibited a hyperactive G2/M checkpoint, with partial checkpoint induction detected after treatment with just 0.1 Gy. Altogether findings suggest that heterochromatin may act as a barrier to ATM-dependent DSB signalling and the efficiency of the G2/M checkpoint. Further, these results demonstrate that this barrier is partially alleviated in cells from patients with disordered chromatin syndromes, resulting in alterations in the IR-induced DDR.

V.1.5 Aims of this chapter

As described above, studies in *S. cerevisiae*, *Drosophila melanogaster*, *Xenopus* and human cells have revealed that various members of the pre-RC are involved in heterochromatin formation. In human cells, members of ORC directly interact with HP1α and impact upon heterochromatin organization (Prasanth et al. 2010). Heterochromatin is thought to act as a barrier to DSB signalling and repair, and this barrier is observed to be alleviated in cells from patients with disordered chromatin syndromes or in cells depleted for heterochromatin factors (Goodarzi et al. 2008; Brunton et al. 2011). Recently, mutations in *ORC1*, *ORC4*, *ORC6*, *CDC6* and *CDT1* were identified in patients with MGS (Bicknell et al. 2011a; Bicknell et al. 2011b). Here, I have examined whether cells depleted for pre-RC components or MGS patient cells deficient in pre-RC components display cellular characteristics consistent with alterations in higher-order chromatin structure.

In Section V.2.1-2, I will present findings which demonstrate that the requirement for ATM in DSB repair is partially alleviated in fibroblasts derived from an ORC1-deficient MGS patient or in cells depleted for ORC1. In Section V.2.3, I will demonstrate that the sub-cellular distribution of heterochromatin markers HP1 and H3K9me3 is altered in these cells. The exploitation of high-resolution microscopy and analysis of γH2AX signal expansion at chromocentres in MEFs has enabled examination of DSB signalling at regions of heterochromatin (Brunton et al. 2011). Here, I have used this methodology to show that ORC1 depletion enhances IR-induced DSB signalling at heterochromatin (Section V.2.4). Section V.2.5 will present results which demonstrate that ORC1-deficient MGS cells or cells depleted for ORC1 or HP1α have a hypersensitive IR-induced G2/M checkpoint. In Section V.2.4, I will demonstrate that cells depleted for ORC6 or cells from an ORC6-deficient MGS patient also display characteristics consistent with alterations in both heterochromatin organization and the IR-induced DDR. Results presented in this subsection will also demonstrate that heterochromatin organization and the IR-induced DDR are not significantly impacted in cells depleted for CDC6 or CDT1 or in cells from patients with CDC6 or CDT1-deficient MGS. Finally, in Section V.3 I will discuss the results presented in this chapter.

V.2 Results

V.2.1 Fibroblast cells from an ORC1-deficient MGS patient display partial alleviation of the DSB repair defect caused by ATM inhibition

Examination of IR-induced DSB repair in ORC1-MGS patient cells was first performed in our lab by Dr. Tom Stiff and colleagues. For these experiments, an hTERT-immortalised fibroblast line derived from an MGS patient carrying mutations in the BAH domain and C-terminus in *ORC1* was utilised (Bicknell et al. 2011b). As previously described, these cells (ORC1-P4hTERT) display reduced levels of chromatin-bound ORC1 protein (Bicknell et al. 2011b) (Figure IV.5.D). Control hTERT-immortalised fibroblasts or ORC1-P4hTERT cells were grown to plateau phase to enrich for G0/G1, treated with an ATMi for 30 minutes, and irradiated with 3 Gy. Cells were fixed at various times after IR and DSB repair was assessed in G0/G1 cells by γH2AX analysis. Using this methodology, Dr. Tom Stiff and colleagues observed that the requirement for ATM was partially alleviated in ORC1-deficient MGS cells during G0/G1.

I next went on to substantiate this finding in sub-confluent cells. 1BR3hTERT control fibroblasts and ORC1-P4hTERT cells were treated with ATMi and IR as described above, and aphidicolin was added at the time of irradiation to prevent the progression of S-phase cells into G2-phase (Figure V.2). As depicted in Figure V.2.A, in the absence of the ATMi, ORC1-P4hTERT cells displayed similar repair kinetics to control fibroblasts during G0/G1. ATM inhibition resulted in a defect in the repair of ~20 % of the induced DSBs in control cells, with ~12 DSBs persisting 24 hours after exposure to 3 Gy. However, consistent with the observations made by Dr. Stiff and colleagues, this defect was partially rescued in ORC1-P4hTERT cells, and only ~5 DSBs persisted 24 hours after IR (Figure V.2).

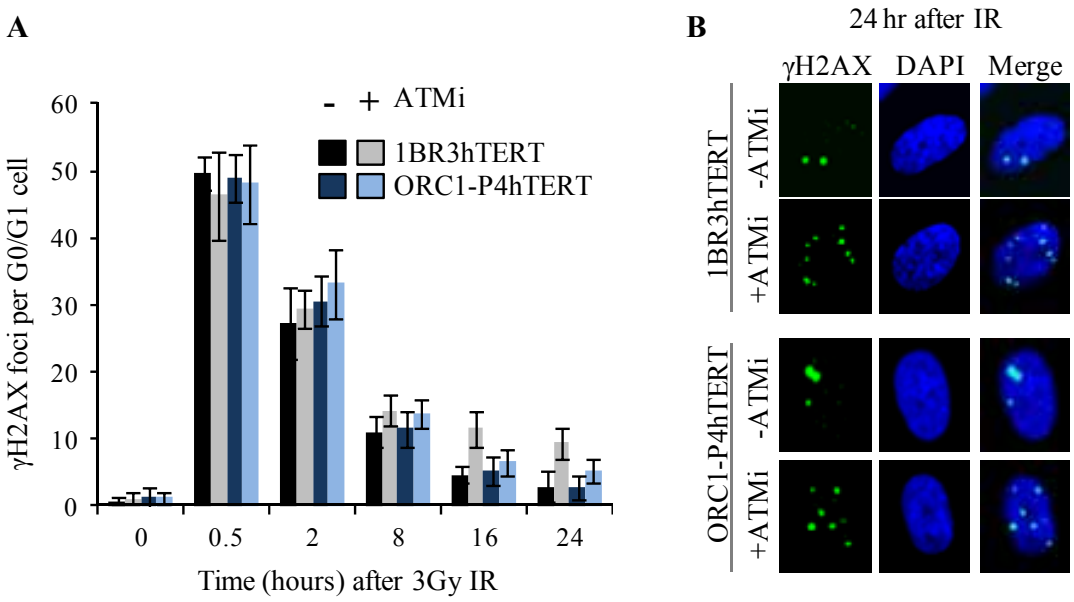

Figure V.2 The requirement for ATM in DSB repair is partially alleviated in cells from an ORC1-deficient MGS patient. hTERT-immortalised cells from a healthy individual (1BR3hTERT) or an MGS patient carrying mutations in *ORC1* (ORC1-P4hTERT) were treated with DMSO (-ATMi) or 10 μM ATMi (+ATMi) for 30 minutes and irradiated with 3 Gy. 4μM aphidicolin was added at the time of irradiation to prevent the progression of cells damaged in S-phase and to facilitate cell cycle discrimination. Cells were fixed at indicated times and subjected to immunofluorescence labelling with γH2AX and CENPF antibodies. DSB repair was assessed by enumeration of γH2AX foci in G0/G1 ($CENPF^-$) **A**. Mean values +/- SD from at least three independent experiments are depicted. **B**. Representative images of γH2AX and DAPI staining in $CENPF^-$ G0/G1 cells 24 hours after 3 Gy IR.

V.2.2 Control fibroblast cells depleted for ORC1 or HP1α display partial alleviation of the DSB repair defect associated with ATM inhibition

To further substantiate this observation and to compare findings with those obtained after depletion of heterochromatin factors, the requirement for ATM in IR-induced DSB repair was assessed in 1BR3hTERT control fibroblasts transfected with a single ORC1-targeting oligonucleotide (siORC1 single), a distinct siORC1 oligonucleotide pool (siORC1 pool), or siKAP-1. As the role of ORC1 in heterochromatin association has been suggested to involve its direct interaction with HP1α (Prasanth et al. 2010), cells depleted for HP1α were also assessed. The combined depletion of the three HP1 subunits (HP1αβγ) has already been demonstrated to result in an alleviation of the requirement for ATM in DSB repair (Goodarzi et al. 2008). Here, I have examined cells transfected with an siRNA oligonucleotide which specifically targets the HP1α subunit (siHP1α). First, cells were transfected with a single ORC1-targeting oligonucleotide (siORC1 single), with a distinct siORC1 oligonucleotide pool (siORC1 pool), siKAP-1, or siHP1α and knockdown was assessed by immunoblotting for ORC1 or KAP-1 (Figure V.3.A) or by immunofluorescence analysis of HP1 levels (using an antibody raised to HP1α but which also recognises HP1β and γ) (Figure V.3.B). Next, DSB repair was assessed by γH2AX foci analysis 0.5 or 24 hours after 3 Gy IR in the presence or absence of an ATMi. Depletion of ORC1, KAP-1, or HP1α did not impact upon the number of DSBs induced 0.5 hours after 3Gy (Figure V.3.C) nor on DSB repair measured 24 hours after IR in absence of ATMi (Figure V.3.D). However, depletion of these components resulted in an alleviation of the requirement for ATM in DSB repair 24 hours after IR (Figure V.3.D-E). KAP-1 depletion resulted in a nearly complete restoration of DSB repair capacity while ORC1 or HP1α depletion resulted in a partial restoration of repair.

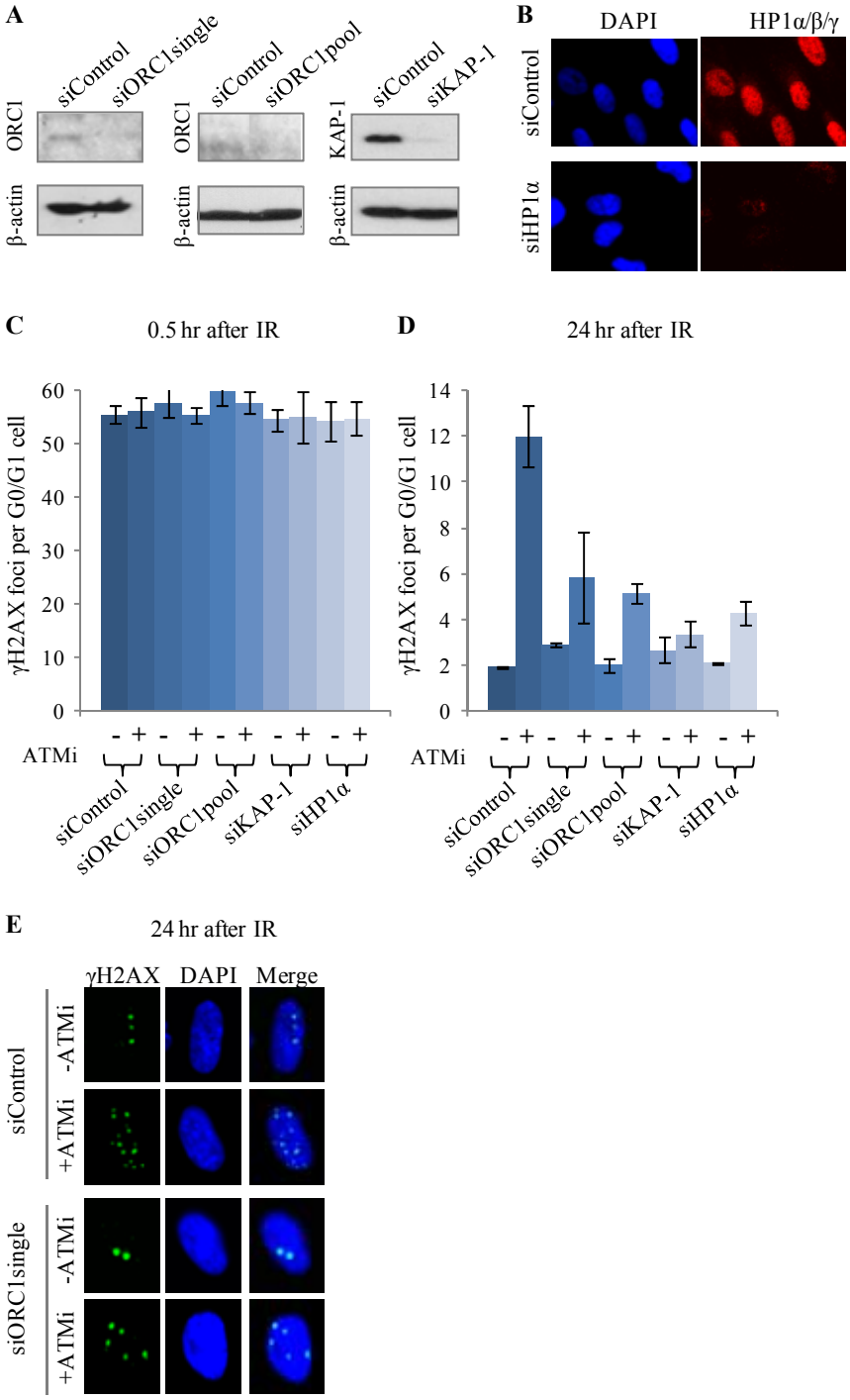

Figure V.3 The requirement for ATM in DSB repair is partially alleviated in control fibroblasts depleted for ORC1 or HP1α. 1BR3hTERT cells were transfected with siORC1single, siORC1pool, siKAP-1, or siHP1α. **A-B**. 48 hours later, ORC1 or KAP-1 levels were assessed by immunoblotting (A) and by immunofluorescence analysis of HP1 using an antibody antibody raised to HP1α but which also recognises HP1β and γ (B). **C-D**. Cells were transfected with siRNA oligonucleotides as in (A) and the requirement for ATM in DSB repair was assessed as in Figure V.2A. **E**. Representative images of cells transfected with siControl or siORC1pool and assessed 24 hours later after IR as in (D).

V.2.3 The sub-cellular distribution of HP1 and H3K9me3 is altered in ORC1-deficient MGS fibroblasts and in cells depleted for ORC1

To evaluate whether changes in heterochromatin can be detected in ORC1-depleted control fibroblasts or in ORC1-deficient MGS cells, nuclear levels of HP1 were assessed by immunofluorescence using an antibody which recognises the three HP1 subunits (α, β, and γ). As controls, I also carried out this analysis following transfection with siHP1α or siKAP1. Quantification of nuclear intensity enabled an approximation of overall nuclear levels of HP1. As described above, depletion of HP1α resulted in markedly reduced nuclear levels of HP1 (Figure V.3.B, Figure V.4.B). In addition, nuclear HP1 levels were reduced (although less dramatically) following KAP-1 depletion (Figure V.4.A-B). Consistent with a previous report that depletion of ORC1 impacts upon HP1 distribution (Prasanth et al. 2010), HP1 levels were observed to be reduced, though this reduction was not as dramatic as that observed after KAP-1 or HP1α depletion. Comparison of HP1 levels in 1BR3hTERT and ORC1-P4 hTERT cells showed a significant decrease in the ORC1-P4 patient.

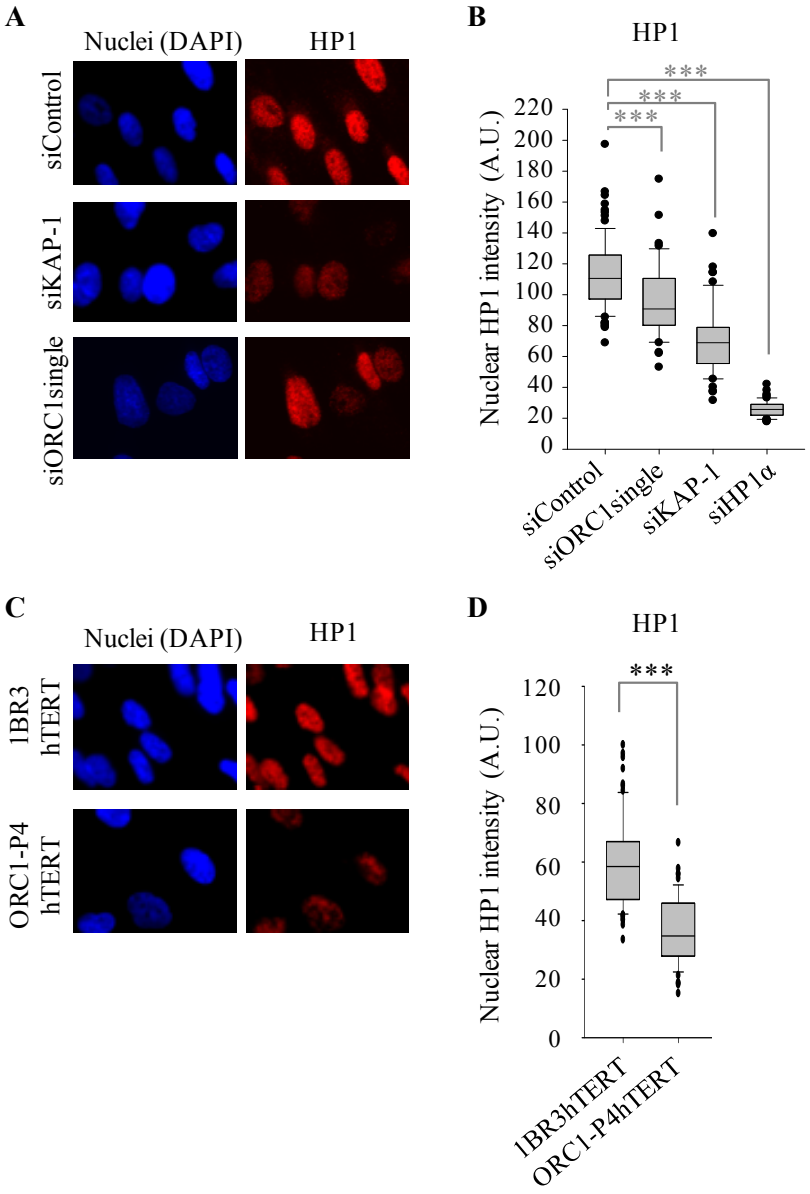

Figure V.4 ORC1-deficient MGS patient cells or control fibroblasts depleted for ORC1 display a reduction in nuclear HP1 levels. A-B. 1BR3hTERT cells were transfected with siRNA oligonucleotides as described in Figure V.3 and nuclear levels of HP1 were assessed by immunofluorescence labelling with an antibody which recognises HP1α, β, and γ. Representative images are depicted in (A). Results from quantification of the nuclear intensity of HP1αβ+γ signal from a single representative experiment are depicted in (B). Similar results were obtained in two further experiments. >40 nuclei were scored per experiment. Statistical significance was assessed using the Mann-Whitney test. Asterisks denote statistical significance (*: $p<0.05$, **: $p<0.01$, ***: $p<0.001$). **C-D**. Nuclear levels of HP1 were assessed in 1BR3hTERT or ORC1-P4hTERT cells as in (A-B).

Next, a similar analysis was carried out using antibodies which recognise two additional heterochromatin markers, H3K9me3 and H4K20me3. As expected, transfection of 1BR3hTERT cells with siKAP-1 or siHP1α resulted in a significant reduction in H3K9me3 (Figure V.5.A). H3K9me3 levels were also observed to be reduced in ORC1-depleted cells (Figure V.5.A) or in ORC1-P4hTERT cells (Figure V.5.B-C). In contrast, while depletion of KAP-1 or HP1α resulted in a reduction in H4K20me3 (Figure V.6.E), no significant change was observed in cells depleted for ORC1 (Figure V.6.D-E) or in ORC1-P4hTERT cells (Figure V.6.F).

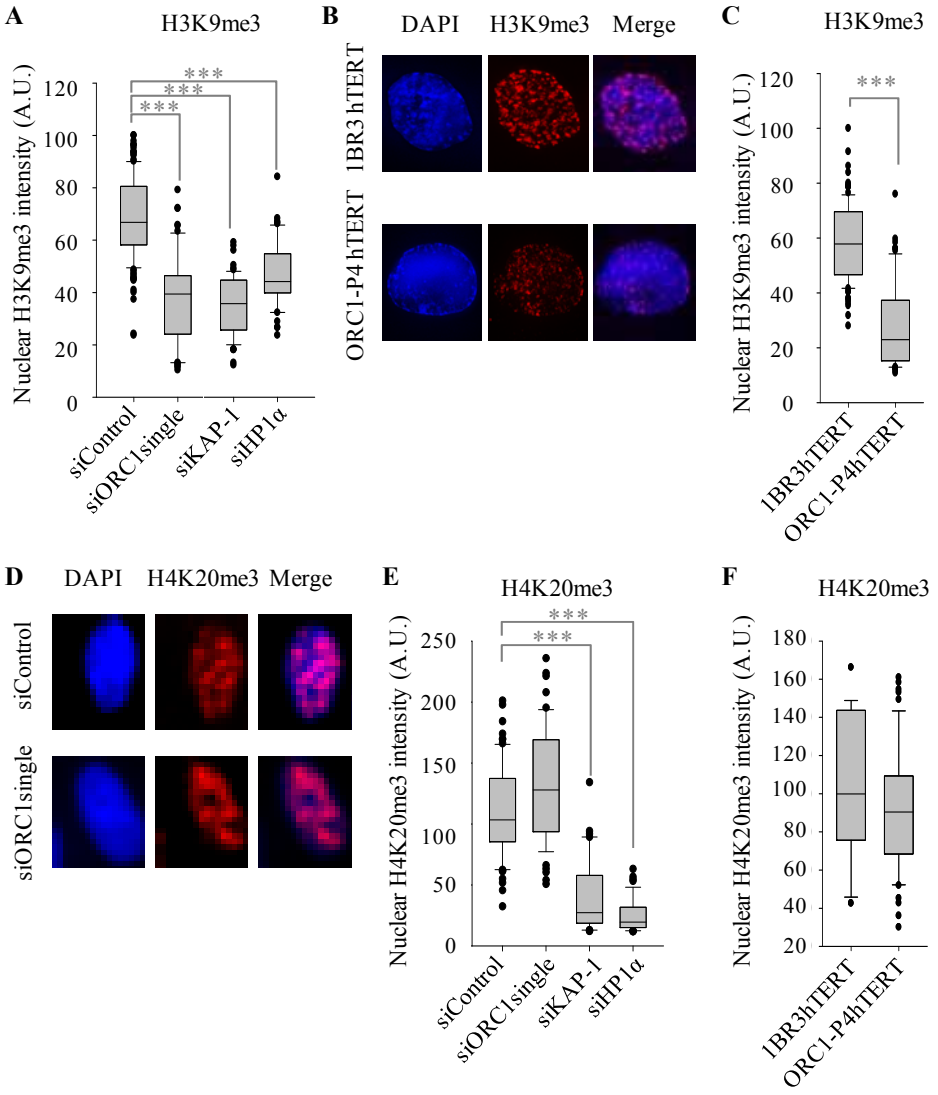

Figure V.5 ORC1-deficient MGS patient cells or control fibroblasts depleted for ORC1 display a reduction in nuclear H3K9me3 levels. A. 1BR3hTERT cells were transfected with siRNA oligonucleotides as described in Figure V.3 and nuclear levels of H3K9me3were assessed by immunofluorescence labelling. Quantification of nuclear H3K9me3 levels was performed as in Figure V.4.B. **B-C**. H3K9me3 levels were assessed in 1BR3hTERT or ORC1-P4hTERT cells as in (A). Representative images captured by high-resolution microscopy are depicted in (B) and quantifications are depicted in (C). **D-F**. As in (A) except cells H4K20me3 analysis was performed. Representative images of H4K20me3 staining in siControl or siORC1-transfected cells are depicted in (D).

V.2.4 ORC1 depletion results in enhanced γH2AX signal expansion at heterochromatin regions

Pericentric and centromeric heterochromatin can be visualised by regions of intense DAPI staining, termed chromocentres, in G0/G1-phase NIH3T3 murine cells (Guenatri et al. 2004; Goodarzi et al. 2008) (Figure V.6.A). As heterochromatin may act as a barrier to DSB signalling, cells depleted for heterochromatin factors such as KAP-1, MeCP2, or DNMT3B display enhanced γH2AX signal expansion at chromocentres (Brunton et al. 2011). Here, I evaluated whether depletion of ORC1 also impacts upon IR-induced DSB signal expansion at heterochromatin regions.

First, the efficiency of ORC1 depletion in MEFs was assessed. Cells were transfected with a pool of siRNA oligonucleotides targeting mouse ORC1. 48 hours later, cells were lysed and extracts were subjected to SDS-PAGE. Immunoblotting demonstrated that transfection with siORC1 results in reduced levels of ORC1 in NIH3T3 cells (Figure V.6.B).

As described previously, analysis of γH2AX foci and chromocentres using high-resolution microscopy may be exploited to assess the overlap of DSB signalling at heterochromatin regions (Brunton et al. 2011). I applied this methodology to assess the impact of ORC1 depletion on DSB signal expansion in NIH3T3 cells. Analysis of chromocentres was restricted to G0/G1-phase cells because these regions become more diffused during G2 (Goodarzi et al. 2009). To enrich for G0/G1, cells were grown to confluency. To further facilitate discrimination of cell cycle phase, aphidicolin was added at the time of IR and cells were labelled with α-Histone H3 phosphorylated on serine 10 (pH3(S10)), which can be readily detected during both G2 and mitosis in NIH3T3 (Brunton et al. 2011). Cells were treated with 3 Gy IR, fixed 30 minutes later, and subjected to immunofluorescence labelling with α-γH2AX and DAPI. Imaging of γH2AX foci, DAPI dense chromocentres, and pH3(S10) signal was performed using a DeltaVision high-resolution microscope. Z-stacked images of γH2AX foci and DAPI dense chromocentres were captured in pH3(S10)$^-$ G0/G1 cells, and images were deconvolved. Background DAPI staining was eliminated from images to highlight only DAPI-dense chromocentres and colocalisation of γH2AX foci with chromocentres was measured and visualised in the red channel (Figure V.6.C). Next, the mean area of -γH2AX foci regions overlapping with chromocentres (depicted in the red channel) was quantified per cell with ImageJ. The area of overlap was then normalised to chromocentre number in each cell. Average cellular values were determined for each experimental condition and normalised to the average area of overlapping regions in siControl-treated cells (arbitrary units (A.U.)). Figure V.6.D depicts the mean A.U. +/- SD from two independent experiments. In order to compare the mean area of γH2AX foci which do not overlap with chromocentres between siControl and siORC1-treated cells, the area of each γH2AX foci (the square pixel number of regions detected in the

green channel) was determined using ImageJ. Regions which overlap with chromocentres (detected in the red channel as described above) were eliminated from the analysis. The average square pixel number of non-overlapping foci regions was determined for each experimental condition and the mean square pixel number +/- SD from two independent experiments is depicted in Figure V.6.E.

Consistent with the previously reported observation that most (80-85 %) IR-induced DSBs occur within regions of euchromatin (Goodarzi et al. 2010), the majority of γH2AX foci were observed to occur within regions not overlapping with chromocentres in both siControl and siORC1-transfected cells. The remaining fraction (~15-20 %) in siControl-transfected cells were observed near the periphery of chromocentres. As depicted, increased expansion of the 15-20 % remaining γH2AX foci into chromocentre regions was observed in siORC1-transfected cells. Quantification of the size of overlapping region revealed a 4 fold increase in siORC1-treated cells compared with the control (Figure V.6.D). Importantly, ORC1 depletion did not impact upon the size of γH2AX foci that did not overlap with chromocentres (Figure V.6.E).

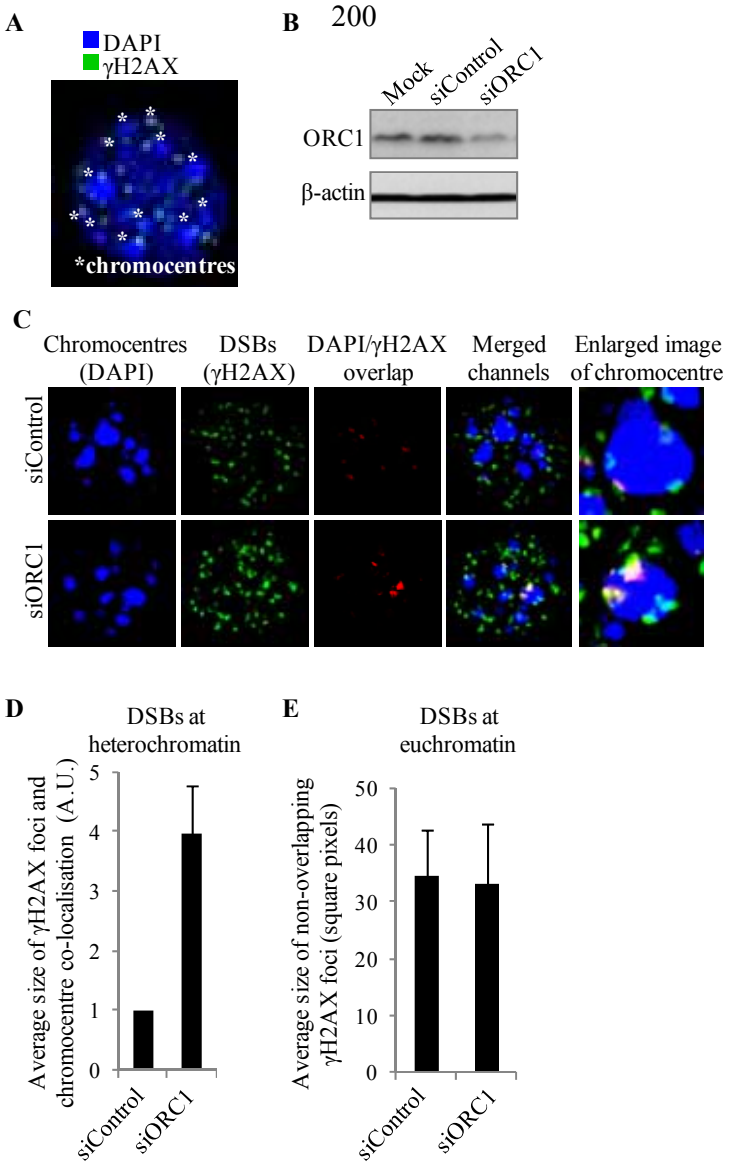

Figure V.6 ORC1 depletion in NIH3T3 murine cells results in increased expansion of IR-induced γH2AX foci at regions of heterochromatin. A. Heterochromatin can be visualised in NIH3T3 cells as DAPI-dense regions. A representative image of NIH3T3 cells treated with 3Gy IR, fixed 30 minutes later, and stained with DAPI and α-γH2AX is depicted. White * indicate DAPI-dense chromocentres. **B**. ORC1 protein levels were assessed in NIH3T3 cells 48 hours after mock transfection (mock), or transfection with siControl or siORC1 by western blotting. β-actin was included as a loading control. **C-E**. siRNA-transfected NIH3T3 cells were exposed to 3Gy IR, treated with 4μM aphidicolin to facilitate discrimination of cell cycle phase, and fixed at indicated times. Immunofluorescence labelling with DAPI and α-γH2AX, and α-pH3(S10) (a marker of G2/M-phase in MEFs) was performed. Z-stacked images were acquired using a DeltaVision Axiovert high resolution microscope. G1 cells were selected for imaging, images were deconvolved, and overlapping DAPI-dense and α-γH2AX labelled regions were visualised using the red channel (SoftWorx). Representative images of DAPI (blue), α-γH2AX (green), overlap (red), merged channels, and enlarged images of chromocentres are depicted in (C). The mean area of -γH2AX foci regions overlapping with chromocentres per cell were quantified with ImageJ and normalised to the number of chromocentres per cell. Average cellular values were determined for each experimental condition and normalised to the average area of overlapping regions in siControl-treated cells (arbitrary units (A.U.)). Results in (D) depict mean A.U. values +/-SD from two independent experiments. The mean area of only γH2AX foci which do not overlap with chromocentres (in square pixels) was quantified using ImageJ. Results depict mean values +/-SD from two independent experiments (E).

V.2.5 Cells from ORC1-deficient MGS patients or cells depleted for ORC1 or HP1α display hypersensitivity of the IR-induced G2/M checkpoint

As previously introduced, cells from patients with disordered chromatin syndromes display hypersensitivity of the G2/M checkpoint which is likely to be attributed to enhanced ATM-dependent DSB signalling (Brunton et al. 2011). As I observed that a reduction in ORC1 partially alleviates the requirement for ATM in DSB repair and enhances IR-induced γH2AX signalling, I next examined the sensitivity of the ATM-dependent IR-induced G2/M checkpoint in these cells.

Cells in mitosis can be visualised after immunofluorescence labelling with DAPI and with an antibody that recognises pH3(S10) (Figure V.7.A). Enumeration of the fraction of cells in mitosis and monitoring the reduction in this fraction after IR provided a measure for efficacy of the G2/M checkpoint.

Using this methodology, I first examined the impact of ORC1, HP1α, or KAP-1 on the initial activation of the checkpoint. 1BR3hTERT cells were transfected with siRNA oligonucleotides, exposed to a range of IR doses (0.1-3 Gy) and fixed 2 hours later. For all G2/M checkpoint analysis, aphidicolin was added at the time of IR to prevent cells damaged in S-phase from progressing through the cell cycle. Immunofluorescence labelling of DAPI and pH3(S10) was performed and the fraction of cells in mitosis was scored. Consistent with previous reports (Deckbar et al. 2007), siControl-treated 1BR3hTERT cells were observed to have an inefficient G2/M checkpoint, and showed very minimal checkpoint induction after 0.1 Gy and complete arrest of cells at doses >1 Gy (Figure V.7.B). Also consistent with a previous results (Brunton et al. 2011), KAP-1 depletion was observed to enhance sensitivity of the G2/M checkpoint. Depletion of HP1α resulted in enhanced cell cycle arrest at lower doses that was comparable to that observed after KAP-1 depletion. Importantly, depletion of ORC1 using distinct siRNA oligonucleotides resulted in enhanced activation of the G2/M checkpoint, though this increase was not as dramatic as that observed in KAP-1 or HP1α-depleted cells.

Next, I examined the impact of ORC1 depletion on the maintenance of the G2/M checkpoint. Cells were transfected with siORC1 and treated with 2 Gy IR. Again, aphidicolin was added at the time of IR as described above. The G2/M checkpoint was then monitored 1, 2, 6, 8, or 12 hours after IR to identify the length of time cells remain arrested. Consistent with reported results, (Deckbar et al. 2007), a fraction of siControl-treated 1BR3hTERT cells were observed to reinitiate cell cycle progression 6 hours after IR (Figure V.7.C). In contrast, ORC1-depleted cells maintained complete G2/M arrest at this time. Mitotic re-entry was observed in ORC1-depleted cells 8 and 12 hours after IR.

These analyses were next applied to ORC1-P4hTERT cells to assess sensitivity of the G2/M checkpoint. As depicted in Figure V.7.D, checkpoint activation in ORC1-P4hTERT was

observed after treatment with 0.1 Gy IR. Further, the fraction of cells exhibiting G2/M arrest was greater at doses <1 Gy in ORC1-P4hTERT MGS patient cells than control fibroblasts. As a control, G2/M checkpoint activation was also monitored in a second control cell line (BJhTERT) and found to be similar to that of 1BR3hTERT (Figure V.7.E). Next, in conjunction with my colleague, Liang Xue, I examined the maintenance of G2/M arrest in ORC1-P4hTERT cells. Similar to findings after ORC1 depletion, we observed that ORC1-P4hTERT cells exhibit prolonged G2/M checkpoint maintenance (Figure V.7.F). 6 hours after IR, a fraction of 1BR3hTERT cells began entering mitosis while ORC1-P4hTERT cells remained arrested. While a fraction of the ORC1-deficient patient cells did eventually progress into mitosis by 8 hours, this fraction was lower than that observed in control cells.

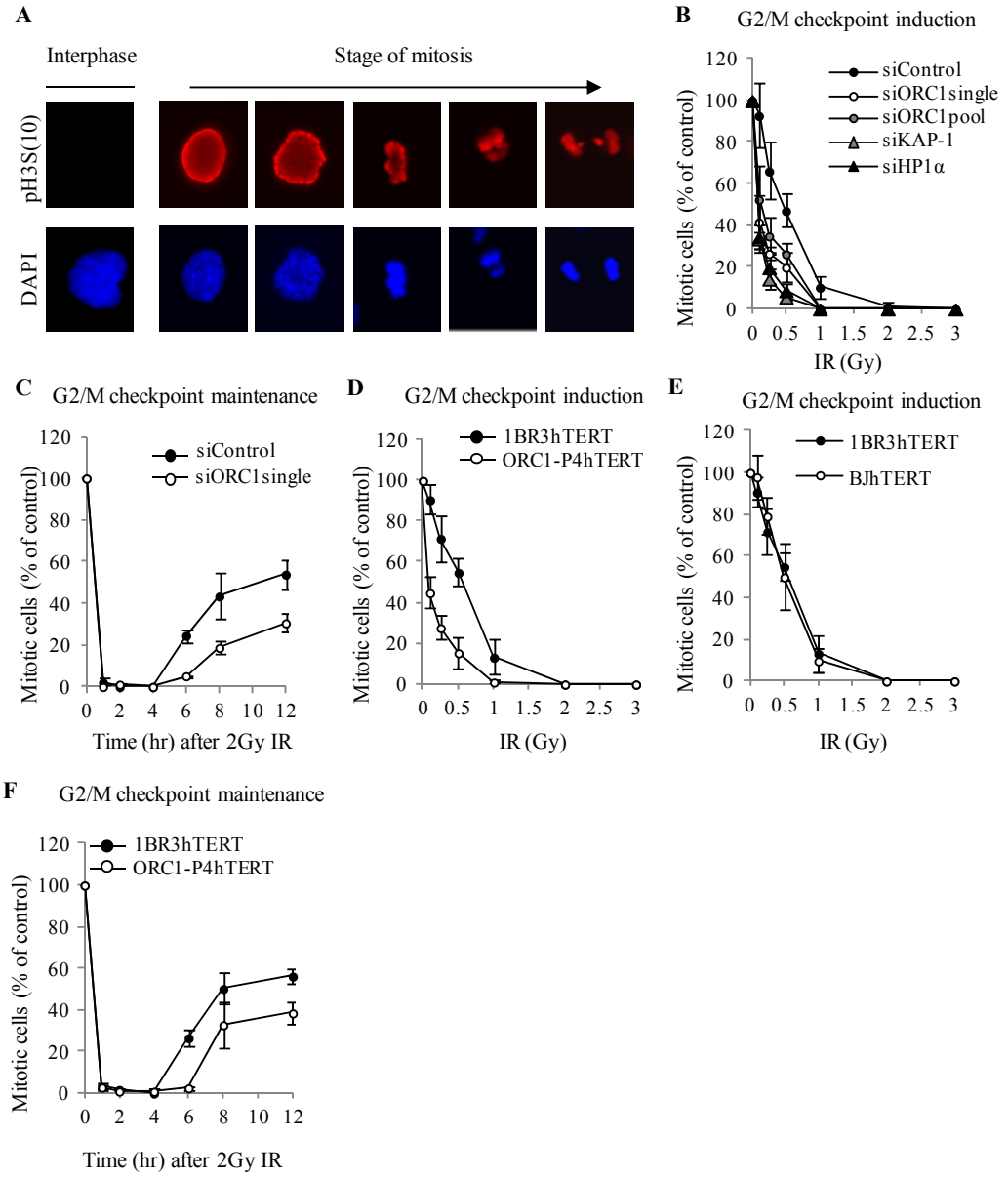

Figure V.7 Cells from an ORC1-deficient MGS patient or cells depleted for ORC1 or HP1α display hypersensitivity of the IR-induced G2/M checkpoint. A. Representative images of a pH3(S10)$^-$ interphase cell or pH3(S10)$^+$ mitotic cells. **B**. Activation of the G2/M checkpoint was assessed in 1BR3hTERT cells transfected with indicated siRNA oligonucleotides. Cells were exposed to a range of IR doses (0.1-3 Gy), aphidicolin was added at the time of IR, and cells were fixed 2 hours later. Immunofluorescence labelling with α-pH3(S10) and DAPI was performed and the number of pH3(S10)$^+$ mitotic cells was scored in >400 cells per condition in each experiment. Plots depict mean values +/- SD from three independent experiments. **C**. As in (B) except G2/M checkpoint maintenance was assessed at various times after treatment with 2 Gy IR. **D-E**. G2/M checkpoint activation was assessed in1BR3hTERT, BJhTERT, and ORC1-P4hTERT cells. **F.** G2/M checkpoint maintenance was assessed as in (C). Results depict mean values +/- SD from six independent experiments performed by myself and Liang Xue.

Next, I aimed to exploit complementation analysis to further substantiate the notion that the hypersensitivity of the G2/M checkpoint observed in ORC1-deficient MGS patient cells is a consequence of reduced ORC1 levels. ORC1-P4 hTERT fibroblasts were not used for this analysis as ORC1 overexpression was found to result in loss of viability in these cells (Section IV.2.2). Instead, complementation analysis was carried out in LBLs derived from an ORC1-deficient MGS patient (ORC1-P1). Consistent with a previous report (Bicknell et al. 2011b), ORC1 levels were observed to be reduced in ORC1-P1 cells compared with GM02188 control LBLs (WT1) (Figure V.8.A). To achieve ORC1 overexpression, LBLs were transfected with an ORC1-GFP expression vector three times over 72 hours. Using these conditions, ORC1-GFP overexpression was found to be highly efficient, with >90 % of cells expressing detectable GFP signal (Figure V.8.B). Examination of G2/M checkpoint activation revealed that ORC1-P1 cells transfected with an empty vector exhibit hypersensitivity of G2/M arrest, similar to observations made in ORC1-P4hTERT cells (Figure V.8.C). Importantly, transfection with ORC1 cDNA relieved this hypersensitivity and conferred a level of G2/M arrest similar to that observed in LBLs derived from a normal individual.

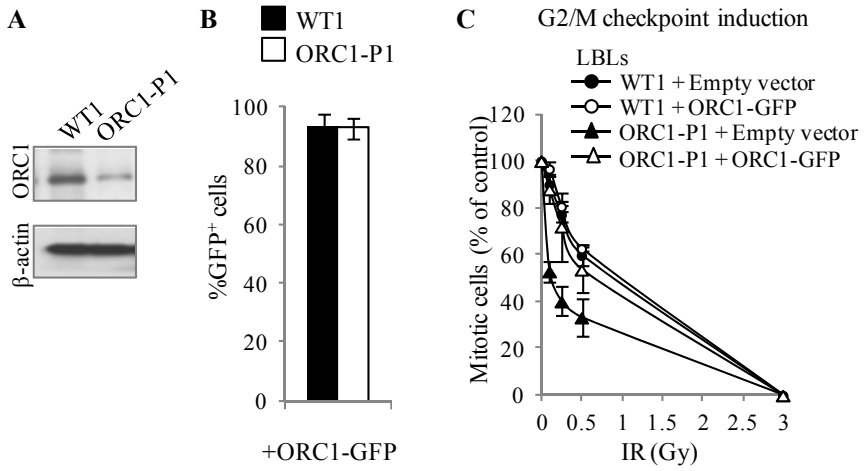

Figure V.8 ORC1 complementation restores normal G2/M checkpoint signalling in ORC1-P1 MGS patient cells. A. ORC1 levels were assessed by immunoblot in WT1 and ORC1-P1 LBLs. **B**. WT1 and ORC1-P1 LBLs were transfected with an ORC1-GFP expressing construct three times over 72 hours. GFP levels were assessed by immunofluorescence and the fraction of cells expressing GFP was estimated. **C**. G2/M checkpoint activation was assessed as in Figure V.7B.

V.2.6 ORC6-deficient MGS patient cells or cells depleted for ORC6 display characteristics consistent with disordered chromatin

To extend my observations that cells with reduced ORC1 levels display alterations in both heterochromatin organization and the IR-induced DDR, I also examined the cellular impact of a reduction in ORC6, CDC6, or CDT1 levels. As previously introduced, hypomorphic mutations in *ORC6*, *CDC6*, and *CDT1* have been reported in patients with MGS (Bicknell et al. 2011a; Bicknell et al. 2011b; Guernsey et al. 2011; de Munnik et al. 2012). While we have obtained LBLs derived from individuals with *ORC6*, *CDC6*, or *CDT1* mutations, fibroblast cell lines from these patients are currently unavailable. Unfortunately, γH2AX foci cannot be accurately quantified in round LBLs, and instead, siRNA-mediated depletion of these licensing components in control fibroblasts was exploited to examine whether a reduction in levels of these proteins impacts upon IR-induced DSB repair.

Efficiency of protein knockdown was first verified by immunoblotting 48 hours following siRNA-mediated depletion (Figure V.9A). Next, the impact of protein depletion on heterochromatin distribution was assessed. Since ORC1 depletion results in a significant reduction in nuclear H3K9me3, this heterochromatin marker was also assessed in cells depleted for ORC6, CDC6, or CDT1. Strikingly, depletion of ORC6 resulted in diminished H3K9me3 levels (Figure V.9.B). However, despite substantial depletion of protein levels as detected by immunoblotting, siCDC6 or siCDT1 did not impact upon H3K9me3.

Next, the requirement for ATM in DSB repair was assessed in siORC6, siCDC6, or siCDT1-transfected cells as previously described. DSB induction was observed to be similar in siControl, siORC6, siCDC6, or siCDT1-transfected cells 0.5 hours after IR (Figure V.9.C). Examination of cells 24 hours after IR revealed that, similar to that observed after ORC1 depletion, ORC6 depletion resulted in a partial alleviation of the requirement for ATM in DSB repair (Figure V.9.D). In contrast, cells depleted for CDC6 or CDT1 were defective in the repair of ~15 % DSBs following treatment with an ATMi.

In addition, examination of the efficiency of G2/M checkpoint activation revealed that depletion of ORC6, but not CDC6 or CDT1, resulted in hypersensitivity of the G2/M checkpoint (Figure V.9.E). Availability of LBLs derived from individuals with mutations in *ORC6, CDC6,* or *CDT1* also enabled analysis of the G2/M checkpoint in MGS patient cells. Similar to findings observed after siRNA-mediated depletion, ORC6-deficient MGS patient cells also displayed enhanced sensitivity of the G2/M checkpoint activation while checkpoint arrest was only minimally affected in CDC6 or CDT1-deficient MGS patient cells (Figure V.9.F). ORC6-deficient MGS patient cells also exhibited delayed mitotic progression after irradiation with 2 Gy (Figure V.9.G).

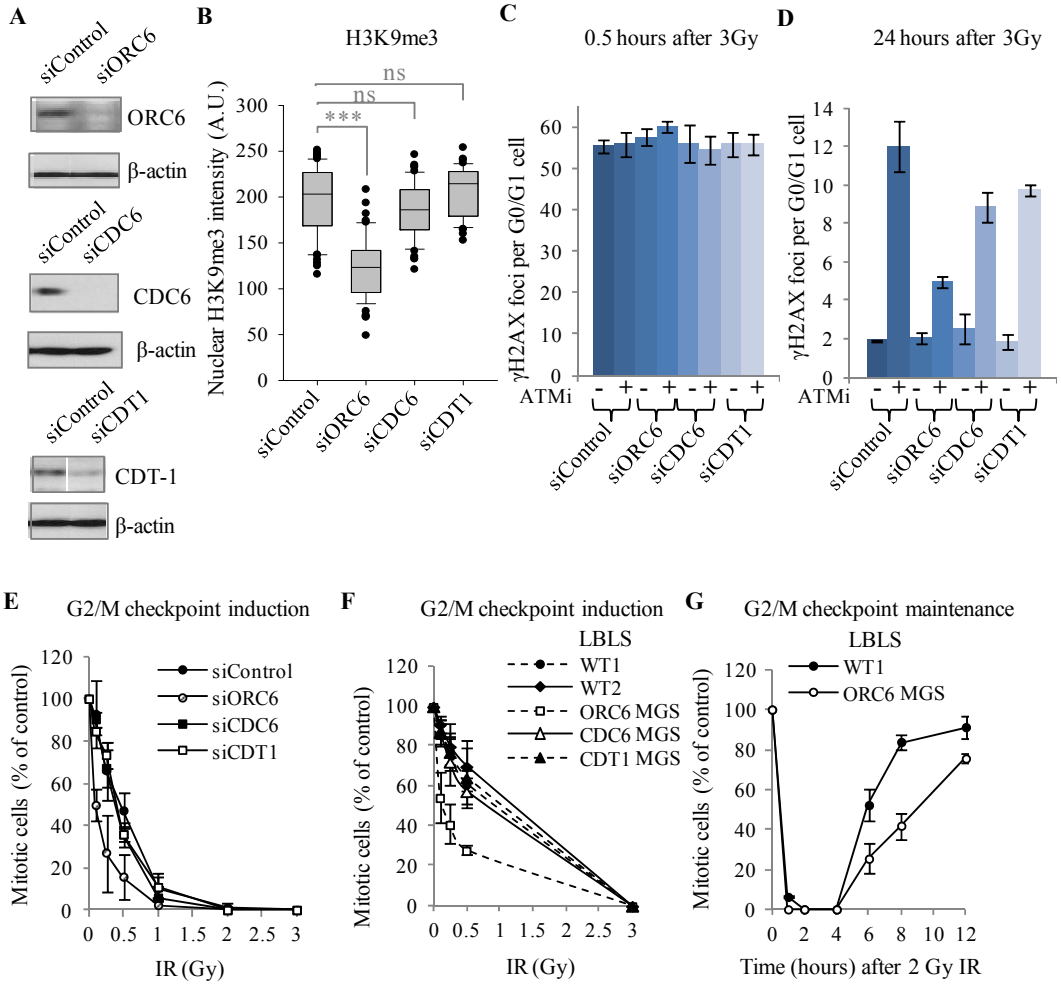

Figure V.9 Depletion of ORC6 but not of CDC6 or CDT1 results in cellular characteristics consistent with disordered chromatin. 1BR3hTERT cells transfected with indicated siRNA oligonucleotides were grown for 48 hours. **A**. ORC6, CDC6, and CDT1 levels were assessed by immunoblotting. β-actin served as a loading control. **B**. Nuclear H3K9me3 levels were assessed as described in Figure V.5. **C-D**. DSB repair was assessed in siRNA-transfected cells treated with DMSO (-ATMi) or 10 μM ATMi (+ATMi) as described in Figures V.2. **E-F**. Efficiency of the G2/M checkpoint activation was assessed in siRNA-transfected cells (E) or LBLs from healthy individuals (GM02188=WT1, AG09387=WT2) and MGS patients with mutations in indicated genes (F). **G**. G2/M checkpoint maintenance was assessed in LBLs from a healthy individual (WT1) or from an ORC6-deficient MGS patient.

V.3 Discussion

Human ORC subunits have previously been reported to contribute to heterochromatin organisation (Prasanth et al. 2010) but, until recently, cells from human patients which harbour mutations in pre-RC components were not available. Several MGS patients with mutations in various ORC components, *CDC6*, and *CDT1* have now been identified. MGS is characterised by bone abnormalities, microcephaly and both pre- and post-natal dwarfism (Bicknell et al. 2011a; Bicknell et al. 2011b; Guernsey et al. 2011; de Munnik et al. 2012). While these features are detected in most MGS patients with mutations in pre-RC components, distinctions in the severity of these symptoms have been observed between patients (de Munnik et al. 2012). Understanding the cellular features which distinguish these patients may shed light on differences in the severity of phenotypes associated with MGS. The impact of these disease-associated mutations on heterochromatin organisation and the IR-induced DDR has not fully been explored. Here I have examined these features in cells from MGS patients and in control fibroblasts depleted for ORC1, ORC6, CDC6, or CDT1.

Following initial observations made by colleagues in our lab, I have substantiated findings that the requirement for ATM in DSB repair is partially bypassed in ORC1-deficient patient cells. Cells from patients with disordered chromatin syndromes such as Rett syndrome also display a reduced requirement for ATM in DSB repair (Brunton et al. 2011). This finding is attributed to the notion that heterochromatin acts as a barrier to DSB repair and that ATM-dependent signalling is required for localised changes in heterochromatin which promote subsequent repair (Goodarzi et al. 2010). ORC1 directly interacts with HP1α via a motif in the BAH domain of ORC1, and depletion of ORC1 has been reported to alter the nuclear distribution of HP1α (Prasanth et al. 2010). Importantly, Prasanth and colleagues have demonstrated that depletion of ORC2 or ORC3 results in the loss of HP1α foci and in abnormal compaction of satellite repeats. In contrast, ORC1 was reported to result in an accumulation of HP1α at the periphery of nucleoli, and the authors proposed that these regions may consist of clustered centromeric heterochromatin (Prasanth et al. 2010). Therefore, a model has been proposed in which ORC1 regulates heterochromatin organisation only at specific regions via its interaction with HP1α. Consequently, in the absence of ORC1, the interaction between ORC3 and HP1α may still promote HP1α recruitment to specific regions of heterochromatin (Chakraborty et al. 2011).

Here, we have found that the alleviation of the requirement for ATM in DSB repair is less dramatic in ORC1-P4hTERT cells than that observed in cells depleted for KAP-1. Several possible explanations may exist. Firstly, as suggested by Prasanth, Stillman, and colleagues, ORC1 may only function in the organization of certain regions of heterochromatin. Thus,

heterochromatin organisation may be functional within specific regions in ORC1-P4hTERT cells and the repair of DSBs occurring in these regions may still require ATM-dependent signalling. Alternatively, even if the interaction between ORC1 and HP1α is disrupted, some ORC1-independent recruitment of HP1α to heterochromatin may still occur. In this scenario, while less HP1α may be associated with chromatin, this may still enable some degree of compaction. Secondly, mutations in ORC1 found in MGS patients are hypomorphic, and therefore result in reduced levels of protein, or in the case of ORC1-P4hTERT cells, reduced chromatin association of ORC1. Only one of the two *ORC1* mutations identified in ORC1-P4hTERT cells is localised within the BAH domain (aa 105) (Bicknell et al. 2011b). Therefore our observations that the requirement for ATM in DSB repair is only partially alleviated in ORC1-P4hTERT cells may reflect the ability of some residual protein to interact with HP1α and function in heterochromatin organisation. Thirdly, our results may reflect the fact that HP1α itself is not exclusively required for heterochromatin organisation.

A partial alleviation of the requirement for ATM in IR-induced DSB repair was also observed in control fibroblasts depleted for ORC1 using multiple siRNA oligonucleotides. While depletion of protein was observed to be efficient by immunoblotting, ORC1 is essential for cellular proliferation; hence, some residual protein is likely to exist in ORC1-depleted control fibroblasts. Consequently, it may not be possible to address the question of why only partial alleviation of the requirement for ATM in DSB repair is observed using siRNA-mediated protein depletion. However, as the requirement for ATM in DSB repair is reduced both in fibroblasts from an ORC1-deficient MGS patient and in cells depleted for ORC1, our observations are likely to reflect a direct impact of ORC1. Depletion of all three HP1 subunits was previously reported to relieve the requirement for ATM for DSB repair (Goodarzi et al. 2008). Here I have also demonstrated that depletion of the HP1α subunit alone provides similar results.

In support of the notion that heterochromatin organisation is altered in ORC1-deficient MGS cells, nuclear levels of the heterochromatin markers HP1αβγ and H3K9me3 were found to be reduced in ORC1-P4hTERT. Similar findings were obtained after siRNA-mediated depletion of ORC1. As alterations in the recruitment of HP1α are likely to result in reduced recruitment of SUV39H1 and in reduced trimethylation of H3K9, these findings may reflect an important role of ORC1 in HP1α recruitment. Perhaps surprisingly, nuclear levels of H4K20me3, an additional heterochromatin marker, were not altered in ORC1-deficient MGS patient cells or in ORC1-depleted fibroblasts. In contrast, a reduction in nuclear H4K20me3 levels were detected in cells depleted for KAP-1 or HP1α. This result may reflect a differential impact of ORC1 on H3K9me3 versus H4K20me3. However, this finding may simply reflect the sensitivity of this analysis. Subtle changes in H4K20me3 may not be detected by analysis of nuclear levels of

protein, and therefore, further exploration of the impact of ORC1 on H4K20me3 using high-resolution microscopy may be informative.

Examination of IR-induced γH2AX foci which colocalise with chromocentres in MEFs revealed that depletion of ORC1also results in the expansion of DDR signalling at heterochromatin regions. Similar to observations in NIH3T3 cells depleted for MeCP2 or DNMT3B, which are altered in Rett syndrome and ICF, respectively, ORC1 depletion was found to result in an increase in the size of γH2AX foci regions which overlap with chromocentres (Brunton et al. 2011). In contrast, the size of γH2AX foci which did not overlap with chromocentres was unaffected in ORC1-depleted cells. These findings suggest that ORC1 depletion specifically impacts upon DSB signalling at heterochromatin regions and does not affect signalling within euchromatin. As heterochromatin is thought to restrict DSB signalling, this observation is consistent with the notion that a reduction in ORC1 results in altered heterochromatin organisation and enhanced ATM-dependent DSB signalling.

Alterations in ATM-dependent signalling and the G2/M checkpoint have also been observed in cells from patients with disordered chromatin syndromes such as Rett syndrome, ICF, and HGPS (Brunton et al. 2011). Similarly, hypersensitivity of the G2/M checkpoint was observed in cells from distinct ORC1-deficient MGS patients and in cells depleted for ORC1. Both activation and maintenance of the checkpoint were observed to be altered in ORC1-P4hTERT cells and ORC1-depleted 1BR3hTERT cells. Further, overexpression of ORC1 was found to restore normal sensitivity of the G2/M checkpoint in ORC1-P1 LBLs. These findings demonstrate that a reduction in ORC1 results in enhanced sensitivity of the G2/M checkpoint, likely as a result of enhanced ATM-mediated DSB signalling.

Finally, I demonstrated that ORC6 also impacts upon heterochromatin organisation and the IR-induced DDR. Similar to observations made after ORC1 depletion, ORC6-depleted fibroblasts displayed reduced levels of H3K9me3, a partial alleviation of the requirement for ATM in DSB repair, and enhanced sensitivity of the G2/M checkpoint. Further, LBLs from an ORC6-deficient MGS patient displayed hypersensitive G2/M checkpoint activation and prolonged maintenance of the checkpoint. In contrast, depletion of CDC6 or CDT1 did not impact these cellular characteristics. Further supporting these findings, G2/M checkpoint efficiency was similar in control LBLs and in LBLs from patients with CDC6 or CDT1-deficient MGS. Therefore, these results have suggested that ORC-dependent heterochromatin organisation is performed either independently of pre-RC formation or prior to CDC6 and CDT1 recruitment. Importantly, these results demonstrate that cellular distinctions exist between ORC-deficient MGS and CDC6 or CDT1-deficient MGS patients.

In considering the evolutionary reason for the close link between ORC and heterochromatin, there are several possible explanations. As DNA replication involves histone deposition, one possible explanation may be that changes in higher-order chromatin structure in

ORC-depleted cells arise indirectly from replication defects. However, as the function of ORC in heterochromatin is genetically separable in *S. cerevisiae* (Bell et al. 1995; Dillin et al. 1997), this explanation is unlikely. A second model proposes that the association of ORC with heterochromatin via interactions with chromatin factors facilitates the replication of these transcriptionally silenced regions which are inherently difficult to replicate (Leatherwood et al. 2003). While this model explains why ORC would be recruited to heterochromatin regions, it does not fully address why ORC is also involved in the formation of heterochromatin. Alternatively, a third explanation may be that ORC recruitment to heterochromatin and ORC-dependent spreading of chromatin compaction functions to regulate the scheduled replication of specific genomic regions during S-phase. As introduced in Chapter I, the timing of replication of DNA regions is regulated, in part, by chromatin compaction, with euchromatin generally replicating early in S-phase and heterochromatin replicating later. Various ORC subunits may contribute to this regulation by promoting heterochromatin formation, for example, via the recruitment of HP1 to chromatin. In support of this notion, mutation of *Drosophila* ORC2 results in altered timing of replication, with some euchromatic regions getting duplicated later than regions normally known to exist as heterochromatin (Loupart et al. 2000; Chakraborty et al. 2011). Further, loss of *Drosophila* HP1 results in alterations in the timing of replication of repeat regions (Schwaiger et al. 2010) and mouse cells lacking SUV39H1/2 duplicate DNA within chromocentre regions earlier in S-phase than control cells (Wu et al. 2006). It may be feasible that the recruitment of ORC to chromatin, mediated by factors such as HMGA1a and ORCA, promotes HP1α recruitment and subsequent chromatin compaction specifically at regions which are replicated late in S-phase. Based on my findings that CDC6 and CDT1 do not have as significant an impact on heterochromatin organisation as ORC components, this process may occur prior to or independently from assembly of the pre-RC. While the model that ORC is specifically involved in the regulation of replication timing in human cells is appealing, further investigation is needed to either confirm or challenge this possibility.

Overall, the results presented in this chapter support a model in which ORC subunits function in heterochromatin formation in human cells to a greater extent than other pre-RC components such as CDC6 and CDT1. The findings presented in this chapter have also implicated ORC1 and ORC6-deficient MGS as a disordered chromatin syndrome, potentially distinguishing these disease phenotypes from CDC6 or CDT1-deficient MGS. The question of whether a defect in heterochromatin organisation contributes to the clinical manifestation of MGS will be discussed in Chapter VI. Finally, I have demonstrated that cells from ORC-deficient MGS patients or in ORC-depleted fibroblasts display a partial alleviation of the requirement for ATM in DSB repair, enhanced DSB signalling, and hypersensitivity of the G2/M checkpoint.

VI Conclusions and perspectives

VI.1 Major thesis aims

The maintenance of genome stability is crucial for the prevention of tumourigenesis. The molecular pathways which regulate replication activity, the segregation of chromosomes during mitosis, cell cycle progression, transcriptional activity, cellular survival or death, and the response to various types of DNA damage are vital in maintaining genome stability. Consequently, aberrations in these pathways may contribute to cancer development and represent cancer biomarkers or therapeutic targets. In addition, the abnormal regulation of some of these molecular pathways may lead to other clinical phenotypes such as premature aging, immunodeficiency, microcephaly, and dwarfism (O'Driscoll et al. 2006). The ongoing study of molecular pathways involved in the maintenance of genome stability has contributed to our understanding of the etiology of various human diseases and potential therapeutic strategies. However, many questions remain.

As presented in this thesis, I have investigated the impact of reduced levels of various molecular components on DNA damage repair and signalling, recovery from replication stress, and heterochromatin formation. While my work presented in Chapter III was focused on examining DSB repair in regions enriched for heterochromatin, my interest in more clinically-relevant research led my pursuit of the work presented in Chapters IV and V. As described in Chapter IV, I embarked on a comprehensive analysis of the impact of diminished dormant origin availability on replication stress recovery in non-tumour and tumour-derived cell lines. Ultimately, this work aimed to assess the potential therapeutic strategy of targeting origin licensing for treatment of cancer and has provided several positive implications. In Chapter V, I aimed to examine the impact of deficient origin licensing capacity on higher-order chromatin structure and the IR-induced DDR in the context of MGS patient cells. This work has had implications in the characterisation of ORC-deficient MGS.

VI.2 Examination of the role of Artemis in DSB repair during G0/G1 using a novel system of site-specific break induction

As previously introduced, the subset of IR-induced DSBs which occur within regions of heterochromatin are specifically repaired with slow kinetics by a pathway involving ATM, the mediator proteins, and the Artemis endonuclease (Riballo et al. 2004; Goodarzi et al. 2008; Noon et al. 2010). Heterochromatin has been proposed to act as a barrier to DSB repair which may be alleviated by ATM-dependent phosphorylation of KAP-1 (Goodarzi et al. 2008) and subsequent changes in chromatin remodelling (Goodarzi et al. 2011). While DSBs persisting in

Artemis-defective cells localise to regions of heterochromatin, in contrast to that observed in ATM-deficient cells, the requirement of Artemis for repair of IR-induced DSBs is not alleviated by heterochromatin relaxation via KAP-1 depletion (Woodbine, Brunton et al. 2011). These results suggest that Artemis has a role in heterochromatic DSB repair distinct to that of ATM and downstream of heterochromatin relaxation. However, the precise role of Artemis is still being examined. The development of new techniques for assessing heterochromatic DSB repair may prove beneficial in further examination of the function of Artemis in DSB repair.

Previous studies of the role of ATM and Artemis in DSB repair have primarily exploited IR to induce DNA damage. However, the relatively low percentage of IR-induced DSBs that localise to heterochromatic regions has posed limitations for monitoring repair at these regions using γH2AX foci enumeration. Routine detection of a defect specifically in IR-induced heterochromatin DSB repair typically relies on distinctions between few γH2AX foci (ie. comparing an average of 2-4 foci per nucleus in repair-efficient cells and an average of 10-12 foci in repair-defective cells at 24 hours after 3 Gy IR). Further, accurate determination of foci number for a sample must be determined in cellular populations which contain cell to cell variations in foci number (Lobrich et al. 2010). Alternative systems of DSB induction involving endonucleases are often limited by low cutting frequency and the capacity of active enzymes to re-cut at the same site. Further, these previously employed systems have generally not been specific to the induction of DSBs occurring within regions enriched for heterochromatin. In Chapter III, I aimed to optimise a system for monitoring the repair of site-specific DSBs occurring within regions enriched for heterochromatin.

VI.2.1 Exploitation of a novel system for monitoring the repair of DSBs likely to occur in heterochromatin regions

In Chapter III, I have described a novel system established by Dr. Jie Wen, Dr. Patrick Concannon, et al. for the induction of site-specific DSBs by CPP-mediated delivery of I-*Ppo*I, an endonuclease which recognises and cleaves a site within 28S rDNA. I was able to successfully optimise the expression and purification of functionally active I-*Ppo*I and observed DSB induction (by detection of γH2AX or 53BP1 foci) following direct delivery of purified I-*Ppo*I using the pep-1-cysteamine CPP. Consistent with a recently published report (Wen et al. 2012), CPP-mediated delivery of I-*Ppo*I was not observed to induce cytotoxity or DSB accumulation in DSB repair-defective cells, suggesting that multiple rounds of enzymatic cutting are unlikely using this system.

The human genome contains multiple I-*Ppo*I recognition sites, precluding the need to integrate a recognition sequence. ~300 possible rDNA I-*Ppo*I recognition sites exist in the

human genome (Monnat et al. 1999) and ~11 additional sites have been recently identified (Berkovich et al. 2007; Wen et al. 2012). As a substantial fraction (~50%) of rDNA is found to be in a transcriptionally silenced state throughout the cell cycle (Conconi et al. 1989), I-*Ppo*I-induced DSBs may occur in regions which have a higher heterochromatin content than that of the entire genome (~20%) (Miklos et al. 1979).

Consistent with a previous report which exploited a tamoxifen-inducible system of I-*Ppo*I expression (Berkovich et al. 2007), cells treated with an ATMi were observed to be defective in the repair of a substantial fraction of I-*Ppo*I-induced DSBs. Here, I have additionally demonstrated that depletion of the Artemis endonuclease or of RNF8 or 53BP1, which mediate ATM-dependent DSB signalling, also results in a substantial defect in I-*Ppo*I-induced DSB repair during G0/G1. Previous work has demonstrated that DSBs persisting in cells with reduced levels of ATM, Artemis, RNF8, or 53BP1 localise to regions of heterochromatin (Goodarzi et al. 2008; Noon et al. 2010; Woodbine et al. 2011) and these factors are thought to be required specifically for heterochromatin DSB repair. Therefore, my observation that inhibition or depletion of ATM, Artemis, or the mediator proteins results in a substantial defect in I-*Ppo*I-induced DSB repair may support a model in which I-*Ppo*I-induced DSBs occur in regions enriched for heterochromatin. In further support of this model, global heterochromatin relaxation, via KAP-1 depletion, was observed to alleviate the requirement for ATM, RNF8, and 53BP1 in repair of I-*Ppo*I-induced DSBs. However, further investigation is needed to prove or disprove the notion that I-*Ppo*I-induced DSBs occur in regions enriched for heterochromatin. Examination of γH2AX foci colocalisation with regions of heterochromatin (ie. labelled with H3K9me3 antibodies or by visualisation of DAPI-dense chromocentres in MEFs) may help to address this point. I have also presented findings which demonstrate that inhibition of the NHEJ factor DNA-PK results in a significant defect in DSB repair during G0/G1. Altogether, these results are consistent with the model that heterochromatic DSBs in G0/G1 cells require ATM-dependent signalling for heterochromatin relaxation and Artemis (potential roles will be discussed below), and are repaired primarily by NHEJ (Beucher et al. 2009).

VI.2.2 Artemis functions in the repair of I-*Ppo*I-induced DSBs in a manner independent of chromatin relaxation

Significantly, global chromatin relaxation via KAP-1 depletion did not alleviate the requirement for Artemis in the repair of I-*Ppo*I-induced DSBs during G0/G1. This finding is similar to observations made after treatment with TBH or IR published last year (Woodbine et al. 2011) and suggests that the role of Artemis in heterochromatic DSB repair is distinct to ATM signalling-dependent heterochromatin relaxation.

Artemis has been demonstrated to promote heterochromatic DSB repair by NHEJ during G0/G1 and by HR during G2. Several possible models exist which explain the functional role of Artemis at these stages of the cell cycle. One model (Beucher et al. 2009) postulates that Artemis functions to remove secondary structures or lesions which block the progression of NHEJ during G0/G1 or of HR-associated resection during G2. During G0/G1, DNA-PK autophosphorylation may activate the endonucleolytic activity of Artemis, enabling the processing of ends which cannot readily be ligated, such as those containing secondary structures (Goodarzi et al. 2006). During G2, secondary structures may feasibly arise during the process of resection-mediated generation of ssDNA. As secondary structures may be more likely to arise in transcriptionally silenced repeat regions such as rDNA, the resolution of DSBs arising in heterochromatin may have a greater requirement for this form of Artemis-dependent processing. However, another model currently favoured in our lab is that Artemis specifically functions to promote DNA end resection. While resection is known to be required for HR during G2, this model postulates that some resection (though less extensive) may also be required for a component of NHEJ-mediated repair during G1, and is specifically required at heterochromatic DSBs. This model poses that heterochromatic DSB repair requires both heterochromatin relaxation and resection of DNA, irrespective of whether cells are in G0/G1 or G2. Following heterochromatin opening and resection, the molecular pathway used to repair heterochromatic DSBs is dependent upon cell cycle phase. The slow kinetics associated specifically with heterochromatic DSBs could then be explained by the need for heterochromatin relaxation and resection to precede repair at these regions.

While my results described above are consistent with the suggestion that Artemis is required for heterochromatic DSB repair but functions downstream of heterochromatin relaxation, further exploitation of this system I-*Ppo*I-mediated DSB induction is needed to clarify the function of Artemis in end resection during G0/G1.

VI.2.3 The nature of I-*Ppo*I-induced DSB repair

While potential limitations in this system of I-*Ppo*I delivery (ie. asynchronous induction of DSBs, variations in cellular uptake, differences sub-cellular protein distribution, and DSB clustering) discussed in Section III.3 preclude the precise monitoring of DSB repair over time, assessment of the range of γH2AX foci per cell at various times has provided an approximation of repair kinetics. Similar to results from quantitative PCR analysis published by our collaborators (Wen et al. 2012), peak DSB induction was observed to occur within 1-3 hours and complete or nearly complete repair was observed ~6-7 hours after CPP-mediated I-*Ppo*I delivery (3-6 hours after peak induction) in control G0/G1 cells. If I-*Ppo*I-induced DSBs do, in fact, occur in rDNA regions enriched for heterochromatin, this result is perhaps surprising,

given our current understanding that repair of IR-induced DSBs within heterochromatin occurs with slow kinetics (> 8 hours) (Goodarzi et al. 2010).

In considering explanations for these observations, several possibilities exist. First, the structure of I-*Ppo*I-dependent DSBs may require less extensive processing prior to their repair. Unlike the range of DSBs which may be induced by IR, DSBs generated by I-*Ppo*I consist of short (4 bp) 3' overhangs (Monnat et al. 1999). If Artemis functions in heterochromatic DSB repair during G0/G1 to process DNA ends incompatible with direct ligation (such as long overhangs), as suggested in previous models (Goodarzi et al. 2006; Beucher et al. 2009), perhaps less processing is required for the repair of I-*Ppo*I-induced DSBs with short overhangs. However, I consider this possibility to be unlikely. While the structure of each unique I-*Ppo*I-induced DSB may be simple relative to most IR-induced DSBs, I-*Ppo*I-induced DSBs may occur in close proximity within clustered rDNA repeats and within regions of high chromatin complexity. Therefore, *in vivo*, I-*Ppo*I-induced DNA damage is likely to be complex in nature as it may consist of clustered DNA lesions, resulting from multiple forms of damage in close vicinity on the DNA. A second explanation may be that differences in the nature of heterochromatin at rDNA impacts upon the kinetics of DSB repair. The reversibility of heterochromatin structure at rDNA is crucial, as under physiological states which require ribosomal synthesis, rDNA genes must be activated for transcription by RNA Polymerase 1 (Preuss et al. 2007). Hence, it may be possible that heterochromatin is more dynamic at rDNA regions than other DNA regions and therefore repair at heterochromatic DSBs in rDNA may require less extensive chromatin remodelling and/or DSB resection. A third possibility which must be considered is that clustering of I-*Ppo*I-induced DSBs within rDNA significantly limits the monitoring of heterochromatic DSB repair by γH2AX foci analysis, therefore impacting upon assessment of DSB repair kinetics. While a limited number of γH2AX foci are visible at later times after protein transduction (ie. 6 hours), these foci may consist of multiple DSBs which cannot be distinguished by eye. Further analysis of γH2AX foci at later times after transduction using high resolution (ie. confocal) microscopy may facilitate the analysis of DSB clustering. The kinetics of I-*Ppo*I-induced DSBs assessed by quantitative PCR by Wen, Concannon, and colleagues were examined using primers which span the non-rDNA recognition sites (Wen et al. 2012). As the higher-order chromatin structure at these sites is less clear, assessment of repair kinetics at rDNA regions likely to be enriched for heterochromatin could therefore be improved by analysis using quantitative PCR primers which span the rDNA recognition site or by southern blot using a 28S rDNA probe. If improvements can be made to the I-*Ppo*I system to address the possibilities described above, it would be important to substantiate the finding that I-*Ppo*I-induced DSBs are in fact repaired more rapidly.

VI.2.4 Summary and implications

In summary, I have optimised a system for monitoring the repair of DSBs likely to occur in regions enriched for heterochromatin. This system exploits a novel method of I-*Ppo*I delivery developed by Dr. Jie Wen, Dr. Patrick Concannon, and colleagues, and enables the analysis of DSB repair during specific stages of the cell cycle. Using this system, I have demonstrated that Artemis is required for the repair of a substantial fraction of I-*Ppo*I-induced DSBs and functions in a process distinct to heterochromatin opening, similar to observations made after TBH and IR (Woodbine et al. 2011). Therefore, this work may contribute to our understanding of heterochromatin DSB repair at rDNA regions and has consolidated findings that Artemis is required for repair at heterochromatic regions in a role independent of chromatin relaxation.

Many interesting questions about heterochromatic DSB repair remain which could potentially be investigated using this novel I-*Ppo*I-dependent system of DSB induction now optimised for routine use. The analysis of I-*Ppo*I-induced cleavage of 28s rDNA recognition sites and repair of these breaks could be assessed in cells deficient in DDR factors by quantitative PCR using primers spanning the 28S rDNA site or by southern blot using a 28S rDNA probe. The extent of DNA end resection at DSBs in rDNA could be examined in G0/G1 cells (ie. cells grown to confluency) using quantitative PCR primer sets which vary in distance from the rDNA recognition site. This method may be useful in examining DNA end resection in cells deficient in enzymes required for resection, such as Artemis and CtIP. This system may be applied to assess chromatin binding of DDR factors by ChIP analysis using primers which recognise sequences at various distances from the 28S rDNA site. Finally, changes in higher-order chromatin structure (ie. the loss of chromatin-bound factors such as H3K9me3) which occur during I-*Ppo*I-induced DSB repair may be investigated in various cellular backgrounds by ChIP-based analysis.

VI.3 The impact of diminished origin licensing capacity on replication stress recovery in tumour versus non-tumour cells

Upon completion of the work described above, my interest in translational medicine inspired a transition in my research project. As described in Chapter IV, I next examined the impact of depleting DNA replication origin licensing factors on the sensitivity of tumour and non-tumour cell lines to replication stress.

One of the hallmarks of cancer cells is a limitless replicative potential (Hanahan et al. 2000), and, consequently, cancer cells are frequently characterised by an increase in DNA replication. The increased availability of replication materials (ie. dNTPs) and overexpression of enzymes required for replication (Scanlon et al. 1989) are thought to contribute to this increase

in replication. In addition, alterations in DNA origin licensing components have been reported in various tumour types (Lau et al. 2007b), perhaps to accommodate increased DNA replication by enhancing replication origin licensing activity (Di Paola et al. 2010; Di Paola et al. 2011).

Enhanced levels of replication stress have been reported in cancer cells and are thought to contribute to the genome instability which drives tumour development (Negrini et al. 2010; Bartek et al. 2012). Cancer-associated alterations in DDR mechanisms may promote sustained proliferation despite enhanced replication fork stalling/collapse. One mechanism used to recover from replication-associated damage is the firing of excess or dormant replication origins (Blow et al. 2011). One model proposed by Blow and colleagues assumes that origin activation occurs in a stochastic manner and that dormant origin activation protects against the hazardous effects of double fork stalling (Blow et al. 2009). Therefore, increased origin density was suggested to correlate with increased protection from replication stress (Blow et al. 2011). Consequently, the overexpression of licensing factors and enhanced origin licensing capacity observed in cancer (Lau et al. 2007b) may not only enable increased replication but also support proliferation under conditions of replication stress by increasing dormant origin availability.

In Chapter IV, I examined whether partial depletion of licensing components enhances sensitivity to replication stress specifically in tumour-derived cell lines. Here, I predicted that non-tumour cells, which express much lower levels of origin licensing components, replication materials, and replication machinery and which display an intact DDR, do not rely as heavily on dormant origin firing to recover from replication stress, instead using alternative recovery mechanisms. This research has both fundamental and translational aspects as discussed below.

VI.3.1 Diminished origin licensing capacity specifically sensitises tumour-derived cell lines to replication stress-inducing agents

To examine my hypothesis described above, several non-tumour (1BR3hTERT, BJhTERT, 48BR, and MRC-5) and tumour-derived (U2OS, HeLa, and MDA-MB-231) cell lines were selected. In support of previous reports that transformed cells display increased expression of origin licensing factors, (Lau et al. 2007b), I observed an increase in the expression of ORC1 in each of the 3 tumour-derived cell lines. In addition, tumour-derived cells were observed to divide more rapidly than non-tumour cell lines, consistent with the notion that increased replication is associated with cancer. Further, shorter exposures to HU were required to achieve complete S-phase arrest in the tumour-derived cell lines. Consistent with the well-established observation that cells license origins in excess, both non-tumour and tumour cells were able to sustain proliferation despite a substantial depletion of origin licensing capacity. Interestingly, in the absence of HU, higher levels of ORC1 were required to maintain viability in the 3 tumour-

derived cell lines examined, perhaps reflecting increased endogenous levels of replication stress. For each cell line, I identified conditions of siRNA-mediated depletion of ORC1 which did not impact upon viability and considered these conditions likely to deplete dormant origin capacity.

Using these conditions, I demonstrated that diminished dormant origin licensing capacity sensitised multiple tumour-derived but not non-tumour cells to replication stress (HU) and oxidative stress (H_2O_2), two types of damage found to be enhanced in cancer. The enhanced HU sensitivity of U2OS osteosarcoma cells partially depleted for ORC1 correlated with diminished new origin firing, reduced recovery of replication, and an accumulation of S-phase associated damage. These findings suggest that the enhanced HU sensitivity of siORC1-treated U2OS cells is associated with impaired recovery from replication stress.

The lack of enhanced sensitivity to replication stress in non-tumour cells depleted for ORC1 was confirmed in 4 primary or hTERT-immortalised cell lines as well as ORC1-deficient MGS patient fibroblasts and LBLs. Therefore my findings were not restricted to a specific cell line or to depletion of ORC1 using siRNA oligonucleotides. Further, diminished licensing capacity did not impact upon sensitivity of non-tumour cells to HU treatment times adjusted to achieve complete S-phase arrest, suggesting that the lack of enhanced sensitivity of ORC1-depleted non-tumour cells was not simply a reflection of slower cell cycle progression. Observations were similar following depletion of other licensing components (ORC6 and CDC6) and therefore not limited to ORC1 depletion. Importantly, despite substantial depletion of ORC1, non-tumour 1BR3hTERT cells were capable of recovering replication at early times after release form HU. This observation suggests that 1BR3hTERT cells may exploit alternative mechanisms of replication recovery under conditions of diminished dormant origin supply. Examination of replication fork restart and new origin firing in ORC1-depleted 1BR3hTERT cells would confirm and extend this observation. In addition, examination of the impact of the increased expression of licensing components or decreased expression of factors required for alternative recovery mechanisms in non-tumour cells may further support this model.

It should be noted, however, that the results presented in Chapter IV are restricted to the tumour-derived and non-tumour cell lines that were examined. Further examination is needed to assess whether these findings represent frequent differences between tumour and non-tumour cell lines and whether they are observed in all cancer types or in specific forms of cancer. Increased ORC1 expression was observed in each of the tumour-derived cell lines that were investigated. Assessment of a broader panel of tumour-derived cell lines with differing levels of ORC1 expression may help to extend these findings and to explore the relationship between ORC1 expression and enhanced HU sensitivity under conditions of reduced origin licensing capacity.

VI.3.2 Depletion of p53 or overexpression of c-Myc results in enhanced loss of viability in non-tumour cells partially depleted for ORC1

Alterations which reduce the expression of tumour suppressor genes such as *TP53* or which increase the expression of oncogenes such as *c-Myc* are frequently found in cancer (Spencer et al. 1991; Vogelstein et al. 2000) and are likely to contribute to enhanced levels of replication stress. Among the many effects of these alterations, reduced levels of p53 or increased expression of *c-Myc* may impact upon the regulation of the G1-S-phase transition, increase replication activity, and/or alter the DDR. Here, I have examined the impact of both alterations on viability in ORC1-depleted non-tumour cells.

Co-depletion of the p53 tumour suppressor gene and ORC1 in non-tumour 1BR3hTERT cells was observed to enhance viability loss, both in the absence and presence of HU treatment. p53 regulates multiple cellular processes such as the G1/S transition (ie. the "origin licensing checkpoint" (Nevis et al. 2009)), DNA damage-induced cell cycle arrest (Wahl et al. 1997), apoptosis, RNR-mediated dNTP production (Xue et al. 2003), and the resolution of stalled replication forks (Sengupta et al. 2003; Ho et al. 2006). Therefore, several possibilities exist which may explain why HU sensitivity is enhanced in non-tumour cells co-depleted for p53 and ORC1.

One possible explanation for the observed increase in viability loss following co-depletion of ORC1 and p53 in non-tumour cells is related to the role for p53 in the replication stress DDR distinct to its function in cell cycle checkpoint activation. p53 is reported to directly associate with stalled forks in a BLM-dependent but ATM-Chk1-independent manner and to negatively regulate HR-based replication fork recovery (Ho et al. 2006) (Sengupta et al. 2003). Further, p53 has been proposed to protect cells from HU-induced one-ended DSBs (Kumari et al. 2004), structures thought to require HR-mediated repair (Petermann et al. 2010a; Petermann et al. 2010b). Given these observations and the fact that p53 localises to structures associated with fork remodelling, one model has been presented which proposes that p53 promotes HR-independent fork restart (Subramanian et al. 2005). As discussed above, HR-mediated repair and dormant origin firing may work together to promote the efficient recovery from replication fork collapse. It may be feasible, therefore, that the loss of p53 may result in greater replication fork collapse and an enhanced reliance on HR and dormant origin firing for replication recovery.

A second possibility is that both the loss of the G1/S DDR checkpoint associated with p53 depletion and enhanced replication stress arising from diminished dormant origin licensing capacity may result in high levels of DNA damage which ultimately impact upon viability. Over

time, cells may accumulate DNA damage from endogenous sources such as ROS or from HU-associated damage which cannot be efficiently resolved in the absence of dormant origin firing. Under conditions of p53 depletion, loss of the G1/S checkpoint may then result in increased levels of replication stress as cells harbouring DNA damage may progress into S-phase. A cellular threshold for replication stress may exist, and when levels rise above this threshold, cells may induce cellular death pathways reflected by the loss of viability observed in my studies.

A third more appealing possibility is related to changes in S-phase entry associated with p53 loss. Both in the presence and absence of DNA damage, cells depleted for p53 display accelerated S-phase entry (Deckbar et al. 2010). As previously introduced, there is some evidence for the existence of a licensing checkpoint which prevents cells from entering S-phase before a sufficient number of origins have been licensed (Ge et al. 2009). This licensing checkpoint has been demonstrated to be regulated by p53 and RB and is deficient in various tumour cell lines such as U2OS and HeLa (Nevis et al. 2009). One possibility is that tumour cells override the origin licensing checkpoint to enhance proliferation and, therefore, partial depletion of ORC1 may result in S-phase entry despite the reduced number of dormant origins; co-depletion of p53 and ORC1 in non-tumour cells may mimic this condition. In support of this notion, co-depletion of p53 and the other licensing factor, Cdc6, in non-tumour cells has been demonstrated to result in premature S-phase entry, reduced rates of DNA replication, and an accumulation of S-phase DNA damage (Nevis et al. 2009).

As presented in Chapter IV, overexpression of the c-Myc oncogene in a non-tumour background also results in enhanced replication stress and loss of viability following ORC1 depletion. As overexpression of c-Myc is reported to enhance DNA damage, hyper-replication, replication stress, and oxidative damage and to disrupt p53 function (Vafa et al. 2002; Dominguez-Sola et al. 2007; Herold et al. 2009b; Robinson et al. 2009), various possible explanations for these results may exist and may be related to those described above. Interestingly, c-Myc has been reported to play a non-transcriptional role in DNA replication by stimulating replication origin activity and in fact, immunoprecipitates with various pre-RC components (Dominguez-Sola et al. 2007). In addition, c-Myc upregulates the transcription of Cdt1 (Watson et al. 2002) and E2F1 (Fernandez et al. 2003) which regulates the expression of various pre-RC components. Therefore, the overexpression of c-Myc may promote increased origin licensing to facilitate hyper-replication. In addition, an increase in dormant origin availability in cells which overexpress c-Myc may promote proliferation under conditions of enhanced replication stress. The examination of c-Myc-induced changes in ORC1 expression in BJ-MYC-ER cells may help to evaluate these possibilities.

Overall, the depletion of p53 or the overexpression of c-Myc may enhance loss of viability in ORC1-depleted non-tumour cells by multiple mechanisms. Further investigation

using ORC1-depleted non-tumour cells depleted for additional components involved in the G1/S transition (such as RB and p16) or which overexpress other oncogenes (such as Ras) would help to extend these findings.

VI.3.3 Diminished origin licensing capacity enhances sensitivity of tumour but not non-tumour cells to HU combined with Chk1 inhibition

As presented in Chapter IV, inhibition of Chk1 just prior to and following release from HU further enhances HU sensitivity in ORC1-depleted osteosarcoma cells. As Chk1 functions to regulate DNA replication origin firing, stabilise forks, and to promote HR, the impact of Chk1 inhibition on viability in HU and siORC1-treated cells may be multifaceted.

DNA damage-activated Chk1 signalling is required to inhibit the activation of late-firing replication clusters but allows dormant origin firing in activated factories which harbour stalled/collapsed replication forks (Ge et al. 2010). Under conditions of replication stress, this function of Chk1 has been proposed to redirect the limited supply of replication machinery towards dormant origin activation in order to promote replication recovery. As previously discussed, enhanced replication stress may accumulate in HU-treated tumour cells depleted for ORC1. In this context, inhibition of Chk1 may result in the inappropriate activation of late-firing origins, resulting in an even greater increase in replication stress and loss of viability.

Chk1 also functions to stabilise stalled replication forks, and consequently, an accumulation of aberrant replication fork structures has been observed after Chk1 inhibition in the absence (Petermann et al. 2006) and presence of replication inhibitors (Kastan et al. 2004). Therefore, Chk1 inhibition combined with HU treatment may result in enhanced replication fork collapse requiring dormant origin firing for recovery.

Finally, Chk1 is also reported to promote the HR-mediated repair of HU-induced lesions (Sorensen et al. 2005). Chk1 has been reported to interact with Rad51, resulting in Chk1-dependent phosphorylation on threonine 309, and this process is thought to directly regulate Rad51 activity. Consequently, inhibition or siRNA-mediated depletion of Chk1 combined with HU treatment results in the deficient formation of Rad51 foci, a reduction in HR-mediated repair, and an accumulation of replication associated-DSBs (Sorensen et al. 2005).

In summary, multiple explanations may exist for the enhanced HU sensitivity observed in ORC1-depleted U2OS inhibited for Chk1. Chk1 inhibitors have shown promise as chemotherapeutic agents (Dai et al. 2010) in combination with replication stress-inducing agents such as HU and gemcitabine (Montano et al. 2012). Therefore this finding may have positive implications for the utility of dormant origin licensing inhibitors.

VI.3.4 Summary and implications

In Chapter IV, I presented results demonstrating that diminished dormant origin capacity specifically sensitises multiple tumour-derived cell lines to HU or H_2O_2-induced replication stress. Further, I have presented findings which indicate that depletion of the p53 tumour suppressor gene or increased expression of the c-Myc oncogene results in enhanced loss of viability in ORC1-depleted non-tumour cells.

Here, I have presented possible explanations to address these observations. First, I have suggested that, in contrast to non-tumour cells which may more readily exploit alternative mechanisms of replication restart or repair, tumour derived cell lines (or non-tumour cells depleted for p53 or which overexpress c-Myc) have a greater reliance on dormant origin firing for replication stress recovery. The expression of origin licensing components may be elevated in tumour-derived cell lines (or cells which overexpress the c-Myc oncogene), resulting in an increased supply of origins which may support hyper-replication. As an increase in dormant origin availability is likely to increase the efficiency of recovery from replication stress, tumour cells may frequently utilise this mechanism. Further, cellular changes associated with cancer may downregulate the use of alternative mechanisms of replication fork recovery. I have also suggested that replication fork collapse may occur more readily in tumour-derived cell lines or in non-tumour cells depleted for p53 or which overexpress c-Myc. An increase in fork collapse may result from cancer-associated changes which prevent fork stabilization, and may preferentially require dormant origin firing and/or HR-mediated repair. Finally, I have suggested that the distinctions between the requirement of non-tumour and tumour-derived cell lines for dormant origin availability may be related to cancer-associated changes in the G1/S checkpoint which result in toxic levels of replication stress. Many tumour cell lines or non-tumour cells which overexpress c-Myc display alterations in S-phase entry, hyper-replication, and enhanced replication stress. Defects in the G1/S DDR checkpoint may result in further replication stress, as cells harbouring DNA damage prematurely enter S-phase. In addition, loss of the licensing checkpoint in tumour cells may result in premature S-phase entry under conditions of diminished origin supply (ie. after ORC1 depletion), again resulting in enhanced levels of replication stress.

The research presented in Chapter IV has both fundamental and translational aspects with several important potential implications. From a fundamental research perspective, these findings may contribute to our understanding of differences in replication stress recovery in tumour vs. non-tumour cells. Further examination of the relative dependence of ORC1-depleted tumour and non-tumour cells on HR-independent replication restart, HR-mediated repair, or dormant origin firing may help to clarify the mechanistic differences which result in the distinctions I have observed. In addition, this research has had a translational aspect, and has

implicated origin licensing as a potentially suitable target for drug-based cancer therapy. My findings that tumour-derived cell lines or cells harbouring cancer-associated changes are hypersensitive to HU-induced damage suggest that administration of a licensing inhibitor at low doses may specifically sensitise tumour cells to replication stress-inducing chemotherapeutic agents. Findings from this work have implied that licensing inhibitors may be particularly effective tumours which overexpress licensing factors such as ORC1, which display increased expression of the c-Myc oncogene, and/or which display defects in the G1/S checkpoint. Further, these results have suggested that a strategy combining replication stress-inducing agents with Chk1 and licensing inhibitors may be particularly effective. Further investigation into tumour backgrounds particularly sensitive to the combined treatment with an inhibitor of origin licensing and replication stress inducing agents may help to expand upon these findings. In addition, assessment of druggability of licensing components such as ORC1 and ORC6 is necessary to validate this approach.

VI.4 The impact of reduced levels of origin licensing factors on higher-order chromatin structure and the IR-induced DDR

An accumulating body of evidence has demonstrated that the components of the pre-RC function in multiple cellular processes other than replication origin licensing such as heterochromatin organisation. Various subunits of ORC have been demonstrated to localise to heterochromatin in human cells, and this localisation is promoted by interactions with chromatin factors such as ORCA, HMGA1a, and HP1α (Alabert et al. 2012). Direct interactions between ORC subunits and HP1α have been identified, and these interactions are proposed to facilitate heterochromatin organisation in human cells (Prasanth et al. 2010).

Mutations in pre-RC components have been identified in MGS, a disorder characterised by bone abnormalities, microcephaly and growth retardation (Bicknell et al. 2011a). In Chapter V, I have examined whether cells from ORC, CDC6, or CDT1-deficient MGS or cells depleted for these components display characteristics associated with alterations in heterochromatin. Additionally, I have examined the sensitivity of the ATM-dependent DNA damage signalling and the G2/M checkpoint in these cells as alterations in these processes have been observed in cells from patients with disordered chromatin syndromes (Brunton et al. 2011). As discussed below, these findings have implications in our understanding of the cellular phenotype of MGS patients which carry mutations in various pre-RC components.

VI.4.1 ORC1-deficient MGS patient cells and ORC1-depleted control fibroblasts display alterations in nuclear levels of heterochromatin markers

Several mutations located in the BAH domain of ORC1 have been identified in cells from MGS patients (Bicknell et al. 2011a; Bicknell et al. 2011b). As ORC1 interacts with HP1α via a region within the BAH domain, and this interaction is thought to facilitate the recruitment of HP1α to chromatin (Prasanth et al. 2010), the BAH domain mutations identified in ORC1-deficient MGS patients may be predicted to impact upon the HP1α-dependent heterochromatin organisation. Consistent with this notion, nuclear levels of HP1 were found to be altered ORC1-P4hTERT cells, which harbour one mutation in the BAH domain and a second mutation in the C-terminus of ORC1 (Bicknell et al. 2011b). Analysis of cells depleted for ORC1 using siRNA oligonucleotides also displayed reduced levels of HP1, substantiating these results. I extended these findings to examine the impact of ORC1 on the heterochromatin marker H3K9me3. Consistent with observations of altered HP1 localisation, H3K9me3 was found to be reduced in ORC1-P4hTERT cells or control fibroblasts depleted for ORC1. As SUV39H1, a methyltransferase which promotes H3K9 trimethylation, is recruited to heterochromatin by HP1 binding and subsequently propagates H3K9 trimethylation across regions of DNA (Craig 2005), the disruption of HP1 localisation in cells with reduced ORC1 may explain this finding.

Perhaps surprisingly, total nuclear levels of H4K20me3 were found to be unaffected by ORC1 depletion or deficiency while depletion of KAP-1 or HP1α resulted in decreased H4K20me3 levels. H4K20 trimethylation is performed by distinct methyltransferases, SUV420H1 and/or SUV420H2, but is thought to be facilitated by SUV39H1-dependent trimethylation of H3K9 (Schotta et al. 2004). However, some H4K20 trimethylation occurs independently of H3K9me3 levels and while the HP1 subunits display dynamic association with chromatin, SUV420H2 remains stably associated with chromatin in a potentially HP1-independent manner (Souza et al. 2009). Therefore, these results could be explained by several models. First, the fact that HP1α localisation, H3K9 trimethylation, and heterochromatin are only partially affected in ORC1-deficient or depleted cells may still provide the platform for SUV420H1/2-dependent trimethylation of H4K20. Alternatively, in support of the findings of Souza and colleagues, some H4K20 trimethylation may occur independently of HP1 and H3K9me3, and therefore is not impacted by ORC1-deficiency or depletion. However, limitations in my analysis must be considered. Subtle changes in heterochromatin structure may not be detected by analysis of overall nuclear levels of H4K20me3. Therefore, further examination of the effect of ORC1 reduction on H4K20me3 may help to clarify these results.

Overall, these findings have indicated that ORC-deficient MGS patient cells display alterations in the distribution of heterochromatin markers and suggest that heterochromatin organisation may be altered.

VI.4.2 The requirement for ATM in DSB repair is partially alleviated in ORC1-deficient MGS patient cells and ORC1-depleted control fibroblasts

ORC1-P4hTERT cells or fibroblasts depleted for ORC1 using multiple siRNA oligonucleotides were observed to display a partial alleviation of the requirement for ATM in IR-induced DSB repair. As previously described, ATM is required specifically for the repair of heterochromatin DSBs, and this requirement is alleviated when heterochromatin becomes disordered (Brunton et al. 2011). Therefore, these findings suggest that heterochromatin organisation is disrupted when ORC1 levels are reduced. As discussed in Chapter V.3, the observation that the DSB repair defect associated with ATM inhibition is only partially alleviated in these cells may have multiple explanations. For example, residual levels of functional ORC1 in these cells may support some HP1α recruitment to all or specific regions of chromatin. This notion is supported by the findings by Prasanth and colleagues that HP1α localization is not completely disrupted in ORC1-depleted cells, but is rather redirected to the periphery of nucleoli (Prasanth et al. 2010). In addition, this observation may reflect the fact that HP1α recruitment to chromatin is only partially driven by binding with ORC1, and therefore some HP1α-dependent heterochromatin formation may occur in the absence of functional ORC1. Finally, recruitment of the HP1α subunit may not be sufficient to support heterochromatin formation at certain regions. Detailed examination of the role of the interaction between ORC1 and HP1α may provide further understanding of the observations made in ORC1- deficient or depleted cells. However, the findings obtained from these studies have demonstrated that the requirements for IR-induced DSB repair are altered in ORC1-deficient MGS patient cells.

VI.4.3 The impact of reduced ORC1 levels on IR-induced DSB signalling and sensitivity of the G2/M checkpoint

Depletion of MeCP2 or DNMT3B, the heterochromatin factors altered in Rett syndrome or ICF, respectively, has been demonstrated to enhance IR-induced DSB signalling at heterochromatin regions (Brunton et al. 2011). Here, I also observed that depletion of ORC1 in NIH3T3 MEFs results in enhanced expansion of γH2AX foci into heterochromatin-rich chromocentres. This finding supports the model that cells with reduced ORC1 levels display enhanced IR-induced DSB signalling at heterochromatin regions, an alteration that is also proposed to impact upon sensitivity of the G2/M checkpoint (Brunton et al. 2011). Therefore, I examined the impact of a reduction in ORC1 levels on G2/M checkpoint activity in ORC1-deficient or depleted cells.

Both hypersensitivity of G2/M checkpoint activation and prolonged G2/M checkpoint maintenance were observed in ORC1-P4hTERT cells or cells depleted for ORC1. Further, overexpression of ORC1 was observed to restore G2/M checkpoint activity in ORC1-P1 LBLs to levels similar to that in control LBLs. These results have substantiated the model that ATM-dependent DSB signalling is enhanced at heterochromatin in ORC1-deficient MGS cells, likely as a result of altered heterochromatin organisation.

VI.4.4 A reduction in ORC6 but not CDC6 or CDT1 results in cellular characteristics associated with disordered chromatin

Finally, I demonstrated that ORC6-depleted 1BR3hTERT cells displayed a similar partial alleviation of the requirement for ATM in DSB repair, hypersensitivity of the IR-induced G2/M checkpoint, and reduction in H3K9me3 levels. Further, LBLs from an ORC6-deficient MGS patient display both hypersensitive activation and prolonged maintenance of the G2/M checkpoint. ORC6 is thought to translocate to the nucleus independently of the other ORC subunits (Chesnokov 2007; Ghosh et al. 2011), displays a more dynamic association with other ORC subunits (Ghosh et al. 2011), and has functions independent of the other ORC subunits (Prasanth et al. 2002). Therefore this observation may reflect a function of ORC6 in heterochromatin formation that is independent of ORC1. The association of ORC6 with HMGA1a at heterochromatin regions (Thomae et al. 2011), for example, may facilitate heterochromatin binding of the other ORC components, including HP1α-bound ORC1 (or ORC3). Therefore, ORC6 may also indirectly promote the recruitment of HP1α to chromatin, facilitating heterochromatin formation. However, as ORC6 is also detected in complex with the remaining ORC components (Ghosh et al. 2011), the role of ORC6 in heterochromatin organisation may be related to that of ORC1 and ORC3-associated HP1α recruitment.

In contrast, cells depleted for CDC6 or CDT1 displayed characteristics similar to siControl treated cells. In addition, sensitivity of the G2/M checkpoint was observed to be similar in control LBLs and LBLs from CDC6- or CDT1-deficient MGS patients. These findings suggest that the role of the pre-RC components in heterochromatin formation may primarily be directed by ORC. In this scenario, CDC6 and CDT1 may be recruited only after ORC binds DNA and promotes heterochromatin spreading, where they function in origin licensing. While further examination would clarify these distinctions in the molecular requirements of pre-RC components in heterochromatin organisation, my results have demonstrated that heterochromatin disruption may be a feature specific to ORC-deficient MGS.

VI.4.5 Summary and Implications

My findings presented in Chapter V have implicated, for the first time, ORC1-deficient MGS as a disordered chromatin syndrome. Further, results from siRNA-mediated depletion of ORC6 and the analysis of ORC6-deficient MGS patient cells suggest that ORC6-deficient MGS may also be classified as a disordered chromatin syndrome. In contrast, CDC6- or CDT1-deficient MGS patient cells do not display alterations in heterochromatin as dramatic as those observed in ORC-deficient MGS patient cells. In addition, I have demonstrated that IR-induced DSB signalling and the ATM-dependent G2/M checkpoint are hypersensitive in cells containing reduced ORC1 or ORC6 levels, consistent with findings in cells from classified disordered chromatin syndrome patients (Brunton et al. 2011).

As speculated in the discussion in Chapter V, ORC and HP1-dependent heterochromatin formation may help to function the timing of replication, as euchromatin regions are replicated early in S-phase, and heterochromatin regions are replicated later in S-phase. In support of this notion, HP1 has recently been reported to modulate replication timing in Drosophila (Schwaiger et al. 2010), and depletion of HP1 results in early replication of heterochromatin regions. If too many origins are activated early in S-phase as a result of altered replication timing in cells defective in ORC-dependent recruitment of HP1, dNTP pools may not be large enough to accommodate synchronous replication and replication may slow. Results from my studies have suggested that CDC6 and CDT1 may not play as much of a role in heterochromatin organisation as the ORC subunits. However, further work is needed to substantiate this model.

While my findings have demonstrated that distinctions exist in the cellular phenotypes of ORC or CDC6/CDT1-deficient patients, it is not clear whether these cellular phenotypes directly impact upon the clinical features of MGS. Interestingly, microcephaly and short stature, two of the key clinical features observed in ORC-deficient MGS patients, have also been reported in patients with various disordered chromatin remodelling syndromes such as Rett syndrome, Rubinstein-Taybi Syndrome, Coffin-Lowry Syndrome, and alpha-thalassemia/mental retardation syndrome (Ausio et al. 2003). However, unlike the nature of these phenotypes in MGS patients, the microcephaly and short stature described in patients with disordered chromatin syndromes are usually observed only after birth and are often progressive. While the disordered chromatin resulting from reduced levels of ORC components may contribute to the microcephaly or growth defects in MGS, these clinical features are also observed in CDC6 and CDT1-deficient MGS patients. Furthermore, no other clinical features have been observed which distinguish ORC-deficient MGS patients from CDC6 or CDT1-deficient MGS patients (de Munnik et al. 2012). Therefore, the disordered chromatin phenotype that I have observed specifically in ORC-deficient cells may contribute but not represent the main cause of the

clinical phenotypes that have been reported. However, one potential clinical manifestation of the impact of ORC deficiency on heterochromatin may be progeria, a feature observed in patients with other disordered chromatin syndromes such as HGPS. Alterations in telomeric heterochromatin, resulting in telomere uncapping, may promote enhanced DDR signalling and/or senescence (d'Adda di Fagagna et al. 2003; Schoeftner et al. 2009). This, in turn, may result in premature ageing. Further examination of MGS patients as they age will be needed to assess whether such a phenotype is apparent in ORC-deficient MGS.

While the limited number of patients identified to date makes it difficult to draw any major conclusions, no increase in cancer incidence has been reported in patients with ORC-deficient MGS or with Rett Syndrome. One potential factor contributing to this observation may be the observations of hypersensitive DNA damage signalling in ORC-deficient MGS and Rett cells as presented here and by other colleagues in our lab (Brunton et al. 2011). In wild-type cells, a threshold of 10-25 DSBs, which corresponds to IR doses >0.5 Gy, is reported to be required for ATM-dependent initiation and maintenance of G2/M checkpoint arrest (Deckbar et al. 2007). The inherent imperfection of the G2/M checkpoint may contribute to genome instability and cancer by allowing the progression of cells harbouring DSBs into mitosis. Chromosome breakage may then ensue in these cells, potentially contributing to tumourigenesis (Krempler et al. 2007; Lobrich et al. 2007). In contract to wild-type cells, both ORC-deficient MGS and Rett Syndrome cells display hypersensitive DSB signalling which prevents cells from progressing from G2 to mitosis when <20 DSBs are present (after <0.5 Gy). Therefore, while defects in heterochromatin formation may result in several adverse clinical phenotypes, they may also help to prevent genome instability and cancer.

VI.5 Final summary

Gaining more insight into the mechanisms which prevent genome instability will help to further our understanding of the molecular basis behind human diseases such as cancer. The molecular mechanisms which regulate DNA replication, DNA damage detection and repair, recovery from replication stress, and the maintenance of higher-order chromatin structure all play a role in the maintenance of genome stability. In this thesis, I have examined the requirement for Artemis in the repair of heterochromatic DSBs. I have exploited a novel system of CPP-mediated I-*Ppo*I delivery to induce site-specific DSBs in regions likely to be enriched for heterochromatin. Using this system, I have demonstrated that there is a substantial requirement for Artemis in the repair of I-*Ppo*I-induced DSBs and that this requirement is not alleviated by global heterochromatin relaxation. These findings have substantiated recently published work from our lab investigating the requirement for Artemis in the repair of IR-induced DSBs in heterochromatin. Further, these findings have suggested that CPP-mediated I-*Ppo*I delivery may be exploited to further study

the molecular mechanisms which govern heterochromatic DSB repair. However, the primary focus of this thesis has been to examine the cellular impact of diminished DNA replication origin licensing capacity. Here, I have demonstrated that partial depletion of origin licensing components specifically sensitises several tumour-derived cell lines to replication stress, without impacting upon the sensitivity of several non-tumour cell lines. I have also shown that depletion of the p53 tumour suppressor or overexpression of the c-Myc oncogene in a non-tumour background results in enhanced loss of viability under conditions of diminished origin licensing capacity. These findings have suggested that origin licensing factors may represent suitable therapeutic targets for the treatment of cancer. In addition, I have demonstrated that a reduction specifically in ORC1 and ORC6, but not in CDC6 or CDT1, results in alterations in heterochromatin organisation and in the IR-induced DDR. These findings have contributed to our understanding of the cellular consequences of ORC depletion and the cellular features of specific forms of MGS.

VII References

Aaltonen, L. A., P. Peltomaki, et al. (1994). "Replication errors in benign and malignant tumors from hereditary nonpolyposis colorectal cancer patients." Cancer Res **54**(7): 1645-1648.

Aasland, R. and A. F. Stewart (1995). "The chromo shadow domain, a second chromo domain in heterochromatin-binding protein 1, HP1." Nucleic Acids Res **23**(16): 3168-3173.

Abdel-Salam, G. M., M. S. Abdel-Hamid, et al. (2012). "Expanding the phenotypic and mutational spectrum in microcephalic osteodysplastic primordial dwarfism type I." Am J Med Genet A **158A**(6): 1455-1461.

Agarwal, N., A. Becker, et al. (2011). "MeCP2 Rett mutations affect large scale chromatin organization." Hum Mol Genet **20**(21): 4187-4195.

Agarwal, N., T. Hardt, et al. (2007). "MeCP2 interacts with HP1 and modulates its heterochromatin association during myogenic differentiation." Nucleic Acids Res **35**(16): 5402-5408.

Aggarwal, B. D. and B. R. Calvi (2004). "Chromatin regulates origin activity in Drosophila follicle cells." Nature **430**(6997): 372-376.

Aggarwal, S. (2010). "Targeted cancer therapies." Nat Rev Drug Discov **9**(6): 427-428.

Akhmanova, A., T. Verkerk, et al. (2000). "Characterisation of transcriptionally active and inactive chromatin domains in neurons." J Cell Sci **113 Pt 24**: 4463-4474.

Al-Dosari, M. S., R. Shaheen, et al. (2010). "Novel CENPJ mutation causes Seckel syndrome." Journal of medical genetics **47**(6): 411-414.

Alabert, C. and A. Groth (2012). "Chromatin replication and epigenome maintenance." Nat Rev Mol Cell Biol **13**(3): 153-167.

Albert, J. M., C. Cao, et al. (2007). "Inhibition of poly(ADP-ribose) polymerase enhances cell death and improves tumor growth delay in irradiated lung cancer models." Clin Cancer Res **13**(10): 3033-3042.

Alt, F. W., E. M. Oltz, et al. (1992). "VDJ recombination." Immunol Today **13**(8): 306-314.

Amente, S., A. Bertoni, et al. (2010). "LSD1-mediated demethylation of histone H3 lysine 4 triggers Myc-induced transcription." Oncogene **29**(25): 3691-3702.

Amir, R. E., I. B. Van den Veyver, et al. (1999). "Rett syndrome is caused by mutations in X-linked MECP2, encoding methyl-CpG-binding protein 2." Nat Genet **23**(2): 185-188.

Anglana, M., F. Apiou, et al. (2003). "Dynamics of DNA replication in mammalian somatic cells: nucleotide pool modulates origin choice and interorigin spacing." Cell **114**(3): 385-394.

Arias, E. E. and J. C. Walter (2006). "PCNA functions as a molecular platform to trigger Cdt1 destruction and prevent re-replication." Nat Cell Biol **8**(1): 84-90.

Arias, E. E. and J. C. Walter (2007). "Strength in numbers: preventing rereplication via multiple mechanisms in eukaryotic cells." Genes Dev **21**(5): 497-518.

Arnaudeau, C., C. Lundin, et al. (2001). "DNA double-strand breaks associated with replication forks are predominantly repaired by homologous recombination involving an exchange mechanism in mammalian cells." J Mol Biol **307**(5): 1235-1245.

Atanasiu, C., Z. Deng, et al. (2006). "ORC binding to TRF2 stimulates OriP replication." EMBO Rep **7**(7): 716-721.

Ausio, J., D. B. Levin, et al. (2003). "Syndromes of disordered chromatin remodeling." Clinical genetics **64**(2): 83-95.

Auth, T., E. Kunkel, et al. (2006). "Interaction between HP1alpha and replication proteins in mammalian cells." Exp Cell Res **312**(17): 3349-3359.

Bakkenist, C. J. and M. B. Kastan (2003). "DNA damage activates ATM through intermolecular autophosphorylation and dimer dissociation." Nature **421**(6922): 499-506.

Baldeyron, C., G. Soria, et al. (2011). "HP1alpha recruitment to DNA damage by p150CAF-1 promotes homologous recombination repair." J Cell Biol **193**(1): 81-95.

Bannister, A. J., P. Zegerman, et al. (2001). "Selective recognition of methylated lysine 9 on histone H3 by the HP1 chromo domain." Nature **410**(6824): 120-124.

Bartek, J., J. Bartkova, et al. (2007a). "DNA damage signalling guards against activated oncogenes and tumour progression." Oncogene **26**(56): 7773-7779.

Bartek, J. and J. Lukas (2001). "Mammalian G1- and S-phase checkpoints in response to DNA damage." Current opinion in cell biology **13**(6): 738-747.

Bartek, J., J. Lukas, et al. (2007b). "DNA damage response as an anti-cancer barrier: damage threshold and the concept of 'conditional haploinsufficiency'." Cell Cycle **6**(19): 2344-2347.

Bartek, J., M. Mistrik, et al. (2012). "Thresholds of replication stress signaling in cancer development and treatment." Nat Struct Mol Biol **19**(1): 5-7.

Bartkova, J., Z. Horejsi, et al. (2005). "DNA damage response as a candidate anti-cancer barrier in early human tumorigenesis." Nature **434**(7035): 864-870.

Bartkova, J., J. Lukas, et al. (1997). "Aberrations of the G1- and G1/S-regulating genes in human cancer." Prog Cell Cycle Res **3**: 211-220.

Bartkova, J., N. Rezaei, et al. (2006). "Oncogene-induced senescence is part of the tumorigenesis barrier imposed by DNA damage checkpoints." Nature **444**(7119): 633-637.

Bartova, E., A. H. Horakova, et al. (2010). "Structure and epigenetics of nucleoli in comparison with non-nucleolar compartments." J Histochem Cytochem **58**(5): 391-403.

Baxevanis, A. D. and D. Landsman (1996). "Histone Sequence Database: a compilation of highly-conserved nucleoprotein sequences." Nucleic Acids Res **24**(1): 245-247.

Belfort, M. and R. J. Roberts (1997). "Homing endonucleases: keeping the house in order." Nucleic Acids Res **25**(17): 3379-3388.

Bell, S. P., J. Mitchell, et al. (1995). "The multidomain structure of Orc1p reveals similarity to regulators of DNA replication and transcriptional silencing." Cell **83**(4): 563-568.

Bell, S. P. and B. Stillman (1992). "ATP-dependent recognition of eukaryotic origins of DNA replication by a multiprotein complex." Nature **357**(6374): 128-134.

Ben-Shem, A., N. Garreau de Loubresse, et al. (2011). "The structure of the eukaryotic ribosome at 3.0 A resolution." Science **334**(6062): 1524-1529.

Bennardo, N., A. Cheng, et al. (2008). "Alternative-NHEJ is a mechanistically distinct pathway of mammalian chromosome break repair." PLoS Genet **4**(6): e1000110.

Bentley, J., C. P. Diggle, et al. (2004). "DNA double strand break repair in human bladder cancer is error prone and involves microhomology-associated end-joining." Nucleic Acids Res **32**(17): 5249-5259.

Berkovich, E., R. J. Monnat, Jr., et al. (2007). "Roles of ATM and NBS1 in chromatin structure modulation and DNA double-strand break repair." Nat Cell Biol **9**(6): 683-690.

Berkovich, E., R. J. Monnat, Jr., et al. (2008). "Assessment of protein dynamics and DNA repair following generation of DNA double-strand breaks at defined genomic sites." Nat Protoc **3**(5): 915-922.

Bernal, J. A. and A. R. Venkitaraman (2011). "A vertebrate N-end rule degron reveals that Orc6 is required in mitosis for daughter cell abscission." J Cell Biol **192**(6): 969-978.

Bertoncini, C. R. and R. Meneghini (1995). "DNA strand breaks produced by oxidative stress in mammalian cells exhibit 3'-phosphoglycolate termini." Nucleic Acids Res **23**(15): 2995-3002.

Beucher, A., J. Birraux, et al. (2009). "ATM and Artemis promote homologous recombination of radiation-induced DNA double-strand breaks in G2." EMBO J **28**(21): 3413-3427.

Bhaumik, S. R., E. Smith, et al. (2007). "Covalent modifications of histones during development and disease pathogenesis." Nat Struct Mol Biol **14**(11): 1008-1016.

Bicknell, L. S., E. M. Bongers, et al. (2011a). "Mutations in the pre-replication complex cause Meier-Gorlin syndrome." Nat Genet **43**(4): 356-359.

Bicknell, L. S., S. Walker, et al. (2011b). "Mutations in ORC1, encoding the largest subunit of the origin recognition complex, cause microcephalic primordial dwarfism resembling Meier-Gorlin syndrome." Nat Genet **43**(4): 350-355.

Blow, J. J. and A. Dutta (2005). "Preventing re-replication of chromosomal DNA." Nat Rev Mol Cell Biol **6**(6): 476-486.

Blow, J. J. and X. Q. Ge (2009). "A model for DNA replication showing how dormant origins safeguard against replication fork failure." EMBO Rep **10**(4): 406-412.

Blow, J. J., X. Q. Ge, et al. (2011). "How dormant origins promote complete genome replication." Trends in biochemical sciences **36**(8): 405-414.

Botuyan, M. V., J. Lee, et al. (2006). "Structural basis for the methylation state-specific recognition of histone H4-K20 by 53BP1 and Crb2 in DNA repair." Cell **127**(7): 1361-1373.

Bowers, J. L., J. C. Randell, et al. (2004). "ATP hydrolysis by ORC catalyzes reiterative Mcm2-7 assembly at a defined origin of replication." Mol Cell **16**(6): 967-978.

Bradley, M. O. and K. W. Kohn (1979). "X-ray induced DNA double strand break production and repair in mammalian cells as measured by neutral filter elution." Nucleic Acids Res **7**(3): 793-804.

Brand, N., T. Faul, et al. (2007). "Interactions and subcellular distribution of DNA replication initiation proteins in eukaryotic cells." Mol Genet Genomics **278**(6): 623-632.

Branzei, D. and M. Foiani (2005). "The DNA damage response during DNA replication." Current opinion in cell biology **17**(6): 568-575.

Branzei, D. and M. Foiani (2010). "Maintaining genome stability at the replication fork." Nat Rev Mol Cell Biol **11**(3): 208-219.

Brun, M. E., E. Lana, et al. (2011). "Heterochromatic genes undergo epigenetic changes and escape silencing in immunodeficiency, centromeric instability, facial anomalies (ICF) syndrome." PLoS One **6**(4): e19464.

Brunton, H., A. A. Goodarzi, et al. (2011). "Analysis of human syndromes with disordered chromatin reveals the impact of heterochromatin on the efficacy of ATM-dependent G2/M checkpoint arrest." Mol Cell Biol **31**(19): 4022-4035.

Bryant, H. E., E. Petermann, et al. (2009). "PARP is activated at stalled forks to mediate Mre11-dependent replication restart and recombination." EMBO J **28**(17): 2601-2615.

Bryant, H. E., N. Schultz, et al. (2005). "Specific killing of BRCA2-deficient tumours with inhibitors of poly(ADP-ribose) polymerase." Nature **434**(7035): 913-917.

Burhans, W. C. and M. Weinberger (2007). "DNA replication stress, genome instability and aging." Nucleic Acids Res **35**(22): 7545-7556.

Burke, T. W., J. G. Cook, et al. (2001). "Replication factors MCM2 and ORC1 interact with the histone acetyltransferase HBO1." J Biol Chem **276**(18): 15397-15408.

Burma, S., B. P. Chen, et al. (2001). "ATM phosphorylates histone H2AX in response to DNA double-strand breaks." J Biol Chem **276**(45): 42462-42467.

Burrow, A. A., A. Marullo, et al. (2010). "Secondary structure formation and DNA instability at fragile site FRA16B." Nucleic Acids Res **38**(9): 2865-2877.

Busby, E. C., D. F. Leistritz, et al. (2000). "The radiosensitizing agent 7-hydroxystaurosporine (UCN-01) inhibits the DNA damage checkpoint kinase hChk1." Cancer Res **60**(8): 2108-2112.

Buscemi, G., P. Perego, et al. (2004). "Activation of ATM and Chk2 kinases in relation to the amount of DNA strand breaks." Oncogene **23**(46): 7691-7700.

Cadet, J., T. Douki, et al. (1997). "Artifacts associated with the measurement of oxidized DNA bases." Environ Health Perspect **105**(10): 1034-1039.

Caldecott, K. W. (2008). "Single-strand break repair and genetic disease." Nat Rev Genet **9**(8): 619-631.

Cayrou, C., P. Coulombe, et al. (2011). "Genome-scale analysis of metazoan replication origins reveals their organization in specific but flexible sites defined by conserved features." Genome Res **21**(9): 1438-1449.

Celeste, A., O. Fernandez-Capetillo, et al. (2003). "Histone H2AX phosphorylation is dispensable for the initial recognition of DNA breaks." Nat Cell Biol **5**(7): 675-679.

Chadwick, K. H. and H. P. Leenhouts (1994). "On the linearity of the dose-effect relationship of DNA double strand breaks." Int J Radiat Biol **66**(5): 549-552.

Chakraborty, A., Z. Shen, et al. (2011). ""ORCanization" on heterochromatin: linking DNA replication initiation to chromatin organization." Epigenetics **6**(6): 665-670.

Charles, M. (2001). "UNSCEAR report 2000: sources and effects of ionizing radiation. United Nations Scientific Comittee on the Effects of Atomic Radiation." J Radiol Prot **21**(1): 83-86.

Chen, C. C., R. D. Kennedy, et al. (2009). "CHK1 inhibition as a strategy for targeting Fanconi Anemia (FA) DNA repair pathway deficient tumors." Mol Cancer **8**: 24.

Chesnokov, I. N. (2007). "Multiple functions of the origin recognition complex." Int Rev Cytol **256**: 69-109.

Cheutin, T., A. J. McNairn, et al. (2003). "Maintenance of stable heterochromatin domains by dynamic HP1 binding." Science **299**(5607): 721-725.

Chien, C. T., S. Buck, et al. (1993). "Targeting of SIR1 protein establishes transcriptional silencing at HM loci and telomeres in yeast." Cell **75**(3): 531-541.

Choi, J. H., L. A. Lindsey-Boltz, et al. (2010). "Reconstitution of RPA-covered single-stranded DNA-activated ATR-Chk1 signaling." Proc Natl Acad Sci U S A **107**(31): 13660-13665.

Ciccia, A., A. L. Bredemeyer, et al. (2009). "The SIOD disorder protein SMARCAL1 is an RPA-interacting protein involved in replication fork restart." Genes Dev **23**(20): 2415-2425.

Ciccia, A. and S. J. Elledge (2010). "The DNA damage response: making it safe to play with knives." Mol Cell **40**(2): 179-204.

Colleaux, L., M. R. Michel-Wolwertz, et al. (1990). "The apocytochrome b gene of Chlamydomonas smithii contains a mobile intron related to both Saccharomyces and Neurospora introns." Molecular & general genetics : MGG **223**(2): 288-296.

Conconi, A., R. M. Widmer, et al. (1989). "Two different chromatin structures coexist in ribosomal RNA genes throughout the cell cycle." Cell **57**(5): 753-761.

Conklin, K. A. (2004). "Chemotherapy-associated oxidative stress: impact on chemotherapeutic effectiveness." Integr Cancer Ther **3**(4): 294-300.

Cook, J. G., D. A. Chasse, et al. (2004). "The regulated association of Cdt1 with minichromosome maintenance proteins and Cdc6 in mammalian cells." J Biol Chem **279**(10): 9625-9633.

Cooke, M. S., M. D. Evans, et al. (2003). "Oxidative DNA damage: mechanisms, mutation, and disease." FASEB J **17**(10): 1195-1214.

Costa, A., I. Ilves, et al. (2011). "The structural basis for MCM2-7 helicase activation by GINS and Cdc45." Nat Struct Mol Biol **18**(4): 471-477.

Coster, G. and M. Goldberg (2010). "The cellular response to DNA damage: a focus on MDC1 and its interacting proteins." Nucleus **1**(2): 166-178.

Cowell, I. G., N. J. Sunter, et al. (2007). "gammaH2AX foci form preferentially in euchromatin after ionising-radiation." PLoS One **2**(10): e1057.

Cowieson, N. P., J. F. Partridge, et al. (2000). "Dimerisation of a chromo shadow domain and distinctions from the chromodomain as revealed by structural analysis." Current biology : CB **10**(9): 517-525.

Craig, J. M. (2005). "Heterochromatin--many flavours, common themes." Bioessays **27**(1): 17-28.

d'Adda di Fagagna, F., P. M. Reaper, et al. (2003). "A DNA damage checkpoint response in telomere-initiated senescence." Nature **426**(6963): 194-198.

Dai, Y. and S. Grant (2010). "New insights into checkpoint kinase 1 in the DNA damage response signaling network." Clin Cancer Res **16**(2): 376-383.

Danis, E., K. Brodolin, et al. (2004). "Specification of a DNA replication origin by a transcription complex." Nat Cell Biol **6**(8): 721-730.

Darroudi, F., W. Wiegant, et al. (2007). "Role of Artemis in DSB repair and guarding chromosomal stability following exposure to ionizing radiation at different stages of cell cycle." Mutat Res **615**(1-2): 111-124.

Darzynkiewicz, Z., G. Juan, et al. (1997). "Cytometry in cell necrobiology: analysis of apoptosis and accidental cell death (necrosis)." Cytometry **27**(1): 1-20.

David, S. S., V. L. O'Shea, et al. (2007). "Base-excision repair of oxidative DNA damage." Nature **447**(7147): 941-950.

Davies, S. L., P. S. North, et al. (2007). "Role for BLM in replication-fork restart and suppression of origin firing after replicative stress." Nat Struct Mol Biol **14**(7): 677-679.

de Bono, J. S. and A. Ashworth (2010). "Translating cancer research into targeted therapeutics." Nature **467**(7315): 543-549.

de Munnik, S. A., L. S. Bicknell, et al. (2012). "Meier-Gorlin syndrome genotype-phenotype studies: 35 individuals with pre-replication complex gene mutations and 10 without molecular diagnosis." Eur J Hum Genet **20**(6): 598-606.

Dechat, T., K. Pfleghaar, et al. (2008). "Nuclear lamins: major factors in the structural organization and function of the nucleus and chromatin." Genes Dev **22**(7): 832-853.

Deckbar, D., J. Birraux, et al. (2007). "Chromosome breakage after G2 checkpoint release." J Cell Biol **176**(6): 749-755.

Deckbar, D., P. A. Jeggo, et al. (2011). "Understanding the limitations of radiation-induced cell cycle checkpoints." Crit Rev Biochem Mol Biol **46**(4): 271-283.

Deckbar, D., T. Stiff, et al. (2010). "The limitations of the G1-S checkpoint." Cancer Res **70**(11): 4412-4421.

Delcuve, G. P., M. Rastegar, et al. (2009). "Epigenetic control." J Cell Physiol **219**(2): 243-250.

Deng, Z., J. Norseen, et al. (2009). "TERRA RNA binding to TRF2 facilitates heterochromatin formation and ORC recruitment at telomeres." Mol Cell **35**(4): 403-413.

Denslow, S. A. and P. A. Wade (2007). "The human Mi-2/NuRD complex and gene regulation." Oncogene **26**(37): 5433-5438.

DePamphilis, M. L. (2005). "Cell cycle dependent regulation of the origin recognition complex." Cell Cycle **4**(1): 70-79.

DePamphilis, M. L., J. J. Blow, et al. (2006). "Regulating the licensing of DNA replication origins in metazoa." Curr Opin Cell Biol **18**(3): 231-239.

Dhar, S. K., L. Delmolino, et al. (2001a). "Architecture of the human origin recognition complex." J Biol Chem **276**(31): 29067-29071.

Dhar, S. K. and A. Dutta (2000). "Identification and characterization of the human ORC6 homolog." J Biol Chem **275**(45): 34983-34988.

Dhar, S. K., K. Yoshida, et al. (2001b). "Replication from oriP of Epstein-Barr virus requires human ORC and is inhibited by geminin." Cell **106**(3): 287-296.

Di Leonardo, A., S. P. Linke, et al. (1994). "DNA damage triggers a prolonged p53-dependent G1 arrest and long-term induction of Cip1 in normal human fibroblasts." Genes Dev **8**(21): 2540-2551.

Di Micco, R., M. Fumagalli, et al. (2006). "Oncogene-induced senescence is a DNA damage response triggered by DNA hyper-replication." Nature **444**(7119): 638-642.

Di Paola, D., E. Rampakakis, et al. (2010). "Increased origin activity in transformed versus normal cells: identification of novel protein players involved in DNA replication and cellular transformation." Nucleic Acids Res **38**(7): 2314-2331.

Di Paola, D. and M. Zannis-Hadjopoulos (2011). "Comparative analysis of pre-replication complex proteins in transformed and normal cells." Journal of cellular biochemistry.

Di Paola, D. and M. Zannis-Hadjopoulos (2012). "Comparative analysis of pre-replication complex proteins in transformed and normal cells." Journal of cellular biochemistry **113**(4): 1333-1347.

Dialynas, G. K., M. W. Vitalini, et al. (2008). "Linking Heterochromatin Protein 1 (HP1) to cancer progression." Mutat Res **647**(1-2): 13-20.

Dijkwel, P. A. and J. L. Hamlin (1995). "The Chinese hamster dihydrofolate reductase origin consists of multiple potential nascent-strand start sites." Mol Cell Biol **15**(6): 3023-3031.

Dillin, A. and J. Rine (1997). "Separable functions of ORC5 in replication initiation and silencing in Saccharomyces cerevisiae." Genetics **147**(3): 1053-1062.

Dimitri, P., R. Caizzi, et al. (2009). "Constitutive heterochromatin: a surprising variety of expressed sequences." Chromosoma **118**(4): 419-435.

Dominguez-Sola, D., C. Y. Ying, et al. (2007). "Non-transcriptional control of DNA replication by c-Myc." Nature **448**(7152): 445-451.

Donovan, S., J. Harwood, et al. (1997). "Cdc6p-dependent loading of Mcm proteins onto pre-replicative chromatin in budding yeast." Proc Natl Acad Sci U S A **94**(11): 5611-5616.

Douglas, P., G. P. Sapkota, et al. (2002). "Identification of in vitro and in vivo phosphorylation sites in the catalytic subunit of the DNA-dependent protein kinase." Biochem J **368**(Pt 1): 243-251.

Downs, J. A. and S. P. Jackson (2004). "A means to a DNA end: the many roles of Ku." Nat Rev Mol Cell Biol **5**(5): 367-378.

Dujon, B. (1989). "Group I introns as mobile genetic elements: facts and mechanistic speculations--a review." Gene **82**(1): 91-114.

Duncker, B. P., I. N. Chesnokov, et al. (2009). "The origin recognition complex protein family." Genome Biol **10**(3): 214.

Duursma, A. and R. Agami (2005). "p53-Dependent regulation of Cdc6 protein stability controls cellular proliferation." Mol Cell Biol **25**(16): 6937-6947.

Eggler, A. L., R. B. Inman, et al. (2002). "The Rad51-dependent pairing of long DNA substrates is stabilized by replication protein A." J Biol Chem **277**(42): 39280-39288.

Eheman, C., S. J. Henley, et al. (2012). "Annual Report to the Nation on the status of cancer, 1975-2008, featuring cancers associated with excess weight and lack of sufficient physical activity." Cancer **118**(9): 2338-2366.

Ehrenhofer-Murray, A. E., M. Gossen, et al. (1995). "Separation of origin recognition complex functions by cross-species complementation." Science **270**(5242): 1671-1674.

Eissenberg, J. C., T. C. James, et al. (1990). "Mutation in a heterochromatin-specific chromosomal protein is associated with suppression of position-effect variegation in Drosophila melanogaster." Proc Natl Acad Sci U S A **87**(24): 9923-9927.

Ekholm-Reed, S., J. Mendez, et al. (2004). "Deregulation of cyclin E in human cells interferes with prereplication complex assembly." J Cell Biol **165**(6): 789-800.

Evrin, C., P. Clarke, et al. (2009). "A double-hexameric MCM2-7 complex is loaded onto origin DNA during licensing of eukaryotic DNA replication." Proc Natl Acad Sci U S A **106**(48): 20240-20245.

Falck, J., J. Coates, et al. (2005). "Conserved modes of recruitment of ATM, ATR and DNA-PKcs to sites of DNA damage." Nature **434**(7033): 605-611.

Farber, S. and L. K. Diamond (1948). "Temporary remissions in acute leukemia in children produced by folic acid antagonist, 4-aminopteroyl-glutamic acid." N Engl J Med **238**(23): 787-793.

Farmer, H., N. McCabe, et al. (2005). "Targeting the DNA repair defect in BRCA mutant cells as a therapeutic strategy." Nature **434**(7035): 917-921.

Feijoo, C., C. Hall-Jackson, et al. (2001). "Activation of mammalian Chk1 during DNA replication arrest: a role for Chk1 in the intra-S phase checkpoint monitoring replication origin firing." J Cell Biol **154**(5): 913-923.

Feng, L., J. R. Barnhart, et al. (2008). "Cdc6 knockdown inhibits human neuroblastoma cell proliferation." Mol Cell Biochem **311**(1-2): 189-197.

Ferguson, D. O. and F. W. Alt (2001). "DNA double strand break repair and chromosomal translocation: lessons from animal models." Oncogene **20**(40): 5572-5579.

Ferlay, J., H. R. Shin, et al. (2010). "Estimates of worldwide burden of cancer in 2008: GLOBOCAN 2008." Int J Cancer **127**(12): 2893-2917.

Fernandez, P. C., S. R. Frank, et al. (2003). "Genomic targets of the human c-Myc protein." Genes Dev **17**(9): 1115-1129.

Fernet, M., F. Megnin-Chanet, et al. (2010). "Control of the G2/M checkpoints after exposure to low doses of ionising radiation: implications for hyper-radiosensitivity." DNA Repair (Amst) **9**(1): 48-57.

Finch, J. T. and A. Klug (1976). "Solenoidal model for superstructure in chromatin." Proc Natl Acad Sci U S A **73**(6): 1897-1901.

Fischle, W., B. S. Tseng, et al. (2005). "Regulation of HP1-chromatin binding by histone H3 methylation and phosphorylation." Nature **438**(7071): 1116-1122.

FitzGerald, J. E., M. Grenon, et al. (2009). "53BP1: function and mechanisms of focal recruitment." Biochem Soc Trans **37**(Pt 4): 897-904.

Flick, K. E., D. McHugh, et al. (1997). "Crystallization and preliminary X-ray studies of I-PpoI: a nuclear, intron-encoded homing endonuclease from Physarum polycephalum." Protein Sci **6**(12): 2677-2680.

Flynn, R. L. and L. Zou (2011). "ATR: a master conductor of cellular responses to DNA replication stress." Trends in biochemical sciences **36**(3): 133-140.

Ford, D., D. F. Easton, et al. (1998). "Genetic heterogeneity and penetrance analysis of the BRCA1 and BRCA2 genes in breast cancer families. The Breast Cancer Linkage Consortium." Am J Hum Genet **62**(3): 676-689.

Forment, J. V., A. Kaidi, et al. (2012). "Chromothripsis and cancer: causes and consequences of chromosome shattering." Nat Rev Cancer **12**(10): 663-670.

Foss, M., F. J. McNally, et al. (1993). "Origin recognition complex (ORC) in transcriptional silencing and DNA replication in S. cerevisiae." Science **262**(5141): 1838-1844.

Fox, C. A., A. E. Ehrenhofer-Murray, et al. (1997). "The origin recognition complex, SIR1, and the S phase requirement for silencing." Science **276**(5318): 1547-1551.

Fritz, A. J., S. Sinha, et al. (2012). "Alterations in replication timing of cancer related genes in malignant human breast cancer cells." Journal of cellular biochemistry.

Fujita, M., C. Yamada, et al. (1999). "Cell cycle regulation of human CDC6 protein. Intracellular localization, interaction with the human mcm complex, and CDC2 kinase-mediated hyperphosphorylation." J Biol Chem **274**(36): 25927-25932.

Gamble, M. J. and W. L. Kraus (2010). "Multiple facets of the unique histone variant macroH2A: from genomics to cell biology." Cell Cycle **9**(13): 2568-2574.

Gaudier, M., B. S. Schuwirth, et al. (2007). "Structural basis of DNA replication origin recognition by an ORC protein." Science **317**(5842): 1213-1216.

Gavin, E. J., B. Song, et al. (2008). "Reduction of Orc6 expression sensitizes human colon cancer cells to 5-fluorouracil and cisplatin." PLoS One **3**(12): e4054.

Ge, X. Q. and J. J. Blow (2009). "The licensing checkpoint opens up." Cell Cycle **8**(15): 2320-2322.

Ge, X. Q. and J. J. Blow (2010). "Chk1 inhibits replication factory activation but allows dormant origin firing in existing factories." J Cell Biol **191**(7): 1285-1297.

Ge, X. Q., D. A. Jackson, et al. (2007). "Dormant origins licensed by excess Mcm2-7 are required for human cells to survive replicative stress." Genes Dev **21**(24): 3331-3341.

Gedik, C. M. and A. Collins (2005). "Establishing the background level of base oxidation in human lymphocyte DNA: results of an interlaboratory validation study." FASEB J **19**(1): 82-84.

Ghosh, S., A. P. Vassilev, et al. (2011). "Assembly of the human origin recognition complex occurs through independent nuclear localization of its components." J Biol Chem **286**(27): 23831-23841.

Gilbert, D. M. (2010). "Evaluating genome-scale approaches to eukaryotic DNA replication." Nature reviews. Genetics **11**(10): 673-684.

Gomez, M. and N. Brockdorff (2004). "Heterochromatin on the inactive X chromosome delays replication timing without affecting origin usage." Proc Natl Acad Sci U S A **101**(18): 6923-6928.

Gonzalez, I. L. and J. E. Sylvester (1995). "Complete sequence of the 43-kb human ribosomal DNA repeat: analysis of the intergenic spacer." Genomics **27**(2): 320-328.

Goodarzi, A. A., P. Jeggo, et al. (2010). "The influence of heterochromatin on DNA double strand break repair: Getting the strong, silent type to relax." DNA Repair (Amst) **9**(12): 1273-1282.

Goodarzi, A. A., T. Kurka, et al. (2011). "KAP-1 phosphorylation regulates CHD3 nucleosome remodeling during the DNA double-strand break response." Nat Struct Mol Biol **18**(7): 831-839.

Goodarzi, A. A., A. T. Noon, et al. (2008). "ATM signaling facilitates repair of DNA double-strand breaks associated with heterochromatin." Mol Cell **31**(2): 167-177.

Goodarzi, A. A., A. T. Noon, et al. (2009). "The impact of heterochromatin on DSB repair." Biochem Soc Trans **37**(Pt 3): 569-576.

Goodarzi, A. A., Y. Yu, et al. (2006). "DNA-PK autophosphorylation facilitates Artemis endonuclease activity." EMBO J **25**(16): 3880-3889.

Gorlin, R. J. (1992). "Microtia, absent patellae, short stature, micrognathia syndrome." Journal of medical genetics **29**(7): 516-517.

Graves, P. R., L. Yu, et al. (2000). "The Chk1 protein kinase and the Cdc25C regulatory pathways are targets of the anticancer agent UCN-01." J Biol Chem **275**(8): 5600-5605.

Grewal, S. I. and S. Jia (2007). "Heterochromatin revisited." Nat Rev Genet **8**(1): 35-46.

Griffith, E., S. Walker, et al. (2008). "Mutations in pericentrin cause Seckel syndrome with defective ATR-dependent DNA damage signaling." Nat Genet **40**(2): 232-236.

Grossel, M. J., G. L. Baker, et al. (1999). "cdk6 can shorten G(1) phase dependent upon the N-terminal INK4 interaction domain." J Biol Chem **274**(42): 29960-29967.

Groth, A., W. Rocha, et al. (2007). "Chromatin challenges during DNA replication and repair." Cell **128**(4): 721-733.

Grummt, I. and A. G. Ladurner (2008). "A metabolic throttle regulates the epigenetic state of rDNA." Cell **133**(4): 577-580.

Gruss, C., J. Wu, et al. (1993). "Disruption of the nucleosomes at the replication fork." EMBO J **12**(12): 4533-4545.

Guenatri, M., D. Bailly, et al. (2004). "Mouse centric and pericentric satellite repeats form distinct functional heterochromatin." J Cell Biol **166**(4): 493-505.

Guernsey, D. L., M. Matsuoka, et al. (2011). "Mutations in origin recognition complex gene ORC4 cause Meier-Gorlin syndrome." Nat Genet **43**(4): 360-364.

Guerra, L., A. Albihn, et al. (2010). "Myc is required for activation of the ATM-dependent checkpoints in response to DNA damage." PLoS One **5**(1): e8924.

Halazonetis, T. D., V. G. Gorgoulis, et al. (2008). "An oncogene-induced DNA damage model for cancer development." Science **319**(5868): 1352-1355.

Hall, J. G., C. Flora, et al. (2004). "Majewski osteodysplastic primordial dwarfism type II (MOPD II): natural history and clinical findings." Am J Med Genet A **130A**(1): 55-72.

Hall, J. R., E. Kow, et al. (2007). "Cdc6 stability is regulated by the Huwe1 ubiquitin ligase after DNA damage." Molecular biology of the cell **18**(9): 3340-3350.

Hanahan, D. and R. A. Weinberg (2000). "The hallmarks of cancer." Cell **100**(1): 57-70.

Hanel, W. and U. M. Moll (2012). "Links between mutant p53 and genomic instability." Journal of cellular biochemistry **113**(2): 433-439.

Hanes, J. W., D. M. Thal, et al. (2006). "Incorporation and replication of 8-oxo-deoxyguanosine by the human mitochondrial DNA polymerase." J Biol Chem **281**(47): 36241-36248.

Hansen, R. S., C. Wijmenga, et al. (1999). "The DNMT3B DNA methyltransferase gene is mutated in the ICF immunodeficiency syndrome." Proc Natl Acad Sci U S A **96**(25): 14412-14417.

Harman, D. (1956). "Aging: a theory based on free radical and radiation chemistry." J Gerontol **11**(3): 298-300.

Hartlerode, A. J. and R. Scully (2009). "Mechanisms of double-strand break repair in somatic mammalian cells." Biochem J **423**(2): 157-168.

Hattori, H., F. Skoulidis, et al. (2011). "Context dependence of checkpoint kinase 1 as a therapeutic target for pancreatic cancers deficient in the BRCA2 tumor suppressor." Mol Cancer Ther **10**(4): 670-678.

Havens, C. G. and J. C. Walter (2009). "Docking of a specialized PIP Box onto chromatin-bound PCNA creates a degron for the ubiquitin ligase CRL4Cdt2." Mol Cell **35**(1): 93-104.

He, H., S. Liyanarachchi, et al. (2011). "Mutations in U4atac snRNA, a component of the minor spliceosome, in the developmental disorder MOPD I." Science **332**(6026): 238-240.

Heinen, C. D., C. Schmutte, et al. (2002). "DNA repair and tumorigenesis: lessons from hereditary cancer syndromes." Cancer Biol Ther **1**(5): 477-485.

Helleday, T., J. Lo, et al. (2007). "DNA double-strand break repair: from mechanistic understanding to cancer treatment." DNA Repair (Amst) **6**(7): 923-935.

Helleday, T., E. Petermann, et al. (2008). "DNA repair pathways as targets for cancer therapy." Nat Rev Cancer **8**(3): 193-204.

Hemerly, A. S., S. G. Prasanth, et al. (2009). "Orc1 controls centriole and centrosome copy number in human cells." Science **323**(5915): 789-793.

Henderson, A. S., D. Warburton, et al. (1972). "Location of ribosomal DNA in the human chromosome complement." Proc Natl Acad Sci U S A **69**(11): 3394-3398.

Henriques, S. T., J. Costa, et al. (2005a). "Re-evaluating the role of strongly charged sequences in amphipathic cell-penetrating peptides: a fluorescence study using Pep-1." FEBS Lett **579**(20): 4498-4502.

Henriques, S. T., J. Costa, et al. (2005b). "Translocation of beta-galactosidase mediated by the cell-penetrating peptide pep-1 into lipid vesicles and human HeLa cells is driven by membrane electrostatic potential." Biochemistry **44**(30): 10189-10198.

Herbig, U., J. W. Griffith, et al. (2000). "Mutation of cyclin/cdk phosphorylation sites in HsCdc6 disrupts a late step in initiation of DNA replication in human cells." Molecular biology of the cell **11**(12): 4117-4130.

Herman, J. G., A. Merlo, et al. (1995). "Inactivation of the CDKN2/p16/MTS1 gene is frequently associated with aberrant DNA methylation in all common human cancers." Cancer Res **55**(20): 4525-4530.

Herold, S., B. Herkert, et al. (2009a). "Facilitating replication under stress: an oncogenic function of MYC?" Nat Rev Cancer **9**(6): 441-444.

Herold, S., B. Herkert, et al. (2009b). "Facilitating replication under stress: an oncogenic function of MYC?" Nature reviews. Cancer **9**(6): 441-444.

Hickson, I., Y. Zhao, et al. (2004). "Identification and Characterization of a Novel and Specific Inhibitor of the Ataxia-Telangiectasia Mutated Kinase ATM." Cancer Res **66**(24): 9152-9159.

Ho, C. C., W. Y. Siu, et al. (2006). "Stalled replication induces p53 accumulation through distinct mechanisms from DNA damage checkpoint pathways." Cancer Res **66**(4): 2233-2241.

Hoeijmakers, J. H. (2009). "DNA damage, aging, and cancer." N Engl J Med **361**(15): 1475-1485.

Hossain, M. and B. Stillman (2012). "Meier-Gorlin syndrome mutations disrupt an Orc1 CDK inhibitory domain and cause centrosome reduplication." Genes Dev.

Hozak, P. and P. R. Cook (1994). "Replication factories." Trends Cell Biol **4**(2): 48-52.

Huberman, J. A. and A. D. Riggs (1966). "Autoradiography of chromosomal DNA fibers from Chinese hamster cells." Proc Natl Acad Sci U S A **55**(3): 599-606.

Huberman, J. A. and A. D. Riggs (1968). "On the mechanism of DNA replication in mammalian chromosomes." J Mol Biol **32**(2): 327-341.

Huen, M. S., R. Grant, et al. (2007). "RNF8 transduces the DNA-damage signal via histone ubiquitylation and checkpoint protein assembly." Cell **131**(5): 901-914.

Huijbregts, R. P., A. Svitin, et al. (2009). "Drosophila Orc6 facilitates GTPase activity and filament formation of the septin complex." Molecular biology of the cell **20**(1): 270-281.

Huyen, Y., O. Zgheib, et al. (2004). "Methylated lysine 79 of histone H3 targets 53BP1 to DNA double-strand breaks." Nature **432**(7015): 406-411.

Ibarra, A., E. Schwob, et al. (2008a). "Excess MCM proteins protect human cells from replicative stress by licensing backup origins of replication." Proc Natl Acad Sci U S A **105**(26): 8956-8961.

Ibarra, A., E. Schwob, et al. (2008b). "Excess MCM proteins protect human cells from replicative stress by licensing backup origins of replication." Proceedings of the National Academy of Sciences of the United States of America **105**(26): 8956-8961.

Iizuka, M. and B. Stillman (1999). "Histone acetyltransferase HBO1 interacts with the ORC1 subunit of the human initiator protein." J Biol Chem **274**(33): 23027-23034.

Jabbari, K. and G. Bernardi (2004). "Cytosine methylation and CpG, TpG (CpA) and TpA frequencies." Gene **333**: 143-149.

Jackson, S. P. and J. Bartek (2009). "The DNA-damage response in human biology and disease." Nature **461**(7267): 1071-1078.

Jackson, S. P. and P. A. Jeggo (1995). "DNA double-strand break repair and V(D)J recombination: involvement of DNA-PK." Trends in biochemical sciences **20**(10): 412-415.

Jakob, B., J. Splinter, et al. (2011). "DNA double-strand breaks in heterochromatin elicit fast repair protein recruitment, histone H2AX phosphorylation and relocation to euchromatin." Nucleic Acids Res **39**(15): 6489-6499.

Jiang, X. R., G. Jimenez, et al. (1999). "Telomerase expression in human somatic cells does not induce changes associated with a transformed phenotype." Nat Genet **21**(1): 111-114.

Jin, J., T. Shirogane, et al. (2003). "SCFbeta-TRCP links Chk1 signaling to degradation of the Cdc25A protein phosphatase." Genes Dev **17**(24): 3062-3074.

KC, S., J. M. Carcamo, et al. (2006). "Antioxidants prevent oxidative DNA damage and cellular transformation elicited by the over-expression of c-MYC." Mutat Res **593**(1-2): 64-79.

Kalay, E., G. Yigit, et al. (2011). "CEP152 is a genome maintenance protein disrupted in Seckel syndrome." Nat Genet **43**(1): 23-26.

Kamath, S. and M. Leffak (2001). "Multiple sites of replication initiation in the human beta-globin gene locus." Nucleic Acids Res **29**(3): 809-817.

Kaneko, T., S. Tahara, et al. (2001). "Accumulation of oxidative DNA damage, 8-oxo-2'-deoxyguanosine, and change of repair systems during in vitro cellular aging of cultured human skin fibroblasts." Mutat Res **487**(1-2): 19-30.

Karakaidos, P., S. Taraviras, et al. (2004). "Overexpression of the replication licensing regulators hCdt1 and hCdc6 characterizes a subset of non-small-cell lung carcinomas: synergistic effect with mutant p53 on tumor growth and chromosomal instability--evidence of E2F-1 transcriptional control over hCdt1." The American journal of pathology **165**(4): 1351-1365.

Karnani, N. and A. Dutta (2011). "The effect of the intra-S-phase checkpoint on origins of replication in human cells." Genes Dev **25**(6): 621-633.

Kastan, M. B. and J. Bartek (2004). "Cell-cycle checkpoints and cancer." Nature **432**(7015): 316-323.

Kawabata, T., S. W. Luebben, et al. (2011a). "Stalled fork rescue via dormant replication origins in unchallenged S phase promotes proper chromosome segregation and tumor suppression." Molecular cell **41**(5): 543-553.

Kawabata, T., S. W. Luebben, et al. (2011b). "Stalled fork rescue via dormant replication origins in unchallenged S phase promotes proper chromosome segregation and tumor suppression." Mol Cell **41**(5): 543-553.

Kawabata, T., S. Yamaguchi, et al. (2011c). "A reduction of licensed origins reveals strain-specific replication dynamics in mice." Mammalian genome : official journal of the International Mammalian Genome Society **22**(9-10): 506-517.

Kellum, R. and B. M. Alberts (1995). "Heterochromatin protein 1 is required for correct chromosome segregation in Drosophila embryos." J Cell Sci **108 (Pt 4)**: 1419-1431.

Keyse, S. M., M. A. McAleer, et al. (1985). "The response of normal and ataxia-telangiectasia human fibroblasts to the lethal effects of far, mid and near ultraviolet radiations." Int J Radiat Biol Relat Stud Phys Chem Med **48**(6): 975-985.

Khanna, K. K. and S. P. Jackson (2001). "DNA double-strand breaks: signaling, repair and the cancer connection." Nat Genet **27**(3): 247-254.

Kirschmann, D. A., R. A. Lininger, et al. (2000). "Down-regulation of HP1Hsalpha expression is associated with the metastatic phenotype in breast cancer." Cancer Res **60**(13): 3359-3363.

Kourmouli, N., Y. M. Sun, et al. (2005). "Epigenetic regulation of mammalian pericentric heterochromatin in vivo by HP1." Biochem Biophys Res Commun **337**(3): 901-907.

Krempler, A., D. Deckbar, et al. (2007). "An imperfect G2M checkpoint contributes to chromosome instability following irradiation of S and G2 phase cells." Cell Cycle **6**(14): 1682-1686.

Kumagai, A. and W. G. Dunphy (2003). "Repeated phosphopeptide motifs in Claspin mediate the regulated binding of Chk1." Nat Cell Biol **5**(2): 161-165.

Kumagai, A., S. M. Kim, et al. (2004). "Claspin and the activated form of ATR-ATRIP collaborate in the activation of Chk1." J Biol Chem **279**(48): 49599-49608.

Kumagai, A., J. Lee, et al. (2006). "TopBP1 activates the ATR-ATRIP complex." Cell **124**(5): 943-955.

Kumari, A., N. Schultz, et al. (2004). "p53 protects from replication-associated DNA double-strand breaks in mammalian cells." Oncogene **23**(13): 2324-2329.

Kunnev, D., M. E. Rusiniak, et al. (2010). "DNA damage response and tumorigenesis in Mcm2-deficient mice." Oncogene **29**(25): 3630-3638.

Kuo, A. J., J. Song, et al. (2012). "The BAH domain of ORC1 links H4K20me2 to DNA replication licensing and Meier-Gorlin syndrome." Nature **484**(7392): 115-119.

Kuschak, T. I., B. C. Kuschak, et al. (2002). "c-Myc initiates illegitimate replication of the ribonucleotide reductase R2 gene." Oncogene **21**(6): 909-920.

Kuzminov, A. (2001). "Single-strand interruptions in replicating chromosomes cause double-strand breaks." Proc Natl Acad Sci U S A **98**(15): 8241-8246.

Labib, K. (2010). "How do Cdc7 and cyclin-dependent kinases trigger the initiation of chromosome replication in eukaryotic cells?" Genes Dev **24**(12): 1208-1219.

Labib, K., J. A. Tercero, et al. (2000). "Uninterrupted MCM2-7 function required for DNA replication fork progression." Science **288**(5471): 1643-1647.

Lachner, M., D. O'Carroll, et al. (2001). "Methylation of histone H3 lysine 9 creates a binding site for HP1 proteins." Nature **410**(6824): 116-120.

Lambert de Rouvroit, C. and A. M. Goffinet (1998). "Cloning of human DAB1 and mapping to chromosome 1p31-p32." Genomics **53**(2): 246-247.

Landschulz, W. H., P. F. Johnson, et al. (1988). "The leucine zipper: a hypothetical structure common to a new class of DNA binding proteins." Science **240**(4860): 1759-1764.

Lau, E., G. G. Chiang, et al. (2009). "Divergent S phase checkpoint activation arising from prereplicative complex deficiency controls cell survival." Molecular biology of the cell **20**(17): 3953-3964.

Lau, E., T. Tsuji, et al. (2007a). "The role of pre-replicative complex (pre-RC) components in oncogenesis." FASEB journal : official publication of the Federation of American Societies for Experimental Biology **21**(14): 3786-3794.

Lau, E., T. Tsuji, et al. (2007b). "The role of pre-replicative complex (pre-RC) components in oncogenesis." FASEB J **21**(14): 3786-3794.

Lau, E., C. Zhu, et al. (2006). "The functional role of Cdc6 in S-G2/M in mammalian cells." EMBO Rep **7**(4): 425-430.

Leatherwood, J. and A. Vas (2003). "Connecting ORC and heterochromatin: why?" Cell Cycle **2**(6): 573-575.

Lee, J., A. Kumagai, et al. (2007). "The Rad9-Hus1-Rad1 checkpoint clamp regulates interaction of TopBP1 with ATR." J Biol Chem **282**(38): 28036-28044.

Lee, K. Y., S. W. Bang, et al. (2012). "Phosphorylation of ORC2 protein dissociates origin recognition complex from chromatin and replication origins." J Biol Chem **287**(15): 11891-11898.

Leahy, J.J., B.T. Golding, et al. (2004) "Identification of a highly potent and selective DNA-dependent protein kinase (DNA-PK) inhibitor (NU7441) by screening of chromenone libraries." Bioorg Med Chem Lett **14**(24): 6083-6087.

Lei, M., Y. Kawasaki, et al. (1996). "Physical interactions among Mcm proteins and effects of Mcm dosage on DNA replication in Saccharomyces cerevisiae." Mol Cell Biol **16**(9): 5081-5090.

Leone, G., J. DeGregori, et al. (1998). "E2F3 activity is regulated during the cell cycle and is required for the induction of S phase." Genes Dev **12**(14): 2120-2130.

Leonhardt, H., H. P. Rahn, et al. (2000). "Dynamics of DNA replication factories in living cells." J Cell Biol **149**(2): 271-280.

LeRoy, G., J. T. Weston, et al. (2009). "Heterochromatin protein 1 is extensively decorated with histone code-like post-translational modifications." Mol Cell Proteomics **8**(11): 2432-2442.

Letessier, A., G. A. Millot, et al. (2011). "Cell-type-specific replication initiation programs set fragility of the FRA3B fragile site." Nature **470**(7332): 120-123.

Li, A. and J. J. Blow (2005). "Cdt1 downregulation by proteolysis and geminin inhibition prevents DNA re-replication in Xenopus." EMBO J **24**(2): 395-404.

Li, C. J., A. Vassilev, et al. (2004). "Role for Cdk1 (Cdc2)/cyclin A in preventing the mammalian origin recognition complex's largest subunit (Orc1) from binding to chromatin during mitosis." Mol Cell Biol **24**(13): 5875-5886.

Li, L., D. Drayna, et al. (1998). "The gene for severe combined immunodeficiency disease in Athabascan-speaking Native Americans is located on chromosome 10p." Am J Hum Genet **62**(1): 136-144.

Little, R. D., T. H. Platt, et al. (1993). "Initiation and termination of DNA replication in human rRNA genes." Mol Cell Biol **13**(10): 6600-6613.

Littlewood, T. D., D. C. Hancock, et al. (1995). "A modified oestrogen receptor ligand-binding domain as an improved switch for the regulation of heterologous proteins." Nucleic Acids Res **23**(10): 1686-1690.

Liu, E., X. Li, et al. (2004). "Cyclin-dependent kinases phosphorylate human Cdt1 and induce its degradation." J Biol Chem **279**(17): 17283-17288.

Liu, J., C. L. Smith, et al. (2000). "Structure and function of Cdc6/Cdc18: implications for origin recognition and checkpoint control." Mol Cell **6**(3): 637-648.

Liu, Y. and S. C. West (2002). "Distinct functions of BRCA1 and BRCA2 in double-strand break repair." Breast Cancer Res **4**(1): 9-13.

Lobrich, M. and P. A. Jeggo (2007). "The impact of a negligent G2/M checkpoint on genomic instability and cancer induction." Nat Rev Cancer **7**(11): 861-869.

Lobrich, M., A. Shibata, et al. (2010). "gammaH2AX foci analysis for monitoring DNA double-strand break repair: strengths, limitations and optimization." Cell Cycle **9**(4): 662-669.

Lord, C. J. and A. Ashworth (2012). "The DNA damage response and cancer therapy." Nature **481**(7381): 287-294.

Loser, D. A., A. Shibata, et al. (2010). "Sensitization to radiation and alkylating agents by inhibitors of poly(ADP-ribose) polymerase is enhanced in cells deficient in DNA double-strand break repair." Mol Cancer Ther **9**(6): 1775-1787.

Loupart, M. L., S. A. Krause, et al. (2000). "Aberrant replication timing induces defective chromosome condensation in Drosophila ORC2 mutants." Current biology : CB **10**(24): 1547-1556.

Loyola, A., H. Tagami, et al. (2009). "The HP1alpha-CAF1-SetDB1-containing complex provides H3K9me1 for Suv39-mediated K9me3 in pericentric heterochromatin." EMBO Rep **10**(7): 769-775.

Lubelsky, Y., T. Sasaki, et al. (2011). "Pre-replication complex proteins assemble at regions of low nucleosome occupancy within the Chinese hamster dihydrofolate reductase initiation zone." Nucleic Acids Res **39**(8): 3141-3155.

Lucas, I., A. Palakodeti, et al. (2007). "High-throughput mapping of origins of replication in human cells." EMBO Rep **8**(8): 770-777.

Luciani, J. J., D. Depetris, et al. (2005). "Subcellular distribution of HP1 proteins is altered in ICF syndrome." Eur J Hum Genet **13**(1): 41-51.

Luger, K., A. W. Mader, et al. (1997). "Crystal structure of the nucleosome core particle at 2.8 A resolution." Nature **389**(6648): 251-260.

Luijsterburg, M. S., C. Dinant, et al. (2009). "Heterochromatin protein 1 is recruited to various types of DNA damage." J Cell Biol **185**(4): 577-586.

Lukas, J., C. Lukas, et al. (2004). "Mammalian cell cycle checkpoints: signalling pathways and their organization in space and time." DNA Repair (Amst) **3**(8-9): 997-1007.

Ma, J., K. K. Hwang, et al. (2001). "Expression and functional analysis of three isoforms of human heterochromatin-associated protein HP1 in Drosophila." Chromosoma **109**(8): 536-544.

Ma, Y., S. B. Jacobs, et al. (2005a). "DNA CpG hypomethylation induces heterochromatin reorganization involving the histone variant macroH2A." J Cell Sci **118**(Pt 8): 1607-1616.

Ma, Y., U. Pannicke, et al. (2005b). "The DNA-dependent protein kinase catalytic subunit phosphorylation sites in human Artemis." J Biol Chem **280**(40): 33839-33846.

Ma, Y., U. Pannicke, et al. (2002). "Hairpin opening and overhang processing by an Artemis/DNA-dependent protein kinase complex in nonhomologous end joining and V(D)J recombination." Cell **108**(6): 781-794.

Ma, Y., K. Schwarz, et al. (2005c). "The Artemis:DNA-PKcs endonuclease cleaves DNA loops, flaps, and gaps." DNA Repair (Amst) **4**(7): 845-851.

Machida, Y. J., J. K. Teer, et al. (2005). "Acute reduction of an origin recognition complex (ORC) subunit in human cells reveals a requirement of ORC for Cdk2 activation." J Biol Chem **280**(30): 27624-27630.

Maddams, J., D. Brewster, et al. (2009). "Cancer prevalence in the United Kingdom: estimates for 2008." Br J Cancer **101**(3): 541-547.

Maga, G. and U. Hubscher (2003). "Proliferating cell nuclear antigen (PCNA): a dancer with many partners." J Cell Sci **116**(Pt 15): 3051-3060.

Mahaney, B. L., K. Meek, et al. (2009). "Repair of ionizing radiation-induced DNA double-strand breaks by non-homologous end-joining." Biochem J **417**(3): 639-650.

Mailand, N., S. Bekker-Jensen, et al. (2007). "RNF8 ubiquitylates histones at DNA double-strand breaks and promotes assembly of repair proteins." Cell **131**(5): 887-900.

Mailand, N., J. Falck, et al. (2000). "Rapid destruction of human Cdc25A in response to DNA damage." Science **288**(5470): 1425-1429.

Maison, C., D. Bailly, et al. (2011). "SUMOylation promotes de novo targeting of HP1alpha to pericentric heterochromatin." Nat Genet **43**(3): 220-227.

Maison, C., K. Romeo, et al. (2012). "The SUMO protease SENP7 is a critical component to ensure HP1 enrichment at pericentric heterochromatin." Nat Struct Mol Biol **19**(4): 458-460.

Maiti, A. K. (2012). "Genetic determinants of oxidative stress-mediated sensitization of drug-resistant cancer cells." Int J Cancer **130**(1): 1-9.

Majewski, F. and T. Goecke (1982). "Studies of microcephalic primordial dwarfism I: approach to a delineation of the Seckel syndrome." Am J Med Genet **12**(1): 7-21.

Mannava, S., V. Grachtchouk, et al. (2008). "Direct role of nucleotide metabolism in C-MYC-dependent proliferation of melanoma cells." Cell Cycle **7**(15): 2392-2400.

Mansilla-Soto, J. and P. Cortes (2003). "VDJ recombination: Artemis and its in vivo role in hairpin opening." J Exp Med **197**(5): 543-547.

Mao, Z., M. Bozzella, et al. (2008). "Comparison of nonhomologous end joining and homologous recombination in human cells." DNA Repair (Amst) **7**(10): 1765-1771.

Marumoto, T., T. Hirota, et al. (2002). "Roles of aurora-A kinase in mitotic entry and G2 checkpoint in mammalian cells." Genes Cells **7**(11): 1173-1182.

Maya-Mendoza, A., E. Petermann, et al. (2007). "Chk1 regulates the density of active replication origins during the vertebrate S phase." EMBO J **26**(11): 2719-2731.

McCord, R. A., E. Michishita, et al. (2009). "SIRT6 stabilizes DNA-dependent protein kinase at chromatin for DNA double-strand break repair." Aging (Albany NY) **1**(1): 109-121.

McNairn, A. J. and D. M. Gilbert (2005). "Overexpression of ORC subunits and increased ORC-chromatin association in transformed mammalian cells." Journal of cellular biochemistry **96**(5): 879-887.

McVey, M. and S. E. Lee (2008). "MMEJ repair of double-strand breaks (director's cut): deleted sequences and alternative endings." Trends Genet **24**(11): 529-538.

Mechali, M. (2010). "Eukaryotic DNA replication origins: many choices for appropriate answers." Nat Rev Mol Cell Biol **11**(10): 728-738.

Melcher, M., M. Schmid, et al. (2000). "Structure-function analysis of SUV39H1 reveals a dominant role in heterochromatin organization, chromosome segregation, and mitotic progression." Mol Cell Biol **20**(10): 3728-3741.

Mendez, J. and B. Stillman (2003). "Perpetuating the double helix: molecular machines at eukaryotic DNA replication origins." Bioessays **25**(12): 1158-1167.

Mendez, J., X. H. Zou-Yang, et al. (2002). "Human origin recognition complex large subunit is degraded by ubiquitin-mediated proteolysis after initiation of DNA replication." Mol Cell **9**(3): 481-491.

Merrick, C. J., D. Jackson, et al. (2004). "Visualization of altered replication dynamics after DNA damage in human cells." J Biol Chem **279**(19): 20067-20075.

Miklos, G. L. and B. John (1979). "Heterochromatin and satellite DNA in man: properties and prospects." Am J Hum Genet **31**(3): 264-280.

Milletti, F. (2012). "Cell-penetrating peptides: classes, origin, and current landscape." Drug Discov Today **17**(15-16): 850-860.

Minc, E., Y. Allory, et al. (1999). "Localization and phosphorylation of HP1 proteins during the cell cycle in mammalian cells." Chromosoma **108**(4): 220-234.

Minc, E., J. C. Courvalin, et al. (2000). "HP1gamma associates with euchromatin and heterochromatin in mammalian nuclei and chromosomes." Cytogenetics and cell genetics **90**(3-4): 279-284.

Monnat, R. J., Jr., A. F. Hackmann, et al. (1999). "Generation of highly site-specific DNA double-strand breaks in human cells by the homing endonucleases I-PpoI and I-CreI." Biochem Biophys Res Commun **255**(1): 88-93.

Montano, R., I. Chung, et al. (2012). "Preclinical development of the novel Chk1 inhibitor SCH900776 in combination with DNA-damaging agents and antimetabolites." Mol Cancer Ther **11**(2): 427-438.

Montecucco, A., R. Rossi, et al. (1998). "DNA ligase I is recruited to sites of DNA replication by an interaction with proliferating cell nuclear antigen: identification of a common targeting mechanism for the assembly of replication factories." EMBO J **17**(13): 3786-3795.

Monteilhet, C., A. Perrin, et al. (1990). "Purification and characterization of the in vitro activity of I-Sce I, a novel and highly specific endonuclease encoded by a group I intron." Nucleic Acids Res **18**(6): 1407-1413.

Morris, M. C., J. Depollier, et al. (2001). "A peptide carrier for the delivery of biologically active proteins into mammalian cells." Nat Biotechnol **19**(12): 1173-1176.

Moshous, D., I. Callebaut, et al. (2001). "Artemis, a novel DNA double-strand break repair/V(D)J recombination protein, is mutated in human severe combined immune deficiency." Cell **105**(2): 177-186.

Murga, M., S. Campaner, et al. (2011). "Exploiting oncogene-induced replicative stress for the selective killing of Myc-driven tumors." Nat Struct Mol Biol **18**(12): 1331-1335.

Murga, M. and O. Fernandez-Capetillo (2007). "Genomic instability: on the birth and death of cancer." Clin Transl Oncol **9**(4): 216-220.

Muscarella, D. E., E. L. Ellison, et al. (1990). "Characterization of I-Ppo, an intron-encoded endonuclease that mediates homing of a group I intron in the ribosomal DNA of Physarum polycephalum." Mol Cell Biol **10**(7): 3386-3396.

Nagy, R., H. Wang, et al. (2012). "Microcephalic osteodysplastic primordial dwarfism type I with biallelic mutations in the RNU4ATAC gene." Clinical genetics **82**(2): 140-146.

Narita, M., S. Nunez, et al. (2003). "Rb-mediated heterochromatin formation and silencing of E2F target genes during cellular senescence." Cell **113**(6): 703-716.

Necsulea, A., C. Guillet, et al. (2009). "The relationship between DNA replication and human genome organization." Mol Biol Evol **26**(4): 729-741.

Negrini, S., V. G. Gorgoulis, et al. (2010). "Genomic instability--an evolving hallmark of cancer." Nat Rev Mol Cell Biol **11**(3): 220-228.

Nevis, K. R., M. Cordeiro-Stone, et al. (2009). "Origin licensing and p53 status regulate Cdk2 activity during G(1)." Cell Cycle **8**(12): 1952-1963.

Nguyen, V. Q., C. Co, et al. (2001). "Cyclin-dependent kinases prevent DNA re-replication through multiple mechanisms." Nature **411**(6841): 1068-1073.

Niemantsverdriet, M., M. J. van Goethem, et al. (2012). "High and low LET radiation differentially induce normal tissue damage signals." Int J Radiat Oncol Biol Phys **83**(4): 1291-1297.

Nigg, E. A. and T. Stearns (2011). "The centrosome cycle: Centriole biogenesis, duplication and inherent asymmetries." Nat Cell Biol **13**(10): 1154-1160.

Nikjoo, H., P. O'Neill, et al. (1997). "Computational modelling of low-energy electron-induced DNA damage by early physical and chemical events." Int J Radiat Biol **71**(5): 467-483.

Nishitani, H., Z. Lygerou, et al. (2004). "Proteolysis of DNA replication licensing factor Cdt1 in S-phase is performed independently of geminin through its N-terminal region." J Biol Chem **279**(29): 30807-30816.

Nishitani, H., Z. Lygerou, et al. (2000). "The Cdt1 protein is required to license DNA for replication in fission yeast." Nature **404**(6778): 625-628.

Nishitani, H., S. Taraviras, et al. (2001). "The human licensing factor for DNA replication Cdt1 accumulates in G1 and is destabilized after initiation of S-phase." J Biol Chem **276**(48): 44905-44911.

Noguchi, K., A. Vassilev, et al. (2006). "The BAH domain facilitates the ability of human Orc1 protein to activate replication origins in vivo." EMBO J **25**(22): 5372-5382.

Noon, A. T., A. Shibata, et al. (2010). "53BP1-dependent robust localized KAP-1 phosphorylation is essential for heterochromatic DNA double-strand break repair." Nat Cell Biol **12**(2): 177-184.

O'Carroll, D., H. Scherthan, et al. (2000). "Isolation and characterization of Suv39h2, a second histone H3 methyltransferase gene that displays testis-specific expression." Mol Cell Biol **20**(24): 9423-9433.

O'Driscoll, M. and P. A. Jeggo (2006). "The role of double-strand break repair - insights from human genetics." Nat Rev Genet **7**(1): 45-54.

O'Driscoll, M., V. L. Ruiz-Perez, et al. (2003). "A splicing mutation affecting expression of ataxia-telangiectasia and Rad3-related protein (ATR) results in Seckel syndrome." Nat Genet **33**(4): 497-501.

Ockey, C. H. and R. Saffhill (1976). "The comparative effects of short-term DNA Inhibition on replicon synthesis in mammalian cells." Exp Cell Res **103**(2): 361-373.

Ogawa, T., A. Shinohara, et al. (1993). "RecA-like recombination proteins in eukaryotes: functions and structures of RAD51 genes." Cold Spring Harb Symp Quant Biol **58**: 567-576.

Ogi, T., S. Walker, et al. (2012). "Identification of the First ATRIP-Deficient Patient and Novel Mutations in ATR Define a Clinical Spectrum for ATR-ATRIP Seckel Syndrome." PLoS Genet **8**(11): e1002945.

Ohno, M., T. Miura, et al. (2006). "A genome-wide distribution of 8-oxoguanine correlates with the preferred regions for recombination and single nucleotide polymorphism in the human genome." Genome Res **16**(5): 567-575.

Ohta, S., Y. Tatsumi, et al. (2003). "The ORC1 cycle in human cells: II. Dynamic changes in the human ORC complex during the cell cycle." J Biol Chem **278**(42): 41535-41540.

Ohtani, K., J. DeGregori, et al. (1996). "Expression of the HsOrc1 gene, a human ORC1 homolog, is regulated by cell proliferation via the E2F transcription factor." Mol Cell Biol **16**(12): 6977-6984.

Ohtani, K., A. Tsujimoto, et al. (1998). "Regulation of cell growth-dependent expression of mammalian CDC6 gene by the cell cycle transcription factor E2F." Oncogene **17**(14): 1777-1785.

Olivier, M., R. Eeles, et al. (2002). "The IARC TP53 database: new online mutation analysis and recommendations to users." Hum Mutat **19**(6): 607-614.

Origanti, S., S. R. Cai, et al. (2012). "Synthetic lethality of Chk1 inhibition combined with p53 and/or p21 loss during a DNA damage response in normal and tumor cells." Oncogene.

Ozeri-Galai, E., R. Lebofsky, et al. (2011). "Failure of origin activation in response to fork stalling leads to chromosomal instability at fragile sites." Mol Cell **43**(1): 122-131.

Pacek, M. and J. C. Walter (2004). "A requirement for MCM7 and Cdc45 in chromosome unwinding during eukaryotic DNA replication." EMBO J **23**(18): 3667-3676.

Pak, D. T., M. Pflumm, et al. (1997). "Association of the origin recognition complex with heterochromatin and HP1 in higher eukaryotes." Cell **91**(3): 311-323.

Palma, J. P., L. E. Rodriguez, et al. (2008). "The PARP inhibitor, ABT-888 potentiates temozolomide: correlation with drug levels and reduction in PARP activity in vivo." Anticancer Res **28**(5A): 2625-2635.

Palmer, D. K., K. O'Day, et al. (1987). "A 17-kD centromere protein (CENP-A) copurifies with nucleosome core particles and with histones." J Cell Biol **104**(4): 805-815.

Paro, R. and D. S. Hogness (1991). "The Polycomb protein shares a homologous domain with a heterochromatin-associated protein of Drosophila." Proc Natl Acad Sci U S A **88**(1): 263-267.

Pedraza-Farina, L. G. (2006). "Mechanisms of oncogenic cooperation in cancer initiation and metastasis." Yale J Biol Med **79**(3-4): 95-103.

Pedroni, M., E. Sala, et al. (2001). "Microsatellite instability and mismatch-repair protein expression in hereditary and sporadic colorectal carcinogenesis." Cancer Res **61**(3): 896-899.

Peltomaki, P. and H. F. Vasen (1997). "Mutations predisposing to hereditary nonpolyposis colorectal cancer: database and results of a collaborative study. The International Collaborative Group on Hereditary Nonpolyposis Colorectal Cancer." Gastroenterology **113**(4): 1146-1158.

Petermann, E. and T. Helleday (2007). "DNA replication-associated lesions: importance in early tumorigenesis and cancer therapy." Biochem Soc Trans **35**(Pt 5): 1352-1354.

Petermann, E. and T. Helleday (2010a). "Pathways of mammalian replication fork restart." Nat Rev Mol Cell Biol **11**(10): 683-687.

Petermann, E., A. Maya-Mendoza, et al. (2006). "Chk1 requirement for high global rates of replication fork progression during normal vertebrate S phase." Mol Cell Biol **26**(8): 3319-3326.

Petermann, E., M. L. Orta, et al. (2010b). "Hydroxyurea-stalled replication forks become progressively inactivated and require two different RAD51-mediated pathways for restart and repair." Mol Cell **37**(4): 492-502.

Petermann, E., M. L. Orta, et al. (2010c). "Hydroxyurea-stalled replication forks become progressively inactivated and require two different RAD51-mediated pathways for restart and repair." Molecular Cell **37**(4): 492-502.

Petersen, B. O., J. Lukas, et al. (1999). "Phosphorylation of mammalian CDC6 by cyclin A/CDK2 regulates its subcellular localization." EMBO J **18**(2): 396-410.

Petersen, B. O., C. Wagener, et al. (2000). "Cell cycle- and cell growth-regulated proteolysis of mammalian CDC6 is dependent on APC-CDH1." Genes Dev **14**(18): 2330-2343.

Pierce, A. J. and M. Jasin (2005). "Measuring recombination proficiency in mouse embryonic stem cells." Methods Mol Biol **291**: 373-384.

Pierce, A. J., R. D. Johnson, et al. (1999). "XRCC3 promotes homology-directed repair of DNA damage in mammalian cells." Genes Dev **13**(20): 2633-2638.

Placek, B. J., L. N. Harrison, et al. (2005). "The H2A.Z/H2B dimer is unstable compared to the dimer containing the major H2A isoform." Protein Sci **14**(2): 514-522.

Poli, J., O. Tsaponina, et al. (2012). "dNTP pools determine fork progression and origin usage under replication stress." EMBO J **31**(4): 883-894.

Pommier, Y., C. Redon, et al. (2003). "Repair of and checkpoint response to topoisomerase I-mediated DNA damage." Mutat Res **532**(1-2): 173-203.

Prasanth, S. G., K. V. Prasanth, et al. (2004). "Human Orc2 localizes to centrosomes, centromeres and heterochromatin during chromosome inheritance." EMBO J **23**(13): 2651-2663.

Prasanth, S. G., K. V. Prasanth, et al. (2002). "Orc6 involved in DNA replication, chromosome segregation, and cytokinesis." Science **297**(5583): 1026-1031.

Prasanth, S. G., Z. Shen, et al. (2010). "Human origin recognition complex is essential for HP1 binding to chromatin and heterochromatin organization." Proc Natl Acad Sci U S A **107**(34): 15093-15098.

Preuss, S. and C. S. Pikaard (2007). "rRNA gene silencing and nucleolar dominance: insights into a chromosome-scale epigenetic on/off switch." Biochim Biophys Acta **1769**(5-6): 383-392.

Pruitt, S. C., K. J. Bailey, et al. (2007). "Reduced Mcm2 expression results in severe stem/progenitor cell deficiency and cancer." Stem Cells **25**(12): 3121-3132.

Quivy, J. P., D. Roche, et al. (2004). "A CAF-1 dependent pool of HP1 during heterochromatin duplication." EMBO J **23**(17): 3516-3526.

Qvist, P., P. Huertas, et al. (2011). "CtIP Mutations Cause Seckel and Jawad Syndromes." PLoS Genet **7**(10): e1002310.

Rabl, J., M. Leibundgut, et al. (2011). "Crystal structure of the eukaryotic 40S ribosomal subunit in complex with initiation factor 1." Science **331**(6018): 730-736.

Radichev, I., S. W. Kwon, et al. (2006). "Genetic analysis of human Orc2 reveals specific domains that are required in vivo for assembly and nuclear localization of the origin recognition complex." J Biol Chem **281**(32): 23264-23273.

Randell, J. C., J. L. Bowers, et al. (2006). "Sequential ATP hydrolysis by Cdc6 and ORC directs loading of the Mcm2-7 helicase." Mol Cell **21**(1): 29-39.

Rauch, A., C. T. Thiel, et al. (2008). "Mutations in the pericentrin (PCNT) gene cause primordial dwarfism." Science **319**(5864): 816-819.

Rea, S., F. Eisenhaber, et al. (2000). "Regulation of chromatin structure by site-specific histone H3 methyltransferases." Nature **406**(6796): 593-599.

Rehman, M. A. and K. Yankulov (2009). "The dual role of autonomously replicating sequences as origins of replication and as silencers." Curr Genet **55**(4): 357-363.

Riballo, E., M. Kuhne, et al. (2004). "A pathway of double-strand break rejoining dependent upon ATM, Artemis, and proteins locating to gamma-H2AX foci." Mol Cell **16**(5): 715-724.

Robinson, K., N. Asawachaicharn, et al. (2009). "c-Myc accelerates S-phase and requires WRN to avoid replication stress." PLoS One **4**(6): e5951.

Rogakou, E. P., D. R. Pilch, et al. (1998). "DNA double-stranded breaks induce histone H2AX phosphorylation on serine 139." J Biol Chem **273**(10): 5858-5868.

Rontgen, W. C. (1896). "On a New Kind of Rays." Science **3**(59): 227-231.

Roth, D. B. and J. H. Wilson (1986). "Nonhomologous recombination in mammalian cells: role for short sequence homologies in the joining reaction." Mol Cell Biol **6**(12): 4295-4304.

Roukos, V., A. Kinkhabwala, et al. (2011). "Dynamic recruitment of licensing factor Cdt1 to sites of DNA damage." J Cell Sci **124**(Pt 3): 422-434.

Rusche, L. N., A. L. Kirchmaier, et al. (2003). "The establishment, inheritance, and function of silenced chromatin in Saccharomyces cerevisiae." Annu Rev Biochem **72**: 481-516.

Saintigny, Y., F. Delacote, et al. (2001). "Characterization of homologous recombination induced by replication inhibition in mammalian cells." EMBO J **20**(14): 3861-3870.

Santocanale, C., K. Sharma, et al. (1999). "Activation of dormant origins of DNA replication in budding yeast." Genes Dev **13**(18): 2360-2364.

Santoro, R. (2005). "The silence of the ribosomal RNA genes." Cell Mol Life Sci **62**(18): 2067-2079.

Scanlon, K. J., M. Kashani-Sabet, et al. (1989). "Overexpression of DNA replication and repair enzymes in cisplatin-resistant human colon carcinoma HCT8 cells and circumvention by azidothymidine." Cancer Commun **1**(4): 269-275.

Schaarschmidt, D., J. Baltin, et al. (2004). "An episomal mammalian replicon: sequence-independent binding of the origin recognition complex." EMBO J **23**(1): 191-201.

Schoeftner, S. and M. A. Blasco (2009). "A 'higher order' of telomere regulation: telomere heterochromatin and telomeric RNAs." EMBO J **28**(16): 2323-2336.

Schotta, G., M. Lachner, et al. (2004). "A silencing pathway to induce H3-K9 and H4-K20 trimethylation at constitutive heterochromatin." Genes Dev **18**(11): 1251-1262.

Schultz, D. C., K. Ayyanathan, et al. (2002). "SETDB1: a novel KAP-1-associated histone H3, lysine 9-specific methyltransferase that contributes to HP1-mediated silencing of euchromatic genes by KRAB zinc-finger proteins." Genes Dev **16**(8): 919-932.

Schwacha, A. and S. P. Bell (2001). "Interactions between two catalytically distinct MCM subgroups are essential for coordinated ATP hydrolysis and DNA replication." Mol Cell **8**(5): 1093-1104.

Schwaiger, M., H. Kohler, et al. (2010). "Heterochromatin protein 1 (HP1) modulates replication timing of the Drosophila genome." Genome Res **20**(6): 771-780.

Sebastian, B., A. Kakizuka, et al. (1993). "Cdc25M2 activation of cyclin-dependent kinases by dephosphorylation of threonine-14 and tyrosine-15." Proc Natl Acad Sci U S A **90**(8): 3521-3524.

Segurado, M. and J. A. Tercero (2009). "The S-phase checkpoint: targeting the replication fork." Biol Cell **101**(11): 617-627.

Semenenko, V. A. and R. D. Stewart (2004). "A fast Monte Carlo algorithm to simulate the spectrum of DNA damages formed by ionizing radiation." Radiat Res **161**(4): 451-457.

Senga, T., U. Sivaprasad, et al. (2006). "PCNA is a cofactor for Cdt1 degradation by CUL4/DDB1-mediated N-terminal ubiquitination." J Biol Chem **281**(10): 6246-6252.

Sengupta, S., S. P. Linke, et al. (2003). "BLM helicase-dependent transport of p53 to sites of stalled DNA replication forks modulates homologous recombination." EMBO J **22**(5): 1210-1222.

Sequeira-Mendes, J., R. Diaz-Uriarte, et al. (2009). "Transcription initiation activity sets replication origin efficiency in mammalian cells." PLoS Genet **5**(4): e1000446.

Shareef, M. M., R. Badugu, et al. (2003). "HP1/ORC complex and heterochromatin assembly." Genetica **117**(2-3): 127-134.

Sheen, J. H. and R. B. Dickson (2002). "Overexpression of c-Myc alters G(1)/S arrest following ionizing radiation." Mol Cell Biol **22**(6): 1819-1833.

Shen, Z., A. Chakraborty, et al. (2012). "Dynamic Association of ORCA with Prereplicative Complex Components Regulates DNA Replication Initiation." Mol Cell Biol **32**(15): 3107-3120.

Shen, Z., K. M. Sathyan, et al. (2010). "A WD-repeat protein stabilizes ORC binding to chromatin." Mol Cell **40**(1): 99-111.

Shibata, A., O. Barton, et al. (2010). "Role of ATM and the damage response mediator proteins 53BP1 and MDC1 in the maintenance of G(2)/M checkpoint arrest." Mol Cell Biol **30**(13): 3371-3383.

Shiloh, Y. (2003). "ATM and related protein kinases: safeguarding genome integrity." Nat Rev Cancer **3**(3): 155-168.

Shima, N., A. Alcaraz, et al. (2007). "A viable allele of Mcm4 causes chromosome instability and mammary adenocarcinomas in mice." Nat Genet **39**(1): 93-98.

Shreeram, S., A. Sparks, et al. (2002). "Cell type-specific responses of human cells to inhibition of replication licensing." Oncogene **21**(43): 6624-6632.

Shumaker, D. K., T. Dechat, et al. (2006). "Mutant nuclear lamin A leads to progressive alterations of epigenetic control in premature aging." Proc Natl Acad Sci U S A **103**(23): 8703-8708.

Siddiqui, K. and B. Stillman (2007). "ATP-dependent assembly of the human origin recognition complex." J Biol Chem **282**(44): 32370-32383.

Sidorova, J. M., N. Li, et al. (2008). "The RecQ helicase WRN is required for normal replication fork progression after DNA damage or replication fork arrest." Cell Cycle **7**(6): 796-807.

Sims, R. J., 3rd, K. Nishioka, et al. (2003). "Histone lysine methylation: a signature for chromatin function." Trends Genet **19**(11): 629-639.

Singer, B. and T. P. Brent (1981). "Human lymphoblasts contain DNA glycosylase activity excising N-3 and N-7 methyl and ethyl purines but not O6-alkylguanines or 1-alkyladenines." Proc Natl Acad Sci U S A **78**(2): 856-860.

Singleton, M. K., M. L. Gonzales, et al. (2011). "MeCP2 is required for global heterochromatic and nucleolar changes during activity-dependent neuronal maturation." Neurobiol Dis **43**(1): 190-200.

Sklar, R., D. Altman, et al. (1986). "An endonuclease from Chlamydomonas reinhardtii that cleaves the sequence TATA." J Biol Chem **261**(15): 6806-6810.

Sorensen, C. S., L. T. Hansen, et al. (2005). "The cell-cycle checkpoint kinase Chk1 is required for mammalian homologous recombination repair." Nat Cell Biol **7**(2): 195-201.

Soulas-Sprauel, P., P. Rivera-Munoz, et al. (2007). "V(D)J and immunoglobulin class switch recombinations: a paradigm to study the regulation of DNA end-joining." Oncogene **26**(56): 7780-7791.

Souza, P. P., P. Volkel, et al. (2009). "The histone methyltransferase SUV420H2 and Heterochromatin Proteins HP1 interact but show different dynamic behaviours." BMC Cell Biol **10**: 41.

Speck, C. and B. Stillman (2007). "Cdc6 ATPase activity regulates ORC x Cdc6 stability and the selection of specific DNA sequences as origins of DNA replication." J Biol Chem **282**(16): 11705-11714.

Spencer, C. A. and M. Groudine (1991). "Control of c-myc regulation in normal and neoplastic cells." Adv Cancer Res **56**: 1-48.

Sripathy, S. P., J. Stevens, et al. (2006). "The KAP1 corepressor functions to coordinate the assembly of de novo HP1-demarcated microenvironments of heterochromatin required for KRAB zinc finger protein-mediated transcriptional repression." Mol Cell Biol **26**(22): 8623-8638.

Stewart, G. S., S. Panier, et al. (2009). "The RIDDLE syndrome protein mediates a ubiquitin-dependent signaling cascade at sites of DNA damage." Cell **136**(3): 420-434.

Stewart, G. S., B. Wang, et al. (2003). "MDC1 is a mediator of the mammalian DNA damage checkpoint." Nature **421**(6926): 961-966.

Stewart, M. D., J. Li, et al. (2005). "Relationship between histone H3 lysine 9 methylation, transcription repression, and heterochromatin protein 1 recruitment." Mol Cell Biol **25**(7): 2525-2538.

Stiff, T., K. Cerosaletti, et al. (2008). "Replication independent ATR signalling leads to G2/M arrest requiring Nbs1, 53BP1 and MDC1." Hum Mol Genet **17**(20): 3247-3253.

Stiff, T., M. O'Driscoll, et al. (2004). "ATM and DNA-PK function redundantly to phosphorylate H2AX after exposure to ionizing radiation." Cancer Res **64**(7): 2390-2396.

Stinchcomb, D. T., K. Struhl, et al. (1979). "Isolation and characterisation of a yeast chromosomal replicator." Nature **282**(5734): 39-43.

Stracker, T. H. and J. H. Petrini (2011). "The MRE11 complex: starting from the ends." Nat Rev Mol Cell Biol **12**(2): 90-103.

Stracker, T. H., T. Usui, et al. (2009). "Taking the time to make important decisions: the checkpoint effector kinases Chk1 and Chk2 and the DNA damage response." DNA Repair (Amst) **8**(9): 1047-1054.

Stratton, M. R. and N. Rahman (2008). "The emerging landscape of breast cancer susceptibility." Nat Genet **40**(1): 17-22.

Stucki, M., J. A. Clapperton, et al. (2005). "MDC1 directly binds phosphorylated histone H2AX to regulate cellular responses to DNA double-strand breaks." Cell **123**(7): 1213-1226.

Stuermer, A., K. Hoehn, et al. (2007). "Mouse pre-replicative complex proteins colocalise and interact with the centrosome." European journal of cell biology **86**(1): 37-50.

Stults, D. M., M. W. Killen, et al. (2008). "Genomic architecture and inheritance of human ribosomal RNA gene clusters." Genome Res **18**(1): 13-18.

Subramanian, D. and J. D. Griffith (2005). "p53 Monitors replication fork regression by binding to "chickenfoot" intermediates." J Biol Chem **280**(52): 42568-42572.

Sugimoto, N., Y. Tatsumi, et al. (2004). "Cdt1 phosphorylation by cyclin A-dependent kinases negatively regulates its function without affecting geminin binding." J Biol Chem **279**(19): 19691-19697.

Sullivan, G. J., J. M. Bridger, et al. (2001). "Human acrocentric chromosomes with transcriptionally silent nucleolar organizer regions associate with nucleoli." EMBO J **20**(11): 2867-2874.

Suto, R. K., M. J. Clarkson, et al. (2000). "Crystal structure of a nucleosome core particle containing the variant histone H2A.Z." Nat Struct Biol **7**(12): 1121-1124.

Szatrowski, T. P. and C. F. Nathan (1991). "Production of large amounts of hydrogen peroxide by human tumor cells." Cancer Res **51**(3): 794-798.

Szeto, H. H., P. W. Schiller, et al. (2005). "Fluorescent dyes alter intracellular targeting and function of cell-penetrating tetrapeptides." FASEB J **19**(1): 118-120.

Szostak, J. W., T. L. Orr-Weaver, et al. (1983). "The double-strand-break repair model for recombination." Cell **33**(1): 25-35.

Taddei, A., C. Maison, et al. (2001). "Reversible disruption of pericentric heterochromatin and centromere function by inhibiting deacetylases." Nat Cell Biol **3**(2): 114-120.

Takeda, D. Y. and A. Dutta (2005). "DNA replication and progression through S phase." Oncogene **24**(17): 2827-2843.

Tatsumi, Y., S. Ohta, et al. (2003). "The ORC1 cycle in human cells: I. cell cycle-regulated oscillation of human ORC1." J Biol Chem **278**(42): 41528-41534.

Taylor, D. J., B. Devkota, et al. (2009). "Comprehensive molecular structure of the eukaryotic ribosome." Structure **17**(12): 1591-1604.

Taylor, J. H. (1977). "Increase in DNA replication sites in cells held at the beginning of S phase." Chromosoma **62**(4): 291-300.

Thiel, G., M. Lietz, et al. (2004). "How mammalian transcriptional repressors work." Eur J Biochem **271**(14): 2855-2862.

Thomae, A. W., J. Baltin, et al. (2011). "Different roles of the human Orc6 protein in the replication initiation process." Cell Mol Life Sci **68**(22): 3741-3756.

Thomae, A. W., D. Pich, et al. (2008). "Interaction between HMGA1a and the origin recognition complex creates site-specific replication origins." Proc Natl Acad Sci U S A **105**(5): 1692-1697.

Thome, K. C., S. K. Dhar, et al. (2000). "Subsets of human origin recognition complex (ORC) subunits are expressed in non-proliferating cells and associate with non-ORC proteins." J Biol Chem **275**(45): 35233-35241.

Triolo, T. and R. Sternglanz (1996). "Role of interactions between the origin recognition complex and SIR1 in transcriptional silencing." Nature **381**(6579): 251-253.

Vafa, O., M. Wade, et al. (2002). "c-Myc can induce DNA damage, increase reactive oxygen species, and mitigate p53 function: a mechanism for oncogene-induced genetic instability." Mol Cell **9**(5): 1031-1044.

Van Der Schans, G. P. (1978). "Gamma-ray induced double-strand breaks in DNA resulting from randomly-inflicted single-strand breaks: temporal local denaturation, a new radiation phenomenon?" Int J Radiat Biol Relat Stud Phys Chem Med **33**(2): 105-120.

van Vugt, M. A., V. A. Smits, et al. (2001). "Inhibition of Polo-like kinase-1 by DNA damage occurs in an ATM- or ATR-dependent fashion." J Biol Chem **276**(45): 41656-41660.

Varley, J. M. (2003). "Germline TP53 mutations and Li-Fraumeni syndrome." Hum Mutat **21**(3): 313-320.

Vas, A., W. Mok, et al. (2001). "Control of DNA rereplication via Cdc2 phosphorylation sites in the origin recognition complex." Mol Cell Biol **21**(17): 5767-5777.

Vashee, S., P. Simancek, et al. (2001). "Assembly of the human origin recognition complex." J Biol Chem **276**(28): 26666-26673.

Venkitaraman, A. R. (2009). "Linking the cellular functions of BRCA genes to cancer pathogenesis and treatment." Annu Rev Pathol **4**: 461-487.

Verschure, P. J., I. van der Kraan, et al. (2005). "In vivo HP1 targeting causes large-scale chromatin condensation and enhanced histone lysine methylation." Mol Cell Biol **25**(11): 4552-4564.

Vogelstein, B., D. Lane, et al. (2000). "Surfing the p53 network." Nature **408**(6810): 307-310.

Wahl, G. M., S. P. Linke, et al. (1997). "Maintaining genetic stability through TP53 mediated checkpoint control." Cancer Surv **29**: 183-219.

Wan, P. T., M. J. Garnett, et al. (2004). "Mechanism of activation of the RAF-ERK signaling pathway by oncogenic mutations of B-RAF." Cell **116**(6): 855-867.

Wang, M., W. Wu, et al. (2006a). "PARP-1 and Ku compete for repair of DNA double strand breaks by distinct NHEJ pathways." Nucleic Acids Res **34**(21): 6170-6182.

Wang, X., L. Zou, et al. (2006b). "Rad17 phosphorylation is required for claspin recruitment and Chk1 activation in response to replication stress." Mol Cell **23**(3): 331-341.

Ward, I. M. and J. Chen (2001). "Histone H2AX is phosphorylated in an ATR-dependent manner in response to replicational stress." J Biol Chem **276**(51): 47759-47762.

Ward, J. F. (1981). "Some biochemical consequences of the spatial distribution of ionizing radiation-produced free radicals." Radiat Res **86**(2): 185-195.

Ward, J. F. (1988). "DNA damage produced by ionizing radiation in mammalian cells: identities, mechanisms of formation, and reparability." Prog Nucleic Acid Res Mol Biol **35**: 95-125.

Watson, J. D., S. K. Oster, et al. (2002). "Identifying genes regulated in a Myc-dependent manner." J Biol Chem **277**(40): 36921-36930.

Weinreich, M. and B. Stillman (1999). "Cdc7p-Dbf4p kinase binds to chromatin during S phase and is regulated by both the APC and the RAD53 checkpoint pathway." EMBO J **18**(19): 5334-5346.

Wen, J., K. Cerosaletti, et al. (2012). "NBN Phosphorylation regulates the accumulation of MRN and ATM at sites of DNA double-strand breaks." Oncogene.

Willems, M., D. Genevieve, et al. (2010). "Molecular analysis of pericentrin gene (PCNT) in a series of 24 Seckel/microcephalic osteodysplastic primordial dwarfism type II (MOPD II) families." Journal of medical genetics **47**(12): 797-802.

Wohlschlegel, J. A., B. T. Dwyer, et al. (2000). "Inhibition of eukaryotic DNA replication by geminin binding to Cdt1." Science **290**(5500): 2309-2312.

Wold, M. S. (1997). "Replication protein A: a heterotrimeric, single-stranded DNA-binding protein required for eukaryotic DNA metabolism." Annu Rev Biochem **66**: 61-92.

Wold, M. S. and T. Kelly (1988). "Purification and characterization of replication protein A, a cellular protein required for in vitro replication of simian virus 40 DNA." Proc Natl Acad Sci U S A **85**(8): 2523-2527.

Wong, P. G., M. A. Glozak, et al. (2010). "Chromatin unfolding by Cdt1 regulates MCM loading via opposing functions of HBO1 and HDAC11-geminin." Cell Cycle **9**(21): 4351-4363.

Wong, P. G., S. L. Winter, et al. (2011). "Cdc45 limits replicon usage from a low density of preRCs in mammalian cells." PLoS One **6**(3): e17533.

Woodbine, L., H. Brunton, et al. (2011). "Endogenously induced DNA double strand breaks arise in heterochromatic DNA regions and require ataxia telangiectasia mutated and Artemis for their repair." Nucleic Acids Res **39**(16): 6986-6997.

Woodward, A. M., T. Gohler, et al. (2006). "Excess Mcm2-7 license dormant origins of replication that can be used under conditions of replicative stress." The Journal of cell biology **173**(5): 673-683.

Wu, R., P. B. Singh, et al. (2006). "Uncoupling global and fine-tuning replication timing determinants for mouse pericentric heterochromatin." J Cell Biol **174**(2): 185-194.

Wutz, A. (2011). "Gene silencing in X-chromosome inactivation: advances in understanding facultative heterochromatin formation." Nat Rev Genet **12**(8): 542-553.

Xue, L., B. Zhou, et al. (2003). "Wild-type p53 regulates human ribonucleotide reductase by protein-protein interaction with p53R2 as well as hRRM2 subunits." Cancer Res **63**(5): 980-986.

Xue, Y., J. Wong, et al. (1998). "NURD, a novel complex with both ATP-dependent chromatin-remodeling and histone deacetylase activities." Mol Cell **2**(6): 851-861.

Yamamoto, K. and M. Sonoda (2003). "Self-interaction of heterochromatin protein 1 is required for direct binding to histone methyltransferase, SUV39H1." Biochem Biophys Res Commun **301**(2): 287-292.

Yan, Z., J. DeGregori, et al. (1998). "Cdc6 is regulated by E2F and is essential for DNA replication in mammalian cells." Proc Natl Acad Sci U S A **95**(7): 3603-3608.

Yap, T. A. and P. Workman (2012). "Exploiting the cancer genome: strategies for the discovery and clinical development of targeted molecular therapeutics." Annu Rev Pharmacol Toxicol **52**: 549-573.

Yoshida, K. and I. Inoue (2004). "Regulation of Geminin and Cdt1 expression by E2F transcription factors." Oncogene **23**(21): 3802-3812.

Yoshida, K., N. Sugimoto, et al. (2010). "CDC6 interaction with ATR regulates activation of a replication checkpoint in higher eukaryotic cells." J Cell Sci **123 Pt 2** : 225-35.

You, Z., C. Chahwan, et al. (2005). "ATM activation and its recruitment to damaged DNA require binding to the C terminus of Nbs1." Mol Cell Biol **25**(13): 5363-5379.

You, Z., L. Z. Shi, et al. (2009). "CtIP links DNA double-strand break sensing to resection." Mol Cell **36**(6): 954-969.

Zeng, L., K. L. Yap, et al. (2008). "Structural insights into human KAP1 PHD finger-bromodomain and its role in gene silencing." Nat Struct Mol Biol **15**(6): 626-633.

Zhang, J., L. Yu, et al. (2010). "The interacting domains of hCdt1 and hMcm6 involved in the chromatin loading of the MCM complex in human cells." Cell Cycle **9**(24): 4848-4857.

Zhang, R. and P. D. Adams (2007). "Heterochromatin and its relationship to cell senescence and cancer therapy." Cell Cycle **6**(7): 784-789.

Zhang, Y. and M. Jasin (2011). "An essential role for CtIP in chromosomal translocation formation through an alternative end-joining pathway." Nat Struct Mol Biol **18**(1): 80-84.

Zhao, H., J. Dobrucki, et al. (2011). "Induction of DNA damage signaling by oxidative stress in relation to DNA replication as detected using "click chemistry"." Cytometry A **79**(11): 897-902.

Zhou, J., C. Chau, et al. (2005). "Epigenetic control of replication origins." Cell Cycle **4**(7): 889-892.

Zhu, Q., G. M. Pao, et al. (2011). "BRCA1 tumour suppression occurs via heterochromatin-mediated silencing." Nature **477**(7363): 179-184.

Ziv, Y., D. Bielopolski, et al. (2006). "Chromatin relaxation in response to DNA double-strand breaks is modulated by a novel ATM- and KAP-1 dependent pathway." Nat Cell Biol **8**(8): 870-876.

Zou, L. and S. J. Elledge (2003a). "Sensing DNA damage through ATRIP recognition of RPA-ssDNA complexes." Science **300**(5625): 1542-1548.

Zou, L., D. Liu, et al. (2003b). "Replication protein A-mediated recruitment and activation of Rad17 complexes." Proc Natl Acad Sci U S A **100**(24): 13827-13832.

Appendix: published work

Published OnlineFirst January 30, 2013; DOI: 10.1158/1541-7786.MCR-12-0491

Molecular Cancer Research

Diminished Origin-Licensing Capacity Specifically Sensitizes Tumor Cells to Replication Stress

Kristin M. Zimmerman, Rebecca M. Jones, Eva Petermann, et al.

Mol Cancer Res 2013;11:370-380. Published OnlineFirst January 30, 2013.

Published OnlineFirst January 30, 2013; DOI: 10.1158/1541-7786.MCR-12-0491

DNA Damage and Repair

Molecular Cancer Research

Diminished Origin-Licensing Capacity Specifically Sensitizes Tumor Cells to Replication Stress

Kristin M. Zimmerman[1], Rebecca M. Jones[2], Eva Petermann[2], and Penelope A. Jeggo[1]

Abstract

Previous studies have shown that dormant licensed replication origins can be exploited to enhance recovery from replication stress. Since tumor cells express high levels of origin-licensing proteins, we examined whether depletion of such factors might specifically sensitize tumor versus nontumor cells. Consistent with previous findings, we observed that three tumor-derived cell lines overexpress ORC1, a licensing component, compared with four nontumor cell lines and that a greater level of ORC1 was required to maintain viability in the tumor cells. We determined siRNA-mediated knockdown conditions for each line that maximally reduced ORC1 but did not impact upon viability, which we considered would optimally deplete dormant origins. ORC1 depletion hypersensitized the tumor-derived cells to hydroxyurea and H_20_2 but did not affect the sensitivity of the nontumor lines. Similar results were observed following depletion of ORC6 or CDC6. Furthermore, codepletion of p53 and ORC1 modestly impaired viability of 1BR3hTERT nontumor fibroblasts and more dramatically caused hypersensitivity to hydroxyurea. Finally, overexpression of the c-Myc oncogene combined with ORC1 depletion in nontumor BJhTERT cells diminished viability. Collectively, these findings suggest that tumor cells may have a reliance on origin-licensing capacity, suggesting that licensing factors could represent a target for drug-based cancer therapy. *Mol Cancer Res; 11(4); 370–80. ©2013 AACR.*

Introduction

To replicate the human genome in a timely manner, replication is initiated bidirectionally from multiple origins. However, this necessitates that replication origins only fire once during each cell cycle to avoid rereplication. Origin licensing occurs from late mitosis to G_1 phase and involves assembly of the origin recognition complex (ORC), encompassing ORC1 to ORC6, onto origin sequences (1, 2). Together with CDC6 and CDT1, ORC loads the heterohexameric MCM2-7 complex which provides helicase activity, generating the prereplication complex (pre-RC; refs. 3–6). Cells exploit several mechanisms to prevent origin refiring, including the inhibition of MCM2-7 loading onto origins during S–G_2 and the tight regulation of other pre-RC components via proteasome-mediated degradation (1, 2).

Only a fraction of licensed origins are used for replication, with nonfired origins being considered dormant (7–9). Following replication stress, the activation of checkpoint kinases stabilizes stalled replication forks (10). In addition, dormant origins can be exploited to promote recovery from replication stress (11–15). However, replication fork stalling also activates an intra-S-phase checkpoint response that inhibits late-firing origins (16–18). Although apparently conflicting with the notion that replication fork stalling exploits dormant origins, recent studies have shown that origins are organized in clusters, with activation occurring stochastically and inactivating further origins within the cluster (14, 19). Although damage response signaling inhibits the firing of origins in new clusters, a distinct process promotes dormant origin firing within a cluster in which double fork stalling has occurred (14). This model is intrinsically appealing as it implies that dormant origins are only activated near a stalled fork where they are needed, whereas new replication is diminished elsewhere to preclude further replication in the presence of DNA damage. Support for this model has come from studies involving siRNA-mediated depletion of MCM2-7 in human cells, which suppresses dormant origin usage, inhibits the rate of DNA synthesis, and reduces cell survival in response to replication-inhibiting agents (11–13).

Until recently, studies on dormant origin usage were predominantly undertaken in tumor cells and it was unclear whether the same process occurs in primary cells. Interestingly, an increase in the number of stalled replication forks in unchallenged S-phase cells was observed in mouse embryonic fibroblasts (MEF) expressing a hypomorphic *Mcm4*^{Chaos3} allele, which impairs MCM2-7 complex stability and reduces the number of dormant origins (15).

Authors' Affiliations: [1]Genome Damage and Stability Centre, University of Sussex, Brighton; and [2]School of Cancer Sciences, University of Birmingham, Edgbaston, Birmingham, United Kingdom

Note: Supplementary data for this article are available at Molecular Cancer Research Online (http://mcr.aacrjournals.org/).

Corresponding Author: Penelope A. Jeggo, University of Sussex, Falmer, Brighton BN1 9RQ, United Kingdom. Phone: 44-1273-678482; Fax: 44-1273-678121; E-mail: p.a.jeggo@sussex.ac.uk

doi: 10.1158/1541-7786.MCR-12-0491

Published OnlineFirst January 30, 2013; DOI: 10.1158/1541-7786.MCR-12-0491

Significantly, *Mcm4*^{Chaos3} mice are cancer prone (20). Importantly, *Mcm4*^{Chaos3} cells have a normal rate of replication and helicase activity. Thus, reducing the number of dormant origins need not affect replication but can impede recovery from either endogenous or damage-induced replication stress. Although other pathways of replication fork recovery exist, a failure to use dormant origins is proposed to cause genomic instability.

Two recent studies identified mutations in origin-licensing components (ORC1, ORC4, ORC6, CDT1, and CDC6) in Meier–Gorlin syndrome (MGS), a disorder characterized by microcephaly, proportionate dwarfism, and bone abnormalities including small or absent patellae (21–23). Cells from patients with MGS, despite having substantially reduced origin licensing capacity, grow well in culture consistent with the notion that only a fraction of licensed origins are required to sustain replication (22).

Carcinogenesis necessitates multiple genetic changes to support often rapid and uncontrolled proliferation. Most tumor cells suffer high replication stress, due to uncontrolled proliferation and/or enhanced genomic instability. Interestingly, several studies have reported that origin-licensing proteins are overexpressed in tumor-derived cell lines (24–27). Given this, we reasoned that tumor cells might have a greater demand for origin licensing than nontransformed cells, either to sustain rapid replication and/or to enhance recovery from the increased level of replication stalling/collapse. Given the finding that nontransformed cells can grow efficiently with substantially reduced licensing capacity, we considered that ORC proteins might represent targets to specifically sensitize tumor cells. Here, we examine this possibility by investigating the impact of diminished origin licensing capacity in tumor versus nontransformed cells. Strikingly, our results suggest that tumor cells more frequently rely on dormant origin usage following exposure to agents that cause replication stress compared with nontumor cells.

Materials and Methods

Cell culture

Cell lines were purchased from the American Type Culture Collection (ATCC) or established and authenticated in-house or by scientific collaborators indicated in references. All cell lines were tested for mycoplasma contamination before use and assessed for ORC1 expression by immunoblot. Control primary skin fibroblasts (48BR), control hTERT-immortalized fibroblasts 1BR3hTERT or BJhTERT (ATCC), and ORC1-P4hTERT, derived from an ORC1-deficient patient with MGS, were cultured in Dulbecco's modified Eagle's medium supplemented with 15% fetal calf serum (FCS, Invitrogen; ref. 22, 28–30). Medium for BJ-MYC-ER, a derivative of BJhTERT expressing a tamoxifen-inducible c-Myc gene, was supplemented with 2 μg/mL puromycin (Invitrogen). MRC-5 is a primary fetal lung fibroblast cell line. MRC5, U2OS, and HeLa cells (ATCC) were cultured in minimal essential medium containing 10% FCS. Cells were transfected with siRNA oligonucleotide pools (Thermo Scientific Dharmacon; ORC1, p53, ORC6, or CDC6) or *Stealth* siRNA targeting ORC1 (Invitrogen; ref. 22) using HiPerFect (Qiagen) or DharmaFECT (Thermo Scientific Dharmacon). siControl represents scrambled oligonucleotides (Thermo Scientific Dharmacon).

Viability assay

siRNA-transfected cells were seeded in 96-well dishes, treated as described and viability was assessed using the CellTiter-Blue assay (Promega). Viability was normalized to the siRNA-transfected but untreated control. The half maximal inhibitory concentration (IC_{50}) values from viability curves were calculated with SigmaPlot (Systat Software, Inc.) using the five-parameter logistic nonlinear regression model. IC_{50} values represent the mean ± SD of 3 independent experiments.

Immunoblotting

For whole-cell extracts, cells were lysed in buffer A (22) containing 500 mmol/L NaCl and supplemented with protease (Sigma-Aldrich) and phosphatase inhibitors (Thermo Fisher Scientific) for one hour on ice and sonicated at 4°C. Fractionation of chromatin-bound and unbound proteins was conducted as previously described (22). Lysates were resolved by electrophoresis, transferred onto polyvinylidene difluoride (GE Healthcare) and immunoblotted using α-ORC1, ORC6, CDC6, p53 (Santa Cruz Biotechnology, Inc.), or β-actin (Abcam) antibodies.

Drug treatments

siRNA-transfected cells were seeded into dishes and grown for 48 hours. Hydroxyurea (Sigma-Aldrich) or H_2O_2 (Fisher Scientific/Acros Organics) was added for the indicated times. Cells were washed 3 times in PBS and incubated in fresh medium as indicated.

Clonogenic survival

Clonogenic survival was assessed as previously described (31). Briefly, cells were transfected with siRNA, treated as described, and incubated for 10 days (U2OS) or for 21 days using irradiated feeder cells to enhance plating efficiency (1BR3hTERT). Survival was normalized to the siRNA-transfected but untreated control. Plotted values represent the mean ± SD of 3 independent experiments.

DNA fibre assay

Cells were labeled with 25 μmol/L chlorodeoxyuridine (CldU) for 20 minutes, washed 3 times with medium, incubated in 2 mmol/L hydroxyurea for 24 hours, washed 3 times again, and pulse-labeled with 250 μmol/L iododeoxyuridine (IdU) for 1 hour. Labeled cells were harvested and DNA fibre spreads were prepared as previously described (32). CldU and IdU were detected by incubating acid-treated fibre spreads with rat α-bromodeoxyuridine (BrdUrd) (1:1,000, AbD Serotec) and mouse α-BrdUrd (1:750, Becton Dickinson) monoclonal antibodies for 1 hour. Slides were fixed with 4% paraformaldehyde and

Published OnlineFirst January 30, 2013; DOI: 10.1158/1541-7786.MCR-12-0491

incubated with AlexaFluor 555-conjugated goat α-rat IgG (1:500, Molecular Probes) and AlexaFluor 488-conjugated goat α-mouse IgG (1:500, Molecular Probes) for 1.5 hours. Images of DNA fibres were acquired on a Nikon E600 microscope using a × 60 (1.3NA) lens, a Hamamatsu digital camera, and the Volocity package (Perkin Elmer). For quantification, at least 130 structures were counted per experiment using ImageJ software (NI H, http://rsbweb.nih.gov/ij/).

Replication recovery assay

siRNA-transfected cells were treated with hydroxyurea and labeled with 50 μmol/L BrdUrd; Becton Dickinson 30 minutes before harvesting. Cells were fixed, BrdUrd-labeled, propidium iodide-stained and analyzed by fluorescence-activated cell sorting (FACS) as previously described (31).

γ-H2AX immunofluorescence

Cells were processed for γ-H2AX analysis as previously described (33) using α-γ-H2AX and α-CENPF (Abcam) and 4′, 6–diamidino–2–phenylindole (DAPI) labeling of DNA. Cells harboring S-phase–associated DNA damage, referred to as γ-H2AX$^+$, were detected by bright, pan-nuclear γ-H2AX and minimal CENPF signal (34, 35). γ-H2AX$^+$ cells were manually scored in more than 500 cells per condition. Images of cells were acquired with identical exposure settings on a Zeiss Axioplan2 microscope using a × 40 (0.75 NA) lens, a Hamamatsu digital camera, and SimplePCI software (Hamamatsu).

Results

Substantial ORC1 depletion does not impact upon proliferation

We aimed to compare how diminished origin licensing capacity affects recovery from replication stress in tumor-derived versus nontumor cell lines. We used 1BR3hTERT and U20S osteosarcoma cells as nontumor and tumor cell lines, respectively. 1BR3hTERT, an hTERT-immortalized fibroblast line derived from a normal individual, has a stable karyotype, shows genomic stability, and has an intact G_1–S checkpoint (Unpublished observations). Because ORC1 is essential, we sought knockdown conditions that reduce ORC1 protein levels without impeding proliferation. Viability, monitored using the CellTiter-Blue assay, was assessed following siRNA-mediated knockdown of ORC1 in 1BR3hTERT and U20S using a range of siRNA oligonucleotide (scrambled or ORC1-specific) concentrations. We observed diminished proliferation with increasing siORC1 concentrations, consistent with the notion that oligonucleotide concentration correlates with knockdown efficiency (Fig. 1A and B). Since tumor and nontumor cell lines differ in the efficiency of siRNA-mediated knockdown and requirement for ORC1, the impact was distinct for each line. The highest siORC1 concentration that did not significantly impede viability was 5 or 0.6 nmol/L for 1BR3hTERT and U20S, respectively (Supplementary Fig. S1A). Immunoblotting revealed that U20S has higher ORC1 protein levels compared with 1BR3hTERT, consistent with previous findings that tumor-derived cells overexpress ORC proteins (Fig. 1C; ref. 24–27). Although α-ORC1 antibodies are inefficient for immunoblotting, a marked reduction in ORC1 protein could be observed in both lines following siORC1 (Fig. 1C). Routinely, low residual ORC1 was detectable in siORC1-treated U20S cells, whereas residual ORC1 was not detectable in siORC1-transfected 1BR3hTERT. As ORC1 is essential, it is likely that 1BR3hTERT retain residual, although undetectable, ORC1. This suggests that U20S cells require a higher level of ORC1 to maintain viability compared with 1BR3hTERT, consistent with the notion that tumor cells have a greater need for origin-licensing proteins compared with nontumor cells. Having identified knockdown conditions that substantially deplete ORC1 without impeding viability, which we anticipated would substantially reduce the level of dormant origins, we proceeded to examine the impact on recovery from damage-induced replication arrest.

ORC1 depletion impairs recovery from hydroxyurea in U20S but not 1BR3hTERT

We examined sensitivity to hydroxyurea, which depletes ribonucleotide reductase and enhances fork stalling/collapse, in 1BR3hTERT and U20S following siControl or siORC1. siRNA transfection was conducted as described above and cells were exposed to differing concentrations of hydroxyurea for 24 hours. Hydroxyurea was removed and viability monitored 4 days later (Fig. 1D and E). To compare the effect of siORC1 between the cell lines, we estimated the hydroxyurea concentration that reduced viability by 50% (the IC_{50} value). The relative IC_{50} value was calculated by comparison with the IC_{50} of siControl-transfected cells (Fig. 1H). Strikingly, while siORC1 did not affect hydroxyurea sensitivity in 1BR3hTERT, it significantly enhanced sensitivity in U20S. Similar effects were observed following transfection of cells with a distinct pool of ORC1 siRNA oligonucleotides (Supplementary Fig. S1B–S1D). To verify that the resistance of 1BR3hTERT cells is not simply a consequence of their slower cell-cycle progression, resulting in a lower fraction of cells progressing into S-phase, we monitored the population doubling time (Supplementary Fig. S1E-S1F) and rate of hydroxyurea -induced γ-H2AX formation in the 2 cell lines (Fig. 1F and G). We estimated that by 48 hours, all 1BRhTERT cells had undergone replication fork arrest after hydroxyurea. However, examination of viability following 48-hour hydroxyurea treatment yielded similar results (Fig. 1H). Thus, the resistance of 1BR3hTERT cells to siORC1-induced hypersensitivity is not explained by their slower cell-cycle progression. To verify that the viability assay reflects clonogenicity, we also examined clonogenic survival of U20S following 24-hour hydroxyurea treatment (Fig. 1I) and of 1BR3hTERT following 48-hour hydroxyurea treatment (Fig. 1J). Although these 2 assays monitor different endpoints, a similar impact was observed, validating use of the viability assay.

To substantiate these findings without relying on siRNA-mediated depletion, we also examined an hTERT-

Published OnlineFirst January 30, 2013; DOI: 10.1158/1541-7786.MCR-12-0491

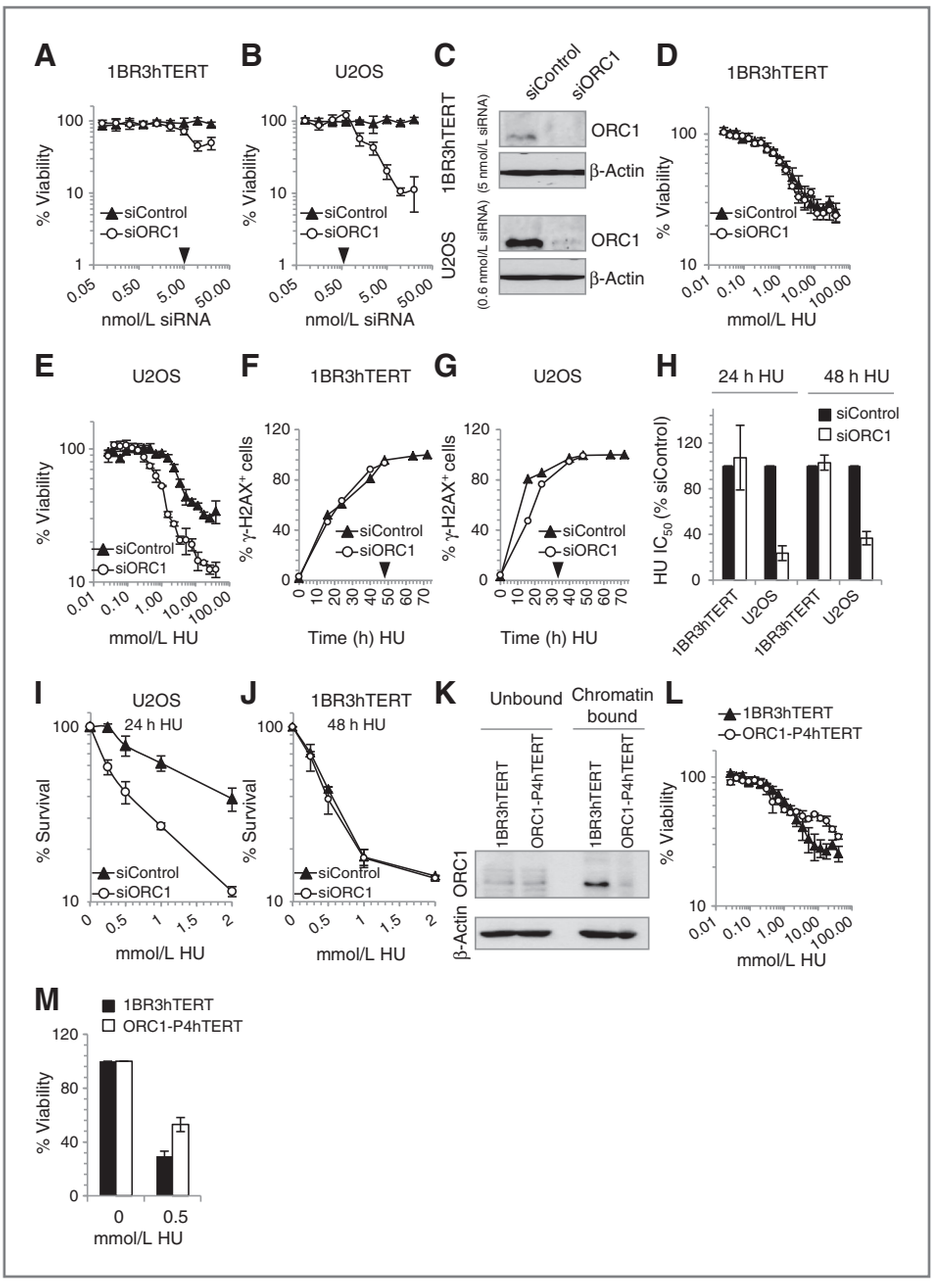

Figure 1. siORC1 impairs recovery of U2OS but not 1BR3hTERT cells from hydroxyurea. 1BR3hTERT (A) or U2OS (B) cells were transfected with siControl or siORC1 oligonucleotides (0.1–20 nmol/L), and viability assessed 7 days later. Results represent mean ± SD from triplicate samples. Black arrows indicate the oligonucleotide concentration subsequently used. C, 1BR3hTERT and U2OS cells were transfected with 5 or 0.6 nmol/L siORC1, respectively. ORC1 protein levels were assessed by immunoblotting 48 hours later. β-actin was a loading control. D and E, 1BR3hTERT and U2OS cells were transfected with siRNA for 48 hours and treated with hydroxyurea (HU; 0.03–40 mmol/L) for 24 hours. Viability was assessed for 4 days following hydroxyurea removal. F and G, 1BR3hTERT and U2OS cells transfected with siRNA as described were treated with 2 mmol/L hydroxyurea for indicated times and hydroxyurea -induced S-phase damage was assessed by immunofluorescence labelling of γ-H2AX. Nuclei containing bright γ-H2AX pan-nuclear staining were scored as γ-H2AX$^+$. Black arrows indicate the time of hydroxyurea treatment required to obtain 100% γ-H2AX$^+$ cells. H, viability was assessed after transfection with siRNA and treatment with hydroxyurea for 24 or 48 hours as in (D and E). Hydroxyurea IC_{50} values were estimated from the viability graphs. I, U2OS cells were treated with siRNA as described above and then with hydroxyurea (0.05–2 mmol/L) for 24 hours. clonogenic survival was estimated at 10 days following hydroxyurea removal. J, as in (I), except 1BR3hTERT cells were treated with hydroxyurea for 48 hours and clonogenic survival was estimated 21 days following hydroxyurea removal. Additional controls are shown in Supplementary Fig. S1. K, ORC1 protein levels were assessed in chromatin-bound and unbound fractions in 1BR3hTERT and ORC1-P4hTERT by immunoblotting. L, 1BR3hTERT or ORC1-P4hTERT were treated with hydroxyurea (0.03–40 mmol/L) for 24 hours. Viability was assessed 4 days after hydroxyurea removal. M, 1BR3hTERT or ORC1-P4hTERT cells were treated with 0.5 mmol/L hydroxyurea for 48 or 72 hours, respectively. Viability was assessed as above.

Published OnlineFirst January 30, 2013; DOI: 10.1158/1541-7786.MCR-12-0491

immortalized fibroblast line derived from an ORC1-deficient MGS patient (ORC1-P4hTERT; ref. 22). ORC1 is expressed at normal levels in ORC1-P4hTERT but chromatin binding of ORC1 is impaired (ref. 22; Fig. 1K).We observed resistance rather than marked sensitivity of ORC1-P4hTERT cells to hydroxyurea at higher concentrations potentially due to a lower number of replication origins (Fig. 1L). We also adjusted hydroxyurea treatment time to achieve complete hydroxyurea-induced S-phase arrest in 1BR3hTERT and ORC-P4hTERT (representing 48 or 72-hour exposures, respectively). Under these conditions, resistance, but not sensitivity, to 0.5 mmol/L hydroxyurea was also observed (Fig. 1M).

U20S cells show diminished recovery of DNA synthesis and accumulated DNA damage following siORC1 compared with 1BR3hTERT

To examine whether siORC1 affects replication recovery, 1BR3hTERT or U20S were treated with siRNA as described above and exposed to 2 mmol/L hydroxyurea for 24 hours. Following hydroxyurea removal, cells were incubated for 2, 4, or 24 hours, and BrdUrd added for the final 30 minutes. BrdUrd incorporation, representing recovery of DNA synthesis, was assessed by FACS (Fig. 2A and B). Hydroxyurea treatment abolished BrdUrd incorporation in both cell lines, consistent with replication inhibition. Strikingly, in 1BR3hTERT, BrdUrd incorporation was substantially recovered at 2 hours after hydroxyurea removal and was similar in siControl or siORC1-treated cells. In marked contrast, although siControl-treated U20S cells also recovered DNA synthesis at 2 hours following hydroxyurea removal, DNA synthesis was dramatically reduced at this time in siORC1-treated U20S cells. Because this difference is observed at early times (2 hours) after hydroxyurea removal, this suggests that siORC1 does not impair rapid recovery of replication in hydroxyurea -treated 1BR3hTERT but does so in U20S.

We also examined whether the inability of siORC1-treated U2OS to recover replication causes accumulated DNA damage. Either immediately (0) or 24 hours following treatment with 2 mmol/L hydroxyurea, cells were examined for γ-H2AX, a marker of DNA damage, and CENPF, a G_2–M-phase marker. Immediately following hydroxyurea treatment, most cells were CENPF$^-$ (consistent with S-phase arrest) and showed pan-nuclear γ-H2AX staining, showing the presence of collapsed/stalled replication forks; untreated cells had a lower fraction of γ-H2AX$^+$ cells (Fig. 2C and D). 24 hours after hydroxyurea removal, few siControl or siORC1-transfected 1BR3hTERT cells were γ-H2AX$^+$ (Fig. 2D), consistent with the observed recovery of replication. Similarly, the number of γ-H2AX$^+$ siControl-treated U20S cells was dramatically reduced 24 hours after hydroxyurea removal (Fig. 2C and D). In stark contrast, approximately 50% of siORC1-treated U20S cells retained γ-H2AX staining 24 hours after hydroxyurea removal. γ-H2AX$^+$ cells were negative for the G_2–M marker, CENPF, consistent with the notion that they represent damaged S-phase cells. This analysis shows that 1BR3hTERT undergo replication fork arrest and activate the DNA damage response after hydroxyurea treatment but efficiently recover despite substantial depletion of ORC1.

ORC1 depletion reduces new origin firing after hydroxyurea in U20S

The DNA fibre assay allows replication at new versus preexisting origins to be monitored (36).We exploited the technique to assess new origin firing in U2OS cells after release from hydroxyurea exposure. siRNA-transfected cells were exposed to CldU for 20 minutes, then either exposed to IdU for 20 minutes (control) or CldU was washed out, and cells were exposed to hydroxyurea for 24 hours. Following hydroxyurea removal, IdU was added for 1 hour. CldU$^+$/IdU$^-$ replication tracks are considered to represent stalled forks that have not reinitiated replication; CldU$^-$/IdU$^+$ tracks represent ones with newly fired origins (Supplementary Fig. S2C–S2D). To monitor new origin firing, the fraction of CldU$^-$/IdU$^+$ tracks was assessed. In untreated U20S cells, ORC1 siRNA did not significantly impact upon new origin firing (Fig. 2E). Following hydroxyurea, although siORC1 did not impact upon the level of stalled forks, new origin firing was substantially diminished. These findings strongly suggest that siORC1 diminishes replication restart by new origin firing after hydroxyurea while not affecting new origin firing in unperturbed cells.

Hypersensitivity of U20S to hydroxyurea following depletion of additional licensing components

We next examined whether the sensitivity of U2OS cells to hydroxyurea is impacted following depletion of additional origin-licensing factors. We examined ORC6 and CDC6 as they are also causal defects for MGS (22). A total of 0.6 nmol/L siORC6 or CDC6 substantially depleted ORC6 or CDC6 but did not impede cellular proliferation (Fig. 3A; data not shown). Viability assessment revealed a similar level of hydroxyurea sensitivity following siORC6 or CDC6 to that observed following siORC1 (Fig. 3B and C). However, neither siORC6 nor siCDC6 affected hydroxyurea sensitivity in 1BR3hTERT (Supplementary Fig. S3).

siORC1 does not affect hydroxyurea sensitivity in additional nontumor lines (BJhTERT, 48BR, and MRC-5) but sensitizes additional tumor-derived lines (HeLa and MDA-MB-231)

To extend our findings, we examined additional nontumor fibroblasts (BJhTERT, 48BR, and MRC-5) and tumor-derived lines (HeLa and MDA-MB-231). 48BR and MRC5 represent primary fibroblast lines to complement the analysis of the hTERT-immortalized line. For all lines, we examined the optimum siORC1 oligonucleotide concentration that failed to impact upon viability (Supplementary Fig. S4). BJhTERT cells showed slightly diminished viability above 5 nmol/L siORC1 similar to 1BR3hTERT cells; 5 nmol/L was chosen for analysis (Supplementary Fig. S4A). HeLa cells were resistant to high oligonucleotide concentrations; 0.6 nmol/L was chosen to allow comparison to U20S (Fig. 4A and B, Supplementary Fig. S4D). 48BR, MDA-MB-231,

Published OnlineFirst January 30, 2013; DOI: 10.1158/1541-7786.MCR-12-0491

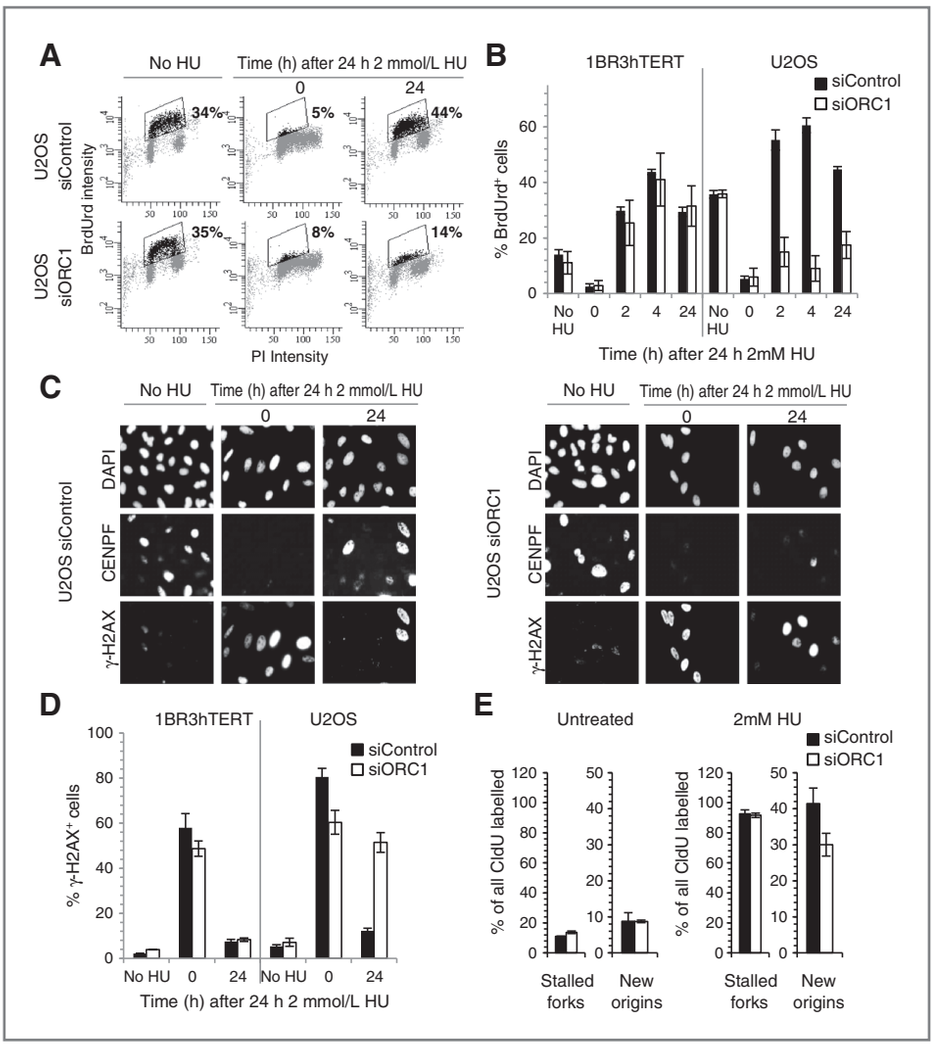

Figure 2. siORC1 impairs recovery of replication following hydroxyurea and reduces hydroxyurea -induced new origin firing in U2OS. A and B, 1BR3hTERT and U2OS cells were transfected with siRNA oligonucleotides (5 or 0.6 nmol/L, respectively). 48 hours later, 2 mmol/L hydroxyurea was added for 24 hours and cells were grown for times shown. BrdUrd was added 30 minutes before processing by FACS. The fraction of replicating ($BrdUrd^+$) cells was determined. A, representative FACS analysis. Boxed regions containing black data points indicate $BrdUrd^+$ cells; numbers represent $BrdUrd^+$ cell fraction. Supplementary Fig. S2A shows additional analyses. B, quantification from 3 experiments using 1BR3hTERT or U2OS cells. C, representative immunofluorescence images showing DAPI (DNA), CENPF (cell-cycle phase), or γ-H2AX (DNA damage) in U20S cells treated as in (A and B). Representative merged channel images are shown in Supplementary Fig. S2B. D, nuclei containing bright γ-H2AX pan-nuclear staining were scored as $γ\text{-H2AX}^+$. Figure shows the fraction of $γ\text{-H2AX}^+$ cells. E, 48 hours following transfection of U2OS cells with 0.6 nmol/L siControl or siORC1, cells were pulse labeled with CldU, treated with 2 mmol/L hydroxyurea for 24 hours and released (or untreated), and pulse labeled with IdU for 1 hour. The number of structures representing fork stalling and new origin firing was normalized to the number of $CldU^+$ replication tracks. The experimental design and representative images are shown in Supplementary Fig. S2C and S2D. Results represent the mean and SD of more than 2 experiments (0 mmol/L hydroxyurea $n = 2$, 2 mmol/L hydroxyurea $n = 3$).

and MRC-5 displayed diminished viability above 1 nmol/L siORC1; 1 nmol/L was chosen for analysis (Supplementary Fig. S4B, S4C, and S4E). The time of hydroxyurea treatment required to achieve complete hydroxyurea -induced S-phase damage was also assessed in each cell line (Supplementary Fig. S5). The time indicated was used for subsequent viability experiments. Similar to 1BR3hTERT and U20S cells, although ORC1 protein levels were greater in siORC1-depleted HeLa and MDA-MB-231 cells compared with BJhTERT, 48BR, or MRC-5 cells, siORC1 enhanced hydroxyurea sensitivity of HeLa and MDA-MB-231 without substantially impacting upon sensitivity of BJhTERT, 48BR, or MRC-5 cells (Fig. 4A, C–G). For MRC-5, slightly enhanced sensitivity was observed at high hydroxyurea doses but there was no impact on the IC_{50} value.

siORC1 diminishes viability of tumor but not primary cells to H_20_2

Having shown that siORC1 hypersensitizes U20S and HeLa but not 1BR3hTERT or BJhTERT cells to hydroxyurea, we used a similar approach to evaluate whether recovery from oxidative damage, which can indirectly

Published OnlineFirst January 30, 2013; DOI: 10.1158/1541-7786.MCR-12-0491

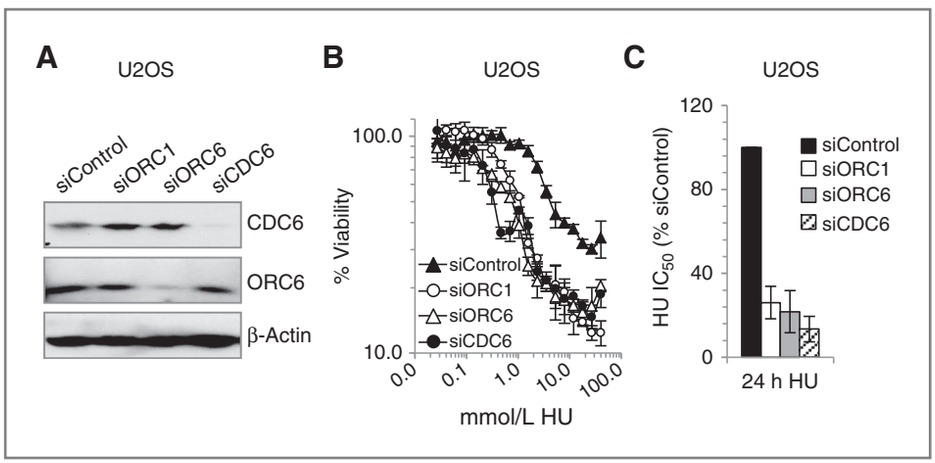

Figure 3. Depletion of additional origin licensing components in U20S enhances hydroxyurea sensitivity. U2OS cells were transfected with 0.6 nmol/L siRNA for 48 hours. A, immunoblotting using α-ORC6 and α-CDC6. B, viability was assessed as in Fig. 1D and E. C, estimated IC_{50} values.

induce replication stress, might also involve differential dormant origin usage. Strikingly, while siORC1 did not affect sensitivity of 1BR3hTERT or BJhTERT to H_20_2, U20S and HeLa cells showed marked hypersensitivity (Fig. 5A–E). The slightly higher resistance of siORC1-treated 1BR3hTERT cells to H_20_2 compared with siControl cells likely reflects their slightly slower replication. Nonetheless, the distinction between 1BR3hTERT/BJhTERT and U20S/HeLa cells to combined siORC1 and H_20_2 was marked.

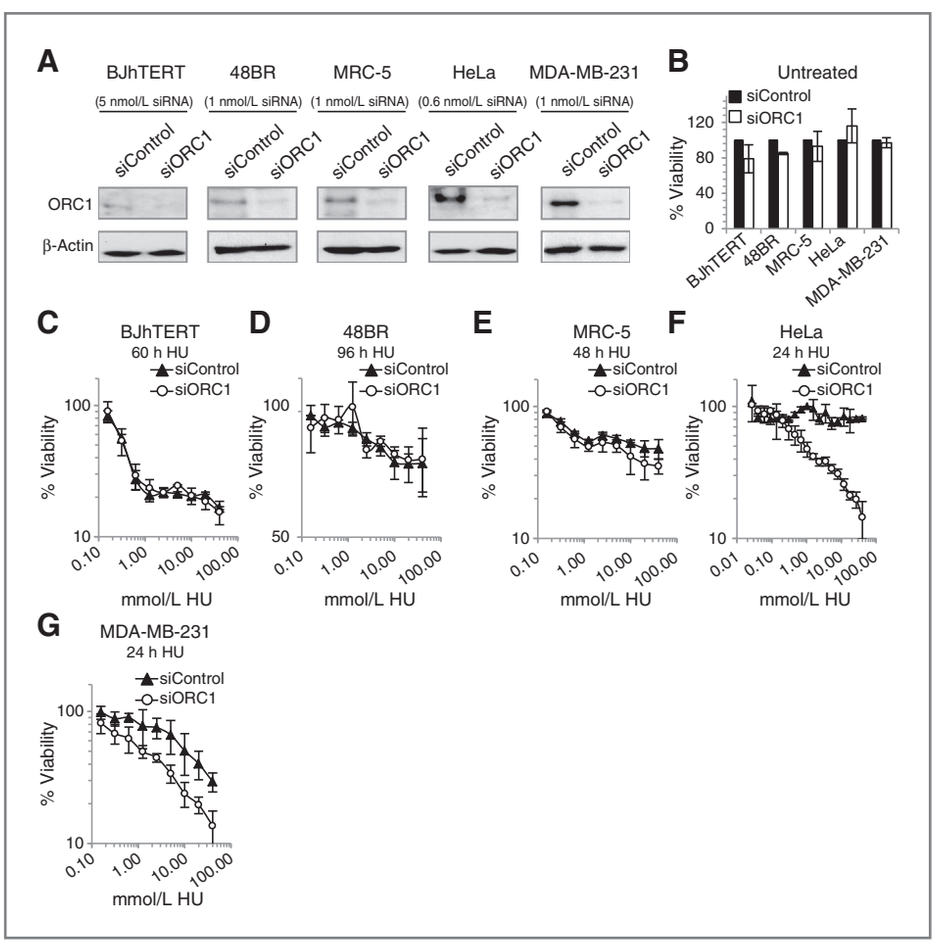

Figure 4. siORC1 enhances hydroxyurea sensitivity of additional tumor-derived cell lines (HeLa and MDA-MB-231) but does not affect nontumor cells (BJhTERT, 48BR, and MRC5). A–G, BJhTERT and were transfected with 5 nmol/L, 48BR, MRC-5, and MDA-MB-231 with 1 nmol/L, and HeLa with 0.6 nmol/L siRNA oligonucleotides. A, ORC1 protein was assessed by immunoblotting 48 hours later. B, viability was assessed 7 days later. Analyses using different siORC1 oligonucleotide concentrations are shown in Supplementary Fig. S4. C–G, viability was assessed as in Fig. 1D and E using indicated hydroxyurea treatment times to achieve complete hydroxyurea -induced S-phase arrest (Supplementary Fig. S5A–S5E).

Published OnlineFirst January 30, 2013; DOI: 10.1158/1541-7786.MCR-12-0491

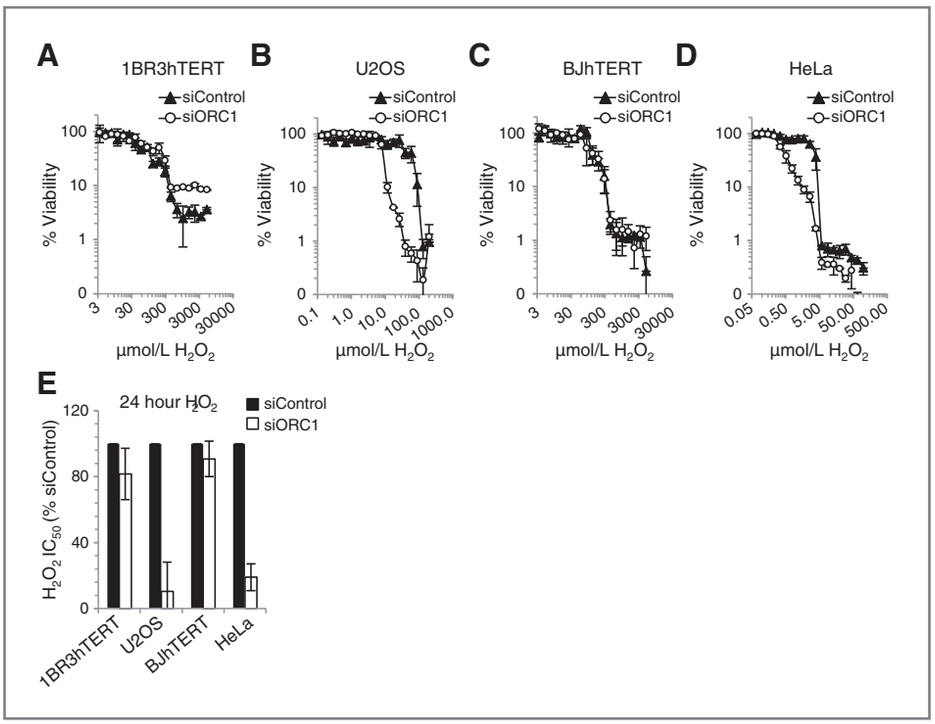

Figure 5. siORC1 specifically enhances sensitivity of tumor-derived cell lines to H_2O_2. A–E, 1BR3hTERT, BJhTERT, U20S or HeLa were transfected with siRNA as described in Figs. 1 and 4. 48 hours later, cells were treated with H_2O_2, with concentrations adjusted to account for substantial differences in sensitivity between cell lines. 24 hours later, H_2O_2 was removed and viability assessed 4 days later. A–D, representative viability plots. E, estimated IC_{50} values.

sip53 mildly sensitizes 1BR3hTERT cells to siORC1 without exogenous DNA damage and causes marked sensitivity to hydroxyurea

p53 loss abrogates the damage-induced G_1–S checkpoint, enhancing S-phase progression and replication stalling (37). In addition, p53 is required for a licensing checkpoint which prevents S-phase entry until sufficient origins have been licensed (38, 39). We examined whether sip53 in 1BR3hTERT affects viability and hydroxyurea sensitivity following siORC1. 1BR3hTERT cells were transfected with siControl, sip53, siORC1 or combined siORC1+sip53 for 48 hours, then viability assessed in untreated or hydroxyurea -treated cells as described above. p53 was efficiently depleted in 1BR3hTERT (Fig. 6A). As above, siORC1 did not affect the viability of 1BR3hTERT cells (Fig. 6B). sip53 alone slightly inhibited viability but combined sip53+siORC1 diminished viability by approximately 1.7 (Fig. 6B). These findings suggest that in undamaged cells, siORC1 more markedly affects viability in the absence of p53. siORC1 did not significantly affect hydroxyurea sensitivity similar to the findings in Fig. 1D; there was a modest but not statistically significant impact of sip53 on hydroxyurea sensitivity but a marked decrease following sip53+siORC1 (Fig. 6C and D).

Depletion of ORC1 confers sensitivity to Myc overexpression

Myc overexpression, which enhances proliferation and replication stress, is frequently observed during carcinogenesis (40–42). We examined whether Myc expression influences the requirement for origin licensing capacity using a BJhTERT derivative that expresses c-Myc fused to a tamoxifen-inducible estrogen receptor (40–42). First, anticipating

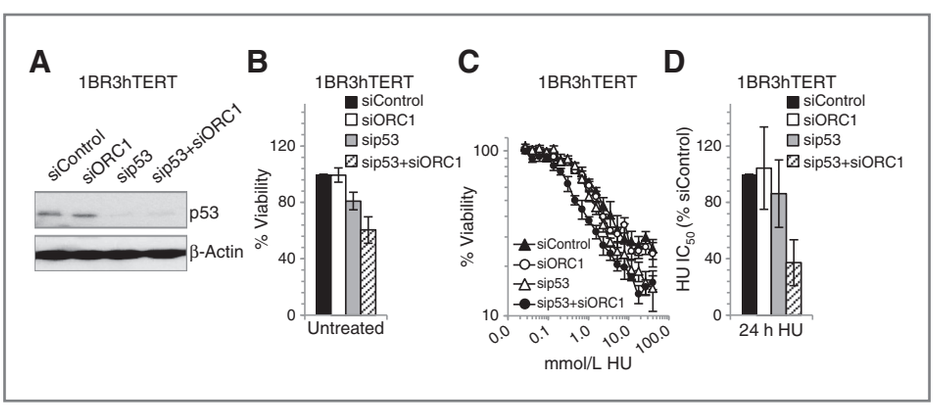

Figure 6. p53 depletion enhances sensitivity of 1BR3hTERT to hydroxyurea. A–D, 1BR3hTERT was transfected with 5 nmol/L siControl, siORC1, sip53 or a combination of siORC1+sip53. A, 48 hours later, p53 levels were assessed by immunoblotting. B, viability was assessed 7 days after siRNA transfection as in Fig. 1A and B. C and D, viability was assessed in hydroxyurea -treated siRNA-transfected cells as in Fig. 1D and E. C, representative viability curves. D, estimated IC_{50} values.

Published OnlineFirst January 30, 2013; DOI: 10.1158/1541-7786.MCR-12-0491

that tamoxifen concentration affects the level of c-Myc expression, we estimated the tamoxifen concentration promoting endogenous DNA damage (assessed by γ-H2AX). 24 hours after 2 μmol/L tamoxifen, 30% of siControl-transfected cells were γ-H2AX$^+$, suggesting that Myc overexpression induces replication stress (Fig. 7A). Following siORC1, 60% of BJhTERT cells were γ-H2AX$^+$, raising the possibility that siORC1 causes enhanced or persistent c-Myc–induced replication arrest. Next, assessment of viability 5 days following exposure to different tamoxifen concentrations revealed substantial sensitivity following siORC1 (Fig. 7B and C) suggesting that depletion of origin-licensing capacity diminishes the ability to cope with c-Myc–induced replication stress.

Discussion

We previously observed that MGS patient-derived cell lines grow efficiently in culture despite 10-fold lower levels of origin-licensing components (21, 22). This ability to sustain substantial proliferation is consistent with findings that only 10% of licensed origins are used during unchallenged replication (7–9). Recent studies have provided evidence that dormant origins can be used to promote recovery from replication fork stalling or collapse (11–15). Because tumor cells show elevated oxidative and replicative stress, we predicted that they might have an enhanced reliance on origin-licensing capacity compared with normal cells, raising the possibility that targeting origin-licensing components could specifically inhibit cancer cell growth. Here, we evaluate this possibility.

Consistent with previous findings, we observed that 3 tumor-derived cell lines showed high ORC1 expression compared with nontumor lines (24–27). In general, higher ORC1 levels were required to maintain viability in the tumor lines (although MRC-5 cells also had a requirement for a higher ORC1 level). Nonetheless, the ability to detect higher residual ORC1 in the tumor than nontumor cell lines shows that our findings cannot simply be explained by more efficient ORC1 knockdown in the tumor versus nontumor cells.

To enhance the applicability to exploit inhibition of origin licensing for tumor therapy, we examined whether partial ORC1 depletion affected the response to hydroxyurea, a chemotherapeutic agent. Significantly, we observed marked sensitization of the tumor -derived lines to hydroxyurea (or H_20_2) compared with the nontumor cells. In addition, we observed that ORC1 depletion enhanced hydroxyurea sensitivity of p53-depleted nontumor cells and also conferred sensitivity to Myc overexpression. This important result suggests that enhancing the level of replication stress and/or rate of proliferation, both of which arise following c-Myc expression, increases the demand for origin-licensing capacity.

Collectively, using our panel of 3 tumor and 4 primary or hTERT-immortalized cell lines, our findings suggest that tumor cells have a greater demand for origin-licensing capacity following replication fork arrest compared with nontumor lines and that loss of p53 or c-Myc expression enhances this demand in nontumor cells. Our findings could have several explanations. One possibility is that following replication stress, stalled forks more readily collapse in tumor compared with nontumor cells and that dormant origin firing enhances recovery from replication fork collapse. However, we are not aware of studies supporting this suggestion. Alternatively, it is possible that fork collapse occurs similarly in tumor and nontumor cells, but that tumor cells more frequently exploit dormant origins for recovery and are hence hypersensitive when this route is unavailable. Although the original studies describing dormant origin usage after replication stress used tumor cells, a recent study involving primary MEFs showed that they also exploit dormant origins for recovery from replicative stress (15). However, it is difficult to evaluate the comparative usage of dormant origins in tumor versus nontumor cells from these studies. An alternative and appealing possibility is that tumor cells override the origin-licensing checkpoint to enhance proliferation and, therefore, enter S-phase with

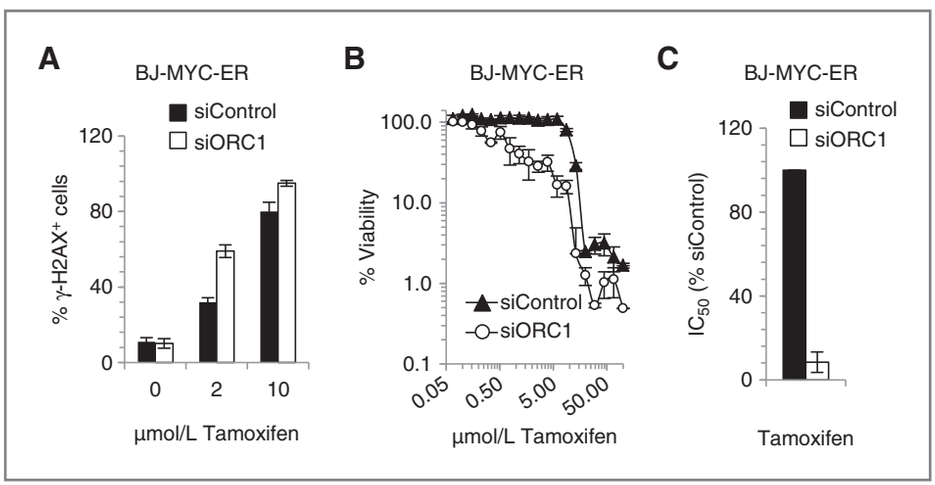

Figure 7. siORC1 enhances viability following Myc overexpression. A–C, BJhTERT cells stably expressing a tamoxifen-inducible Myc oncogene (BJ-MYC-ER) were transfected with 5 nmol/L siRNA for 48 hours. Tamoxifen was added as indicated. A, 24 hours following transfection, cells were examined by immunofluorescence for γ-H2AX (DNA damage), CENPF (cell-cycle phase), and DAPI (DNA). Nuclei containing bright γ-H2AX pan-nuclear staining were scored as γ-H2AX$^+$. B, BJ-MYC-ER fibroblasts were transfected with siRNA as in (A) and treated with tamoxifen (0.07–100 μmol/L) to induce Myc expression. Viability was assessed 5 days later. C, estimated IC_{50} values.

Published OnlineFirst January 30, 2013; DOI: 10.1158/1541-7786.MCR-12-0491

diminished dormant origins. Indeed, the upregulation of origin licensing proteins in tumor cells may reflect their need to effect rapid origin licensing during their short G_1 phase. Thus, further reducing licensing capacity may provide a situation where there are insufficient dormant origins to exploit following replication fork arrest. It should be noted that our knockdown conditions were designed to prevent any impact on unperturbed cell growth. This model is consistent with the known function of p53 in enhancing G_1-phase progression and/or abolishing the G_1–S checkpoint. Importantly, in the present context, p53 is also required for the origin-licensing checkpoint as codepletion of p53 and CDC6, another licensing component, in normal fibroblasts permits S-phase entry with insufficient origin capacity (43). c-Myc also enhances G_1-phase progression and disrupts p53 activity (44, 45). However, both p53 loss and c-Myc expression have multiple additional impacts including an influence on replication (44–46). Thus, although the latter explanation is appealing, further work is required to define the basis underlying our observations. It is likely, moreover, that there could be multiple impacts. Our findings to date are based on a restricted number of tumor or nontumor cell lines. Nonetheless, the relationship seems marked and further work will be required to examine the extent to which this represents a phenotype of many tumor cell lines. It should be noted that around 50% of tumor cell lines show an upregulation of origin-licensing components (24–27).

Our goal was to examine whether the origin-licensing complex represents a suitable target to specifically sensitize tumor cells. Importantly, we report that 3 tumor cells require greater origin-licensing capacity following exposure to DNA damaging agents than 4 nontumor cells. In addition, we show that p53 loss (in the presence of hydroxyurea) or c-Myc expression in nontumor cells enhances the reliance on ORC1. Interestingly, the BAH domain of ORC1 was recently reported to bind H4K20me2 with high specificity and affinity via an aromatic cage, which could provide a route for drug targeting (47). In summary, we provide evidence that the downregulation of ORC1 and other origin-licensing proteins enhances the sensitivity of tumor but not nontumor cell lines to replicative stress, providing a potential route for specific sensitization of tumor cells.

Disclosure of Potential Conflicts of Interest

No potential conflicts of interest were disclosed.

Authors' Contributions

Conception and design: E. Petermann, P.A. Jeggo
Development of methodology: P.A. Jeggo, K.M. Zimmerman
Acquisition of data (provided animals, acquired and managed patients, provided facilities, etc.): R.M. Jones, K.M. Zimmerman
Analysis and interpretation of data (e.g., statistical analysis, biostatistics, computational analysis): K.M. Zimmerman, R.M. Jones, P.A. Jeggo
Writing, review, and/or revision of the manuscript: K.M. Zimmerman, E. Petermann, P.A. Jeggo
Study supervision: P.A. Jeggo

Acknowledgments

The authors thank Drs. M. O'Driscoll for discussions and O. Fernandez-Capetillo for kindly providing BJ-MYC-ER.

Grant Support

The P.A. Jeggo laboratory is supported by an MRC programme grant, the Association for International Cancer Research, the Wellcome Research Trust, and the EMF Biological Research Trust. The E. Petermann laboratory is supported by an MRC project grant, Cancer Research UK, and the University of Birmingham.

The costs of publication of this article were defrayed in part by the payment of page charges. This article must therefore be hereby marked *advertisement* in accordance with 18 U.S.C. Section 1734 solely to indicate this fact.

Received August 18, 2012; revised December 11, 2012; accepted December 31, 2012; published OnlineFirst January 30, 2013.

References

1. Blow JJ, Dutta A. Preventing re-replication of chromosomal DNA. Nat Rev Mol Cell Biol 2005;6:476–86.
2. Arias EE, Walter JC. Strength in numbers: preventing rereplication via multiple mechanisms in eukaryotic cells. Genes Dev 2007;21:497–518.
3. Bell SP, Stillman B. ATP-dependent recognition of eukaryotic origins of DNA-replication by a multiprotein complex. Nature 1992;357:128–34.
4. Nishitani H, Lygerou Z, Nishimoto T, Nurse P. The Cdt1 protein is required to license DNA for replication in fission yeast. Nature 2000;404:625–8.
5. Blow JJ, Ge XQ, Jackson DA. How dormant origins promote complete genome replication. Trends Biochem Sci 2011;36:405–14.
6. Remus D, Beuron F, Tolun G, Griffith JD, Morris EP, Diffley JF. Concerted loading of Mcm2-7 double hexamers around DNA during DNA replication origin licensing. Cell 2009;139:719–30.
7. Anglana M, Apiou F, Bensimon A, Debatisse M. Dynamics of DNA replication in mammalian somatic cells: nucleotide pool modulates origin choice and interorigin spacing. Cell 2003;114:385–94.
8. DePamphilis ML, Blow JJ, Ghosh S, Saha T, Noguchi K, Vassilev A. Regulating the licensing of DNA replication origins in metazoa. Curr Opin Cell Biol 2006;18:231–9.
9. Gilbert DM. Evaluating genome-scale approaches to eukaryotic DNA replication. Nat Rev Genet 2010;11:673–84.
10. Caspari T, Carr AM. Checkpoints: how to flag up double-strand breaks. Curr Biol 2002;12:R105–7.
11. Ibarra A, Schwob E, Mendez J. Excess MCM proteins protect human cells from replicative stress by licensing backup origins of replication. Proc Natl Acad Sci U S A 2008;105:8956–61.
12. Woodward AM, Gohler T, Luciani MG, Oehlmann M, Ge X, Gartner A, et al. Excess Mcm2-7 license dormant origins of replication that can be used under conditions of replicative stress. J Cell Biol 2006;173:673–83.
13. Ge XQ, Jackson DA, Blow JJ. Dormant origins licensed by excess Mcm2-7 are required for human cells to survive replicative stress. Genes Dev 2007;21:3331–41.
14. Blow JJ, Ge XQ. A model for DNA replication showing how dormant origins safeguard against replication fork failure. EMBO Rep 2009;10:406–12.
15. Kawabata T, Luebben SW, Yamaguchi S, Ilves I, Matise I, Buske T, et al. Stalled fork rescue via dormant replication origins in unchallenged S phase promotes proper chromosome segregation and tumor suppression. Mol Cell 2011;41:543–53.
16. Lambert S, Carr AM. Checkpoint responses to replication fork barriers. Biochimie 2005;87:591–602.
17. Bartek J, Lukas C, Lukas J. Checking on DNA damage in S phase. Nat Rev Mol Cell Biol 2004;5:792–804.
18. Branzei D, Foiani M. The DNA damage response during DNA replication. Curr Opin Cell Biol 2005;17:568–75.

Published OnlineFirst January 30, 2013; DOI: 10.1158/1541-7786.MCR-12-0491

19. Lebofsky R, Heilig R, Sonnleitner M, Weissenbach J, Bensimon A. DNA replication origin interference increases the spacing between initiation events in human cells. Mol Biol Cell 2006;17:5337–45.
20. Shima N, Alcaraz A, Liachko I, Buske TR, Andrews CA, Munroe RJ, et al. A viable allele of Mcm4 causes chromosome instability and mammary adenocarcinomas in mice. Nat Genet 2007;39:93–8.
21. Bicknell LS, Bongers EM, Leitch A, Brown S, Schoots J, Harley ME, et al. Mutations in the pre-replication complex cause Meier-Gorlin syndrome. Nat Genet 2011;43:356–9.
22. Bicknell LS, Walker S, Klingseisen A, Stiff T, Leitch A, Kerzendorfer C, et al. Mutations in ORC1, encoding the largest subunit of the origin recognition complex, cause microcephalic primordial dwarfism resembling Meier-Gorlin syndrome. Nat Genet 2011;43:350–5.
23. Gorlin RJ. Microtia, absent patellae, short stature, micrognathia syndrome. J Med Genet 1992;29:516–7.
24. McNairn AJ, Gilbert DM. Overexpression of ORC subunits and increased ORC-chromatin association in transformed mammalian cells. J Cell Biochem 2005;96:879–87.
25. Lau E, Tsuji T, Guo L, Lu SH, Jiang W. The role of pre-replicative complex (pre-RC) components in oncogenesis. FASEB J 2007; 21:3786–94.
26. Di Paola D, Zannis-Hadjopoulos M. Comparative analysis of pre-replication complex proteins in transformed and normal cells. J Cell Biochem 2012;113:1333–47.
27. Karakaidos P, Taraviras S, Vassiliou LV, Zacharatos P, Kastrinakis NG, Kougiou D, et al. Overexpression of the replication licensing regulators hCdt1 and hCdc6 characterizes a subset of non-small-cell lung carcinomas: synergistic effect with mutant p53 on tumor growth and chromosomal instability–evidence of E2F-1 transcriptional control over hCdt1. Am J Pathol 2004;165:1351–65.
28. Shibata A, Barton O, Noon AT, Dahm K, Deckbar D, Goodarzi AA, et al. Role of ATM and the damage response mediator proteins 53BP1 and MDC1 in the maintenance of G(2)/M checkpoint arrest. Mol Cell Biol 2010;30:3371–83.
29. Morales CP, Holt SE, Ouellette M, Kaur KJ, Yan Y, Wilson KS, et al. Absence of cancer-associated changes in human fibroblasts immortalized with telomerase. Nat Genet 1999;21:115–8.
30. Keyse SM, McAleer MA, Davies DJ, Moss SH. The response of normal and ataxia-telangiectasia human fibroblasts to the lethal effects of far, mid and near ultraviolet radiations. Int J Radiat Biol Relat Stud Phys Chem Med 1985;48:975–85.
31. Loser DA, Shibata A, Shibata AK, Woodbine LJ, Jeggo PA, Chalmers AJ. Sensitization to radiation and alkylating agents by inhibitors of poly (ADP-ribose) polymerase is enhanced in cells deficient in DNA double-strand break repair. Mol Cancer Ther 2010;9:1775–87.
32. Henry-Mowatt J, Jackson D, Masson JY, Johnson PA, Clements PM, Benson FE, et al. XRCC3 and Rad51 modulate replication fork progression on damaged vertebrate chromosomes. Mol Cell 2003; 11:1109–17.
33. Woodbine L, Brunton H, Goodarzi AA, Shibata A, Jeggo PA. Endogenously induced DNA double strand breaks arise in heterochromatic DNA regions and require ataxia telangiectasia mutated and Artemis for their repair. Nucleic Acids Res 2011;39:6986–97.
34. Murga M, Campaner S, Lopez-Contreras AJ, Toledo LI, Soria R, Montana MF, et al. Exploiting oncogene-induced replicative stress for the selective killing of Myc-driven tumors. Nat Struct Mol Biol 2011;18:1331–5.
35. Lobrich M, Shibata A, Beucher A, Fisher A, Ensminger M, Goodarzi AA, et al. gamma H2AX foci analysis for monitoring DNA double-strand break repair: Strengths, limitations and optimization. Cell Cycle 2010;9:662–9.
36. Petermann E, Orta ML, Issaeva N, Schultz N, Helleday T. Hydroxyurea-stalled replication forks become progressively inactivated and require two different RAD51-mediated pathways for restart and repair. Mol Cell 2010;37:492–502.
37. Wahl GM, Linke SP, Paulson TG, Huang LC. Maintaining genetic stability through TP53 mediated checkpoint control. Cancer Surv 1997;29:183–219.
38. Shreeram S, Sparks A, Lane DP, Blow JJ. Cell type-specific responses of human cells to inhibition of replication licensing. Oncogene 2002;21:6624–32.
39. Ge XQ, Blow JJ. The licensing checkpoint opens up. Cell Cycle 2009;8:2320–2.
40. Robinson K, Asawachaicharn N, Galloway DA, Grandori C. c-Myc accelerates S-phase and requires WRN to avoid replication stress. PLoS ONE 2009;4:e5951.
41. Herold S, Herkert B, Eilers M. Facilitating replication under stress: an oncogenic function of MYC? Nat Rev Cancer 2009;9:441–4.
42. Dominguez-Sola D, Ying CY, Grandori C, Ruggiero L, Chen B, Li M, et al. Non-transcriptional control of DNA replication by c-Myc. Nature 2007;448:445–51.
43. Nevis KR, Cordeiro-Stone M, Cook JG. Origin licensing and p53 status regulate Cdk2 activity during G(1). Cell Cycle 2009;8:1952–63.
44. Vafa O, Wade M, Kern S, Beeche M, Pandita TK, Hampton GM, et al. c-Myc can induce DNA damage, increase reactive oxygen species, and mitigate p53 function: a mechanism for oncogene-induced genetic instability. Mol Cell 2002;9:1031–44.
45. Ceballos E, Munoz-Alonso MJ, Berwanger B, Acosta JC, Hernandez R, Krause M, et al. Inhibitory effect of c-Myc on p53-induced apoptosis in leukemia cells. Microarray analysis reveals defective induction of p53 target genes and upregulation of chaperone genes. Oncogene 2005;24:4559–71.
46. Kumari A, Schultz N, Helleday T. p53 protects from replication-associated DNA double-strand breaks in mammalian cells. Oncogene 2004;23:2324–9.
47. Kuo AJ, Song J, Cheung P, Ishibe-Murakami S, Yamazoe S, Chen JK, et al. The BAH domain of ORC1 links H4K20me2 to DNA replication licensing and Meier-Gorlin syndrome. Nature 2012;484:115–9.

Supplementary Figure Legends

Figure S1. Growth parameters of 1BR3hTERT and U2OS cells. (A) 1BR3hTERT and U2OS cells were transfected with 5 or 0.6 nM siRNA oligonucleotides, respectively, and grown in normal growth medium. 7 days later, viability was assessed and normalized to that of siControl-transfected cells. Results represent the mean +/- SD from three independent experiments**. (B)** 1BR3hTERT and U2OS cells were transfected with indicated concentrations of siControl or a distinct siRNA oligonucleotide pool targeting ORC1 (siORC1pool). 48 hours later, cells were lysed and ORC1 protein levels were assessed by immunoblotting. **(C-D)** 1BR3hTERT and U2OS cells were transfected with siControl, siORC1 (single), or siORC1pool, grown for 48 hours, and treated with HU for 24 hours. Viability was assessed 4 days later. **(E)** Exponentially growing cells were seeded at densities comparable to those used for the viability assay and grown in normal growth medium. Cells were harvested at the indicated time points, non-viable cells were labelled with trypan blue, and viable cells were manually scored. Cell number was then normalized to initial seeding density. Results represent the mean +/- SD of from three experiments. **(F)** Cell doubling time was estimated from data in (E).

Figure S2. Additional images of BrdU replication recovery and γH2AX staining in HU-treated U2OS and/or 1BR3hTERT; description of DNA fibre assay. (A) Experimental conditions were as described in the legend to Fig 2A-B. Images from FACS analysis showing BrdU vs. PI intensity for all time points tested in U2OS cells are depicted. Boxed regions containing blue data points indicate $BrdU^+$ cells; adjacent numbers represent $BrdU^+$ cell fraction. **(B)** Experimental conditions were as described in the legend to Fig 2C. Representative images of DAPI (blue), γH2AX (green), and CENPF (red) staining in 1BR3hTERT and U2OS cells are presented. All three channels have been merged and images

have been cropped with identical settings. **(C)** Schematic of experimental setup for the DNA fibre assay. Briefly, U2OS cells were transfected with 0.6 nM siControl or siORC1. 48 hours later, cells were pulsed with CldU (red) for 20 minutes, washed, treated with 2 mM HU for 24 hours, washed again, and labelled with IdU (green) for 1 hour. Acid treated fibre spreads were then stained and imaged using immunofluorescence methodology. **(D)** Representative images of labelled DNA fibres. CldU (red) and IdU (green)-labelled tracks represent ongoing/progressing forks. CldU-only (red) tracks represent fork stalling. IdU-only (green) tracks represent new origin firing. Levels of each were assessed as in Fig. 2E.

Figure S3. Depletion of ORC6 and CDC6 does not affect HU sensitivity in 1BR3hTERT. **(A)** 1BR3hTERT cells were transfected with 5 nM indicated siRNA oligonucleotides. 48 hours later, cells were lysed and ORC6 or CDC6 protein levels were assessed by immunoblotting. **(B)** Viability was assessed in siRNA-transfected cells treated with HU for 24 hours as in Fig. 1D-E.

Figure S4. Selected concentrations of siRNA oligonucleotides do not significantly impair viability in additional cell lines selected. Non-tumour BJhTERT, 48BR, and MRC-5 cells (A-C) or tumour-derived HeLa and MDA-MB-231 cells (D-E) were transfected with siControl or siORC1 oligonucleotides (0.1-20 nM) and viability assessed 7 days later as in Fig. 1A-B. Black arrows indicate the oligonucleotide concentration subsequently utilised.

Figure S5. Assessment of HU treatment time required for complete HU-induced S phase damage induction. Non-tumour BJhTERT, 48BR, and MRC-5 cells (A-C) or tumour-derived HeLa and MDA-MB-231 (D-E) were transfected with siControl or siORC1 oligonucleotides indicated above. ORC1-P4hTERT cells (F) were grown in normal growth

medium for 48 hours. Cells were treated with 2 mM HU for indicated times, and HU-induced S phase damage was assessed by γH2AX analysis as in Fig. 1F-G.

Figure S1

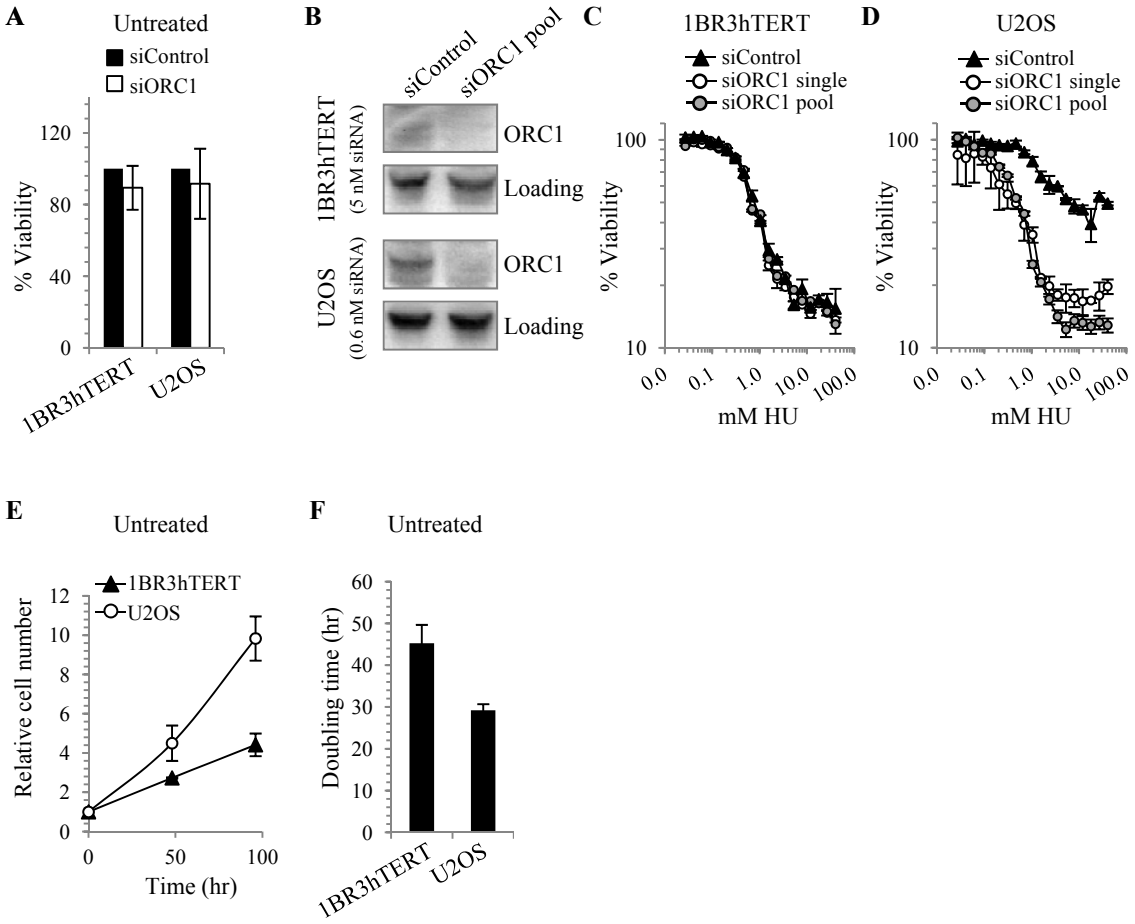
A
Untreated
siControl
siORC1
% Viability
120
80
40
0
1BR3hTERT
U2OS
B
siControl
siORC1 pool
1BR3hTERT
(5 nM siRNA)
ORC1
Loading
U2OS
(0.6 nM siRNA)
ORC1
Loading
C
1BR3hTERT
siControl
siORC1 single
siORC1 pool
% Viability
100
10
0.0
0.1
1.0
10.0
100.0
mM HU
D
U2OS
siControl
siORC1 single
siORC1 pool
% Viability
100
10
0.0
0.1
1.0
10.0
100.0
mM HU
E
Untreated
1BR3hTERT
U2OS
Relative cell number
12
10
8
6
4
2
0
0
50
100
Time (hr)
F
Untreated
Doubling time (hr)
60
50
40
30
20
10
0
1BR3hTERT
U2OS

Figure S2

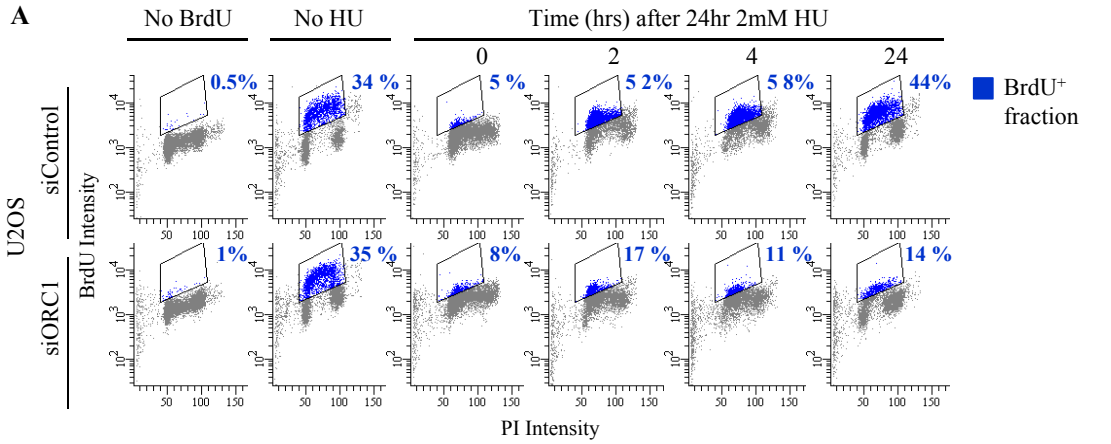
A
No BrdU
No HU
Time (hrs) after 24hr 2mM HU
0
2
4
24
U2OS
siControl
siORC1
BrdU Intensity
PI Intensity
0.5%
34 %
5 %
5 2%
5 8%
44%
1%
35 %
8%
17 %
11 %
14 %
BrdU+ fraction

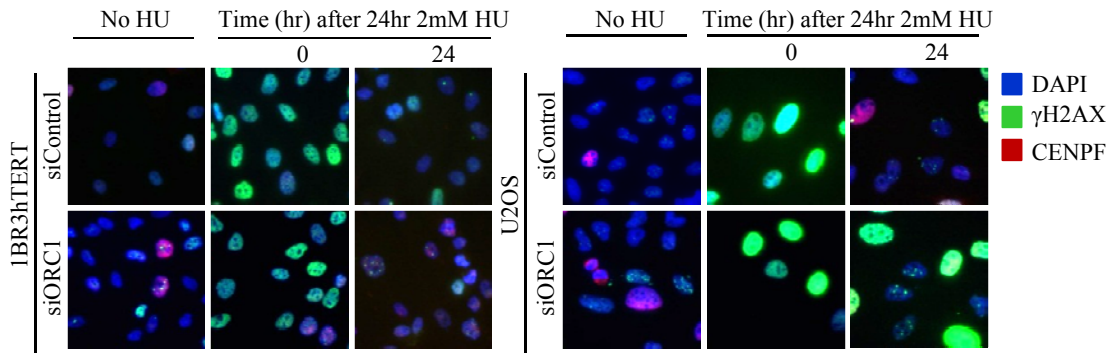
B
No HU
Time (hr) after 24hr 2mM HU
0
24
1BR3hTERT
U2OS
siControl
siORC1
DAPI
γH2AX
CENPF

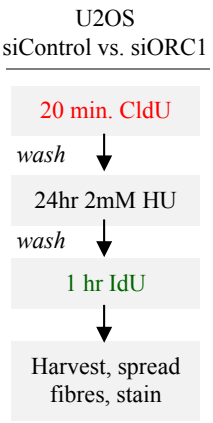
C
U2OS
siControl vs. siORC1
20 min. CldU
wash
24hr 2mM HU
wash
1 hr IdU
Harvest, spread fibres, stain

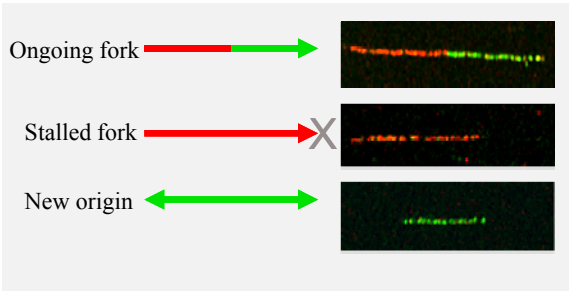
D
Ongoing fork
Stalled fork
New origin

Figure S3

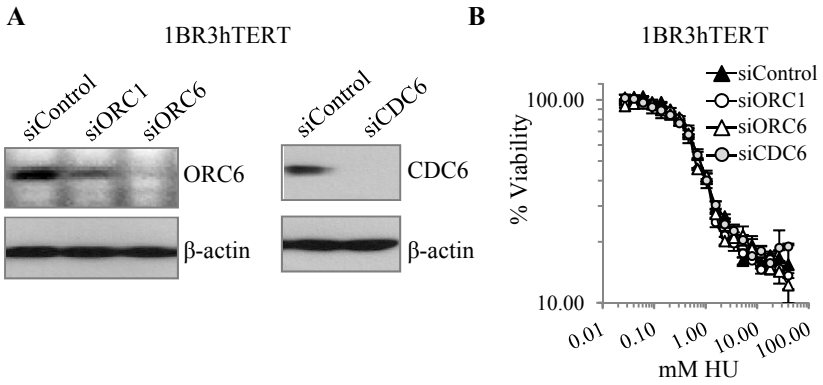
A
1BR3hTERT
siControl
siORC1
siORC6
ORC6
β-actin
siControl
siCDC6
CDC6
β-actin
B
1BR3hTERT
siControl
siORC1
siORC6
siCDC6
% Viability
100.00
10.00
0.01
0.10
1.00
10.00
100.00
mM HU

Figure S4

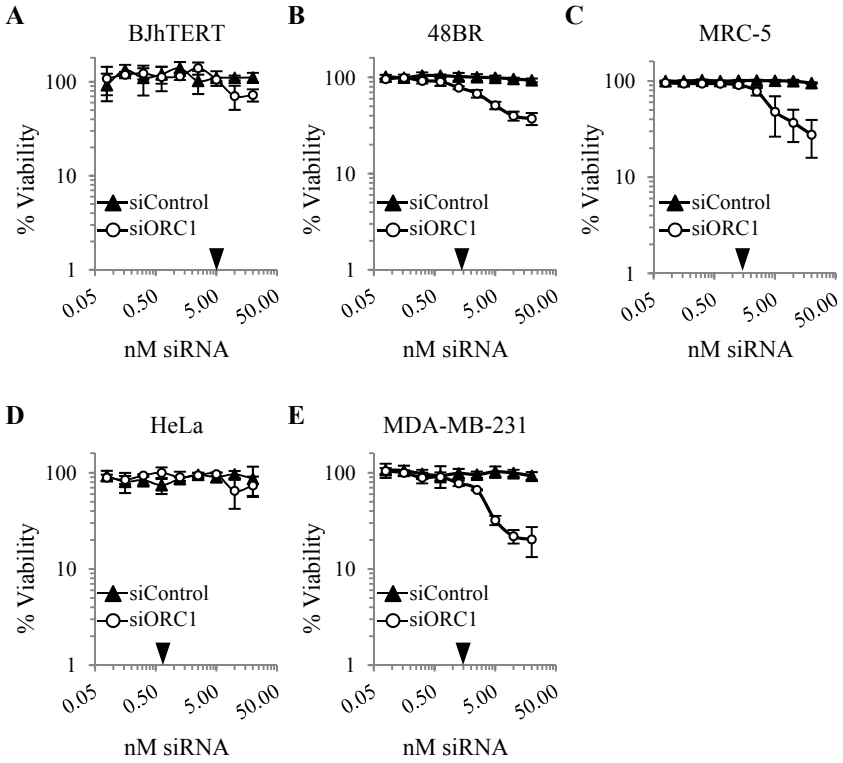
A
BJhTERT
B
48BR
C
MRC-5
D
HeLa
E
MDA-MB-231
% Viability
100
10
1
siControl
siORC1
0.05
0.50
5.00
50.00
nM siRNA

Figure S5

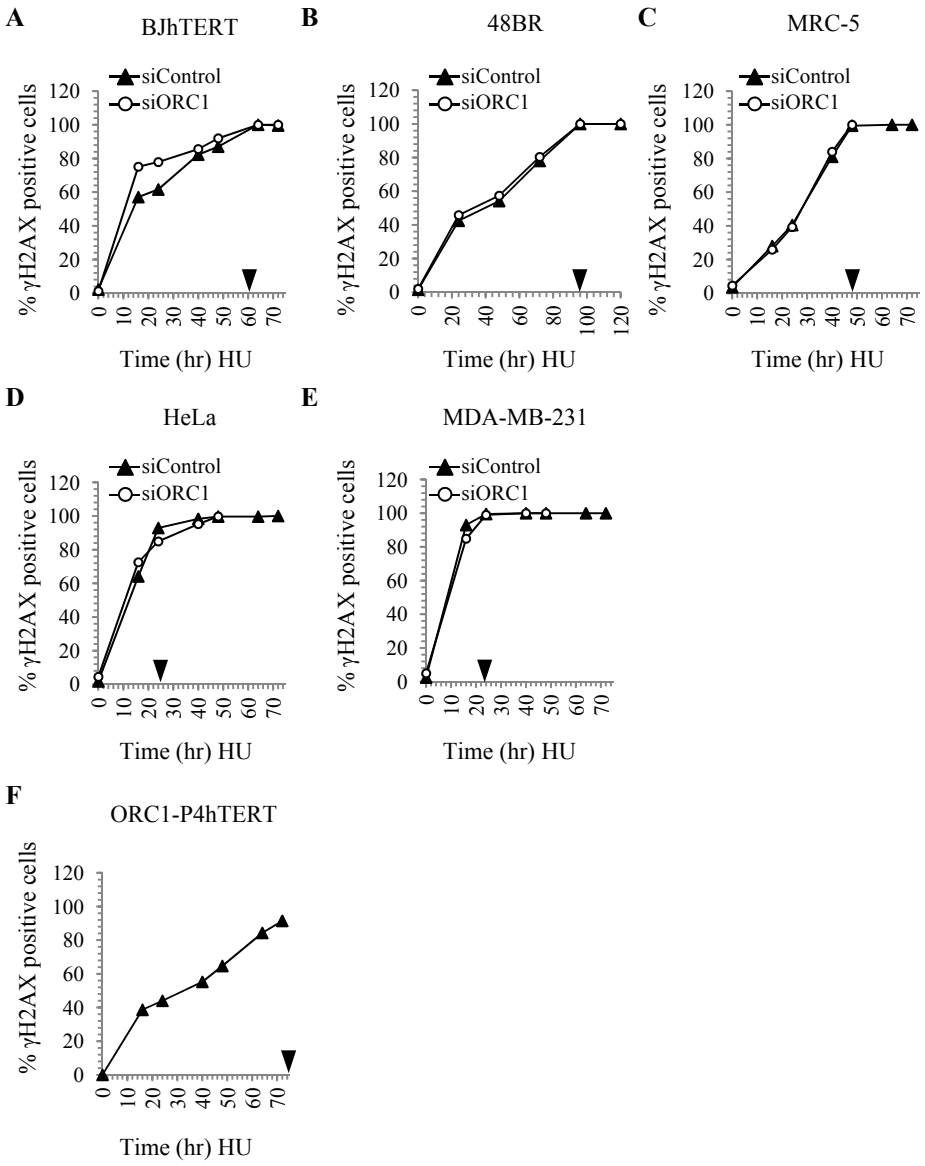
A
BJhTERT
B
48BR
C
MRC-5
D
HeLa
E
MDA-MB-231
F
ORC1-P4hTERT
siControl
siORC1
% γH2AX positive cells
Time (hr) HU